„Molekulare Ursachen und therapeutische Intervention bei der Alzheimer-Demenz“

Dissertation

zur Erlangung des Grades

„Doktor der Naturwissenschaften“

im Promotionsfach Biochemie

am Fachbereich Chemie, Pharmazie und Geowissenschaften

der Johannes Gutenberg Universität

in Mainz

Sven Reinhardt

geboren am 22.08.1984 in Bad Dürkheim

Mainz 2014

Dekan: [redacted].

Erster Berichterstatter: [redacted].

Zweiter Berichterstatter: [redacted].

Dritter Berichterstatter: [redacted].

Datum der mündlichen Prüfung: 03.11.2014.

Die vorliegende Arbeit wurde im Zeitraum von Mai 2010 bis Juni 2014 unter Betreuung von [redacted] im Biochemischen Labor der Klinik für Psychiatrie und Psychotherapie, Universitätsmedizin Mainz angefertigt.

EIDESSTATTLICHE ERKLÄRUNG

Ich erkläre an Eides statt, dass ich die vorliegende Dissertation selbstständig verfasst habe und keine anderen Hilfsmittel/Quellen benutzt habe als die in dieser Arbeit angegebenen.

Weiterhin erkläre ich, dass kein anderes Prüfungsverfahren beantragt oder diese Arbeit anderweitig als Prüfungsarbeit in einer anderen Fakultät vorgelegt wurde.

Ort:……

Datum:……

Unterschrift:……

Danksagung

[redacted]

Inhaltsverzeichnis

I. Abkürzungsverzeichnis

5xFAD	Alzheimer-Mausmodell (Mutationen: APP KM670/671NL (Swedish), APP I716V (Florida), APP V717I (London), PSEN1 M146L (A>C), PSEN1 L286V)
A-beta	Amyloid-beta
AD	*Alzheimer's disease* (Alzheimersche Krankheit)
ADAM	*A disintegrin and metalloproteinase* (Disintegrin Metalloproteinase)
AICD	*APP intracellular domain* (APP intrazelluläre Domäne)
APLP	*Amyloid precursor like protein* (Amyloid Vorläufer ähnliches Protein)
ApoE	Apolipoprotein E
APP	*Amyloid precursor protein* (Amyloid Vorläufer Protein)
APP/PS1	Alzheimer-Mausmodell (Mutationen: APP KM670/671NL (Swedish), PSEN1-dE9)
ATF 4/6	*Activating transcription factor* 4/*6* (aktivierender Transkriptionsfaktor 4/6)
ATP	Adenosintriphosphat
AVC	*Atrioventricular channel* (Atrioventrikulär Kanal)
BACE-1	*Beta site APP cleaving enzyme-1* (beta Stelle des APP spaltendes Enzym-1)
BHS	Blut-Hirn Schranke
Bmp2	*Bone morphogenetic protein 2* (knochenmorphogenetisches Protein 2)
bp	Basenpaare
CDK5	*Cyclin dependent protein kinase 5* (Zyklin abhängige Proteinkinase 5)
CDKI	*Cyclin-dependent kinase inhibitor* (Zyklin abhängige Kinase Inhibitor)
CK 1	Casein Kinase 1
CSF	*Cerebrospinal fluid* (Zerebrospinalflüssigkeit)
DAPT	N-[N-(3,5-Difluorophenacetyl)-L-alanyl]-S-phenylglycine t-butylester
DMSO	Dimethylsulfoxid
DNA	*Deoxyribonucleic acid* (Deoxyribonukleinsäure)
ELISA	*Enzyme-linked-immunosorbent-assay* (enzymatisches Immunadsorptionsverfahren)
ER	Endoplasmatisches Retikulum
ERK	*Extracellular signal regulated kinases* (Extrazellulär Signal regulierte Kinasen)
ERSE	*ER-stress responsive element* (ER-Stress sensitive Bindestelle)
EST	*Expressed sequence tag* (kurze DNA Sequenzen zur Expressionsanalyse)
FDA	*Food and Drug Administration* (Arzneimittelzulassungsbehörde der Vereinigten Staaten)
FITC	Fluoresceinisothiocyanat
GRP78	*glucose-regulated protein 78* (Glukose reguliertes Protein 78)
GSK 3-beta	*Glycogen synthase kinase 3-beta* (Glykogen Synthase Kinase 3-beta)
HDAC-1	Histon-Deacetylase-1
HEK293	humane embryonale Nierenzellen
HMG-CoA	3-Hydroxy-3-Methylglutaryl-Coenzym-A
HNE	4-Hydroxy-2-Nonenal
HPLC	*high performance liquid chromatography* (Hochleistungsflüssigkeitschromatographie)
HSF-1	*Heat shock factor-1* (Hitzeschock Faktor-1)
IDE	*Insulin degrading enzyme* (Insulin abbauendes Enzym)
IGF-1	*Insulin like growth factor 1* (Insulin ähnlicher Wachstumsfaktor 1)
IL-1 beta	Interleukin-1 beta
IR	Insulin-Rezeptor
IRE1-alpha	*Inositol requiring enzyme 1-alpha* (Inositol benötigendes Enzym 1-alpha)
kDa	Kilo Dalton
LRP-1	*low-density lipoprotein receptor-related protein-1 (*LDL Rezeptor verwandtes Protein-1)
MCI	*Mild cognitive impairment* (Milde kognitive Beeinträchtigung)
miRNA	microRNA
mRNA	*Messenger RNA* (Boten-RNA)
NL-1	Neuroligin-1
NR-1	Neuregulin-1
NSAID	*Non-steroidal anti-inflammatory drugs* (Nicht-steroidale anti-entzündliche Medikamente)
P_{app}	*Permeability coefficient* (Permeabilitäts Koeffizient)
PBEC	*Porcine brain endothelial cells* (Schweine Hirn Endothelzellen)
PERK	*Double-stranded RNA-activated protein kinase (PKR)-like ER kinase* (PKR-ähnliche ER Kinase)
PAC-1	*pituitary adenylate cyclase-activating polypeptide 1* (pituitäres Adenylatzyklas-aktivierendes Polypeptid 1)
P-gp	P-Glykoprotein
PI3K	Phosphatidylinositol 3 Kinase
PK A	Proteinkinase A
PP2A	Proteinphosphatase 2A
QAlb	Albumin-Quotient

RAGE	*receptor for advanced glycation end products* (Rezeptor für Glykationsendprodukte)
RB-1	Retinoblastoma Protein-1
ROS	*Reactive oxygen species* (Reaktive Sauerstoffspezies)
RT-PCR	*Reverse transcriptase-polymerase chain reaction* (Reverse Transkriptase-Polymerasekettenreaktion)
RXR	Retinoid-X-Rezeptor
siRNA	*Small interfering RNA* (Kleine Interferenz RNA)
SH-SY5Y	Humane Neurobastomzellen
TACE	*Tumor necrosis factor alpha converting enzyme* (Tumor Nekrose Faktor alpha konvertierendes Enzym)
Tbx2	*T box 2* (T Box 2)
TEER	*Trans endothelial electrical resistance* (Transendotheliale elektrische Resistenz)
TF	Transkriptionsfaktor
UPR	*Unfolded protein response* (Stressantwort auf ungefaltete Proteine)
UTR	*Untranslated region* (Untranslatierte Region)
ZNS	zentrales Nervensystem

II. Abbildungsverzeichnis

III. Zusammenfassung

Ein charakteristisches, neuropathologisches Merkmal der Alzheimer-Demenz (AD), der am häufigsten vorkommenden Demenz-Form des Menschen, ist das Auftreten von senilen Plaques im Gehirn der Patienten. Hierbei stellt das neurotoxische A-beta Peptid den Hauptbestandteil dieser Ablagerungen dar. Einen Beitrag zu der pathologisch erhöhten A-beta Generierung liefert das verschobene Expressions-gleichgewicht der um APP-konkurrierenden Proteasen BACE-1 und ADAM10 zu Gunsten der beta-Sekretase BACE-1. In der vorliegenden Dissertation sollten molekulare Mechanismen identifiziert werden, die zu einem pathologisch veränderten Gleichgewicht der APP-Spaltung und somit zum Entstehen und Fortschritt der AD beitragen. Des Weiteren sollten Substanzen identifiziert werden, die durch Beeinflussung der Genexpression einer der beiden Proteasen das physiologische Gleichgewicht der APP-Prozessierung wiederherstellen können und somit therapeutisch einsetzbar sind.

Anhand eines „*Screenings*“ von 704 Transkriptionsfaktoren wurden 23 Faktoren erhalten die das Verhältnis ADAM10- pro BACE-1-Promotor Aktivität beeinflussten. Exemplarisch wurden zwei der molekularen Faktoren auf ihren Wirkmechanismus untersucht: Der TF „*X box binding protein-1*“ (XBP-1), der die so genannte „*unfolded protein response*“ (UPR) reguliert, erhöhte die Expression von ADAM10 in Zellkultur-Experimenten. Die Menge dieses Faktors war in AD-Patienten im Vergleich zu gesunden, Alters-korrelierten Kontrollen signifikant erniedrigt. Im Gegensatz dazu verminderte der Seneszenz-assoziierte TF „*T box 2*“ (Tbx2) die Menge an ADAM10 in SH-SY5Y Zellen. Die Expression des Faktors selbst war in post-mortem Kortexgewebe von AD-Patienten erhöht. Zusätzlich zu den TFs konnten in einer Kooperation mit dem Helmholtz Zentrum München drei microRNAs (miRNA 103, 107, 1306) bioinformatisch prädiziert und experimentell validiert werden, die die Expression des humanen ADAM10 reduzierten.

Im Rahmen dieser Arbeit konnten damit körpereigene Faktoren identifiziert werden, die die Menge an ADAM10 regulieren und folglich potenziell an der Entstehung der gestörten Homöostase der APP-Prozessierung beteiligt sind. Somit ist die AD auch im Hinblick auf eine A-beta-vermittelte Pathologie als multifaktorielle Krankheit zu verstehen, in der verschiedene Regulatoren zur gestörten APP-Prozessierung und somit zur pathologisch gesteigerten A-beta Generierung beitragen können.

Eine pharmakologische Erhöhung der ADAM10 Genexpression würde zu der Freisetzung von neuroprotektivem APPs-alpha und gleichzeitig zu einer reduzierten A-beta Generierung führen. Deshalb war ein weiteres Ziel dieser Arbeit die Evaluierung von Substanzen mit therapeutischem Potenzial im Hinblick auf eine erhöhte ADAM10 Expression. Von 640 FDA-zugelassenen Medikamenten einer Substanz-Bibliothek wurden 23 Substanzen identifiziert, die die Menge an ADAM10 signifikant steigerten während die Expression von BACE-1 und APP unbeeinflusst blieb. In Zusammenarbeit mit dem Institut für Pathologie (Johannes Gutenberg Universität Mainz) wurde ein Zellkultur-basiertes Modell etabliert, um die Permeationsfähigkeit der potenziellen Kandidaten-Substanzen über die Blut-Hirn Schranke (BHS) zu untersuchen. Von den 23 Medikamenten konnten neun im Rahmen des etablierten Modells als BHS-gängig charakterisiert werden. Somit erfüllen diese verbleibenden Medikamente die grundlegenden Anforderungen an ein AD-Therapeutikum.

ADAM10 spaltet neben APP eine Vielzahl anderer Substrate mit unterschiedlichen Funktionen in der Zelle. Zum Beispiel reguliert das Zelladhäsionsmolekül Neuroligin-1 (NL-1), das von ADAM10 prozessiert wird, die synaptische Funktion exzitatorischer Neurone. Aus diesem Grund ist die Abschätzung potenzieller, Therapie-bedingter Nebenwirkungen sehr wichtig. Im Rahmen eines Forschungsaufenthalts an der Universität von Tokio konnte in primären, kortikalen Neuronen der Ratte bei einer Retinoid-induzierten Erhöhung von ADAM10 neben einer vermehrten alpha-sekretorischen APP-Prozessierung auch eine gesteigerte Spaltung von NL-1 beobachtet werden. Dies lässt vermuten, dass bei einer Behandlung mit dem Retinoid Acitretin neben einer vermehrten APP-Spaltung durch ADAM10 auch die Regulation glutamaterger Neurone durch die Spaltung von NL-1 betroffen ist. Anhand eines geeigneten Alzheimer-Tiermodells sollten diese Befunde weiter analysiert werden, um so auf einen sicheren therapeutischen Ansatz bezüglich einer vermehrten ADAM10 Genexpression schließen zu können.

IV. Englischsprachige Zusammenfassung (Abstract)

A characteristic, neuropathological hallmark of Alzheimer's disease (AD), the most common form of dementia in humans, is the appearance of senile plaques in the brain of patients. The neurotoxic A-beta peptide, which is pathologically increased due to the disturbed homeostasis of APP-processing pathways, is the main component of these deposits. A shifted expression-balance of two proteases (BACE-1 and ADAM10) competing for their substrate APP in favor of BACE-1 contributes to the disturbed proteolytical balance. The aim of this thesis was to identify molecular mechanisms that contribute to pathological changes in APP-cleavage and thus to the development and progression of the disease. Furthermore, substances were identified, which might be able to restore the physiological balance of APP-processing by influencing the gene expression of one of the two proteases (ADAM10 and BACE-1).

Regarding the molecular factors, two transcription factors (TFs), identified from a high-throughput method of 704 human TFs, were examined for their distinct mechanism of action: the TF X-box binding protein-1 (XBP-1), which regulates the so called unfolded protein response (UPR), increased the expression of ADAM10 in cell culture experiments. However, the amount of this factor in AD-patients compared to healthy, age-matched controls was significantly decreased. In contrast, the senescence-associated TF T-box 2 (Tbx2) reduced the amount of ADAM10 in SH-SY5Y cells. The expression of this factor was increased in post-mortem cortical tissue samples of AD-patients. In addition to these TFs, three microRNAs (miRNA 107, 103, 1306) were bioinformatically predicted and experimentally validated regarding their potential to reduce the expression of human ADAM10 in a cooperation with the Helmholtz Centre Munich.

In sum, endogenous molecules were identified that regulate ADAM10 expression and consequently might be responsible for the disturbed homeostasis of APP-processing. Thus, AD in regard to A-beta-mediated pathology might be understood as a multifactorial disease, in which an interplay of different molecules can contribute to the disturbed APP-processing and thus to pathologically increased A-beta generation.

A pharmacological increase of ADAM10 gene expression would lead to the release of neuroprotective APPs-alpha and moreover to a reduced A-beta generation. Therefore, another objective of this work was the evaluation of substances with

therapeutic potential regarding an increased ADAM10 gene expression. Out of 640 FDA-approved drugs of a substance library, 23 compounds were identified that significantly increased the amount of ADAM10 while the expression of APP and BACE -1 were not affected. In collaboration with the Institute of Pathology (Johannes Gutenberg University Mainz), a cell culture-based model was established to investigate the permeability of the potential candidate-substances across the blood-brain barrier (BBB). Nine of the 23 candidate-substances were characterized with the established model as being BBB-permeable. Thus, these nine remaining drugs meet the basic requirements of an AD-therapeutic. However, ADAM10 cleaves many other substrates with different physiological roles in the cell besides APP. For example, the cell adhesion molecule neuroligin-1 (NL-1), that regulates the synaptic function of excitatory neurons, is shed by ADAM10. Therefore, the assessment of potential, therapy-related side effects is very important. As part of a research stay at the University of Tokyo, the expression of ADAM10 in rat primary cortical neurons was induced by synthetic retinoids such as acitretin. Under these conditions, in addition to an increased alpha-secretory APP-processing, an enhanced cleavage of NL-1 was observed. These results suggest that besides an enhanced APP cleavage by ADAM10 also the regulation of glutamatergic neurons via shedding of NL-1 might be affected. Investigations in an appropriate AD-animal model will provide further data to establish a safe therapeutic application regarding an increased expression of ADAM10.

1. Einleitung

1.1 Neurodegenerative Erkrankungen

Aufgrund des demographischen Wandels erreichen immer mehr Menschen ein höheres Lebensalter. Dies geht mit einem erhöhten Risiko eine neurodegenerative Erkrankung zu entwickeln einher. Schätzungsweise 36 Millionen Menschen leiden heutzutage an einer Demenz (*The Global Impact of Dementia* 2013–2050, Alzheimer's Disease International (ADI) 2013). Die Anzahl an Demenz-Erkrankten wird Schätzungen zufolge auf 115 Millionen im Jahre 2050 ansteigen. Ein gemeinsames Merkmal aller Demenzerkrankungen ist ein fortschreitender Verlauf, der in allen Fällen zum Verlust von Nervenzellen des Gehirns führt. Klinische Symptome manifestieren sich hierbei durch Gedächtnisverlust, Veränderung des Wesens sowie Verlust der Sprachfähigkeit und des Urteilsvermögens. Der Verlauf einer Demenz geht hin bis zur völligen Pflegebedürftigkeit des Betroffenen. Somit ist die Aufdeckung molekularer Ursachen sowie therapeutischer Ansatzmöglichkeiten aktuell von großem Interesse.

1.1.1 Die Alzheimer-Demenz

Mit circa 70% ist die am häufigsten auftretende Form einer Demenz die Alzheimer-Krankheit („*Alzheimer's disease*", AD) (*The Global Impact of Dementia* 2013–2050, Alzheimer's Disease International (ADI) 2013). Der deutsche Neurologe Alois Alzheimer beschrieb die klinischen Merkmale bereits im Jahr 1907 (Alzheimer *et al.*, 1907). Trotz der ausgeprägten pathologischen Kennzeichen im Gehirn der betroffenen Patienten, bleiben die genauen Ursachen der AD weitestgehend unverstanden (Karantzoulis und Galvin, 2011).

1.1.2 Grundlagen der Alzheimer-Pathogenese

Alois Alzheimer beschrieb bereits im Jahre 1907 histopathologische Auffälligkeiten im Gehirn einer Patientin (Alzheimer *et al.*, 1907). Hierbei war die Pathologie geprägt von intrazellulär auftretenden neurofibrillären Bündeln, die aus dem Protein Tau bestehen, sowie extrazellulär vorkommenden Ablagerungen in der Hirnrinde - den senilen Plaques. Diese bestehen hauptsächlich aus den so genannten A-beta Peptiden (Glenner und Wong, 1984; Kapitel 1.1.3). Neuere Befunde weisen allerdings auf ein viel komplexeres Krankheitsbild hin, in dem verschiedene Faktoren

im Zusammenspiel zur Entstehung der Krankheit beitragen könnten. Nachfolgend werden einige in der Forschung diskutierte Ansätze erläutert:

1.1.2.1 Entzündliche Prozesse

Eine wichtige Rolle in neurodegenerativen Prozessen spielt die Entzündungsreaktion im Gehirn der Patienten (Übersicht in Halliday *et al.*, 2000). Es konnten aktivierte Mikrogliazellen nachgewiesen werden, die an den Plaque Ablagerungen assoziiert sind. Hierbei unterscheidet sich der aktivierte Phänotyp dieser Immunzellen durch die erweiterte Ausbildung von Ausläufern, die die A-beta enthaltenen Ablagerungen zu einem großen Teil bedecken (Bolmont *et al.*, 2008; Bornemann *et al.*, 2001). Dies führt zu einer vermehrten Sekretion an entzündungsfördernden Stoffen wie Zytokinen, Chemokinen und Proteasen, die vor allem bei chronischem Verlauf zum Fortschritt neurodegenerativer Prozesse beitragen können (Akiyama *et al.*, 2000). Zum Beispiel konnte eine erhöhte Zytokin-Sekretion in A-beta positiven Neuronen von humanem APP-transgenen Ratten beobachtet werden (Hanzel *et al.*, 2014). Des Weiteren führen Plaque Ablagerung zur Sekretion der Vorläufer-Form des entzündungsfördernden Zytokins Interleukin 1-beta (IL1-bata) (Prinz *et al.*, 2011). Das Inflammasom, ein zytosolischer Proteinkomplex der Immunantwort, führt dadurch zur Aktivierung der Caspase 1 (Heneka *et al.*, 2013; Qazi *et al.*, 2013). Die Caspase 1-vermittelte Spaltung von IL1-beta führt zur Generierung der aktiven Form des Zytokins und trägt somit zu einem entzündlichen Milieu im Bereich der Plaque Ablagerungen bei (Fukumoto *et al.*, 2013; Kolliputi *et al.*, 2012; Kolliputi *et al.*, 2010). Allerdings werden der Mikroglia-induzierten Immunantwort auch positive Eigenschaften in der AD-Pathogenese zugesprochen. Aktivierte Mikroglia entfernen Zelltrümmer abgestorbener Zellen und verringern die Freisetzung toxischer Produkte und dadurch den programmierten Zelltod (Elkabes *et al.*, 1996). Darüber hinaus spielen diese Immunzellen eine wichtige Rolle bei der Phagozytose und beim Abbau von A-beta Peptiden (Paresce *et al.*, 1997). In Studien konnte gezeigt werden, dass frühe dementielle Veränderungen im Gehirn mit einer Astrozytenatrophie einhergehen. Dies äußert sich durch eine verminderte synaptische Plastizität und dem Absterben von Neuronen (Verkhratsky *et al.*, 2010). Des Weiteren sezernieren aktivierte Astrozyten wichtige Wachstumsfaktoren, die das Überleben von Neuronen propagieren können (Verkhratsky *et al.*, 2010).

1.1.2.2 Die Rolle der Blut-Hirn Schranke

Ein weiterer Ansatz zur Erklärung der AD-Pathogenese ist die zerebrovaskuläre Dysfunktion. Die damit verbundene strukturell bedingte Funktionsänderungen der Blutgefäße des Gehirns führen unter anderem zu einer beeinträchtigten Funktion der Blut-Hirn Schranke (BHS) und reduzieren somit die Kapazität des Gehirns, um auf äußere Einflüsse durch bestimmte Reparaturmechanismen reagieren zu können (Sun *et al.*, 2006; Sutton *et al.*, 1997; Thomas *et al.*, 1996). Jedoch weist die Literatur eine gewisse Heterogenität in Bezug auf endotheliale Dysfunktion in der AD-Pathogenese auf. In einer Übersichtsarbeit wurden insgesamt 15 klinische Studien verglichen (Kelleher und Soiza, 2013). Zehn Untersuchungen konnten beim Vergleich von AD-Patienten mit gesunden Kontrollen eine Beeinträchtigung der BHS sowie Endotheldysfunktion zeigen, wohingegen fünf Analysen ohne signifikante Unterschiede blieben. Zum Beispiel konnten durch Messung des Albumin-Quotienten (QAlb), der ein Indikator für die Funktion der BHS ist, keine signifikanten Unterschiede zwischen verschiedenen Apolipoprotein E (ApoE)-Genotypträgern erhalten werden (Karch *et al.*, 2013), wobei das ApoE4 Allel der maßgeblichste genetische Risikofaktor für die AD ist (Corder *et al.*, 1993). Im Gegensatz dazu zeigte eine mikrovaskuläre Verletzung im Gehirn eine Korrelation mit dem Fortschreiten der Krankheitspathologie gemessen in Form von Braak Stadien (Zipser *et al.*, 2007). Somit könnte ein Teil des im Blut zirkulierenden A-betas in einem gewissen Ausmaß durch eine beeinträchtigte BHS in das Gehirn gelangen (Stewart *et al.*, 1992). Jedoch wurde auch ein aktiver Rezeptor-vermittelter Transport von A-beta über die BHS beschrieben (Monro *et al.*, 2002; Poduslo *et al.*, 1999). Zwei der beteiligten Rezeptoren wurden genauer charakterisiert: Der Rezeptor für Glykationsendprodukte („*receptor for advanced glycation end products*“, RAGE) transportiert A-beta über die BHS in das Gehirn. Dies sorgt dort für dessen vermehrtes Auftreten und Akkumulierung (Deane *et al.*, 2003). Das „*low-density lipoprotein receptor-related protein-1*” (LRP-1) transportiert A-beta aus dem Gehirn in das Blut (Shibata *et al.*, 2000). Untersuchungen von hippokampalen Gewebeproben von AD-Patienten zeigten eine starke Immunreaktivität von RAGE in mikrovaskulären Strukturen, wohingegen die Expression von LRP-1 in denselben Proben reduziert vorlag (Donahue *et al.*, 2006). Dies deutet darauf hin, dass unter pathologischen Bedingungen ein vermehrter Transport von A-beta in das Gehirn stattfindet. Darüber hinaus wurde für RAGE eine Ektodomänen-Spaltung beschrieben, die durch

Metalloproteasen vermittelt und durch G-Protein gekoppelten Rezeptoren wie zum Beispiel dem PAC1 Rezeptor („*pituitary adenylate cyclase-activating polypeptide 1 receptor*“) reguliert wird (Metz *et al.*, 2012; Raucci *et al.*, 2008; Zhang *et al.*, 2008). Die Injektion des löslichen Spaltprodukts von RAGE in das Gehirn eines AD-Mausmodells führt zu reduzierten Mengen an A-beta Peptiden sowie Plaque Ablagerungen (Cho *et al.*, 2009). Für LRP-1 konnte ebenfalls eine Beteiligung an der AD-Pathogenese aufgezeigt werden: ein Polymorphismus innerhalb des Exon 3 des LRP-1 Gens (C766T), der mit einem späteren Krankheitsentstehen assoziiert war, war in AD-Patienten unterrepräsentiert (Kang *et al.*, 1997). Des Weiteren konnte gezeigt werden, dass LRP-1 an der Beseitigung der A-beta Peptide aus dem Gehirn beteiligt ist und eine reduzierte LRP-1 Expression mit vermehrten Plaque Ablagerungen in post-mortem Kortexgewebe von AD-Patienten korreliert (Kang *et al.*, 2000).

1.1.2.3 Zelluläre Stressantworten

Eine Ursache der zuvor diskutierten zerebrovaskulären Dysfunktion liegt vermutlich am verstärkten Auftreten von oxidativem Stress in Form von reaktiven Sauerstoffspezies (ROS) (Faraci, 2006; Simpson *et al.*, 2010). Diese Moleküle haben ungepaarte Elektronen in ihrem äußeren Orbital und sind daher sehr reaktionsfreudig. Somit sind ROS die Ursache für Schäden in den Zellorganellen und beeinträchtigen folglich die zelluläre Funktion. Diese spezifische Form von Stress steht auch im Fokus vieler Forschungsberichte in Bezug auf die Entstehung der AD (Übersicht in Smith *et al.*, 2000). Hierbei überwiegt das Auftreten von freien Radikalen die endogene Abwehrfähigkeit der Zelle durch Antioxidantien. Vor allem sind bei oxidativem Stress Neuronenpopulationen derjenigen Hirnareale betroffen, bei denen es im Laufe einer AD zum vermehrten Absterben von Nervenzellen kommt (Smith *et al.*, 1994). Die zu Grunde liegenden Mechanismen, die letzten Endes zur Pathogenese der AD beitragen, bleiben bisher unverstanden. Diskutiert werden zum Beispiel mitochondriale Dysfunktion, Übergangsmetall-Ablagerungen oder auch genetische Faktoren wie zum Beispiel ApoE (Smith *et al.*, 2000). Zum Beispiel ist ApoE4 sehr stark mit dem Auftreten des Lipid-Peroxidationsprodukts HNE (4-Hydroxy-2-Nonenal) im Gehirngewebe von AD-Patienten korreliert (Montine *et al.*, 1996) und ist ebenso ein Chelator für redoxaktive Übergangsmetalle (Miyata und Smith, 1996). Das vermehrte Vorkommen von Eisen geht stark mit dem Auftreten

von neurofibrillären Bündeln (Good *et al.*, 1992) und senilen Plaque Ablagerungen einher (Smith *et al.*, 1997). Hierbei setzt Eisen Radikale frei, indem es die Oxidation von Wasserstoffperoxid katalysiert. Immunhistochemische Untersuchungen von hippokampalen Gewebeschnitten von AD-Patienten zeigen eine reduzierte Redoxaktivität in Hirnläsionen bei entsprechender Vorinkubation mit Eisen-Chelatoren (Sayre *et al.*, 2000). Die Analyse der zu Grunde liegenden Mechanismen, die die genaue Beziehung zwischen oxidativem Stress und der AD aufzeigen, würde zu neuen therapeutischen Ansätzen wie zum Beispiel dem Einsatz von Chelatoren oder Antioxidantien führen. Letztere wurden durch den Einsatz von Vitamin E in Form von alpha-Tocopherol, die Hauptkomponente der Vitamin E Klasse, bereits in klinischen Studien mit AD-Patienten untersucht. Jedoch ist die aktuelle Datenlage diesbezüglich nicht eindeutig: In einer aktuellen Arbeit waren die Gehirn-Spiegel von alpha-Tocopherol nicht mit dem Vorkommen von amyloiden Plaques sowie neurofibrillären Bündeln assoziiert (Morris *et al.*, 2014). Im Gegensatz dazu konnte im selben Jahr gezeigt werden, dass bei Patienten mit leichter bis mittelschwerer AD durch die Behandlung mit alpha-Tocopherol der kognitive Abfall verlangsamt wurde (Dysken *et al.*, 2014). Auch andere zelluläre Stressantworten wie zum Beispiel der so genannte Endoplasmatische Retikulum Stress (ER-Stress) konnten mit der AD-Pathogenese mechanistisch verknüpft werden (Bernales *et al.*, 2012). Die Zelle reagiert hierbei auf das Vorkommen ungefalteter Proteine und induziert durch drei parallel ablaufende Signalwege die Genexpression so genannter Faltungshelfer (Chaperone). Somit tragen diese Signalwege dazu bei, ein bestimmtes Maß an Stress zu bewältigen. Bei chronischer lang anhaltender Stressantwort wird jedoch der programmierte Zelltod (Apoptose) eingeleitet (Teske *et al.*, 2013). Die Summe dieser drei Signalwege nennt man „*unfolded protein response*“ (UPR). Die detaillierte Beteiligung eines der drei UPR-Signalwege an der AD-Pathogenese wird in Kapitel 3 (Ergebnisse und Diskussion) erläutert.

1.1.2.4 Insulin als zentrales Signalmolekül

Die wechselseitige Beeinflussung von Komponenten der ER-Stress Antwort mit anderen Signalmolekülen wie zum Beispiel Insulin (Park *et al.*, 2010; Winnay *et al.*, 2010) erschweren die genaue Analyse zellulärer Mechanismen der AD. So konnte in einigen Arbeiten eine gestörte, Insulin-abhängige Signalweiterleitung mit dem Entstehen der AD in Verbindung gebracht werden (Übersicht in Kojro und Postina,

2009). Bei einer chronischen Hyperinsulinämie werden die zerebralen Insulin Level durch eine Herunterregulation der Insulin-Rezeptoren (IR) reduziert (Cavalieri *et al.*, 2010; Craft, 2009). Darüber hinaus führt eine Hyperinsulinämie zu entzündungsfördernden Prozessen im Gehirn, die in einem vorherigen Abschnitt dieser Arbeit (Kapitel 1.1.2.1) bereits mit der Pathogenese der AD verknüpft werden konnten (Fishel *et al.*, 2005). Des Weiteren konnte auch eine gesteigerte Aktivität des „*Insulin-like growth factor-1*“ (IGF-1) mit einer höheren Krankheitshäufigkeit korreliert werden (de Bruijn *et al.*, 2014). Unter physiologischen Bedingungen verringert Insulin die Generierung von neurotoxischen A-beta Peptiden, den Hauptkomponenten der senilen Plaques, und induziert gleichzeitig deren Abbau. Der zu Grunde liegende Mechanismus ist die Bindung von Insulin an den entsprechenden Tyrosinkinase Rezeptor und die dadurch verbundene Aktivierung der Phosphatidylinositol 3 Kinase (PI3K) (Solano *et al.*, 2000). Darüber hinaus konnte gezeigt werden, dass eine intranasale Insulin-Applikation zu einer gesteigerten Gedächtnisleistung bei AD-Patienten führt (Reger *et al.*, 2008). Die Rezeptordichte der Insulinrezeptoren im Gehirn ist sehr hoch (Young *et al.*, 2006). Vor allem Regionen, die mit Gedächtnis- und Erinnerungs-Leistung in Verbindung gebracht werden, wie der Hippokampus und das limbische System, zeigen eine starke Rezeptor Expression (Young *et al.*, 2006). Durch diese aufgeführten Aspekte wird eine klare Korrelation zwischen Insulin, als zentralem Signalmolekül, und kognitiven Defiziten deutlich.

1.1.3 Neuropathologische Merkmale der Alzheimer-Demenz

Die AD manifestiert sich klinisch in dem Verlust von Nervenzellen im Gehirn und einem progressiven und graduellen Abfall der kognitiven Fähigkeiten. Neben den oben diskutierten Grundlagen der AD-Pathogenese, die zum Fortschritt der Krankheit beitragen können, stehen die zwei von Alois Alzheimer bereits beschriebenen pathologischen Auffälligkeiten bis heute im Blickpunkt vieler Forschungsarbeiten. Sowohl die A-beta enthaltenen Plaque Ablagerungen als auch die intraneuronalen fibrillären Bündel gelten als die maßgeblichen pathologischen Merkmale der AD, die in früheren Arbeiten als Ursache für die Entwicklung einer AD diskutiert wurden (Hardy und Higgins, 1992). Die Menge und die Verteilung der A-beta Ablagerungen in spezifischen Hirnregionen korrelieren jedoch oft nur schwach mit den klinischen Symptomen der Krankheit (Arriagada *et al.*, 1992). In einigen kognitiv unauffälligen Menschen konnte eine vergleichbare Menge sowie Topologie von A-beta Plaques

gefunden werden, die sich mit denen eines typischen AD-Patienten deckt (Aizenstein *et al.*, 2008). Ein möglicher Ansatz, um dieses Phänomen zu erklären, ist, dass A-beta relativ früh in der Entstehung der Krankheit eine Kaskade an zellulären Prozessen initiiert, die dann A-beta-unabhängig fortschreiten und zur Entwicklung der Pathogenese beitragen (Holtzman, 2008). Dies lässt Anlass zur Spekulation, dass A-beta neurodegenerative Prozesse auslöst, welche auch dann fortschreiten wenn A-beta therapeutisch reduziert wird, und könnte erklären, warum bislang A-beta-basierte Therapieansätze in der klinischen Prüfung fehlschlugen: Zum Beispiel konnte in einer Studie durch Immunisierung mit humanem A-beta zwar eine Reduzierung der Plaque Ablagerungen im Gehirn von Patienten erhalten werden (Holmes *et al.*, 2008). Jedoch blieb der Fortschritt des kognitiven Abbaus unbeeinflusst und mündete letztlich in einem Endstadium der AD, das klinisch nicht von unbehandelten AD-Patienten zu unterscheiden war. Demnach ist eine sehr frühe Behandlung notwendig, um erfolgreiche Therapieeffekte zu erzielen (Gauthier, 2005). Es konnte gezeigt werden, dass pathologische Veränderungen wie zum Beispiel die amyloid Ablagerungen bereits in präklinischen Phasen nachweisbar sind (Vos *et al.*, 2013). Probanden, die die entsprechenden Kriterien einer präklinischen AD aufwiesen, hatten ein erhöhtes Risiko eine AD zu entwickeln.

Die intrazellulären Bündel bestehen aus dem Protein Tau, welches unter physiologischen Bedingungen Tubulin stabilisiert und somit die Mikrotubuli-Polymerisation unterstützt (Avila *et al.*, 2004). Für dieses Protein konnten Änderungen der Konformation sowie verkürzte Formen in AD-Patienten nachgewiesen werden (Cotman *et al.*, 2005; Gamblin *et al.*, 2003; Jicha *et al.*, 1999a; Jicha *et al.*, 1997; Jicha *et al.*, 1999b; Novak *et al.*, 1991). Jedoch stellt die Phosphorylierung von Tau die maßgeblichste Modifikation dar, die zum Entstehen der intrazellulären Ablagerungen beiträgt (Grundke-Iqbal *et al.*, 1986). Die Hyperphosphorylierung des Tau Proteins führt zu einer fehlerhaften Assemblierung der Mikrotubuli sowie der Ablagerung von Tau in Form von fibrillären Strukturen in den Nervenzellen (Übersicht in Iqbal und Grundke-Iqbal, 2008; Iqbal *et al.*, 1986). Neben Proteinkinasen wie CDK5 („*cyclin dependent protein kinase 5*“), CK 1 („*casein kinase 1*“) und PK A („*protein kinase A*“) gilt die GSK 3-beta („*glycogen synthase kinase 3-beta*“) als maßgebliches Tau phosphorylierendes Enzym (Ishiguro *et al.*, 1993; Ishiguro *et al.*, 1992). Die Expression dieses Enzyms im Gehirn ist sehr hoch und die Expressionsstärke von GSK3-beta ist mit allen Stadien der Tau-induzierten

Pathologie korreliert (Pei *et al.*, 1999; Pei *et al.*, 1998). Zudem konnte gezeigt werden, dass auch Tau dephosphorylierende Enzyme wie zum Beispiel die Proteinphosphatase 2A (PP2A) im Gehirn von AD-Patienten reduziert sind (Liu *et al.*, 2005). Dies trägt ebenfalls zum hyperphosphorylierten Stadium des Proteins in der AD-Pathogenese bei. Das Vorkommen von hyperphosphoryliertem Tau konnte auch mit Prozessen wie zum Beispiel einer Reduzierung dendritischer Ausläufer oder der Änderung deren Morphologie in Verbindung gebracht werden (Messing *et al.*, 2013).
Die extrazellulär auftretenden Plaque Ablagerungen im Gehirn von AD-Patienten bestehen aus Amyloid-beta (A-beta) Peptiden, die Glenner und Wong bereits 1984 aus vaskulären Ablagerungen isolieren konnten (Glenner und Wong, 1984) und kurz darauf als Hauptkomponenten der Plaques beschrieben wurden (Masters *et al.*, 1985b). Diese Peptide weisen ein Molekulargewicht von 4 kDa auf und besitzen beta-Faltblattstruktur. Somit haben diese Fragmente ein erhöhtes Potenzial zur Oligomerisierung. Das neurotoxische A-beta Peptid wird aus dem Amyloid Vorläufer Protein (APP) proteolytisch freigesetzt (Kang *et al.*, 1987; Masters *et al.*, 1985a). Untersuchungen zur physiologischen Funktion von APP gestalten sich bis heute schwierig, da die entsprechenden zellulären Funktionen kompensatorisch von den APP-verwandten Proteinen APLP1 und APLP2 übernommen werden können (Herms *et al.*, 2004). Während APP „*Knock-Out*“ Mäuse lebensfähig sind, sterben die entsprechenden APP/APLP2 Doppel „*Knock-Out*“ Mäuse kurz nach der Geburt durch gestörte neuromuskuläre Übertragung sowie Fehlbildungen der zentralen Synapsen (Heber *et al.*, 2000; Herms *et al.*, 2004; Wang *et al.*, 2005). Die Expression von APPs-alpha, ein durch Proteolyse generiertes Fragment des APP, in APLP2-deffizienten Tieren verminderte die erhöhte Sterberate nach der Geburt im Vergleich zu APP/APLP2 Doppel „*Knock-Out*“ Mäusen (Weyer *et al.*, 2011). Diese Mäuse wiesen eine beeinträchtigte neuromuskuläre Signalübertragung sowie eine gestörte Aufrechterhaltung von Synapsen auf. Zudem wurde eine hippokampale Dysfunktion im Vergleich zu entsprechenden Kontrolltieren detektiert (Aydin *et al.*, 2011; Weyer *et al.*, 2011). Diese Befunde zeigen eine Beteiligung der APP Protein Familie an Prozessen wie synaptischer Plastizität und folglich Lern- und Gedächtnis-Leistung. Auch Mutationen innerhalb der APP-Sequenz konnten mit dem Entstehen der AD verknüpft werden (Bekris *et al.*, 2010): Zum Beispiel führt der Austausch eines Alanins zu Glycin innerhalb der APP kodierenden DNA-Sequenz (Kodon 692) zu einer erhöhten Generierung von toxischen A-beta Peptiden und somit zur so

genannten präsenilen AD, deren Beginn bereits in einem Lebensalter unter 60 Jahren beginnt (Hendriks *et al.*, 1992). Darüber hinaus führt eine Mutation (E693G) innerhalb der A-beta Sequenz des APP zu aggregationsfähigeren A-beta Peptiden, die dann zum vermehrten Auftreten von Plaque Ablagerungen führen (Nilsberth *et al.*, 2001). In einigen Arbeiten konnte gezeigt werden, dass A-beta Peptide synaptische Dysfunktion induzieren, die neuronale Konnektivität stören und mit dem Absterben von Neuronen in AD-spezifischen Hirnregionen korreliert sind (Cao *et al.*, 2012; Übersicht in Carter und Lippa, 2001; Parihar und Brewer, 2010). Neben der isolierten Betrachtung von A-beta und Tau als Krankheits-auslösend konnte ein mechanistisches Zusammenspiel zwischen beiden Spezies nachgewiesen werden: Die Injektion von löslichen Gehirnextrakten aus 6 Monate alten APP transgenen Mäusen, in denen A-beta Ablagerungen nachgewiesen wurden, in junge Tau transgene Mäuse, zeigte eine verstärkte Tau Pathologie im Hippokampus nach 6 Monaten im Vergleich zu Kontroll-Tieren, denen Gehirnextrakte von gealterten nicht-transgenen Mäusen oder gealterten Tau transgenen Mäusen injiziert wurden (Bolmont *et al.*, 2007). Des Weiteren induzierten A-beta Oligomere, die aus kortikalem Gewebe von AD-Patienten isoliert wurden, die Hyperphosphorylierung von Tau und folglich das Absterben von neuronalen Zellen (De Felice *et al.*, 2008; Jin *et al.*, 2011). Somit sind A-beta Spezies in der Lage pathologische Prozesse der AD zu initiieren. Eine entscheidende Rolle des APP in der AD-Pathogenese konnte ebenfalls mit der Identifizierung einer protektiven APP-Mutation aufgezeigt werden (Jonsson *et al.*, 2012). Die Mutation (A673T) innerhalb des APP Gens schützt vor dem Alters-bedingten kognitiven Abfall bzw. der Entwicklung einer AD (Jonsson *et al.*, 2012). Hierbei ergaben Untersuchungen von Genom-weiten Sequenzanalysen, dass diese Mutation an eine A-beta-generierende Spaltstelle des APP angrenzt und folglich zu einer Reduktion der A-beta Peptide um 40% führt.
Im nachfolgenden Abschnitt wird nun das Entstehen der A-beta Peptide auf zellbiologischer Ebene erläutert.

1.1.3.1 Die proteolytische Prozessierung des Amyloid Vorläufer Proteins (APP)

A-beta Peptide stellen mit etwa 90% den Hauptanteil der AD-charakteristischen Plaque Ablagerungen dar (Selkoe, 1994). Des Weiteren konnte das Vorkommen von Fragmenten APP verwandter Proteine wie APLP1 (Bayer *et al.*, 1997) und APLP2 (Crain *et al.*, 1996) sowie das Prion Protein (Ferrer *et al.*, 2001) nachgewiesen

werden. Die neurotoxischen A-beta Peptide, die maßgeblich an der Entstehung der AD beteiligt sind, werden proteolytisch aus dem Amyloid Vorläufer Protein (APP) freigesetzt (Kang *et al.*, 1987; Masters *et al.*, 1985a). Das APP-Gen ist auf dem Chromosom 21 lokalisiert (Korenberg *et al.*, 1989). Eine Trisomie dieses Chromosoms führt zum Entstehen des Down Syndroms (Antonarakis *et al.*, 2004), das einen neuropathologischen Phänotyp vergleichbar mit dem der AD zeigt (Mann *et al.*, 1990; Masters *et al.*, 1985b). Hierbei ist das Auftreten von A-beta Ablagerungen gefolgt von einer AD-ähnlichen Neurodegeneration, die in den meisten Fällen zur beeinträchtigten kognitiver Funktion führt. APP ist evolutionär hochkonserviert (Slunt *et al.*, 1994) und ein Typ I Transmembranprotein. Charakteristisch hierbei ist eine große extrazelluläre Domäne, eine Transmembrandomäne sowie eine relativ kurze zytoplasmatische Domäne (Kitaguchi *et al.*, 1988; Tanzi *et al.*, 1988). Es werden verschiedene Isoformen des Proteins exprimiert, wobei die Isoform APP695 hauptsächlich in Neuronen vorkommt. Zwei weitere Hauptformen des APP, APP751 und 770, werden in peripherem Gewebe exprimiert (Sandbrink *et al.*, 1994). Innerhalb des konstitutiv sekretorischen Weges wird das entstehende Protein N- und O-glykosyliert (Weidemann *et al.*, 1989) sowie phosphoryliert (Hung und Selkoe, 1994; Suzuki *et al.*, 1997). Das reife Protein gelangt dann durch vesikulären Transport über den Golgi-Apparat an die Plasmamembran der Zelle. Auf diesem Weg kann das APP durch verschiedene Enzyme proteolytisch gespalten werden. Grundsätzlich unterscheidet man die Spaltung des reifen Proteins durch zwei Wege: 1) den amyloidogenen Weg und 2) den nicht amyloidogenen Weg (Abb. 1).

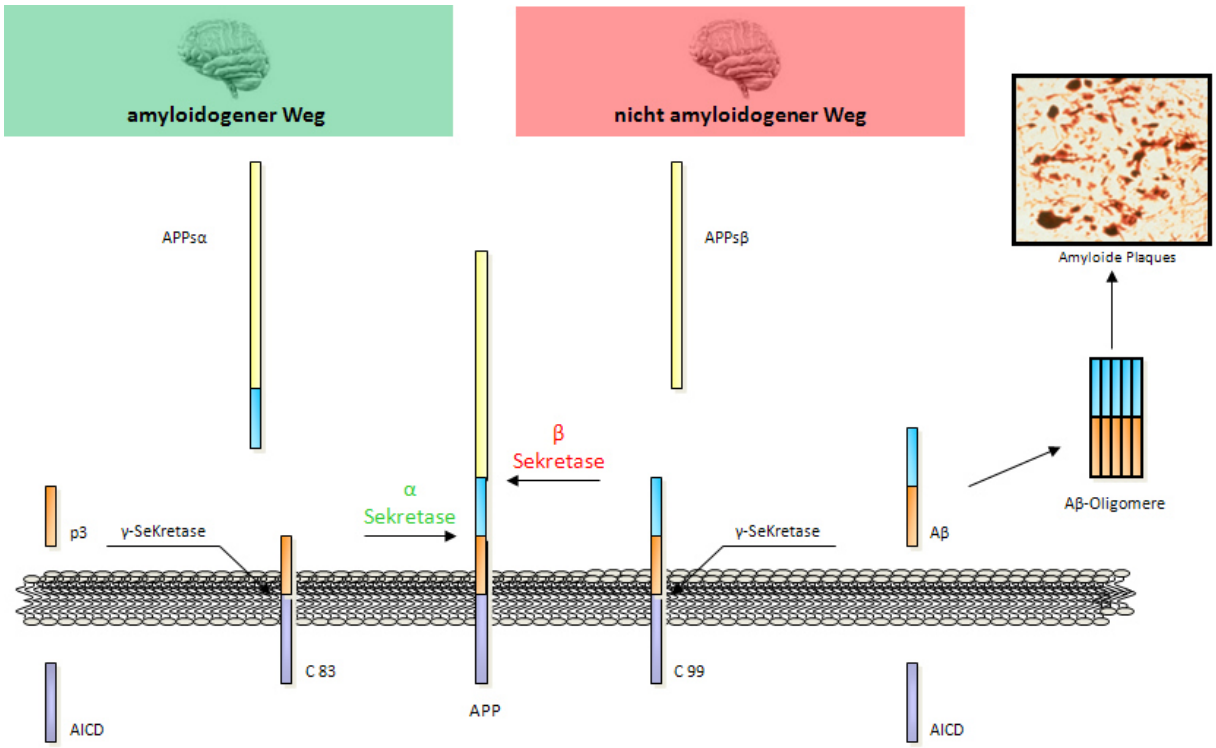

Abbildung 1: Proteolytische Prozessierung des Amyloid Vorläufer Proteins (APP): Initial wird das APP durch die alpha-oder beta-Sekretase gespalten. Dies führt zum Freisetzen löslicher Fragmente (APPs-alpha oder -beta). Das resultierende Membran-gebundene C-terminale Fragment (C83 oder C99) wird in beiden Fällen vom gamma-Sekretase Komplex in der Transmembran-Region gespalten. Erfolgt zunächst der beta-Sekretase Schnitt werden A-beta Peptide zusammen mit der APP intrazellulären Domäne (AICD) freigesetzt. Bei vorangehender alpha-Sekretase Spaltung entstehen die Fragmente p3 und AICD. (Abbildung der Plaques von: National Institute on Aging)

1) Entlang des amyloidogenen Prozessierungswegs wird das APP initial durch die beta-Sekretase BACE-1 („*beta site APP cleaving enzyme-1*“) in der Ektodomänensequenz gespalten. Hieraus resultieren zum einen das lösliche Fragment APPs-beta und zum anderen das Membran-gebundene C-terminale Fragment C99 (Hussain *et al.*, 1999; Sinha *et al.*, 1999; Vassar *et al.*, 1999). Dieses Spaltprodukt wird vom gamma-Sekretase Komplex innerhalb der Transmembran-domäne gespalten (Simmons *et al.*, 1994; Yankner *et al.*, 1989). Dies führt hauptsächlich zur Freisetzung von 40 bzw. 42 Aminosäure großen A-beta Peptiden. Vor allem die größere Variante weist neurotoxischen Charakter auf und ist wie im vorherigen Abschnitt (Kapitel 1.1.3) beschrieben an der Entstehung neurodegenerativer Prozesse im Gehirn beteiligt.

2) Der zweite Weg der APP-Proteolyse (nicht amyloidogener Weg) wird durch die Spaltung des APP durch die alpha-Sekretase initiiert. Entscheidend hierbei ist, dass der Schnitt innerhalb der A-beta Sequenz stattfindet (Abbildung 1). Das daraus

resultierende lösliche Fragment APPs-alpha weist neuroprotektive und neurotrophe Eigenschaften auf (zum Beispiel Corrigan *et al.*, 2011; Thornton *et al.*, 2006). APPs-alpha ist ein Modulator der synaptischen Plastizität, die vor allem eine entscheidende Rolle bei Lern- und Gedächtnisvorgängen im Gehirn spielt (Ishida *et al.*, 1997). Das C-terminale Fragment von 83 Aminosäuren Länge (C83) wird ebenfalls vom gamma-Sekretase Komplex gespalten. Diese Spaltung führt zur Freisetzung eines so genannten p3-Peptids, welches im Gegensatz zu A-beta keine neurotoxischen Eigenschaften aufweist und nicht in den Plaque Ablagerungen vorkommt (Lichtenthaler und Haass, 2004). Die bereits erwähnte intrazelluläre Domäne des APP (AICD), die in beiden Proteolyse-Wegen entsteht, fungiert vermutlich als klassischer Transkriptionsfaktor, indem es in den Zellkern transloziert und transkriptionell aktiv ist (Cao und Südhof, 2004; Hebert *et al.*, 2006; Roncarati *et al.*, 2002).

Als potenzielle alpha-Sekretasen konnten bereits ADAM10 und ADAM17 (TACE: „*tumor necrosis factor alpha converting enzyme*“) identifiziert werden (ADAM: „*a disintegrin and metalloproteinase*“) (Buxbaum *et al.*, 1998; Lammich *et al.*, 1999; Slack *et al.*, 2001). Beide Enzyme weisen ein typisches Zink-Bindemotiv auf und haben die gleiche Domänen-Struktur (Übersicht in Endres und Fahrenholz, 2010). Die Spaltung des APP erfolgt zum einen konstitutiv durch ADAM10 oder zum anderen durch einem Aktivitäts-abhängigen Mechanismus, der durch die Proteinkinase C regulierbar ist und durch beide ADAM Proteasen katalysiert werden kann (Buxbaum *et al.*, 1993; le Blanc *et al.*, 1998). *In vitro* konnte gezeigt werden, dass ADAM10 APP an der physiologischen Spaltstelle zwischen K16 und L17 innerhalb der A-beta Sequenz spaltet (Lammich *et al.*, 1999). In der gleichen Studie führte eine Überexpression von ADAM10 in HEK293 Zellen zu einer erhöhten Sekretion an APPs-alpha in den Zellkultur-Überstand. Zudem zeigte die Überexpression einer dominant negativen Mutante des Enzyms eine signifikante Erniedrigung der APPs-alpha Sekretion. Die physiologische Relevanz der APP-Spaltung durch ADAM10 konnte in verschiedenen Studien belegt werden: In primären kortikalen Neuronenkulturen der Maus blieb die Spaltung des APP durch alpha-Sekretase Aktivität bei einem siRNA vermittelten „*Knock-Down*“ von ADAM10 - nicht aber von ADAM17 - aus (Kuhn *et al.*, 2010). Mäuse mit konditionellem ADAM10 „*Knock-Out*“ zeigten eine drastisch reduzierte alpha-Sekretase Aktivität (Jorissen *et al.*, 2010). Des Weiteren zeigten APP (V717I) transgene Mäuse bei gleichzeitiger

Überexpression von ADAM10 eine erhöhte Menge an sekretiertem APPs-alpha und eine verminderte Menge an Plaque Ablagerungen im Gehirn *in vivo* (Postina *et al.*, 2004). Jedoch scheint es für die alpha-Sekretase-vermittelte Spaltung von APP kompensatorische Mechanismen zu geben. Fibroblasten von ADAM10 „*Knock-Out*" Mäusen waren immer noch in der Lage APP proteolytisch zu spalten (Hartmann *et al.*, 2002). Einige Studien belegen, dass auch ADAM17 APP Aktivitäts-abhängig spalten kann. Im Zellkulturmodell führte die Überexpression der Protease zu einer vermehrten APPs-alpha Sekretion (Endres *et al.*, 2005; Slack *et al.*, 2001). In TACE „*Knock-Out*" Mäusen war die Sekretion an APPs-alpha bei gleichzeitiger Aktivierung der Proteinkinase C gestört (Buxbaum *et al.*, 1998).
Unter den dargestellten Gesichtspunkten nahm man an, dass die Generierung von A-beta Peptiden ausschließlich als pathologischer Prozess zu sehen ist. Jedoch laufen beide Prozessierungswege des APP initiiert durch ADAM10 bzw. BACE-1 unter physiologischen Bedingungen in einer Balance ab. So konnten A-beta Peptide unter nicht-pathologischen Bedingungen zum Beispiel in konditioniertem Medium von primären Neuronenkulturen der Ratte detektiert werden (Busciglio *et al.*, 1993). Zudem wurde auch das Vorkommen von A-beta Peptiden in der Cerebrospinalflüssigkeit (CSF) von gesunden Menschen beschrieben (Seubert *et al.*, 1993; Shoji *et al.*, 1992).

1.1.3.2 Die Homöostase der APP-Prozessierung

Einen pathologisches Level an A-beta Peptiden kann durch verschiedene Mechanismen erklärt werden: Eine beeinträchtigte Beseitigung („Clearance") der A-beta Peptide kann durch zwei Wege stattfinden: proteolytischer Abbau und Rezeptor-vermittelter Transport aus dem Gehirn (Tanzi *et al.*, 2004). In einem vorherigen Abschnitt dieser Arbeit (Kapitel 1.1.2.2) konnte bereits die Rolle von LRP-1 als Effluxtransporter von A-beta aus dem Gehirn dargelegt werden (Übersicht in Zlokovic, 2004). Auch ein gestörter proteolytischer Abbau von A-beta durch zum Beispiel dem „*insulin degrading enzyme*" (IDE) kann zu einem gesteigerten Vorkommen dieser Peptide führen (Übersicht in Selkoe, 2001). Des Weiteren kann das vermehrte Auftreten an A-beta durch eine gesteigerte Produktion erklärt werden. Dieser liegt eine gestörte Homöostase der APP-Prozessierung zu Grunde. Die Menge bzw. Aktivität der alpha- bzw. beta-Sekretase hat einen entscheidenden Einfluss auf die Entstehung von APP-Proteolyseprodukten wie den A-beta Peptiden.

Allerdings sind beide Spaltereignisse nicht unbedingt voneinander abhängig: In primären kortikalen Neuronen der Maus konnte gezeigt werden, dass bei genetischer sowie pharmakologischer Inhibierung der beta-Sekretase BACE-1 APP vermehrt durch ADAM10 gespalten wurde (Colombo *et al.*, 2012). Im Gegensatz dazu führte eine Reduktion an ADAM10 nicht zu einer gesteigerten beta-Sekretase Spaltung im gleichen Modell. Zudem wurde beschrieben, dass in Zellkulturexperimenten APP zum größten Teil von alpha-Sekretase Aktivität gespalten wird (Simons *et al.*, 1996). In kultivierten Neuronen überwiegt jedoch die Spaltung durch BACE-1 (Colombo *et al.*, 2012). Somit kann man unter physiologischen Bedingungen im Gehirn nicht auf eine ausgewogene Spaltung des APP schließen. Jedoch kann eine veränderte Genexpression ein Ungleichgewicht der beiden um APP konkurrierenden Proteasen ADAM10 und BACE-1 hervorrufen und zu einem pathologischen Anstieg von A-beta Peptiden und somit zur Entstehung der Pathogenese beitragen (Abbildung 2).

Abbildung 2: Die Homöostase der APP-Prozessierung: Unter physiologischen Bedingungen laufen sowohl der alpha- als auch der beta-Sekretase-abhängige Prozessierungsweg des APP ab. Dies wurde bereits vor 20 Jahren deutlich, indem das Vorkommen von A-beta Peptiden in Zellkulturen und primären Neuronen der Ratte unter normalen Kulturbedingungen beschrieben wurde (Busciglio *et al.*, 1993; Haass *et al.*, 1992). Hierbei dominiert die beta-Sekretase Spaltung im ZNS, so dass nicht unbedingt von einer „eins zu eins" Spaltung unter physiologischen Bedingungen ausgegangen werden kann (Colombo *et al.*, 2012). Entlang der AD-Pathogenese liegt dieses Gleichgewicht der APP-Prozessierung verschoben vor zu Gunsten von BACE-1. Somit kommt es zur Generierung eines pathologischen Levels an A-beta Peptiden, die dann zur Entstehung und zum Fortschritt der Krankheit beitragen können (Übersicht in Endres und Fahrenholz, 2012).

In mehreren Arbeiten konnte demonstriert werden, dass in AD-Patienten das Gleichgewicht der beiden Proteasen ADAM10 und BACE-1 zu Gunsten von BACE-1 verschoben ist (Übersicht in Endres und Fahrenholz, 2012). Die Proteinmenge der beta-Sekretase BACE-1 ist signifikant erhöht im zerebralen und frontalen Kortex von AD-Patienten im Vergleich zu gesunden Kontrollpersonen (Ahmed *et al.*, 2010; Cai *et al.*, 2010). Diese Befunden korrelieren auch mit einer erhöhten Aktivität des Enzyms

(Ahmed *et al.*, 2010; Miners *et al.*, 2010). Dahingegen gilt eine reduzierte Menge bzw. Aktivität der alpha-Sekretase ADAM10 in der Literatur als anerkannt. So konnte gezeigte werden, dass das ADAM10 mRNA Level in kortikalem Hirngewebe von AD-Patienten reduziert ist (Marcinkiewicz und Seidah, 2000). Dies geht einher mit Analysen, die eine verminderte Menge von ADAM10 auf Proteinebene beschreiben (Bernstein *et al.*, 2003). Hierbei ist die Anzahl ADAM10 immunreaktiver Neurone in Gehirnen von AD-Patienten im Vergleich zu gesunden Kontrollen reduziert. Auch die Aktivität dieses Enzyms ist in temporalem Kortexgewebe sporadischer AD-Fälle drastisch vermindert (Tyler *et al.*, 2002). Für das ADAM10-abhängige Spaltprodukt des APP, APPs-alpha, konnte eine Reduktion in CSF-Proben von dementen Personen beschrieben werden (Fellgiebel *et al.*, 2009). Eine gestörte Sekretion dieses neuroprotektiven und neurotrophen Faktors könnte potenziell zusätzlich zur erhöhten A-beta Menge zu neurodegenerativen Prozessen beitragen.

a) Die beta-Sekretase als therapeutischer Ansatz

Aus der Hypothese der gestörten Homöostase der APP-Prozessierung wurden verschiedene therapeutische Ansätze entwickelt. Hierbei stellt die pharmakologische Inhibition der beta-Sekretase BACE-1 ein intensiv erforschtes Therapieziel dar (Übersicht in Yan und Vassar, 2014). BACE-1 „*Knock-Out*“ Mäuse bilden keine neurotoxischen A-beta Peptide (Cai *et al.*, 2001; Luo *et al.*, 2001; Roberds *et al.*, 2001) und zeigen phänotypische Merkmale wie zum Beispiel Hypomyelinisierung (Hu *et al.*, 2006; Willem *et al.*, 2006). Seit der Aufdeckung der Kristallstruktur von BACE-1 in der Gegenwart eines Inhibitors wird intensiv an der Entwicklung selektiver beta-Sekretase Hemmer geforscht (Ghosh *et al.*, 2001; Sauder *et al.*, 2000). Zum Beispiel stellte die Firma CoMentis ihren BACE-1 Inhibitor CTS-21166 vor, der vielversprechende Eigenschaften im Hinblick auf BHS-Gängigkeit, Selektivität, Stabilität und Bioverfügbarkeit aufwies (Ghosh *et al.*, 2012). Intraperitoneale Injektion des Inhibitors in AD-Modellmäuse führte zu einer Reduktion der A-beta Level um circa 40% und war gefolgt von einer reduzierten Menge an Plaque Ablagerungen im Hippokampus der Tiere (Ghosh *et al.*, 2012). Jedoch sind klinische Testungen nötig, um den therapeutischen Nutzen in der AD-Therapie vollends zu belegen (Übersicht in Luo und Yan, 2010). Bei einer therapeutischen Inhibition von BACE-1 besteht die Gefahr, dass unerwünschte Nebenwirkungen auftreten können. Diese könnten auf physiologisch relevanten Substrate von BACE-1 beruhen wie zum Beispiel dem „*seizure protein 6*“ oder Proteine der Neuroligin-Genfamilie, die eine zentrale Rolle in

der exzitatorischen Informationsverarbeitung einnehmen (Kuhn *et al.*, 2012). Hierbei könnte auch die Neuregulin-1 vermittelte Myelinisierung von peripheren Nervenzellen eine Rolle spielen (Willem *et al.*, 2006). Neuregulin-1 kann von BACE-1 gespalten werden, was unter anderem auch die Ausbildung der Muskelspindel reguliert (Cheret *et al.*, 2013). Für potenzielle unerwünschte Nebenwirkungen bei einer pharmakologischen Inhibierung der beta-Sekretase spricht auch eine gestörte Informationsweiterleitung zwischen den Axonen sensorischer Neurone und dem *Bulbus Olfaktorius* des Gehirns in BACE-1 „*Knock-Out*" Mäusen (Rajapaksha *et al.*, 2011).

b) Die Induktion der alpha-sekretorischen APP-Spaltung als Therapieziel

Neben der im vorherigen Abschnitt diskutierten pharmakologischen Inhibition der beta-Sekretase BACE-1 ist die Aktivierung des alpha-sekretorischen Signalwegs eine weitere vielversprechende Alternative, um therapeutisch in die gestörte Homöostase der APP-Prozessierung einzugreifen (Übersicht in Endres und Fahrenholz, 2012; Saftig und Reiss, 2011). Zum Beispiel führte die Überexpression von ADAM10 im APP-transgenen Mausmodell zu einer signifikanten Reduktion der Plaque Ablagerungen im Gehirn der Tiere (Postina *et al.*, 2004). Eine Therapie-basierte Modulation der alpha-Sekretase Expression bzw. Aktivität hätte neben einer verminderten Menge an toxischen A-beta Peptiden den Vorteil, dass das neuroprotektive und neurotrophe Fragment APPs-alpha generiert wird (siehe Kapitel 1.1.3.1). In einem AD-Mausmodell konnte im Vergleich zu entsprechenden Wildtyp Mäusen eine beeinträchtigte Lern- und Gedächtnisleistung beschrieben werden (Schmitt *et al.*, 2006). Bei Überexpression von ADAM10 war die Lern- und Gedächtnisleistung wieder mit der von entsprechenden Wildtyp Mäusen vergleichbar. Jedoch ist im Falle einer pharmakologischen Aktivierung der ADAM10-vermittelten Spaltung des APP durch ein relativ großes Substratspektrum mit potenziellen unerwünschten Nebenwirkungen zu rechnen (Übersicht in Pruessmeyer und Ludwig, 2009). Zum Beispiel spaltet ADAM10 neuronales Cadherin (N-Cadherin) und reguliert somit die Ausbildung von Zell-Zell Kontakten (Reiss *et al.*, 2005). Auch das Zelladhäsionsmolekül Neuroligin-1 (NL-1), welches eine fundamentale Rolle bei der exzitatorischen Signalweiterleitung glutamaterger Neurone spielt wird von ADAM10 gespalten (Suzuki *et al.*, 2012). Deshalb ist die Identifizierung sowie Charakterisierung physiologisch relevanter Substrate von ADAM10 von großer Bedeutung, um potenzielle Nebenwirkungen einer ADAM10-basierten Therapie

besser abschätzen zu können. Dennoch sind erste Experimente, die den therapeutischen Nutzen einer Modulation der alpha-Sekretase untersuchen, vielversprechend. Hierbei scheint das Maß an Induktion entscheidend zu sein: Das Genexpressionsprofil in einer Microarray-Analyse von ADAM10 transgenen Mäusen mit moderater Überexpression zeigte bei einer vergleichsweise geringen Anzahl von Genen nur sehr milde Änderungen um einen Faktor von maximal 1,4 im Vergleich zu entsprechenden Wildtyp Mäusen (Prinzen *et al.*, 2009). Jedoch führt eine milde Überexpression der Protease bereits zur verminderten Ablagerung von A-beta Peptiden in transgenen Mäusen, während es keine phänotypische Auffälligkeiten gab (Postina *et al.*, 2004). Erst bei einer starken Überexpression des Enzyms konnte eine reduzierte Akt-Signalweiterleitung sowie eine lokale Verdickung der Myelinscheide beschrieben werden (Freese *et al.*, 2009). Zusammenfassend wird ADAM10 in der Literatur als überaus interessantes und vielversprechendes Therapieziel für die Alzheimer-Demenz diskutiert (Endres und Fahrenholz, 2010; Postina, 2012). Um die Menge an ADAM10 zu modulieren und somit in das gestörte Gleichgewicht der APP-Prozessierung einzugreifen gibt es verschiedene Ansatzpunkte, die im Folgenden vorgestellt werden:

Beeinflussung der ADAM10 Genexpression

Ein Bereich eines Gens, in dem regulatorisch Einfluss auf dessen Transkription genommen werden kann, ist der so genannte Promotorbereich. Studien zeigten, dass der Kernbereich des humanen ADAM10-Promotors im Bereich -508 bis -300 Basenpaaren ("*baise pairs*", bp) stromaufwärts des Translationsinitiationsstarts lokalisiert ist und eine Vielzahl funktioneller Bindestellen ausweist (Prinzen *et al.*, 2005). Innerhalb der Volllängen-Promotorsequenz konnten zwei Retinoid-X-Rezeptor (RXR) Bindestellen identifiziert werden, die im Bereich -203 bzw. -302 bp liegen (Prinzen *et al.*, 2005). Die Behandlung von murinen sowie humanen neuronalen Zellen mit Retinsäure, einem endogenen Liganden für die korrespondierenden Retinoid-Rezeptoren, führte zu einer gesteigerten Menge an ADAM10 sowohl auf mRNA- als auch auf Protein-Ebene (Tippmann *et al.*, 2009). Dies führte ebenfalls zu einer vermehrten Sekretion an APPs-alpha in neuronalen Zellkulturmodellen (Endres *et al.*, 2005; Tippmann *et al.*, 2009). Der direkte Ligand Retinsäure kann ein relativ breites Spektrum an unerwünschten Nebenwirkungen wie zum Beispiel allergische Reaktionen oder einen Pseudotumor cerebri bei der Behandlung von akuter promyelozytischer Leukämie erzeugen (Sano *et al.*, 1998; Wansley *et al.*, 2013).

Synthetische Retinoide hingegen erfüllen entsprechende Anforderungen an eine Langzeitgabe als Medikament und wurden bereits für verschiedene Krankheiten wie zum Beispiel Hautkrankheiten (Psoriasis) eingesetzt. RAR-alpha Subtyp spezifische synthetische Retinoide konnten identifiziert werden, die die Menge an ADAM10 im Tiermodell beeinflussten: Tamibaroten (Am80) erhöht die Proteinmenge an ADAM10 und daraus folgend die Sekretion an neuroprotektivem APPs-alpha (Kawahara *et al.*, 2009; Kitaoka *et al.*, 2013). Zudem wurden die Level an toxischen A-beta Peptide reduziert und die AD-charakteristische Neuroinflammation gesenkt. Des Weiteren konnte Acitretin als Aktivator der alpha-Sekretase Genexpression identifiziert werden (Tippmann *et al.*, 2009). Hierbei hat Acitretin einen eher indirekten Mechanismus, indem es den endogenen Liganden Retinsäure aus seinem intrazellulären Bindeprotein freisetzt und somit dessen Konzentration in einem physiologischen Rahmen in der Zelle erhöht (Armstrong *et al.*, 2005). Analysen in transgenen AD Modellmäusen, die pathologische Merkmale wie amyloide Plaques entwickeln, zeigten bei einmaliger stereotaktischer Injektion von Acitretin eine circa 50%ige Reduktion der A-beta Peptide im Gehirn der Tiere (Tippmann *et al.*, 2009). Die Analysen legten den Grundstein für eine „*proof of mechanism*“ klinische Studie vom Typ IIa, um den therapeutischen Nutzen von Acitretin an Patienten mit leichter bis mittelschwerer AD zu prüfen (http://clinicaltrial.gov, Nr.: NCT01078168).

Beeinflussung der Menge an ADAM10 auf translationaler Ebene

Effekte auf translationaler Ebene können durch bestimmte nicht-kodierende Bereiche innerhalb der entsprechenden mRNA vermittelt werden, den so genannten UTRs („*untranslated regions*“). Für ADAM10 wurde eine 444 Nukleotide umfassende regulatorische UTR beschrieben, die 5‘ ausgehend vom Translationsinitiationspunkt der kodierenden Sequenz liegt (Lammich *et al.*, 2010). Innerhalb dieses Bereichs konnte eine Repressor-Sequenz identifiziert werden, die die Menge an Protein in der Zelle vermindert, wohingegen die entsprechenden mRNA Level unbeeinflusst blieben (Lammich *et al.*, 2010). In einer weiteren Studie konnte gezeigt werden, dass dieser Effekt durch eine spezifische Guanin-reiche Sequenz innerhalb der 5’UTR des ADAM10, die einen stabilen intramolekularen Guanin-Quadruplex bildet, vermittelt wird und somit die Translation von ADAM10 inhibiert (Lammich *et al.*, 2011). Auch für BACE-1 wurde eine 5‘ UTR beschrieben, die die Translation des Proteins maßgeblich reguliert (Lammich *et al.*, 2004). Die Transfektion einer BACE-1 Mutante, deren 5’UTR deletiert wurde, zeigte eine Senkung der Protein Menge um 90%

verglichen mit der entsprechenden Wildtyp Sequenz in Zellkulturversuchen (Lammich *et al.*, 2004). Des Weiteren kann die Translation eines Proteins durch so genannte microRNAs (miRNAs) beeinflusst werden (Wienholds und Plasterk, 2005). Durch Bindung an komplementäre Sequenzen innerhalb der 3'UTR des entsprechenden Zielgens, blockieren miRNAs die Translation des Proteins oder initiieren den Abbau der korrespondierenden mRNA (McDaneld, 2009). Bezüglich der AD zeigte ein RT-PCR Ansatz ein Muster an differenziell regulierten miRNAs im Gehirn von AD-Patienten im Vergleich zu Kontrollen (Cogswell *et al.*, 2008). Für die beta-Sekretase BACE-1 konnte gezeigt werden, dass das miRNA Cluster 29a/29b1 die Expression in neuronalen Zellkulturen vermindert (Hebert *et al.*, 2008). Zudem waren diese miRNAs im Gehirn von AD-Patienten, die eine erhöhte Expression von BACE-1 aufwiesen, gesenkt (Hebert *et al.*, 2008). Auch für die protektive Protease ADAM10 konnten bislang zwei miRNAs identifiziert werden, die deren Expression regulieren: Die Überexpression der miRNA 122 in kultivierten Leberzellen führte zur Verminderung von ADAM10 auf Protein Ebene (Bai *et al.*, 2009). In einer weiteren Arbeit konnte gezeigt werden, dass die A-beta-induzierte Überexpression der miRNA 144 zu einer reduzierten Mengen an ADAM10 in neuronalen SH-SY5Y Zellen führt (Cheng *et al.*, 2013). Die Transkription der miRNA selbst in der Zelle wurde dabei von dem TF AP1 („*activator protein 1*“) gesteuert. Somit haben miRNAs prinzipiell das Potenzial in die Balance der APP-Prozessierung einzugreifen und vermutlich zur vermehrten A-beta Generierung beizutragen.

Lokalisierung und Aktivität von ADAM10

Das Protein ADAM10 entsteht durch Translation am rauen Endoplasmatischen Retikulum (ER) und durchläuft den sekretorische Weg. Hierbei wird die Proform des Enzyms durch Proproteinkonvertasen wie zum Beispiel Furin gespalten und somit die Prodomäne entfernt (Anders *et al.*, 2001). Die Reifung von ADAM10 und somit dessen Aktivität ist ein stark regulierter Prozess, der unter anderem von posttranslationaler Modifikation abhängt. Es wurden vier potenzielle N-Glykosylierungsstellen in der extrazellulären Sequenz des ADAM10 identifiziert, die mit der Reifung und folglich der Aktivität stark korreliert sind (Escrevente *et al.*, 2008). Ein weiterer Mechanismus, der die Menge/Aktivität an ADAM10 an seinem Bestimmungsort determiniert, ist die Zusammensetzung der Plasmamembran. Die Entfernung von Cholesterin aus der Membran führt zu einer vermehrten Aktivität des Enzyms (Kojro *et al.*, 2001; Matthews *et al.*, 2003). Hingegen führte die Lokalisierung

von ADAM10 in Cholesterin-reichen Domänen innerhalb der Membran zu einer verminderten Enzymaktivität (Harris *et al.*, 2009; Kojro *et al.*, 2010). Die Gabe von Statinen, die therapeutisch in Fettstoffwechselstörungen als HMG-CoA Reduktase Hemmer eingesetzt werden, führte in neuronalen Zellkulturen zu einer erhöhten Aktivität von ADAM10 (Kojro *et al.*, 2001). Allerdings konnte die klinische Relevanz einer therapeutischen Nutzung von Statinen bei AD bislang nicht eindeutig belegt werden (Übersicht in McGuinness und Passmore, 2010)

c) Die Passage der Blut-Hirn Schranke als Kriterium für ein Alzheimer-Therapeutikum

Bei einem frühen therapeutischen Eingriff in der präklinischen Phase der AD muss mit einer intakten BHS gerechnet werden, die ein zu testendes Therapeutikum überwinden muss. Zum Beispiel sind viele der entwickelten Inhibitoren für BACE-1 Substrate für das P-Glykoprotein (P-gp), den wichtigsten Effluxtransporter der BHS (Hussain *et al.*, 2007; Meredith, Jr. *et al.*, 2008). Es wurden auch verschiedene NSAIDs („*non steroidal anti inflammatory drugs*“) bezüglich ihres Potenzials als AD-Therapeutikum untersucht. Dieser Substanzklasse konnte die Eigenschaft nachgewiesen werden die A-beta Produktion in Zellkultur und AD-Modellmäusen drastisch zu reduzieren (Eriksen *et al.*, 2003; Weggen *et al.*, 2001). Jedoch mussten weitere klinische Entwicklungen bezüglich des NSAID, Tarenflurbil, gestoppt werden, nachdem bei einer Behandlung über 18 Monaten kein Einfluss auf den geistigen Abbau in einer Phase IIa Studie gemessen werden konnte (Green *et al.*, 2009). Weitere Untersuchungen erhärteten den Verdacht, dass die ausbleibenden Effekte durch eine sehr geringe BHS-Gängigkeit und somit durch eine unzureichende Anreicherung des Medikaments im Gehirn der Patienten erklärt werden konnten (Green *et al.*, 2009). Neuere Studien zeigen alternative Wege, um Substanzen mit schlechter Penetrationsfähigkeit an ihren Bestimmungsort zu bringen. Hierbei stellt das Koppeln mit Nanopartikeln, die den Transport über die BHS maßgeblich erleichtern sollen, ein aktuelles Themengebiet dar (Gidwani und Singh, 2014). Auch in Bezug auf die NSAID vermittelte Reduktion der A-beta Peptide, konnte durch den Einsatz von Nanopartikeln Fortschritte gemacht werden. Das NSAID Flurbiprofen, welches bereits von der FDA („*Food and Drug Administration*“) als Medikament zugelassen ist, zeigt eine durch gamma-Sekretase Modulation vermittelte Senkung der A-beta Level (Meister *et al.*, 2013). Durch Kopplung dieser Substanz mit Nanopartikeln konnte ein Transport in einem *in vitro* BHS Modell mit primären

Endothelzellen der Maus erzielt und somit therapeutisch nutzbar gemacht werden (Meister *et al.*, 2013).

Zusammenfassend lässt sich sagen, dass die gestörte Homöostase der APP-Prozessierung nicht der einzige Einflussfaktor auf die A-beta-vermittelte Pathologie der AD ist. Zudem könnten auch ein verminderter Abbau oder fehlerhafte Transportprozesse eine Rolle spielen. Dennoch ist die Spaltung des APP grundlegend für die Generierung der A-beta Peptide. Somit würde die Analyse von molekularen Faktoren, die die Menge bzw. Aktivität einer der beiden Proteasen (ADAM10 und BACE-1) regulieren, zum Verständnis der AD-Pathogenese beitragen. Die pharmakologische Intervention in das unter pathologischen Bedingungen gestörte Gleichgewicht der APP-Prozessierung bietet einen interessanten Ansatzpunkt für die Entwicklung neuer Alzheimer-Therapeutika.

2. Zielsetzung der Arbeit

Eine verminderte Expression der protektiven alpha-Sekretase ADAM10 ist ein zentraler Prozess in der Alzheimer-Demenz. Die Aufdeckung von zellulären Signalwegen, die letztlich zu einer reduzierten Menge an ADAM10 und folglich zur gestörten Homöostase der APP-Prozessierung beitragen, würde zum Verständnis der Alzheimer-Pathogenese beitragen und gegebenenfalls neue therapeutische ADAM10-basierte Ansatzpunkte hervorbringen. Die Anhebung der ADAM10 Expression auf ein physiologisches Ursprungsniveau ist ein aktuelles vielversprechendes Therapieziel in der Alzheimer-Forschung.

Im Rahmen dieser Arbeit sollten im Wesentlichen zwei potenzielle molekulare Mechanismen untersucht werden: die Regulation auf Genexpressionsebene sowie die Steuerung durch microRNAs. Als Ausgangspunkt für die Analyse an der Genexpression beteiligter TFs wurden 704 humane Transkriptionsfaktoren in einem Hochdurchsatzverfahren untersucht. 48 Transkriptionsfaktoren beeinflussten den Quotienten ADAM10- pro BACE-1-Promotor Aktivität und sollten anschließend durch Datenbankanalyse („*expressed sequence tag*“ EST-Profile) auf ein ausreichend hohes Expressionsprofil im adulten Gehirn des Menschen untersucht werden. Daraus sollten geeignete Kandidaten ausgewählt und näher analysiert werden: Es wurden exemplarisch XBP-1 („*X box binding protein-1*“), als Vertreter eines alpha-Sekretase Induktors, und Tbx2 („*T box 2*“), welches die Expression von ADAM10 senkt, detaillierter untersucht. Hierbei sollten zum einen die jeweiligen zellulären Wirkmechanismen aufgeklärt und potenzielle Interaktionspartner identifiziert werden. Zum anderen sollte die pathophysiologische Relevanz beider Transkriptionsfaktoren in entsprechenden Alzheimer-Mausmodellen sowie post-mortem Hirngewebeproben von Alzheimer-Patienten evaluiert werden. Auf Translationsebene kann die Menge eines Proteins durch so genannte microRNAs moduliert werden. In Kooperation mit dem Helmholtz-Zentrum München (Prof. Wolfgang Wurst) sollten bislang unbekannte miRNAs bioinformatisch identifiziert werden, die an die 3'UTR („*untranslated* region“) des humanen ADAM10 Gens binden. Darüber hinaus sollten experimentelle Daten mittels eines ADAM10 3'UTR Reporter Konstrukts die physiologische Relevanz des bioinformatischen Ansatzes belegen und die Funktionalität dieser miRNAs bezüglich einer Regulation von ADAM10 aufzeigen.

Ein weiteres Ziel dieser Dissertation war die Identifizierung neuer Substanzen, die die Menge an ADAM10 erhöhen und/oder die Expression von BACE-1 senken und somit

therapeutisches Potenzial hinsichtlich der Alzheimer Krankheit besitzen. In einem dualen Luziferase Reportergen Experiment sollten 640 Wirkstoffe einer Substanz-Bibliothek auf die Induktion des Quotienten ADAM10- pro BACE-1-Promotor Aktivität hin untersucht werden. Als initiales Filterkriterium hinsichtlich der klinischen Relevanz sollten verbleibende Kandidaten durch Reportergen-Analysen auf die Beeinflussung des humanen APP-Promotors analysiert werden. Eine weitere Selektion sollte die Evaluierung der Blut-Hirn-Schranke Permeabilität der einzelnen Kandidaten sein. Hierzu sollte in Zusammenarbeit mit Dr. Christian Freese (Institut für Pathologie Mainz, AG Prof. Charles J. Kirkpatrick) ein *in vitro* Blut-Hirn-Schranke Modell, das auf einem Ko-Kultur System bestehend aus primären Schweine Hirn Endothelzellen und neuronalen SH-SY5Y Zellen basiert, anhand der Modell-Substanz Acitretin entwickelt werden. Durch das große Substratspektrum von ADAM10 muss bei einer pharmakologischen Intervention mit etwaigen Nebenwirkungen wie zum Beispiel eine gestörte exzitatorische Signalweiterleitung an zentralen Synapsen gerechnet werden. Im Rahmen eines Forschungsaufenthaltes an der Universität von Tokio (Graduate School of Pharmaceutical Sciences, Prof. Taisuke Tomita) sollte untersucht werden, inwieweit eine pharmakologische Induktion der alpha-Sekretase durch das synthetische Retinoid Acitretin zu potenziellen unerwünschten Nebenwirkungen führt. Hierbei sollte der Effekt von Acitretin auf die ADAM10-vermittelte Spaltung des Zelladhäsionsproteins Neuroligin-1 in primären kortikalen Neuronen der Ratte untersucht werden.

3. Ergebnisse und Diskussion

Bei der AD-Pathogenese führt eine Dysbalance zwischen den beiden konkurrierenden Proteasen, ADAM10 und BACE-1, zu einem Anstieg an A-beta Peptiden. Die Aufdeckung molekularer Mechanismen, die letztlich zu einer gestörten Homöostase der APP-Prozessierung führen, würden zum Verständnis der AD-Pathogenese beitragen. Des Weiteren stellt die Evaluierung von Substanzen, die regulatorisch in die proteolytische Spaltung des APP eingreifen, einen interessanten Ansatzpunkt für eine A-beta vermindernde AD-Therapie dar.

3.1 Identifikation von regulatorischen Einflussfaktoren der APP-Prozessierung

Nachfolgend werden die Ergebnisse bezüglich des TF „*X box binding protein-1*“ (XBP-1) beschrieben und diskutiert, die zum Teil in Reinhardt et al. 2014 (Kapitel 6 (B)) publiziert und in Endres und Reinhardt 2013 (Kapitel 6 (D)) zusammenfassend beschrieben wurden. Die Studie bezüglich der miRNAs wurde in Augustin et al. 2012 (Kapitel 6 (A)) veröffentlicht. Zudem werden auch Daten einer bisher unveröffentlichten Studie bezüglich des Transkriptionsfaktors T box 2 (Tbx2) behandelt.

Um ein gestörtes Gleichgewicht der APP-Prozessierung zu erklären gibt es verschiedene Ansatzpunkte wie zum Beispiel die Regulation auf Genexpressionsebene. Jene wird in der Regel durch so genannte Transkriptions-faktoren (TFs), die an spezielle Bindesequenzen innerhalb regulatorischer Abschnitte eines Gens, den Promotoren, binden, vermittelt. Um Transkriptionsfaktoren zu identifizieren, die letztlich zu einer gestörten Homöostase der APP-Prozessierung und folglich zur Entstehung der AD beitragen, wurde ein Hochdurchsatz Verfahren entwickelt. Hierzu wurde ein dualer Luziferase-basierter Reporter Vektor generiert. Die Expression einer *Firefly*-Luziferase wird hierbei von der Promotorsequenz des humanen ADAM10 (Prinzen *et al.*, 2005) gesteuert. Gleichzeitig reguliert der humane BACE-1-Promotor (Christensen *et al.*, 2004) die Expression einer *Renilla*-Luziferase. Initial wurden 704 humane Transkriptionsfaktoren (*Transcription Factor GFC-Transfection Array*, Origene, Rockville MD, USA) untersucht. Die Transfektion des dualen Reportervektors zusammen mit einem der 704 TFs in neuronalen SH-SY5Y Zellen ergab 48 TFs die den Quotient ADAM10- pro BACE-1-Promotor Aktivität signifikant beeinflussen (Abbildung 3, Reinhardt *et al.*, 2014). Hierbei konnten bereits bekannte Regulatoren der BACE-1 Genexpression wie zum Beispiel Sp1

(Christensen *et al.*, 2004) oder YY-1 (Lahiri *et al.*, 2006) anhand eines veränderten Quotienten identifiziert werden, die die Validität des Ansatzes bestätigten. 23 dieser so erhaltenen TFs zeigten durch Datenbankanalyse (EST-Profil Analyse) auch eine ausreichend hohe Expression im Gehirn von Erwachsenen und somit das Potenzial in die AD-Pathogenese eingreifen zu können.

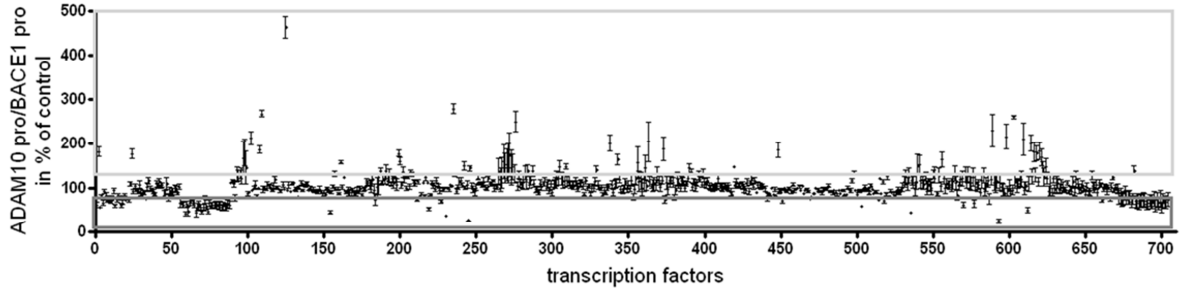

Abbildung 3: Identifikation von Transkriptionsfaktoren (TFs), die regulatorisch in die Homöostase der APP-Prozessierung eingreifen: Die Analyse einer TF Expressionsvektoren Bibliothek mit einem dualen Luziferase Reporter für die humanen Promotoren von ADAM10 und BACE-1 in SH-SY5Y Zellen ergab 48 TFs, die den Quotient ADAM10/BACE-1 im Vergleich zu Leervektor-transfizierten Zellen signifikant modulieren (130% > Quotient ADAM10/BACE-1 < 70%) (nach Reinhardt et al. 2014, Abbildung 1).

Nachfolgend werden zwei selektierte Kandidaten TFs beschrieben, für die der molekulare Mechanismus der Regulation von ADAM10 genauer untersucht wurde. Hierbei werden XBP-1 als Induktor sowie Tbx2 als Inhibitor der ADAM10 Genexpression vorgestellt.

3.1.1 Der Stress-Faktor XBP-1 als Induktor der ADAM10 Genexpression

Die initialen Analysen des TF-„*Screenings*“ ergaben vier TFs (ATF4 („*activating transcription factor 4*“), HSF1 („*heat shock factor 1*“), p53 und XBP-1 („*X box binding protein-1*“)), deren physiologische Aufgabe sehr stark mit zellulären Stressantworten korreliert sind: p53 wird zum Beispiel durch DNA Schäden aktiviert und senkt das Verhältnis ADAM10- zu BACE-1-Promotor Aktivität auf 33% im Vergleich zu Leervektor-transfizierten Zellen. Nur einer der Stress-assoziierten Faktoren „*X box binding protein-1*“ (XBP-1) zeigte eine signifikante Steigerung der ADAM10-Promotor Aktivität während die von BACE-1 unbeeinflusst blieb.

XBP-1 ist ein wesentlicher Bestandteil der so genannten „*unfolded protein response*“ (UPR), ein Signalnetzwerk, welches bei ER-Stress aktiviert wird (Schröder und Kaufman, 2005). Im Allgemeinen operieren hierbei drei parallel ablaufende

Signalwege: IRE1-alpha (*inositol requiring enzyme 1*), PERK (*double-stranded RNA-activated protein kinase (PKR)-like ER kinase*) und ATF6 (*activating transcription factor 6*). Nach Induktion der UPR durch das Auftreten von ungefalteten Proteinen führen letztlich alle drei Signalwege zur Aktivierung von speziellen Transkriptionsfaktoren, die das Ablesen spezifischer UPR-Zielgene wie zum Beispiel Chaperone, so genannte Faltungshelfer, verstärken (Abbildung 4, Übersicht in Endres und Reinhardt, 2013, Kapitel 6 (D)).

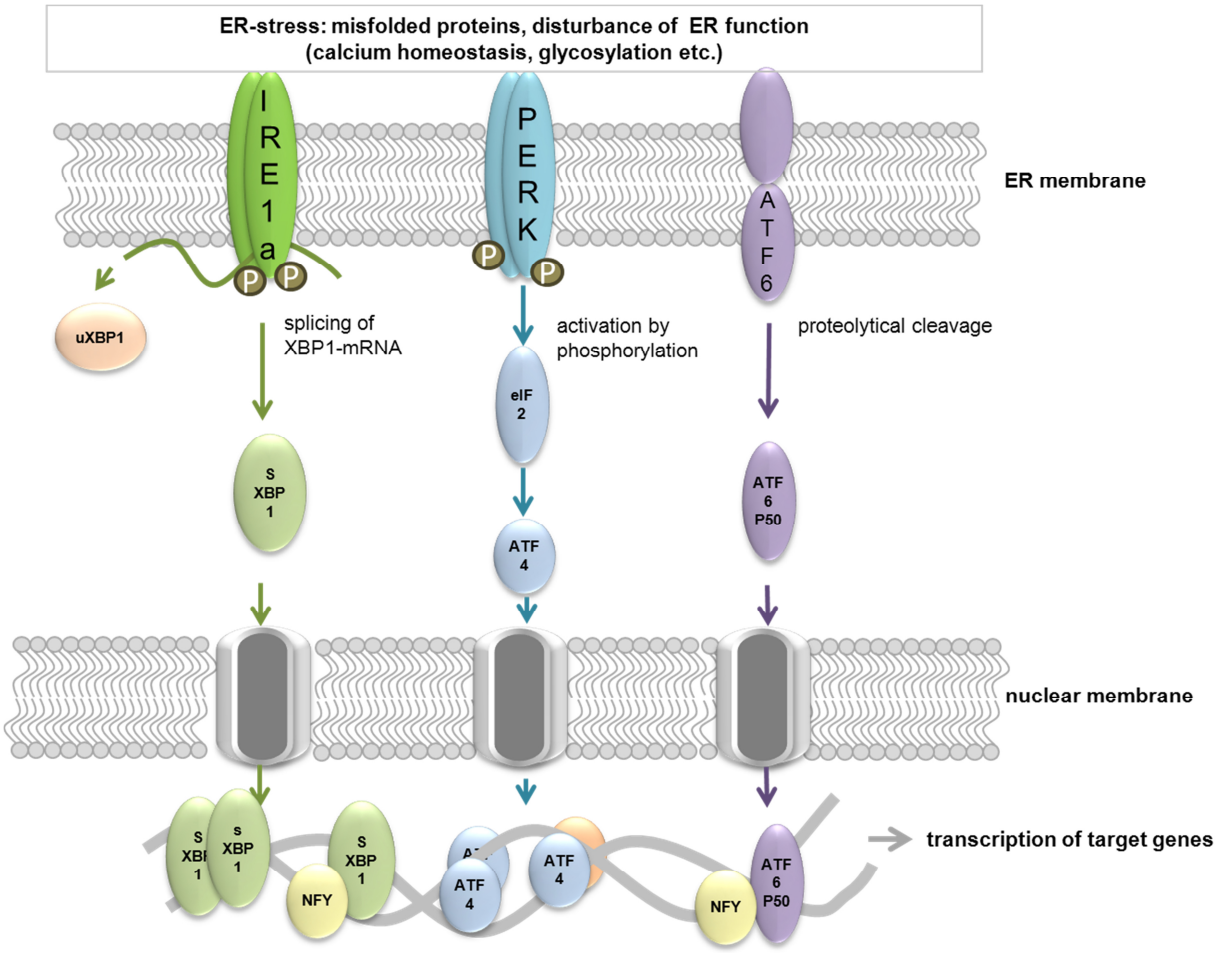

Abbildung 4: Die drei Signalwege der "*unfolded protein response*" (UPR): Die ER-Stress Antwort wird vermittelt durch drei an der ER-Membran assoziierte Sensoren: IRE1-alpha, PERK und ATF6. Die Aktivierung der Sensorproteine findet vor allem durch die Bindung von ungefalteten Proteinen statt und führt zu intrazellulären Signalkaskaden. Im Falle von PERK wird zum Beispiel der TF eIF2-alpha phosphoryliert und somit weitere intrazelluläre Signalkaskaden über ATF4 initiiert. IRE1-alpha dimerisiert nach dessen Aktivierung. Dadurch kommt es zur Autophosphorylierung und nachfolgend zu Endonuklease-Aktivität. Dies führt zum Spleißen der XBP-1 mRNA und zur Translation des aktiven Proteins. ATF6 transloziert nach Aktivierung in den Golgi-Apparat, wo es nach Spaltung zum aktiven Transkriptionsfaktor wird. Die Aktivierung der UPR-Zielgene führt zur Translation von Proteinen, die in Prozesse wie zum Beispiel Protein-Faltung, -Reifung, -Sekretion aber auch -Abbau verknüpft sind (modifiziert nach Endres und Reinhardt 2013, Abbildung 1).

XBP-1 wird durch den IRE1-alpha-abhängigen Signalweg aktiviert, indem jenes Enzym nach Dimerisierung in der ER-Membran Endonuklease-Aktivität entwickelt und aus der ungespleißten XBP-1 mRNA ein 26 Nukleotid großes Intron entfernt (Calfon *et al.*, 2002; Yoshida *et al.*, 2001). Charakteristisch hierbei ist die Ausbildung von zwei Haarnadel-Schleifen als Sekundärstruktur der XBP-1 mRNA, die Donor- bzw. Akzeptor-Seiten für das Spleißen repräsentieren und somit die IRE1-alpha-vermittelte Spaltung ermöglichen (Nagashima *et al.*, 2011). Ein veränderter Leserahmen führt bei der Translation zur aktiven Proteinform von 54 kDa (Korennykh *et al.*, 2011; Liu *et al.*, 2000; Tirasophon *et al.*, 2000). Diese zeichnet sich durch eine Transkriptions-Aktivierungsdomäne sowie dem Verlust einer Kernausschluss-Sequenz aus. Die Translation der ungespleißten XBP-1 mRNA unter nicht-Stress Bedingungen führt zur Synthese eines 33 kDa großen Proteins (Abbildung 5), welches in der Literatur als negativ Regulator der UPR diskutiert wird (Guo *et al.*, 2010; Lee *et al.*, 2003; Yoshida *et al.*, 2006). Darüber hinaus trägt die hydrophobe Region der ungespleißten XBP-1 mRNA zur Verankerung an der ER-Membran bei (Yanagitani *et al.*, 2009). Diese räumliche Nähe von Substrat und Endonuklease führt vermutlich dazu, dass die XBP-1 mRNA bei dem Auftreten von Stresssignalen sehr viel einfacher und schneller prozessiert werden kann, was zu einer vermehrten Bildung von aktivem XBP-1 führt.

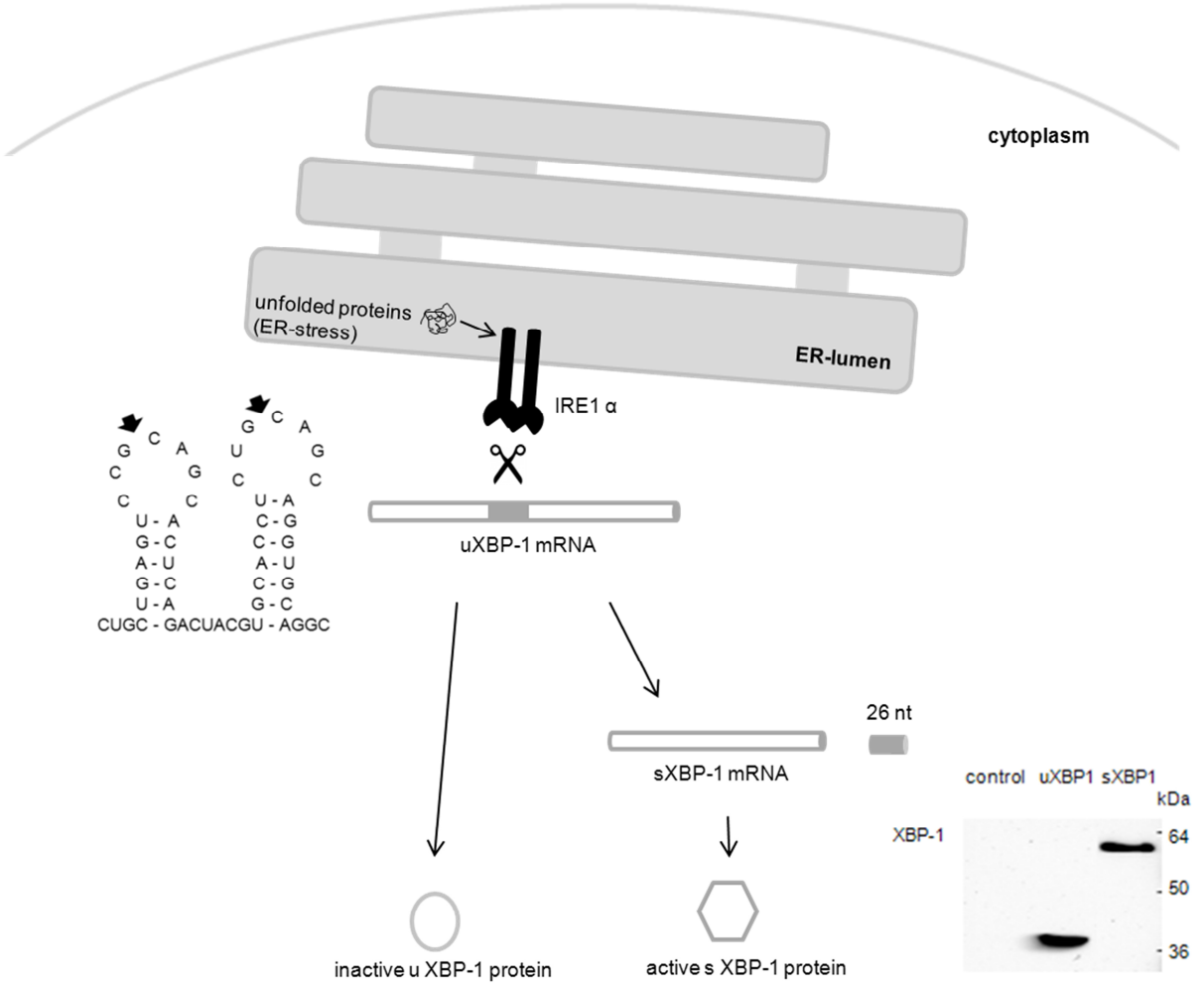

Abbildung 5: IRE1-alpha-abhängige Aktivierung des Transkriptionsfaktors XBP-1: Durch das Auftreten von fehlgefalteten Proteinen, kommt es zur Dimerisierung von IRE1-alpha in der ER-Membran. Dies hat eine Autophosphorylierung zur Folge, welche die Entwicklung von Endonuklease-Aktivität ermöglicht. Das enzymatisch aktive IRE1-alpha entfernt ein 26 nt großes Intron aus der ungespleißten XBP-1 mRNA, die durch die Ausbildung von zwei Haarnadel-Schleifen Spleiß Donor- bzw. Akzeptor-Seiten aufweist. Dies führt zur Translation eines Proteins mit höherem Molekulargewicht (54 kDa, s XBP-1) verglichen mit dem Protein, das ausgehend von der Translation der ungespleißten mRNA entsteht (33 kDa, u XBP-1). Das transkriptionell aktive Protein transloziert in den Zellkern und führt zum Ablesen UPR-spezifischer Zielgene (zusammengestellt aus den Abbildungen 2 und 10, Reinhardt et al. 2014).

ER-Stress im Allgemeinen und insbesondere die UPR wurden bereits in einigen Arbeiten mit der Pathogenese der AD korreliert (Übersicht in Endres und Reinhardt, 2013, Kapitel 6 (D)). Hierbei wurde die UPR als früh auftretendes Merkmal in AD-Patienten beschrieben. Zum Beispiel zeigten Analysen von post-mortem Hirngewebeproben von AD-Patienten eine starke Korrelation zwischen ersten Stadien der Akkumulierung und Aggregation toxischer Produkte und klassischen UPR Aktivierungsmarkern (Hoozemans *et al.*, 2012). Im Rahmen dieser Promotion konnte eine mögliche Rolle von XBP-1 in der AD-Pathogenese aufgezeigt werden. In

Zellkulturexperimenten konnte gezeigt werden, dass XBP-1 als TF die Genexpression von ADAM10 reguliert (Reinhardt *et al.*, 2014, Kapitel 6 (B)). Insbesondere die aktive Spleißform des XBP-1 induziert in einer Dosis-Abhängigkeit die Expression der protektiven Protease ADAM10 in neuronalen SH-SY5Y Zellen. Weitere Analysen identifizierten eine „*ER-stress responsive element*" (ERSE)-ähnliche Bindestelle innerhalb der humanen ADAM10-Promotor Sequenz, die maßgeblich an der Vermittlung des Effekts beteiligt ist. *Western blot* Analysen bestätigten die Regulation, indem die Sekretion des ADAM10-abhängigen APP-Spaltprodukts in XBP-1 überexprimierenden SH-SY5Y Zellen signifikant erhöht war, während die Expression von APP selbst unbeeinflusst blieb. Die Überexpression von XBP-1 hatte hierbei keinen Einfluss auf die Genexpression von ADAM17, das als zum Beispiel Proteinkinase C induzierbare alpha-Sekretase beschrieben wurde (Endres *et al.*, 2005; Slack *et al.*, 2001). Des Weiteren zeigte eine siRNA vermittelte Verminderung der Menge an XBP-1 in der Zelle eine gesenkte ADAM10-Promotor Aktivität im Vergleich zu einer Kontroll-siRNA mit zufälliger Nukleotidabfolge und minimaler Bindekapazität. Ein physiologisch relevanter Ko-Regulator von XBP-1 ist Insulin (Ueki und Kadowaki, 2011). Nach der Bindung von Insulin an dessen Rezeptor, wird p85, eine Untereinheit der Phosphatidyinositol 3 Kinase, intrazellulär aktiviert und dimerisiert mit der aktiven Form von XBP-1 (Park *et al.*, 2010; Winnay *et al.*, 2010). Dieser Komplex induziert die Translokation von XBP-1 in den Zellkern und führt folglich zu einer gesteigerten transkriptionellen Aktivität dieses TFs. Inkubation von XBP-1 überexprimierenden neuronalen Zellkulturen mit Insulin zeigte eine synergistische, Dosis-abhängige Verstärkung des XBP-1-vermittelten Effekts auf die Aktivität des humanen ADAM10-Promotors, wohingegen Insulin alleine keinen Effekt zeigte (Reinhardt *et al.*, 2014, Kapitel 6 (B)). Die Ko-Regulation von XBP-1 und Insulin ist von großem Interesse, da *Diabetes mellitus* vom Typ II als Risikofaktor für die Entwicklung einer AD definiert wurde (Biessels *et al.*, 2006). Eine Hochregulation von ADAM10 durch XBP-1 im Kontext der Insulin-Signalkaskade könnte eine physiologische Antwort auf akute Stresssituationen in der Zelle repräsentieren (Übersicht in Ueki und Kadowaki, 2011).

Die Analyse zweier AD-Mausmodelle (5xFAD (Oakley *et al.*, 2006) und APP/PS1 (Casas *et al.*, 2004)) zeigte, dass zu frühen Zeitpunkten (1 und 2 Monate) pathologischer Veränderungen in den Tieren der XBP-1 Metabolismus gesteigert ist. Dies war begleitet von einer gesteigerten ADAM10 mRNA Menge und deutet

vermutlich auf ein funktionales Zwischenspiel von TF und Zielprotein hin. Zu fortgeschrittenen pathologischen Stadien (9 Monate) lag das Level des aktiven TFs vermindert vor, was mit einer Senkung der ADAM10 Menge einherging (Abbildung 6 A). Diese Ergebnisse sind in Einklang mit vorhergehenden Berichten, die die Aktivierung der UPR als relativ frühes Ereignis in der AD-Pathogenese beschreiben (Hoozemans *et al.*, 2012). Zum Beispiel zeigten *Western blot* Analysen, dass die Expression von GRP78 („*glucose-regulated protein 78*“), einem Indikator für eine aktivierte UPR, im Kortex und Hippokampus von AD-Patienten im Vergleich zu gesunden Kontrollen induziert ist (Hoozemans *et al.*, 2005). Des Weiteren konnten die ER-Stress Sensoren PERK und IRE1-alpha in aktiver phosphorylierter Form in Neuronen von AD-Patienten nachgewiesen werden (Hoozemans *et al.*, 2009). Somit könnte lang anhaltender Stress durch zum Beispiel fehlgefaltete Proteine wie A-beta zu einer Fehlregulation des Systems und letztlich zum Absterben der entsprechenden Nervenzellen führen. Diese Vermutungen konnten auch in *post-mortem* Kortex Proben von AD-Patienten in den eigenen Analysen bestätigt werden. Die Menge der ADAM10 mRNA lag im Vergleich zu gesunden Kontrollen in Proben von AD-Patienten vermindert vor. Auch die Menge an gespleißter XBP-1 mRNA war unter diesen Bedingungen reduziert (Abbildung 6 B). Hierbei korrelierte die Menge an ADAM10 mRNA signifikant mit der von XBP-1 (Reinhardt *et al.*, 2014), was eine gestörte XBP-1 Signalkaskade und eine funktionelle Korrelation zwischen TF und Protease vermuten lässt.

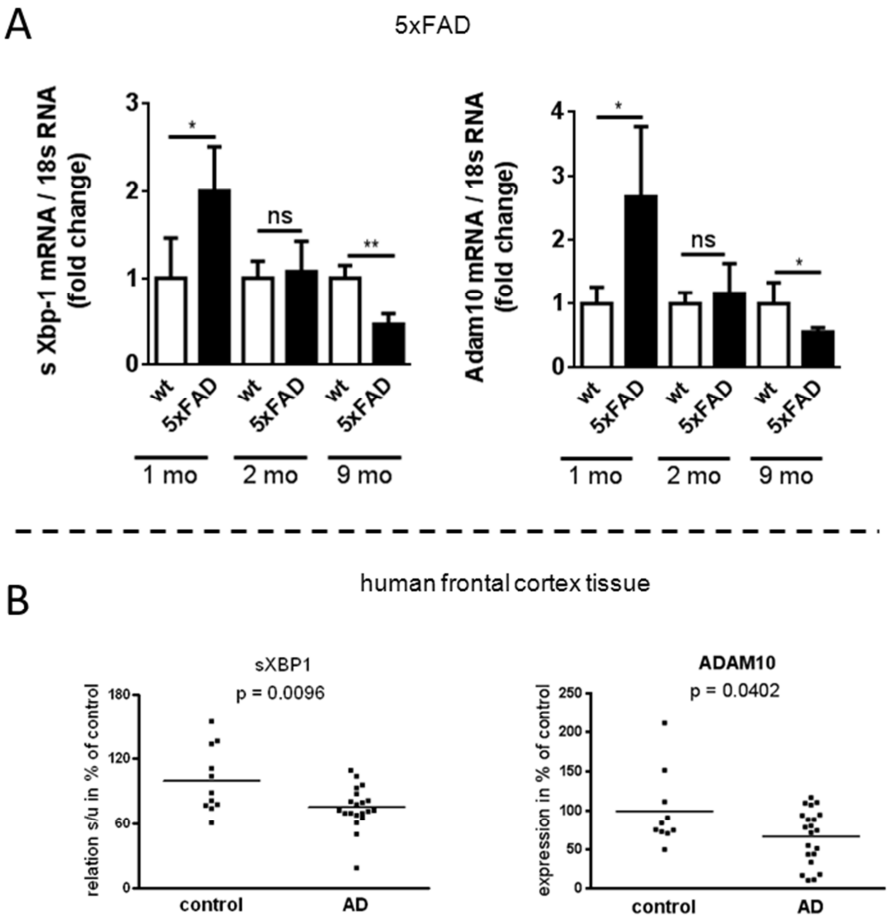

Abbildung 6: Analyse der XBP-1 und ADAM10 mRNA Level in AD-Modellmäusen und AD-Patienten: A) Evaluierung der s XBP-1 sowie ADAM10 mRNA Level in 5xFAD Modellmäusen. Die gemessenen Quantitäten wurden auf 18 S rRNA normiert und in Relation zu nicht-transgenen Kontrolltieren gesetzt. Das Alter der entsprechenden Tiere ist in der Abbildung gekennzeichnet. Die Daten sind gezeigt in Mittelwerten ± SD von 4 Tieren jeder Gruppe (ns = nicht signifikant, * $p < 0,05$, ** $p < 0,01$). B) Analyse von post-mortem Kortexgewebe von AD-Patienten. Die Quantitäten der s XBP-1 bzw. ADAM10 mRNA aus frontalem Kortexgewebe wurden per *real-time* RT-PCR bestimmt und in Relation zu gesunden, Alters-korrelierten Patienten gesetzt (modifiziert nach Reinhardt et al. 2014, Abbildungen 7-9).

3.1.2 Der Seneszenz-assoziierte Faktor Tbx2 als transkriptioneller Repressor der ADAM10 Expression

Ein weiterer aus den vorangegangenen Versuchen identifizierter TF war T box 2 (Tbx2), die hierzu erfolgten Analysen sind bislang unveröffentlicht. Die Überexpression dieses Proteins zeigte im initialen „*Screening*“ eine signifikante Verminderung der ADAM10-Promotor Aktivität auf 45% im Vergleich zu Leervektor-transfizierten SH-SY5Y Zellen. Die BACE-1-Promotor Aktivität zeigte bei Überexpression von Tbx2 eine tendenzielle Reduktion um 20%, die allerdings keine statistische Signifikanz erreichte. Die Expressionsprofil Analyse von Tbx2 ergab, dass der TF mit 16 Transkripten pro Millionen relativ stark im Gehirn im Vergleich zu

anderen Geweben und mit 31 Transkripten pro Millionen ausreichend stark im Erwachsenen exprimiert wird (EST-Profil Analyse, http://www.ncbi.nlm.nih.gov/) und somit die Anforderungen erfüllt an einer Alters-abhängigen Gehirn-Erkrankung beteiligt zu sein. Im Gegensatz dazu zeigten die weiteren im „*Screening*“ inkludierten Mitglieder der T-box Protein Familie (Tbx5 und Tbx21) keinen signifikanten Einfluss auf die Promotoren von ADAM10 bzw. BACE-1. Dieser Befund lässt schließen, dass der Effekt auf ADAM10 Tbx2-spezifisch ist und nicht allgemein von allen Proteinen dieser Genfamilie vermittelt werden kann.

Tbx2 gehört zu einer Familie von Transkriptionsfaktoren, die durch eine hoch-konservierten DNA-Bindedomäne – die T-box – gekennzeichnet sind (Reim *et al.*, 2003; Showell *et al.*, 2004). Die Mitglieder dieser Proteinfamilie können generell in fünf Klassen unterteilt werden, wobei Tbx2 zur Tbx2-Subfamilie zählt (Papaioannou und Silver, 1998). Im Gegensatz zu anderen Vertretern der T-box Familie, gilt Tbx2 als Repressor seiner Zielgene (Carreira *et al.*, 1998; He *et al.*, 1999). Der TF bindet mit seiner DNA-Bindedomäne an spezifische Sequenzen innerhalb der Promotoren der Zielgene – die so genannten T-„*sites*“ *(Carreira et al., 1998)*. Vermittelt wird der Effekt auf die Expression der Zielgene letztlich immer in einem Zusammenspiel aus verschiedenen Ko-Faktoren. Zum Beispiel wurde für Tbx2 eine Wechselwirkung mit dem nicht-DNA bindenden Ko-Repressor Histon-Deacetylase-1 (HDAC-1) beschrieben (Vance *et al.*, 2005). Des Weiteren zeigte das Retinoblastom-Protein-1 (RB-1) eine synergistische Beteiligung an der Tbx2-vermittelten Repression des p21-Promotors (Vance *et al.*, 2010). Im folgenden Text werden gemeinsame Korrelationspunkte von Tbx2 und ADAM10 aufgezeigt, die sich bei der Herzentwicklung, pathobiologischen Prozessen wie Krebs und bei der Zellalterung finden:

a) Herzentwicklung: Die Spaltung des Notch Rezeptors durch ADAM10 führt nach anschließender gamma-Sekretase Spaltung zum Entstehen einer intrazellulären Domäne mit transkriptioneller Aktivität (NICD) (Hartmann *et al.*, 2002). Vor allem die Notch-spezifischen Zielgene Hey1 und Hey2 stehen im Zusammenhang mit der Entwicklung des Atrioventrikularkanals („*atrioventricular channel*“ AVC) (Ehebauer *et al.*, 2006). Beide Proteine regulieren die Expression von spezifischen Zielgenen der Herzmuskelentwicklung. Zum Beispiel wird die Expression von Bmp2 („*bone morphogenetic protein 2*“) reprimiert (Rutenberg *et al.*, 2006). Während der Entwicklung des Myokards führt die Expression von Bmp2 zu einem gesteigerten

Vorkommen von Tbx2, welches wiederum die Menge an Hey1 und Hey 2 regulieren kann (Kokubo *et al.*, 2007). Somit steht Tbx2 zentral in einem zirkulären Regulationsmechanismus der Herzentwicklung, der von ADAM10 durch Spaltung des Notch-Rezeptors initiiert wird.

b) Karzinogenese: ADAM10 spaltet unter physiologischen Bedingungen eine Vielzahl von Substraten. Darunter auch das Typ I Transmembranprotein E-Cadherin, welches für Zell-Zell Kontakte sowie Entwicklungsprozesse der Zelle verantwortlich ist (Halbleib und Nelson, 2006; Maretzky *et al.*, 2005). Eine gesteigerte Spaltung von E-Cadherin durch ADAM10 führt im Rahmen einer Tumorgenese zur Bildung invasions-aggressiveren Zellen mit einem beweglicheren Phänotyp, was die Gefahr einer Metastasierung erhöht (Mechtersheimer *et al.*, 2001). Tbx2 bindet direkt an den Promotor von E-Cadherin und reduziert folglich dessen Expression (Rodriguez *et al.*, 2008). Des Weiteren konnte gezeigt werden, dass durch die Tbx2 vermittelte Reduktion von E-Cadherin ein aggressiver mesenchymaler Brustkrebs-Phänotyp propagiert wird (Wang *et al.*, 2012). Somit stellt das Zelladhäsionsprotein E-Cadherin im Rahmen der Karzinogenese ein Korrelationspunkt zwischen ADAM10 und Tbx2 dar, da es von ADAM10 gespalten wird und seine Expression von Tbx2 reguliert werden kann.

c) Zellalterung: Des Weiteren wurde Tbx2 als Seneszenz-assoziierter Faktor beschrieben, was dessen Erforschung in Hinblick auf Alters-bedingte neurodegenerative Erkrankungen sehr attraktiv erscheinen lässt (Jacobs *et al.*, 2000). Ein wesentliches Merkmal der Seneszenz ist der Arrest des Zellzyklus in der G1 Phase, wobei die Zelle metabolisch aktiv bleibt (Di *et al.*, 1994; Ogryzko *et al.*, 1996). Dieser Arrest wird vorrangig von den Zyklin-abhängigen Kinase Inhibitoren („*cyclin-dependent kinase inhibitors*“ CDKIs) p16 und p21 vermittelt. In vorhergehenden Studien konnte gezeigt werden, dass Tbx2 ein direkter Repressor von p21 ist (Prince *et al.*, 2004) und folglich Seneszenz-verhindernde Eigenschaften aufweist. Somit steht Tbx2 im direkten Zusammenhang mit regulatorischen Faktoren der Seneszenz und konnte in einer unabhängigen Studie durch ein genetisches „*Screening*“ Verfahren als immortalisierender Faktor in primären Fibroblasten identifiziert werden (Jacobs *et al.*, 2000).

Durch die zuvor dargestellten Ergebnisse und die aufgezeigten Korrelationspunkte zwischen ADAM10 und Tbx2 in der Literatur wurde dieser TF für weitere Analysen herangezogen. Im Rahmen von bislang unveröffentlichten Untersuchungen sollte

eine gemeinsame funktionale Korrelation von Tbx2 und ADAM10 in Hinblick auf neurodegenerative Prozesse und insbesondere der AD aufgezeigt werden, die die initialen Befunde des „*Screenings*“ untermauern. Die Senkung der ADAM10-Promotor Aktivität bei Tbx2 Überexpression in neuronalen Zellen konnte auf das endogene ADAM10 neuronaler SH-SY5Y Zellen übertragen werden. Eine vermehrte Expression des TFs führte zu einer reduzierten Menge an ADAM10 mRNA (Abbildung 7 A). *Western blot* Analysen konnten dies auf Protein Ebene bestätigen, indem sowohl die Proform als auch das reife, enzymatisch aktive ADAM10 bei Tbx2 Überexpression signifikant vermindert waren. Folglich war auch die Sekretion des ADAM10-abhängigen Spaltprodukts des APP, APPs-alpha, in den Zellkultur-Überstand signifikant verringert (Abbildung 7 B). Bei einer siRNA-vermittelte Reduzierung von Tbx2 in der Zelle (Abbildung 7 C) konnte gezeigt werden, dass der Tbx2-spezifische Effekt auf die ADAM10-Promotor Aktivität signifikant schwächer ausfällt als bei Zellkulturproben, in denen kein „*Knock-Down*“ stattfand (Abbildung 7 D). Diese Befunde zeigen deutlich, dass Tbx2 unter zellulären Bedingungen in der Lage ist die Menge an ADAM10 zu regulieren, was ebenfalls Effekte auf ADAM10-abhängige Spaltereignisse bezüglich des Substrats APP hat.

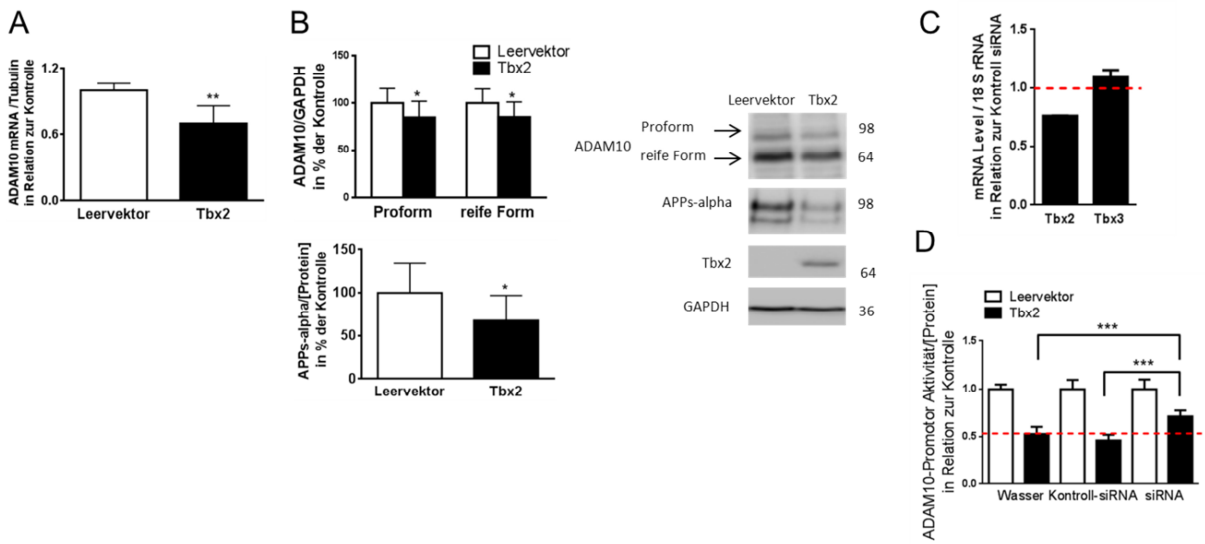

Abbildung 7: Tbx2 reguliert die ADAM10 Genexpression in neuronalen SH-SY5Y Zellen: A) Quantifizierung des ADAM10 mRNA Levels bei Tbx2 Überexpression durch *real-time* RT-PCR. Die gemessenen Werte wurden auf jene von Tubulin normiert und in Bezug zu Leervektor-transfizierten Zellen gesetzt. B) Tbx2 Überexpression senkt die ADAM10 Genexpression. *Western blot* Analysen zeigten bei Tbx2 überexprimierenden SH-SY5Y Zellen eine signifikante Reduzierung des ADAM10 Protein Levels im Vergleich zu Kontroll-transfizierten Zellen. Zudem ergab die Analyse des Zellkultur-Überstandes eine verminderte Sekretion an APPs-alpha. Gezeigt sind die quantitativen Analysen sowie exemplarische *Western blot* Bilder. C) Das Einbringen einer Tbx2-spezifischen siRNA senkt die mRNA Menge von Tbx2 in der Zelle, nicht aber von Tbx3. D) Der „*Knock-Down*" von Tbx2 vermindert den Effekt von Tbx2 auf die ADAM10-Promotor Aktivität. Neuronale Zellen wurden mit einem Kontrollvektor oder mit einem Tbx2 Expressionsvektor transfiziert in Kombination mit Wasser, einer Kontroll-siRNA oder einer Tbx2 spezifischen siRNA. Bei den Kombinationen von Wasser oder Kontroll-siRNA zusammen mit Tbx2 konnte der Effekt auf die ADAM10-Promotor Aktivität dargestellt werden. Der Effekt war signifikant schwächer bei Ko-Transfektion mit Tbx2 siRNA im Vergleich zur Kontrolle.
Gezeigt sind die Mittelwerte ± SD von drei unabhängigen Versuchen. (* $p < 0,05$, ** $p < 0,01$, *** $p < 0,001$).

Auch im Zusammenhang mit Seneszenz wurden im Rahmen dieser Arbeit Experimente durchgeführt, weil dies den wohl stärksten Verknüpfungspunkt von Tbx2 mit Alters-bedingter Neurodegeneration darstellt. Hierbei wird die Seneszenz als Alters-bedingter Arrest des Zellzyklus definiert. Dieser ist geprägt vom Auftreten einer Seneszenz-assoziierten beta-Galaktosidase (Dimri *et al.*, 1995). Dieses Phänomen macht man sich zu Nutze, um gezielt Seneszenz in Zellkulturen nachzuweisen. Hierbei wird die Aktivität des Enzyms durch den Zusatz eines fluorogenen Substrats nachgewiesen (Debacq-Chainiaux *et al.*, 2009). Durch Kontakt-Inhibition wurde in neuronalen SH-SY5Y Zellen Seneszenz induziert (Abbildung 8 A) und so das Zellwachstum temporär gestoppt (Munro *et al.*, 2001). Hierbei wurde die Expression von Tbx2 in der Zelle drastisch nach oben reguliert (Abbildung 8 B). Unter diesen Bedingungen war die Protein Menge an ADAM10 signifikant reduziert. Dies war gefolgt von einer Senkung der APPs-alpha Sekretion in den Zellkultur-Überstand auf

7% im Vergleich zur Kontrolle (Abbildung 8 B). Somit kann gefolgert werden, dass Tbx2 im Kontext von zellulärer Seneszenz vermutlich zur Senkung der ADAM10 Expression beiträgt und somit in diesem Zusammenhang in neurodegenerative Prozesse eingreifen kann.

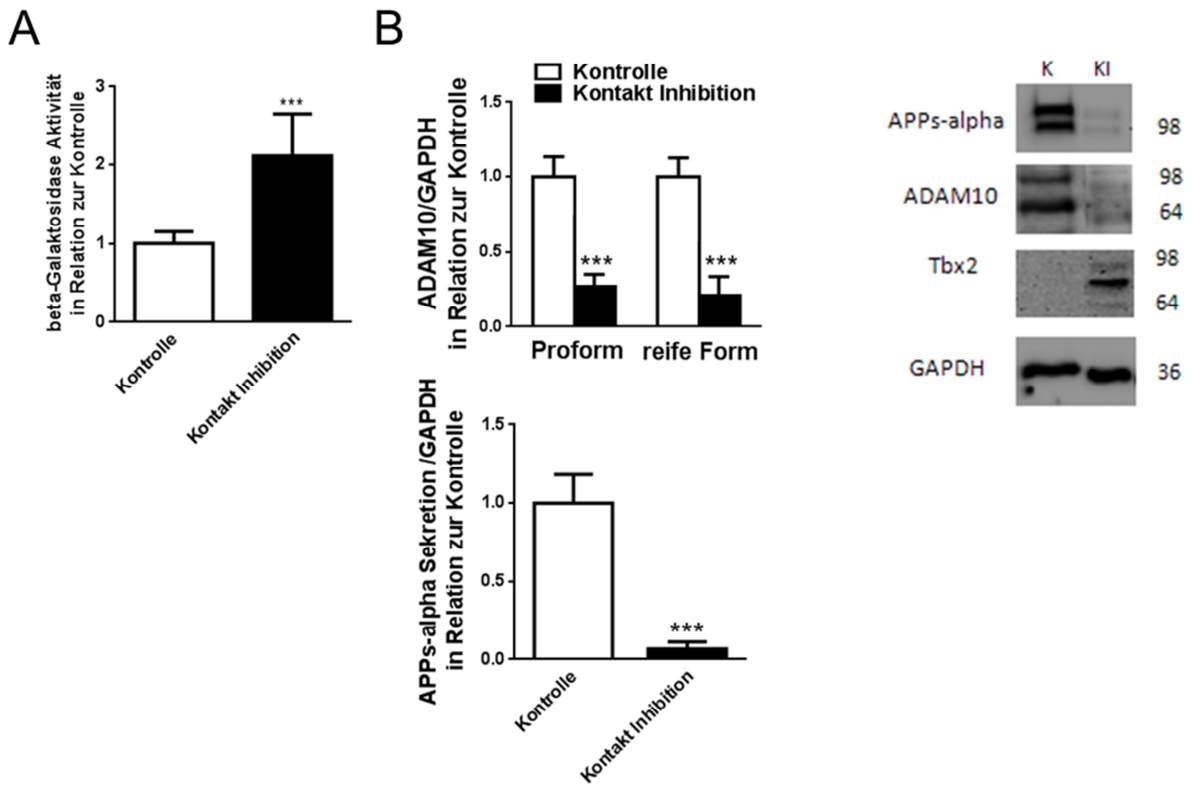

Abbildung 8: Die Regulation von ADAM10 durch Tbx2 im Kontext von zellulärer Seneszenz: A) Nachweis von Seneszenz in Kontakt inhibierten neuronalen SH-SY5Y Zellen. Der Nachweis der Seneszenz-assoziierten beta-Galaktosidase erfolgte durch ein fluorogenes Substrat. B) Tbx2 und ADAM10 sind unter Seneszenz-Bedingungen gegenläufig reguliert. Seneszenz-induzierte SH-SY5Y Zellen zeigten eine Verminderung des ADAM10 Protein Level sowie eine verminderte Sekretion an APPs-alpha in *Western blot* Analysen. Zeitgleich war die Expression von Tbx2 deutlich erhöht.
In dieser Abbildung sind die Mittelwerte ± SD von drei unabhängigen Versuchen gezeigt. (*** $p < 0{,}001$).

Eine Analyse von frontalem Kortexgewebe von AD-Patienten ergab eine signifikante Hochregulation der Tbx2 mRNA Level im Vergleich zu gesunden, Alters-korrelierten Kontrollen (Abbildung 9). In den gleichen Proben blieb die Expression eines weiteren Mitglieds der Tbx-Genfamilie (Tbx21) unbeeinflusst. Aus diesen Ergebnissen geht hervor, dass unter pathologischen Bedingungen Tbx2 signifikant erhöht ist und somit das Potenzial besitzt zu einer verminderten Menge an ADAM10 beizutragen.

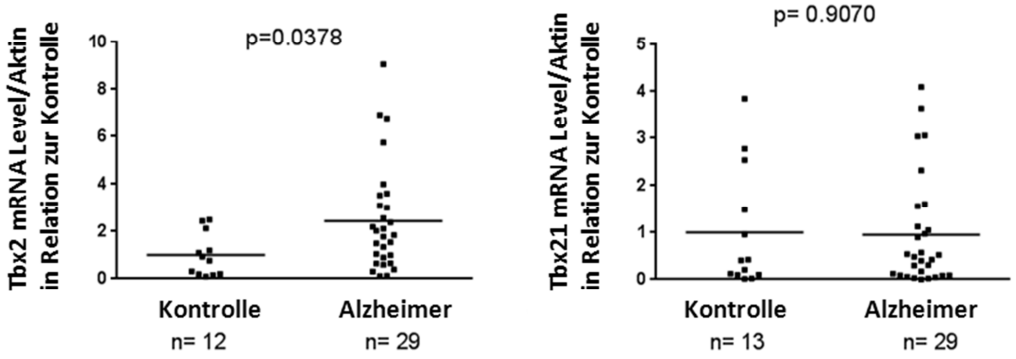

Abbildung 9: Analyse der Tbx2 mRNA Level in post-mortem Kortexgewebe von AD-Patienten: Die Quantitäten der Tbx2 bzw. 21 mRNA aus frontalem Kortexgewebe wurden per *real-time* RT-PCR bestimmt, auf Aktin normiert und in Relation zu gesunden, Alters-korrelierten Patienten gesetzt. Die Anzahl an Proben jeder Gruppe sowie die entsprechenden Signifikanzniveaus sind in den Graphen vermerkt.

Zusammenfassend konnten von 23 TFs bezüglich einer regulativen Funktion der ADAM10 Genexpression identifiziert werden. Zwei TFs (XBP-1 und Tbx2) konnten hinsichtlich ihres molekularen Wirkmechanismus genauer untersucht werden. Zudem wurden die Befunde bezüglich dieser TFs durch Analysen in entsprechenden AD-Modellmäusen (XBP-1) sowie humanem post-mortem Kortexgewebe (XBP-1 und Tbx2) untermauert. Somit haben beide analysierten TFs das Potenzial zur gestörten Homöostase der APP-Prozessierung beizutragen: XBP-1 beeinflusst positiv die Expression von ADAM10. Allerdings sind dessen mRNA Level in AD-Patienten reduziert. Die mRNA Level von Tbx2 nicht aber von Tbx21 sind in post-mortem Kortexgewebe von AD-Patienten signifikant erhöht. In Zellkulturversuchen konnte gezeigt werden, dass Tbx2, in seiner Funktion als Repressor (Carreira *et al.*, 1998; He *et al.*, 1999), die Expression von ADAM10 senkt. Abschließend bleibt zu sagen, dass mit den weiteren 21 TFs interessante Kandidaten verbleiben, deren regulative Funktion sowie pathologische Bedeutung für neurodegenerative Prozesse im Gehirn es zu analysieren gilt, um ein funktionales Netzwerk an pathomechanistisch relevanten Faktoren erstellen zu können, das in seiner Gesamtheit zur Entstehung und zum Fortschreiten der AD beiträgt.

3.1.3 MicroRNAs als Regulatoren der ADAM10 Expression

Ein weiterer Aspekt, der während dieser Promotion erarbeitet wurde, ist die Regulation der AD-relevanten Protease ADAM10 durch microRNAs (miRNAs). Dieser Teil der Dissertation entstand in Zusammenarbeit mit dem Helmholtz Zentrum München und wurde in Augustin et al. 2012 (Kapitel 6 (A)) veröffentlicht. Hierbei

leisteten die Mitarbeiter der Arbeitsgruppe von Prof. Wolfgang Wurst die bioinformatischen Analysen, deren biologische Relevanz durch meine experimentellen Daten unterstrichen wurde. Der Einfluss von miRNAs auf AD-relevante Gene wie zum Beispiel ADAM10 wurde im entsprechenden Abschnitt der Einleitung bereits dargelegt (Kapitel 1.1.3.2). Schätzungen gehen davon aus, dass miRNAs etwa 20-30 % aller humanen Gene regulieren, wobei eine miRNA eine Vielzahl an Zielgenen besitzen kann (Wienholds und Plasterk, 2005). Die zumeist translationale Repression findet durch zwei unterschiedliche Mechanismen statt (Abbildung 10, McDaneld, 2009). Zum einen kann die Bindung einer miRNA an den 3'UTR Bereich der entsprechenden Zielgen-mRNA deren Abbau induzieren (Abbildung 10 A). Zum anderen führen miRNAs zur Dissoziation der Ribosomen von der mRNA und folglich zu einer Blockade der Proteinbiosynthese ohne die Menge der entsprechenden mRNA zu beeinflussen (Abbildung 10 B).

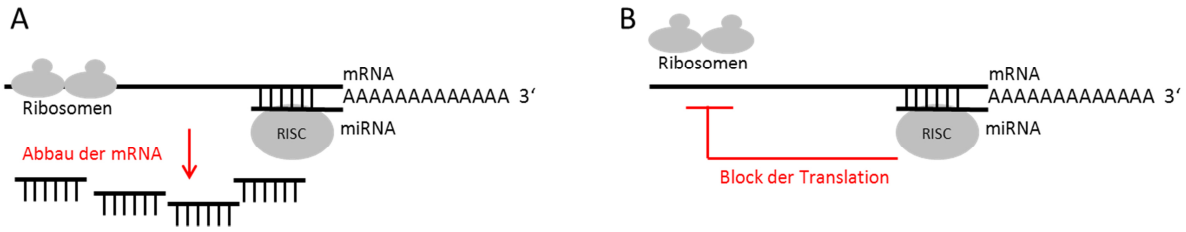

Abbildung 10: Zellulärer Wirkmechanismus von miRNAs: MiRNAs können ihren translationalen Wirkmechanismus auf zwei unterschiedlichen Wegen vermitteln: A) Die Bindung der entsprechenden miRNA an den 3'UTR Bereich des Zielgens führt zum Abbau der mRNA und somit zur verminderten Translation. B) Die Bindung der miRNA führt zur Dissoziation der Ribosomenuntereinheiten von der zu translatierenden mRNA und führt zur Blockade der Proteinbiosynthese.

MiRNAs, die mechanistisch in die AD-Pathogenese eingreifen können, indem sie AD-relevante Zielgene wie zum Beispiel ADAM10 oder BACE-1 regulieren, wurden bislang eher selten erforscht. Vor allem für die protektive Protease ADAM10 konnten erst zwei Veröffentlichungen die Beteiligung von miRNAs an der Regulation von ADAM10 aufzeigen (Kapitel 1.1.3.2, Bai *et al.*, 2009; Cheng *et al.*, 2013). Um nun pathologisch relevante miRNAs zu identifizieren, wurde vom Helmholtz Zentrum München ein bioinformatischer Algorithmus entwickelt, der potenzielle miRNAs, die an den 3'UTR Bereich der humanen ADAM10 mRNA binden, prädiziert. Hierzu wurde folgender Aufbau für die bioinformatischen Analysen gewählt (Abbildung 11 A, Augustin *et al.*, 2012, Kapitel 6 (A)): Die Programme RNA22, RNA Hybrid und miRanda prädizierten 122 miRNAs, die potenziell an den 3'UTR Bereich des humanen ADAM10 binden können. Die erhaltenen miRNAs wurden weiter nach folgenden Kriterien selektiert: Expression im humanen Gehirn und Bindung der murinen miRNA an den entsprechenden 3'UTR Bereich des murinen ADAM10. Zudem wurden die prädizierten miRNAs nach einer Veröffentlichung von Cogswell und Kollegen (Cogswell *et al.*, 2008) auf eine differenzielle Regulation in AD-Patienten analysiert. Die verbleibenden 52 miRNAs wurden weiter auf ihre evolutionäre Konservierung hin untersucht, um eine Spezies übergreifende Funktion dieser miRNAs bezüglich der Regulation von ADAM10 zu gewährleisten. Hierbei wurden letztlich 11 miRNAs als potenzielle Kandidaten selektiert von denen 3 miRNAs experimentell validiert wurden. Die Auswahl der miRNAs 103, 107 und 1306 erfolgte aufgrund ihrer starken Korrelation zu AD-relevanten Zielgenen und wegen ihrem hohen Maß an Konservierung zwischen den verschiedenen Spezies.

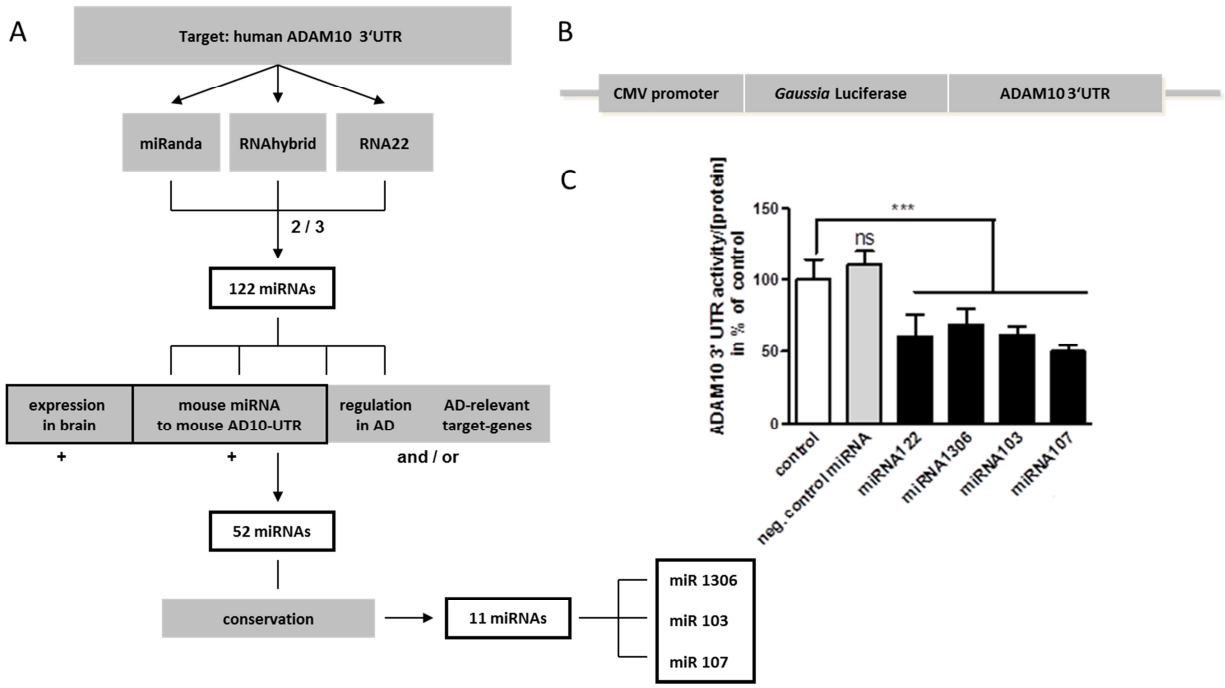

Abbildung 11: Bioinformatische Prädiktion und experimentelle Validierung von ADAM10-bindenden miRNAs: A) Die potenzielle Bindung von miRNAs an den 3'UTR Bereich des humanen ADAM10 wurde mit drei unterschiedlichen Programmen analysiert. Weitere Selektionskriterien wie zum Beispiel die Expression im Gehirn und die differenzielle Regulation in AD-Patienten ergaben 52 verbleibende Kandidaten miRNAs, von denen 11 miRNAs zwischen verschiedenen Spezies evolutionär konserviert waren. Drei durch ihre starke Korrelation zu AD und sehr hohe Konservierung selektierten miRNAs (miRNA 103, 107 und 1306) wurden für weitere Analysen herangezogen. B) Zur experimentellen Validierung wurde ein Luziferase-basierter ADAM10 3'UTR Reporter Vektor generiert, der in der obigen Abbildung schematisch dargestellt ist. Hierbei wird die Expression einer sekretierten Luziferase unter der Kontrolle des CMV-Promotors durch den 3'UTR Bereich des humanen ADAM10 reguliert. C) Experimentelle Validierung der Kandidaten miRNAs durch eine ADAM10 3'UTR Luziferase Reportergen Analyse. Neuronale SH-SY5Y Zellen wurden mit dem Reporter-Konstrukt in Kombination mit einer der selektierten miRNAs oder einer Kontroll-miRNA transfiziert. Die Analyse der miRNA 122 diente als Positivkontrolle (Bai *et al.*, 2009). Nach einer Inkubation von 48 h wurde die Lumineszenz im Zellkultur-Überstand gemessen und die Werte auf den Proteingehalt der Zelllysate normiert. Die Werte wurden in Relation zu Wasser-behandelten Zellen gesetzt und sind als Mittelwerte ± SD von drei unabhängigen Versuchen gezeigt. (ns = nicht signifikant, *** $p < 0{,}001$). (modifiziert nach Augustin et al. 2012 Abbildung 7)

Um die drei selektierten miRNAs experimentell zu validieren, wurde zunächst ein geeignetes Reporter-System etabliert (Abbildung 11 B). Hierzu wurde der Bereich der 3'UTR des humanen ADAM10 bis 738 nt nach dem Stopp-Kodon der ADAM10 kodierenden Sequenz an chromosomaler DNA humaner Zellen nach Bai und Kollegen amplifiziert (Bai *et al.*, 2009) und in einen entsprechenden Reportervektor stromabwärts zu einer *Gaussia*-Luziferase kodierenden Sequenz eingefügt (Augustin *et al.*, 2012, Kapitel 6 (A)). Somit wurde die Expression dieser sekretierten Luziferase

durch die Sequenz der humanen ADAM10 3'UTR reguliert. Neuronale SH-SY5Y Zellen wurden mit dem Reporter-Konstrukt und den entsprechenden miRNAs transient ko-transfiziert. Als Kontrolle wurde eine miRNA verwendet, die eine zufällige Abfolge an Nukleotiden hat und somit eine minimale Bindekapazität bezüglich humaner Sequenzen besitzt. Um potenzielle Nebeneffekte dieser Negativkontrolle auszuschließen, wurden die Zellen in einem Parallelansatz nur mit Wasser als Lösungsmittel der miRNAs behandelt und die experimentell erhaltenen Werte der übrigen Ansätze hiermit verglichen. Die erfolgreiche Überexpression der jeweiligen miRNAs wurde mittels *real-time* RT-PCR nachgewiesen (Daten nicht gezeigt). Die miRNA 122, für die ein regulatorischer Effekt auf den 3'UTR Bereich des ADAM10 bereits beschrieben war (Bai *et al.*, 2009), wurde als Positivkontrolle herangezogen. Eine zeitaufgelöste Messung des Reportersignals im Zellkultur-Überstand abhängig von der Überexpression dieser miRNA ergab einen optimalen Zeitpunkt für eine voll ausgeprägter Effektstärke von 48 h (Daten nicht gezeigt). Die Überexpression der selektierten miRNAs 103, 107 und 1306 sowie der Kontroll-miRNA 122 ergab eine signifikante Reduktion des Reportersignals von circa 40% (Abbildung 11 C, Augustin *et al.*, 2012, Kapitel 6 (A)). Die Verminderung der Lumineszenz ist vermutlich zurückzuführen auf die Bindung der entsprechenden miRNA an den 3'UTR Bereich von ADAM10 innerhalb des Reporter-Konstrukts. Somit konnten alle bioinformatisch selektierten miRNAs experimentell erfolgreich auf ihre Funktionalität bezüglich eines ADAM10-regulierenden Effekts hin verifiziert werden. Durch die Senkung der ADAM10 Expression und die differenzielle Regulation in AD-Patienten als zusätzliches Selektionskriterium könnten diese miRNAs zu der gestörten Homöostase der APP-Prozessierung beitragen und folglich eine regulative Funktion in der AD-Pathogenese haben. Hierzu sind jedoch weitere Analysen notwendig (4. Schlussfolgerungen und Ausblick). Des Weiteren könnten mit diesem etablierten Modell auch miRNAs identifiziert werden, die relevante Zielgene anderer Krankheiten regulieren, indem der 3'UTR Reporter Vektor sowie die Selektionskriterien entsprechend angepasst werden.

3.2 Therapeutische Intervention bei der Alzheimer-Pathogenese

Die nachfolgend dargestellten Ergebnisse wurden zum Teil in Freese *et al.* 2014 (Kapitel 6 (C)) veröffentlicht. Die Befunde werden zusätzlich durch unveröffentlichte Ergebnisse bezüglich der Evaluierung von potenziellen AD-Therapeutika ergänzt. Hierzu werden auch Ergebnisse bezüglich der Spaltung des Zelladhäsionsmoleküls Neuroligin-1 (NL-1) durch ADAM10 besprochen, die im Rahmen eines Forschungsaufenthaltes an der Universität von Tokio erhalten wurden.

Wie bereits im entsprechenden Kapitel der Einleitung (Kapitel 1.1.3.2) beschrieben, wurden in den letzten Jahren vor allem BACE-1- und gamma-Sekretase Inhibitoren untersucht, um die gesteigerte Generierung neurotoxischer A-beta Peptide zu vermindern. Ein therapeutischer Aspekt, der im Rahmen dieser Dissertation untersucht wurde, besteht in dem Eingreifen in die gestörte Homöostase der APP-Prozessierung durch eine Erhöhung der ADAM10 Genexpression (Übersicht in Endres und Fahrenholz, 2012). Bei dieser pharmakologischen Intervention würde neben der Senkung der A-beta Menge auch das neuroprotektive und neurotrophe Fragment APPs-alpha entstehen. Allerdings sollten auch bei diesem Ansatz potenzielle Nebenwirkungen abgewogen werden, da ADAM10 neben APP weitere physiologisch relevante Substrate besitzt (Pruessmeyer und Ludwig, 2009). Für eine Induktion der ADAM10 Genexpression stellt der Einsatz synthetischer Retinoide ein gut erforschtes Gebiet dar (Shudo *et al*., 2009). Zum Beispiel induziert Tamibaroten (Am80) die Menge an ADAM10 in APP-transgenen Mäusen und führt zudem zur Linderung der A-beta vermittelten Neuroinflammation (Kawahara *et al*., 2009). Zudem konnte gezeigt werden, dass das synthetische Retinoid Acitretin durch Erhöhung der intrazellulären Retinsäure Konzentration die Genexpression der protektiven Protease ADAM10 erhöht (Tippmann *et al*., 2009). Des Weiteren konnte in Gehirnen von AD-Modellmäusen gezeigt werden, dass eine einmalige stereotaktische Injektion von Acitretin zu einer erhöhten Sekretion von APPs-alpha führt und gleichzeitig die Menge an neurotoxischen A-beta Peptiden signifikant senkt (Tippmann *et al*., 2009).

Die Identifizierung von weiteren Substanzen, die die ADAM10 Expression induzieren, könnte zum Beispiel zu einem verminderten Potenzial an Nebenwirkungen führen.

3.2.1 Untersuchung einer Wirkstoff-Bibliothek auf die Expression von ADAM10

Im Rahmen dieser Dissertation sollten Substanzen auf eine mögliche ADAM10 Expressions-steigernde Wirkung untersucht werden. Hierzu wurde eine 640 Wirkstoffe umfassende Substanz-Bibliothek (*FDA approved drug library*, Enzo Life Science, Farmingdale, NY, USA) herangezogen. Hierbei sind alle verwendeten Medikamente bereits von der FDA für verschiedene Krankheiten zugelassen. Durch die bereits bestehende Zulassung könnte die Initiierung von klinischen Studien an Patienten beschleunigt werden, da alle Medikamente zum Beispiel hinsichtlich Dosierung und Verträglichkeit im Menschen bereits charakterisiert sind.

Um zunächst die Zell-Viabilität neuronaler Zellen unter dem Einfluss einer der 640 Substanzen zu analysieren, wurde ein Luziferase-basierter, ATP-abhängiger Assay verwendet, der direkt auf die metabolische Aktivität der Zellen schließen lässt. Auch nach seriellen Verdünnungen zeigten 13 Substanzen eine generelle Reduktion der Zell-Viabilität und wurden somit für das nachfolgende „*Screening*“ ausgeschlossen (Daten nicht gezeigt). Für die Analyse der verbleibenden 627 Substanzen, die in der getesteten Konzentration keinen Einfluss auf die Zell-Viabilität hatten, wurden SH-SY5Y Zellen mit dem dualen Vektor, der auch zur Analyse der 704 TFs verwendet wurde (Kapitel 3.1), transfiziert und anschließend mit der entsprechenden Substanz für 48 h inkubiert. Hierbei konnten 44 Substanzen identifiziert werden, die therapeutisches Potenzial haben, indem sie die ADAM10 Genexpression steigern und/oder die BACE-1-Promotor Aktivität senken (Abbildung 12 A, grünes Kästchen). Die erhaltenen Werte wurden prozentual in Relation zu DMSO behandelten Zellen gesetzt und Acitretin diente als Positivkontrolle für eine Steigerung der ADAM10-Promotor Aktivität (siehe Markierung in Abbildung 12 A). Zur weiteren Selektion der Medikamente bezüglich des Potenzials in die gestörte APP-Prozessierung einzugreifen, wurde der Effekt auf den humanen APP-Promotor untersucht. Eine zusätzliche pharmakologische Beeinflussung des Substrats APP wäre im Rahmen einer Therapie unvorteilhaft, da somit die physiologische Funktion des APP in der Zelle beeinträchtigt werden könnte. Der Luziferase-basierte Reportergen Assay zeigte, dass von den 44 Substanzen 35 keinen Einfluss auf die humane APP-Promotor Aktivität hatten (Abbildung 12 B).

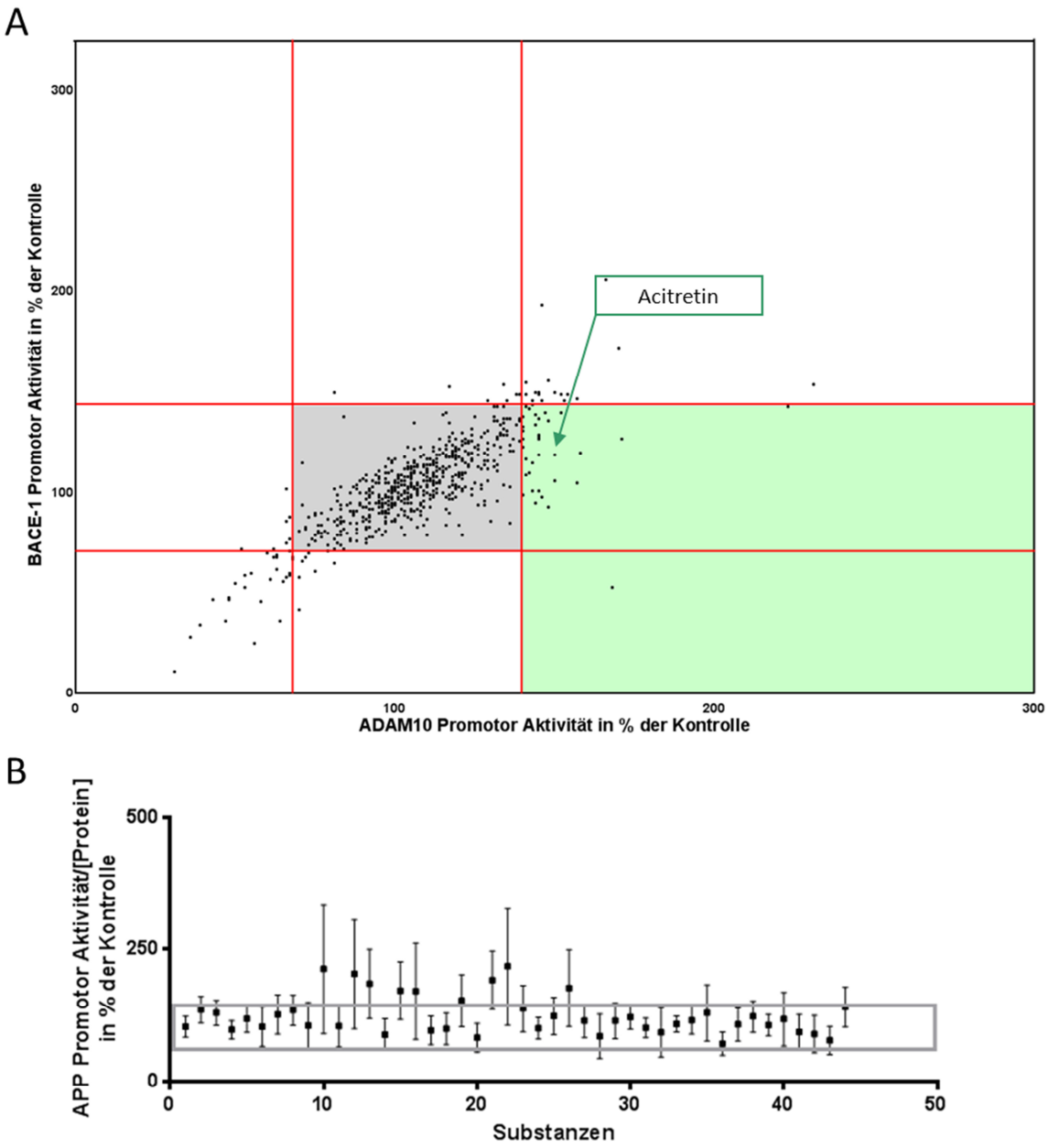

Abbildung 12: Untersuchung von 627 Medikamenten einer Wirkstoffbibliothek auf die ADAM10 und BACE-1 Genexpression: A) „*Screening*" der Substanzen auf ihren Effekt bezüglich der ADAM10- und BACE-1-Promotor Aktivität. Die Transfektion von neuronalen SH-SY5Y Zellen mit dem dualen Reportergen Vektor und anschließende Inkubation mit einer der 627 Substanzen ergab 45 Substanzen (inklusive Acitretin) die die ADAM10-Promotor Aktivität erhöhen und/oder die BACE-1-Promotor Aktivität senken und somit therapeutisches Potenzial besitzen. (140% > Quotient ADAM10/BACE-1 < 70%, grünes Kästchen). B) Analyse der Kandidaten-Substanzen auf die Beeinflussung des humanen APP-Promotors. 35 von den zuvor evaluierten 44 Substanzen zeigten keinen signifikanten Einfluss auf den humanen APP-Promotor (Punkte innerhalb des grauen Kästchens) und wurden folglich für weitere Analysen ausgewählt.
(Die Daten sind gezeigt als Mittelwerte ± SD von drei unabhängigen Versuchen)

3.2.2 Evaluierung der Blut-Hirn Schranke-Gängigkeit der Kandidaten-Substanzen

Wie schon in der Einleitung beschrieben (Kapitel 1.1.3.2) ist eine maßgebliche Anforderung an eine therapeutisch wirksame Substanz, die gegen Erkrankungen des zentralen Nervensystems (ZNS) gerichtet ist, die Fähigkeit die BHS zu überwinden. Jedoch gibt es nicht für alle FDA-zugelassenen Medikamente Daten zur BHS-Gängigkeit, da viele Substanzen für ihre gedachte Applikation nicht zwingend zentral-nervös wirksam sein müssen. Bioinformatische Prädiktionen können mit einer gewissen Wahrscheinlichkeit die Permeationsfähigkeit einer Substanz voraussagen. Dies ist abhängig von Moleküleigenschaften wie Größe, Lipophilie oder räumlicher Struktur (Crivori *et al.*, 2000; Waterhouse, 2003). Um die BHS-Penetrationsfähigkeit der zuvor selektierten Kandidaten-Substanzen zu untersuchen, wurde in Zusammenarbeit mit Dr. Christian Freese (Institut für Pathologie, Universitätsmedizin Mainz, AG Prof. Dr. Charles J. Kirkpatrick) ein Zellkultur-basiertes *in vitro* BHS Modell entwickelt, welches Rückschlüsse über die Penetrationsfähigkeit von Substanzen, für die ein therapeutisches Potenzial hinsichtlich ADAM10 nachgewiesen wurde, gibt. Die nachfolgend vorgestellten Ergebnisse wurden in Freese *et al.* 2014 (Kapitel 6 (C)) veröffentlicht.

Das Modell besteht im Wesentlichen aus einem Transwell-System, in dem das obere Kompartiment mit primären Schweine-Hirn Endothelzellen („*porcine brain endothelial cells*“, PBECs), die die physiologische Barriere bilden, besetzt ist und das untere Kompartiment des Systems mit neuronalen SH-SY5Y Zellen (Abbildung 13). Die neuronalen Zellen sind mit einem Luziferase-basierten Reporter Vektor transfiziert, der abhängig von der Aktivität des humanen ADAM10-Promotors die Expression einer Luziferase steuert.

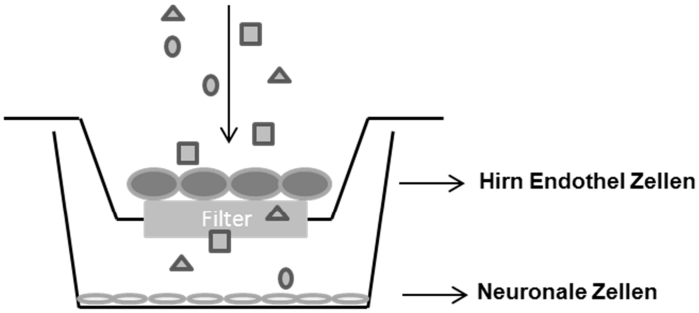

Abbildung 13: Schematische Darstellung des *in vitro* Blut-Hirn Schranke (BHS) Modells: Zur Selektion von therapeutisch bedeutsamen Substanzen wurde ein Ko-Kultur System etabliert. Hierbei werden als Barriere-bildende Zellen Schweine Hirn Endothel Zellen (PBECs) verwendet, die im oberen Kompartiment eines Transwell-Systems ausgesät sind. Im unteren Kompartiment befinden sich neuronale SH-SY5Y Zellen, die mit einem ADAM10-Promotor-abhängigen Luziferase Reporter Konstrukt transfiziert sind. Somit können Substanzen, die bereits auf einen Effekt auf die ADAM10 Genexpression hin analysiert wurden, auf ihre BHS Gängigkeit untersucht werden (in Anlehnung an Freese et al. 2014, Abbildung 1).

Das System wurde zunächst auf eine wechselseitige Beeinflussung beider Zelllinien untersucht (Freese *et al.*, 2014, Kapitel 6 (C)). Hierzu wurden die Endothelzellen sowie die neuronalen SH-SY5Y Zellen hinsichtlich Zell-Viabilität und Caspase 3/7 Induktion bei Ko-Kultivierung im Vergleich zu den entsprechenden Mono-Kulturen analysiert. Des Weiteren wurden die PBECs bei gleichzeitiger Ko-Kultivierung mit SH-SY5Y Zellen auf eine veränderte Expression von „*Tight Junction*“ Proteinen, die die Ausbildung von intakten Zell-Zell Kontakten indizieren, untersucht sowie die Expression des wichtigsten Effluxtransporters der BHS - P-Glykoprotein (P-gp) - analysiert. Keiner der gemessenen Parameter zeigte signifikante Veränderungen bei Ko-Kultivierung im Vergleich zur entsprechenden Mono-Kultur. Die Eigenschaften der Barriere wurden durch Messungen der elektrischen Widerstandsfähigkeit über beide Kompartimente („*trans endothelial electrical* resistance“, TEER) sowie des so genannten Durchlässigkeitskoeffizienten („*permeability* coefficient“, P_{app}) ermittelt. Hierbei zeigte die Barriere eine signifikante Steigerung des TEER Wertes bei Ko-Kultivierung mit SH-SY5Y Zellen im Vergleich zu PBEC Mono-Kulturen. Dies deutet auf verbesserte Barriere-Eigenschaften hin. Dieser Befund konnte auch mit der Bestimmung des P_{app}-Werts bestätigt werden. Der parazelluläre Transport eines fluoreszierenden Moleküls (Natrium-Fluoresceinisothiocyanat, Na-FITC) war bei Ko-Kultur-Bedingungen signifikant niedriger als bei Endothelzellen alleine. Die neuronalen Zellen wurden zu den Messungen bezüglich Zell-Viabilität und Caspase 3/7 Induktion auch auf klassische Proteine typischer Signaltransduktionswege wie zum Beispiel ERK1/2 und Proteine des Glukoneogenese-Stoffwechsels in Form von

GSK3-beta (Glykogen-Synthase Kinase 3-beta) analysiert (Freese *et al.*, 2014, Kapitel 6 (C)). In *Western blot* Analysen zeigten die aktiven Formen beider Proteine keine signifikante Beeinflussung bei Ko-Kultivierung beider Zelllinien. Dies deutet darauf hin, dass sowohl wichtige Signaltransduktionswege sowie metabolische Parameter unter Ko-Kultivierung nicht beeinträchtigt sind. Mit dem Nachweis von GSK3-beta konnten auch Rückschlüsse auf ein wesentliches pathologisches Merkmal der AD gemacht werden, da dieses Enzym das Protein Tau phosphoryliert (Ishiguro *et al.*, 1993; Ishiguro *et al.*, 1992) und folglich zum Entstehen von neurofibrillären Bündeln beiträgt. Um ein weiteres Hauptmerkmal der AD-Pathogenese, die A-beta Generierung, zu untersuchen, wurden die SH-SY5Y Zellen auch auf einen veränderten ADAM10-abhängigen APP-Metabolismus bei Ko-Kultivierung mit PBECs untersucht. Protein biochemische Analysen bezüglich der Expression von ADAM10 und APP sowie der Sekretion von APPs-alpha zeigten keine signifikanten Veränderungen verglichen mit entsprechenden einzeln kultivierten SH-SY5Y Zellen. Somit konnten keine negativen Parameter bei einer Ko-Kultivierung beider Zelllinien erhalten werden und zudem eine gesteigerte Dichtigkeit der Barriere, wenn PBECs zusammen mit neuronalen Zellen kultiviert werden.

Um die erfolgreiche Etablierung des Systems hinsichtlich des Transports von Substanzen über die von PBECs gebildete Barriere zu analysieren, wurde Acitretin als Modell-Substanz verwendet. Das synthetische Retinoid ist bereits etabliert hinsichtlich eines steigernden Effekts auf die ADAM10 Genexpression (Tippmann *et al.*, 2009) und ist zudem auch als BHS-gängig *in vivo* charakterisiert (Eisenhardt und Bickel, 1994; Holthoewer *et al.*, 2012). Die Menge an transportiertem Acitretin in das untere, neuronale Zellen enthaltene Kompartiment wurde durch HPLC Analysen detektiert (Abbildung 14 A, Freese *et al.*, 2014, Kapitel 6 (C)). Die Konzentration an Acitretin wurde so eingesetzt, dass bei ungehinderter Passage (w/o PBECs) eine Konzentration von 2 µM im unteren Kompartiment zu erwarten gewesen wäre. Dies ist in etwa im Einklang mit den erhaltenen Ergebnissen für das Modell ohne Endothelzell-Barriere (1,77 µM, Abbildung 14 A). Für das System mit PBECs konnte eine Acitretin-Konzentration von 1,24 µM per HPLC detektiert werden (Abbildung 14 A). Dies deutet darauf hin, dass wohlmöglich ein Teil des Acitretins in den Zellen verbleibt und dort vermutlich Stoffwechselprozessen unterliegt. Um parallel einen potenziellen parazellulären Transport zu detektieren, wurde der Durchlässigkeits-koeffizient von Fluoreszein bestimmt. Die Daten zeigen, dass der parazelluläre

Transport signifikant erniedrigt ist, sobald eine Barriere durch PBECs in dem System vorhanden ist (Abbildung 14 A). Unter diesen Bedingungen wurde Acitretin dennoch in das untere Kompartiment transportiert, was auf einen Transport durch die Endothelzellen schließen lässt. Hierbei erreicht Acitretin in bioaktiver Form das untere Kompartiment, da die Aktivität des humanen ADAM10-Promotors im Vergleich zu DMSO behandelten Zellen signifikant erhöht war (Abbildung 14 B).

Die Etablierung des BHS-Modells ermöglicht die Untersuchung potenzieller Induktoren der ADAM10 Genexpression auf ihre BHS-Gängigkeit. Somit sind keine HPLC Messungen notwendig, die für jede Substanz neu zu etablieren wären. Des Weiteren wird die Anzahl an notwendigen Tierversuchen reduziert, da zunächst eine Zellkultur-basierte Selektion mit diesem Modell möglich ist.

A

	Acitretin [µM]*	P_{app} (Acitretin) [cm x min^{-1}]	P_{app} (NaFITC$_{Acitretin}$) [cm x min^{-1}]
w/o PBEC	1.77 ± 0.22	1.55×10^{-4}	1.48×10^{-4}
PBEC	1.24 ± 0.29	1.09×10^{-4}	6.05×10^{-5}

* concentrations in lower compartment measured by HPLC

B

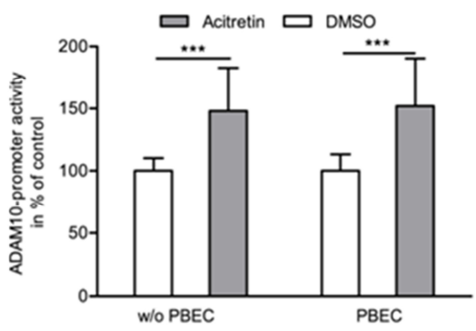

Abbildung 14: Etablierung des BHS-Systems an der Modell-Substanz Acitretin: A) Acitretin wird über die Endothelzell-Barriere transportiert. Um einen parazellulären Transport von Acitretin auszuschließen, wurde parallel der Durchlässigkeitskoeffizient von Fluoreszein bestimmt. Der Transport von Fluoreszein war signifikant erniedrigt, wenn eine Endothelzell-Barriere im System enthalten war. Unter diesen Bedingungen wurde Acitretin in das untere Kompartiment transportiert, was mit HPLC Messungen detektiert werden konnte. B) Acitretin induziert die ADAM10 Expression. Das transportierte Acitretin erreichte das untere Kompartiment in bioaktiver Form, da es die Aktivität des humanen ADAM10-Promotors im Vergleich zur Lösungsmittel-Kontrolle signifikant erhöhte. Gezeigt sind Mittelwerte ± SD von drei unabhängigen Versuchen (*** $p < 0{,}001$). (modifiziert nach Freese et al 2014 Abbildung 4)

23 der 35 aus dem „*Screening*“ evaluierten Substanzen zeigten einen induzierenden Effekt auf die ADAM10-Promotor Aktivität während die BACE-1 sowie APP

Genexpression unbeeinflusst blieben. Somit kommen diese 23 Substanzen für eine ADAM10-gerichtete Therapie gegen die AD prinzipiell in Frage und wurden nachfolgend mit dem etablierten BHS-Modell auf ihre Permeationsfähigkeit analysiert. Um eine intakte Barriere zum Zeitpunkt der Transportversuche zu gewährleisten, wurde jeweils vor und nach der Behandlung mit den entsprechenden Substanzen der TEER Wert bestimmt. Zu jedem Zeitpunkt der Analyse lag eine dichte Barriere durch die PBECs vor (Daten nicht gezeigt). Acitretin als Positivkontrolle induzierte signifikant die humane ADAM10-Promotor Aktivität in den neuronalen Zellen des unteren Kompartiments. Unter diesen Bedingungen konnte für neun Substanzen der induzierende Effekt auf den ADAM10-Promotor aus vorhergehenden Analysen unter Transport-Bedingungen reproduziert werden. Somit gelten im Rahmen des etablierten *in vitro* Modells diese neun Substanzen als BHS-permeabel und erfüllen die grundlegenden Anforderungen an ein Medikament, welches die Menge an ADAM10 im Gehirn von AD-Patienten erhöhen soll. Jedoch konnte im Rahmen dieses Versuchs nicht geklärt werden, ob die restlichen Substanzen generell die Barriere nicht überqueren können, wieder heraus transportiert werden oder durch metabolisierende Enzyme nur in inaktiver Form das untere Kompartiment erreichen. In weiteren Studien muss für die identifizierten neun Substanzen der genaue zelluläre Wirkmechanismus im Detail geklärt werden.

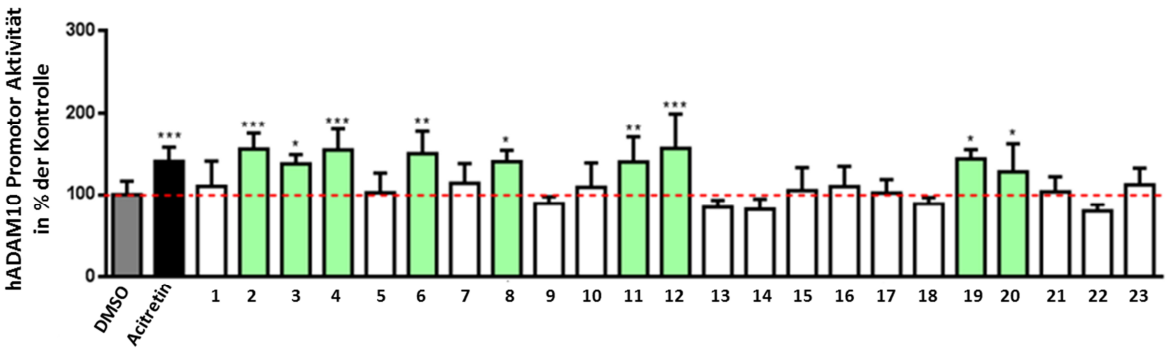

Abbildung 15: Analyse der BHS-Gängigkeit der Kandidaten-Substanzen: 23 Substanzen aus den initialen Versuchen zeigten einen induzierenden Effekt auf die ADAM10-Promotor Aktivität während die BACE-1 und APP Expression unbeeinflusst blieb. Diese Substanzen haben somit therapeutisches Potenzial und wurden mit dem *in vitro* BHS-Modell analysiert. Als Positivkontrolle wurde Acitretin verwendet, das die ADAM10 Expression signifikant erhöhte. Neun der 23 analysierten Substanzen zeigten eine signifikante Erhöhung der ADAM10-Promotor Aktivität in neuronalen Zellen nach dem Transport über die Endothelzell-Barriere und gelten somit als BHS-permeabel. Gezeigt sind die Mittelwerte ± SD von drei unabhängigen Versuchen. (* $p < 0,05$, ** $p < 0,01$, *** $p < 0,001$).

3.2.3 Die Spaltung von Neuroligin-1 durch ADAM10

Wie schon zuvor in der Einleitung besprochen (Kapitel 1.1.3.2) ist ein wichtiger Aspekt, den man bei einer ADAM10-basierenden Therapie beachten muss, dass ADAM10 als Protease neben APP viele verschiedene Substrate besitzt. Allerdings wurden einige davon lediglich durch Zellkultur-basierte Studien identifiziert. Weiterführende Analysen in geeigneten Tiermodellen wiederlegten zum Teil die Substrateigenschaften für ADAM10 *in vivo*. Zum Beispiel wurde beschrieben, dass Neuregulin-1 (NR-1), das unter anderem wichtig für die Myelinisierung von peripheren Nerven ist (Willem *et al.*, 2006), durch ADAM10 gespalten werden kann (Luo *et al.*, 2011). Ein siRNA vermittelter „*Knock Down*" von ADAM10 führte zu einer verminderten Spaltung von NR-1 in HEK293 Zellen. Im Gegensatz dazu konnte gezeigt werden, dass in Mäusen, die ADAM10 überexprimieren, die NR-1 Spaltung im Vergleich zu Kontroll-Tieren unbeeinflusst blieb (Freese *et al.*, 2009). Dies war ebenfalls gefolgt von einer unveränderten Dicke der Myelinhülle von peripheren Nerven. Ein weiteres Beispiel ist die Spaltung des Prion Proteins, das als zerebrale Ablagerungen bei spongiformer Enzephalopathie auftritt. In ADAM10 deffizienten Fibroblasten der Maus konnte eine reduzierte Sekretion von N1, dem löslichen Fragment des Prion Proteins, detektiert werden (Vincent *et al.*, 2000; Vincent *et al.*, 2001). Zudem führte eine stabile Überexpression von ADAM10 in HEK293 Zellen zu einer verstärkten Sekretion von N1. Im Gegensatz dazu zeigten Mäuse mit neuronaler Überexpression von ADAM10 eine Reduzierung aller Prion Protein Spezies im Gehirn der Tiere (Endres *et al.*, 2009). Dies lässt eher auf eine Beeinflussung der Menge des zellulären Prion Proteins als auf eine ADAM10-regulierte Spaltung schließen.

Ein aktuelles Beispiel für ein physiologisches ADAM10-Substrat ist das neuronale Zelladhäsionsprotein Neuroligin-1 (NL-1), durch dessen Spaltung die exzitatorische Signalweiterleitung glutamaterger Neurone reguliert wird (Song *et al.*, 1999). Hierbei konnte von der Gruppe um Prof. Taisuke Tomita ADAM10 als hauptverantwortliche Protease für die Spaltung von NL-1 identifiziert und zudem deren Auswirkung auf die synaptische Funktion im Gehirn charakterisiert werden (Suzuki *et al.*, 2012). Im Rahmen eines Forschungsaufenthalts an der Universität von Tokio (Graduate School of Pharmaceutical Siences, Department of Neuropathology and Neuroscience, Prof. Taisuke Tomita) sollte untersucht werden, ob Acitretin als Modell-Substanz mit therapeutischem Potenzial auch zu einer vermehrten Spaltung von NL-1 führen

kann. Um hierbei die Ergebnisse mit dem Einsatz eines physiologisch relevanten Systems zu untermauern, wurden alle Experimente mit primären kortikalen Neuronen der Ratte durchgeführt.

Um zunächst die Grundlage für eine Untersuchung der ADAM10-basierten Spaltung von NL-1 zu schaffen, wurde der Effekt von Acitretin auf die ADAM10 Expression in primären Neuronen untersucht. Nach Inkubation mit Acitretin war die Expression von ADAM10 sowohl auf mRNA als auch auf Protein Ebene signifikant erhöht (Abbildung 16 A, B). Unter diesen Bedingungen konnte auch eine gesteigerte Sekretion des ADAM10-abhängigen Spaltprodukts, APPs-alpha, in den Zellkultur-Überstand detektiert werden, während die Genexpression des APP nicht beeinflusst wurde (Abbildung 16 C). Zudem konnte gezeigt werden, dass gleichzeitig das Spaltprodukt, welches durch BACE-1 generiert wird, APPs-beta, vermindert vorliegt (Abbildung 16 C). In einer vorhergehenden Arbeit konnte gezeigt werden, dass die alpha- bzw. beta-Sekretase Spaltung nicht immer kompetitiv ablaufen (Colombo *et al.*, 2012). Trotz einer verminderten Menge an ADAM10 konnte keine gesteigerte Spaltung von APP durch BACE-1 in primären Neuronen der Maus detektiert werden. Die Ergebnisse der eigenen Arbeit zeigen jedoch eine gewisse Konkurrenz zwischen ADAM10 und BACE-1 um das gemeinsame Substrat APP, zumindest bei einer Retinoid-induzierten Menge an ADAM10. Dies ist in Einklang mit vorherigen Arbeiten die zeigen konnten, dass die beiden Spaltereignisse in Modellen mit Überexpression oder pharmakologischer Induktion der Proteasen invers gekoppelt sind: Eine pharmakologische Aktivierung der alpha-Sekretase durch muskarinische Acetylcholinrezeptor Agonisten führte zu einer gesenkten Menge an A-beta Peptiden (Nitsch *et al.*, 1992). Darüber hinaus zeigte die Überexpression von BACE-1 in Mäusen eine Reduktion der ADAM10-regulierten Spaltung des APP (Kuhn *et al.*, 2010; Vassar *et al.*, 1999; Willem *et al.*, 2004).

Auch die Sekretion der neurotoxischen A-beta Peptide lag bei Acitretin Inkubation im Vergleich zur Lösungsmittel Kontrolle signifikant vermindert vor (Abbildung 16 D). Hierbei wurden sowohl A-beta 40 bzw. 42, die je nach Schnittmechanismus der gamma-Sekretase entstehen, durch spezifische ELISAs nachgewiesen. Da im Rahmen dieser Analysen die Entstehung sowohl von A-beta 40 als auch von A-beta 42 verringert wurde, lässt dies auf einen gamma-Sekretase unabhängigen Mechanismus schließen. Somit war zunächst gesichert, dass die Modell-Substanz Acitretin den gewünschten Effekt auch in dem gewählten Test-System hat.

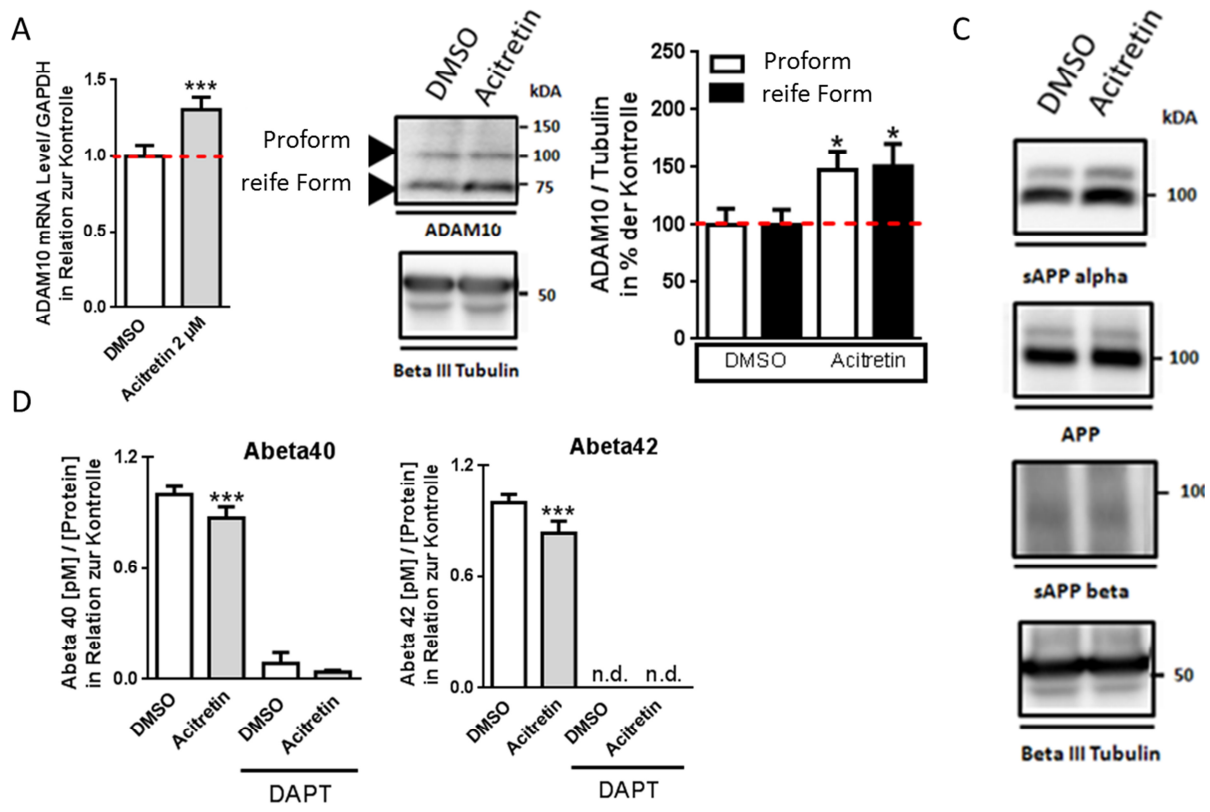

Abbildung 16: Acitretin induziert die ADAM10-abhängige Spaltung von APP in primären kortikalen Neuronen der Ratte: A-B) Eine 48 stündige Inkubation der primären Zellkulturen mit Acitretin führte zu einer gesteigerten Menge der ADAM10 mRNA sowie der entsprechenden Protein Level. Zur Normierung der Ergebnisse wurde zusätzlich das Neuronen-spezifische beta-III-Tubulin nachgewiesen. Exemplarisch sind Bilder der entsprechenden *Western blot* Analysen gezeigt sowie die quantitative Auswertung. C) Die erhöhte Menge an ADAM10 führte auch zur vermehrten nicht-amyloidogenen Spaltung von APP. Gezeigt sind exemplarische Nachweise aus den Zellkultur-Überständen (APPs-alpha, APPs-beta) sowie aus den Lysaten (APP und beta-III-Tubulin). D) Die Menge an A-beta 40 bzw. 42 wurde durch ELISA im Überstand nachgewiesen. Hierbei diente die Inhibition der gamma-Sekretase mit DAPT als Spezifitätskontrolle. A,B,D) Gezeigt sind die Mittelwerte ± SD von drei unabhängigen Versuchen. (nd = nicht detektiert, * $p < 0,05$, *** $p < 0,001$).

Unter diesen Bedingungen wurde die Sekretion der löslichen Ektodomäne von NL-1 in den Zellkultur-Überstand per *Western blot* Methode untersucht. Bei Inkubation mit Acitretin wurde vermehrt NL-1 gespalten und folglich das lösliche Fragment vermehrt in den Zellkulturüberstand abgegeben (Abbildung 17). Da der verwendete Antikörper ein Epitop in der extrazellulären Domäne des NL-1 erkennt, das nicht spezifisch für das ADAM10-abhängige Fragment ist, wird bei diesem Nachweis die Summe aller Spaltereignisse nachgewiesen. Die Sekretion des löslichen NL-1 Fragments war durch den Matrix-Metalloproteinase Inhibitor GM6001 hemmbar (Daten nicht gezeigt). Zudem konnte von der Gruppe um Prof. Taisuke Tomita nachgewiesen werden, dass von den potenziellen alpha-Sekretasen NL-1 nur von ADAM10

gespalten wird (Suzuki *et al.*, 2012). Um Rückschlüsse geben zu können, ob der beobachtete Effekt auf einer veränderten Genexpression von NL-1 beruht, wurden auch die Protein Level von NL-1 in den entsprechenden Zell-Lysaten nachgewiesen, wobei keine signifikante Veränderung detektiert werden konnte (Abbildung 17). Somit führt Acitretin in primären Neuronen der Ratte nicht nur zu einer gesteigerten, von ADAM10-regulierten Spaltung von APP sondern auch von NL-1. Allerdings ist der Effekt auf die Spaltung von NL-1 nicht sehr stark ausgeprägt jedoch statistisch signifikant unterschiedlich zu DMSO behandelten Zellkulturen (Abbildung 17).

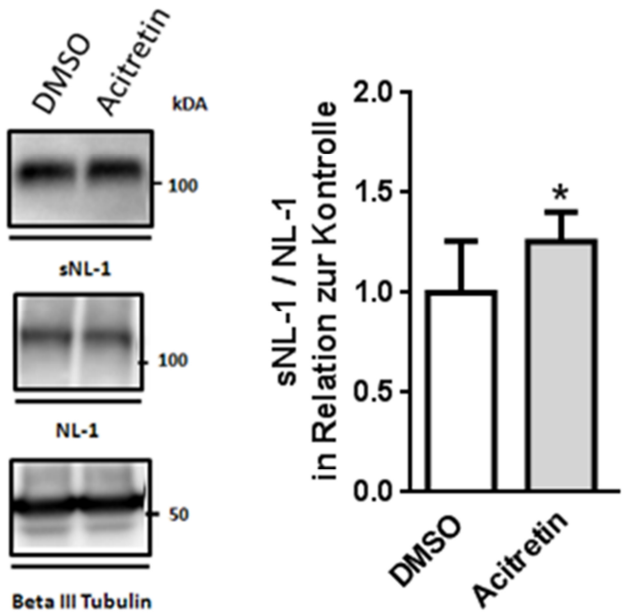

Abbildung 17: Acitretin erhöht die Spaltung von Neuroligin-1 in primären Neuronen der Ratte: Die Analyse der Zellkultur-Überstände nach 48 stündiger Inkubation mit Acitretin, ergab eine signifikante Erhöhung der löslichen NL-1-Ektodomäne. Unter diesen Bedingungen war die Expression von NL-1 im Zell-Lysat im Vergleich zu DMSO behandelten Zellen unverändert. Die Werte des löslichen NL-1 Fragments (sNL-1) wurden auf die des Volllängenproteins (NL-1) normiert. Dargestellt sind repräsentative *Blot* Bilder sowie die quantitative Analyse von drei unabhängigen Versuchen in Triplikaten. Gezeigt sind die Mittelwerte ± SD. (* $p < 0,05$).

Die Spaltung von NL-1 durch ADAM10 an der Postsynapse könnte zu dem Verlust der Interaktion mit dessen Bindungspartner Neurexin und folglich der trans-synaptischen Signalweiterleitung führen (Baudouin und Scheiffele, 2010). Somit ist bei einer Acitretin-basierten Therapie der AD vermutlich mit einer verminderten Aktivität glutamaterger Neurone zu rechnen. Es konnte gezeigt werden, dass die Prävalenz für Krampfanfälle in AD-Patienten zehnmal höher ist als in einer entsprechenden Kontroll-Population (Hauser *et al.*, 1986). Dies deutet auf eine gestörte exzitatorische Signalweiterleitung im Gehirn von AD-Patienten hin. Eine

moderate Überexpression von ADAM10 in APP-transgenen Mäusen führte zu einer milderen Auswirkung von Kainat-induzierten Krampfanfällen bezüglich einer schwächeren Intensität und einer kürzeren Erholungsphase (Clement *et al.*, 2008). Es wäre denkbar, dass bei einer pharmakologisch-induzierten Spaltung von NL-1 durch ADAM10, das damit verbundene Abschalten der glutamatergen Signalweiterleitung auch zu einer geringeren Anzahl an Krampfanfällen in AD-Patienten führen könnte.

Eine pharmakologisch-induzierte Erhöhung der NL-1 Spaltung könnte auch im Rahmen anderer Erkrankungen interessant sein. Mutationen innerhalb der Neuroligin-Genfamilie konnten zum Beispiel in einigen Arbeiten mit der Autismus-Erkrankung kausal korreliert werden (Jamain *et al.*, 2003; Laumonnier *et al.*, 2004; Übersicht in Zoghbi, 2003). In einem Autismus-Mausmodell, welches zu sozialem Fehlverhalten führt und somit einen autistischen Phänotyp aufweist, konnte eine gesteigerte Menge an Volllängen-NL-1 detektiert werden (Gkogkas *et al.*, 2013). Dies führte folglich zu einer übermäßigen synaptischen Aktivität glutamaterger Neuronen der Tiere. Nach einer siRNA-vermittelten Reduzierung des NL-1 Levels in hippokampalen Neuronen war die synaptische Aktivität wieder vergleichbar mit Wildtyp Mäusen (Gkogkas *et al.*, 2013). Daher könnte auch eine Retinoid-vermittelte Induktion der NL-1 Spaltung, zu einer Reduktion der gestörten NL-1-vermittelten Signalweiterleitung im Kontext von autistischen Störungsbildern führen.

4. Schlussfolgerungen und Ausblick

In der hier vorliegenden Dissertation wurden sowohl molekulare Faktoren identifiziert, die zu der Dysbalance der APP-Prozessierung und somit zum Entstehen und Fortschritt der Krankheit beitragen, als auch Substanzen evaluiert, die in die gestörte Homöostase der APP-Prozessierung eingreifen können und somit therapeutisches Potenzial aufzeigen.

Im Rahmen einer Hochdurchsatz-Analyse von 704 humanen Transkriptionsfaktoren (TFs) konnten 23 TFs identifiziert werden, die das Verhältnis von ADAM10- zu BACE-1-Promotor Aktivität signifikant modulieren. Hierbei wurden zwei Faktoren (XBP-1, Tbx2) bezüglich ihres detaillierten Wirkmechanismus analysiert. Der TF XBP-1 erhöht die ADAM10 Genexpression. Jedoch ist die XBP-1-vermittelte Signalweiterleitung sowohl in zwei verschiedenen AD-Mausmodellen als auch in post-mortem Kortexgewebe von AD-Patienten signifikant vermindert. Ein interessanter Punkt wäre die Analyse von Gehirnproben von Patienten mit „*mild cognitive impairment*“ (MCI), um eine Regulation von XBP-1 in frühen pathologischen Stadien im Menschen analysieren zu können. Der Seneszenz-assoziierte TF Tbx2 verminderte die Expression von ADAM10 in Zellkultur-Experimenten. Zudem sind die mRNA Level von Tbx2 in Kortexgewebe von AD-Patienten im Vergleich zu gesunden Kontrollen signifikant erhöht. In weiteren Studien sollte die Tbx2-Bindestelle innerhalb der ADAM10-Promotor Sequenz durch Protein-DNA Bindungsstudien identifiziert werden. Des Weiteren sollte der Beitrag von Ko-Faktoren wie zum Beispiel des Retinoblastom Protein 1 (RB1) (Vance *et al.*, 2010) zu der Tbx2-vermittelten Regulation von ADAM10 analysiert werden. Datenbankanalysen (EST-Profil Analyse) könnten eine ausreichend starke Expression der analysierten TFs zum Beispiel in Leukozyten aufzeigen. Ein möglicher Nachweis der TFs in peripherem Gewebe könnte als potenzieller Biomarker in der Diagnostik eingesetzt werden. Voraussetzung hierbei wäre allerdings, dass das periphere Expressionsprofil mit dem des ZNS übereinstimmt. Zudem verbleiben 21 TFs, die in den initialen Analysen identifiziert wurden. Jene sollten ebenfalls auf ihren zellulären Mechanismus und deren Bedeutung für die AD hin untersucht werden. Somit wäre es möglich ein funktionales Netzwerk an relevanten Faktoren erstellen zu können, das dazu beiträgt die zugrunde liegenden Mechanismen der gestörten APP-Prozessierung zu verstehen.

Des Weiteren konnten drei microRNAs identifiziert werden, die die Expression des humanen ADAM10 senken. Die miRNAs sollten zudem auf ihren Effekt auf das zelleigene ADAM10 (mRNA und Protein) untersucht werden, um auf den genauen zellulären Mechanismus der miRNAs schließen zu können (Abbau der mRNA oder Stopp der Translation). Denkbar wäre auch die Analyse eines Mausmodells, das eine der Kandidaten-miRNAs überexprimiert, um die Auswirkung dieser miRNA auf die Expression von ADAM10 *in vivo* zu untersuchen. Des Weiteren konnte die miRNA 107 in einem bereits durchgeführten Vortest in humanem Plasma nachgewiesen werden (Daten nicht gezeigt). Weitere Untersuchungen, wie zum Beispiel die differenzielle Regulation dieser miRNAs in Blutproben von AD-Patienten, könnten den Einsatz der selektierten miRNAs als Biomarker in der AD ermöglichen.

Bezüglich der Evaluierung von Substanzen, die die Menge an ADAM10 erhöhen, konnten in einem Hochdurchsatz-Verfahren von 640 FDA-zugelassenen Medikamenten einer Substanz-Bibliothek 23 Substanzen identifiziert werden, die die ADAM10-Promotor Aktivität signifikant induzierten. Neun dieser Substanzen wurden durch ein entwickeltes Modell als BHS-permeabel klassifiziert. Hierbei muss der genaue zelluläre Wirkmechanismus einer jeden verbleibenden Substanz in weiteren Zellkultur-Experimenten und geeigneten AD-Mausmodellen analysiert werden. Da die identifizierten Substanzen bereits von der FDA zugelassen sind und im Alltag für verschiedene Krankheiten angewendet werden, wäre die Analyse bezüglich einer gesteigerten ADAM10 Expression in Proben von Patienten, die im Rahmen anderer Indikationen die Medikamente erhalten, interessant.

Im Rahmen eines Forschungsaufenthalts an der Universität von Tokio (Prof. Taisuke Tomita) konnte anhand einer Acitretin-induzierten Erhöhung von ADAM10 eine gesteigerte Spaltung von NL-1 beobachtet werden. Interessant wäre die Analyse der NL-1 Spaltung in BACE-1 transgenen Mäusen. Die vermehrte Expression der beta-Sekretase würde in diesem Modell die AD-Pathologie besser abbilden. Ebenfalls denkbar wäre der Einsatz von induzierbaren pluripotenten Stammzellen von AD-Patienten, die zu Neuronen umprogrammiert werden, um eine genaue Beteiligung von ADAM10 bei der Spaltung von NL-1 in diesem Kontext zu analysieren. Interessant wäre auch die Analyse des löslichen Spaltprodukts von NL-1 im Vergleich zu APPs-alpha in CSF-Proben von AD-Patienten.

5. Literaturverzeichnis

Ahmed RR, Holler CJ, Webb RL, Li F, Beckett TL, and Murphy MP (2010) BACE1 and BACE2 enzymatic activities in Alzheimer's disease. *J Neurochem,* **112,** 1045-1053.

Aizenstein HJ, Nebes RD, Saxton JA, Price JC, Mathis CA, Tsopelas ND, Ziolko SK, James JA, Snitz BE, Houck PR, Bi W, Cohen AD, Lopresti BJ, DeKosky ST, Halligan EM, and Klunk WE (2008) Frequent amyloid deposition without significant cognitive impairment among the elderly. *Arch Neurol,* **65,** 1509-1517.

Akiyama H, Barger S, Barnum S, Bradt B, Bauer J, Cole GM, Cooper NR, Eikelenboom P, Emmerling M, Fiebich BL, Finch CE, Frautschy S, Griffin WS, Hampel H, Hull M, Landreth G, Lue L, Mrak R, Mackenzie IR, McGeer PL, O'Banion MK, Pachter J, Pasinetti G, Plata-Salaman C, Rogers J, Rydel R, Shen Y, Streit W, Strohmeyer R, Tooyoma I, Van Muiswinkel FL, Veerhuis R, Walker D, Webster S, Wegrzyniak B, Wenk G, and Wyss-Coray T (2000) Inflammation and Alzheimer's disease. *Neurobiol Aging,* **21,** 383-421.

Alzheimer A, Stelzmann RA, Schnitzlein HN, and Murtagh FR (1995) An English translation of Alzheimer's 1907 paper, "Uber eine eigenartige Erkankung der Hirnrinde". *Clin Anat,* **8,** 429-431.

Anders A, Gilbert S, Garten W, Postina R, and Fahrenholz F (2001) Regulation of the alpha-secretase ADAM10 by its prodomain and proprotein convertases. *FASEB J,* **15,** 1837-1839.

Antonarakis SE, Lyle R, Dermitzakis ET, Reymond A, and Deutsch S (2004) Chromosome 21 and down syndrome: from genomics to pathophysiology. *Nat Rev Genet,* **5,** 725-738.

Armstrong JL, Ruiz M, Boddy AV, Redfern CP, Pearson AD, and Veal GJ (2005) Increasing the intracellular availability of all-trans retinoic acid in neuroblastoma cells. *Br J Cancer,* **92,** 696-704.

Arriagada PV, Growdon JH, Hedley-Whyte ET, and Hyman BT (1992) Neurofibrillary tangles but not senile plaques parallel duration and severity of Alzheimer's disease. *Neurology,* **42,** 631-639.

Augustin R, Endres K, Reinhardt S, Kuhn PH, Lichtenthaler SF, Hansen J, Wurst W, and Trümbach D (2012) Computational identification and experimental validation of microRNAs binding to the Alzheimer-related gene ADAM10. *BMC Med Genet,* **13,** 35.

Avila J, Lucas JJ, Perez M, and Hernandez F (2004) Role of tau protein in both physiological and pathological conditions. *Physiol Rev,* **84,** 361-384.

Aydin D, Filippov MA, Tschape JA, Gretz N, Prinz M, Eils R, Brors B, and Müller UC (2011) Comparative transcriptome profiling of amyloid precursor protein family members in the adult cortex. *BMC Genomics,* **12,** 160.

Bai S, Nasser MW, Wang B, Hsu SH, Datta J, Kutay H, Yadav A, Nuovo G, Kumar P, and Ghoshal K (2009) MicroRNA-122 inhibits tumorigenic properties of hepatocellular carcinoma cells and sensitizes these cells to sorafenib. *J Biol Chem,* **284,** 32015-32027.

Baudouin S and Scheiffele P (2010) SnapShot: Neuroligin-neurexin complexes. *Cell,* **141,** 908, 908.

Bayer TA, Paliga K, Weggen S, Wiestler OD, Beyreuther K, and Multhaup G (1997) Amyloid precursor-like protein 1 accumulates in neuritic plaques in Alzheimer's disease. *Acta Neuropathol,* **94,** 519-524.

Bekris LM, Yu CE, Bird TD, and Tsuang DW (2010) Genetics of Alzheimer disease. *J Geriatr Psychiatry Neurol,* **23,** 213-227.

Bernales S, Soto MM, and McCullagh E (2012) Unfolded protein stress in the endoplasmic reticulum and mitochondria: a role in neurodegeneration. *Front Aging Neurosci,* **4,** 5.

Bernstein HG, Bukowska A, Krell D, Bogerts B, Ansorge S, and Lendeckel U (2003) Comparative localization of ADAMs 10 and 15 in human cerebral cortex normal aging, Alzheimer disease and Down syndrome. *J Neurocytol,* **32,** 153-160.

Biessels GJ, Staekenborg S, Brunner E, Brayne C, and Scheltens P (2006) Risk of dementia in diabetes mellitus: a systematic review. *Lancet Neurol,* **5,** 64-74.

Bolmont T, Clavaguera F, Meyer-Luehmann M, Herzig MC, Radde R, Staufenbiel M, Lewis J, Hutton M, Tolnay M, and Jucker M (2007) Induction of tau pathology by intracerebral infusion of amyloid-beta -containing brain extract and by amyloid-beta deposition in APP x Tau transgenic mice. *Am J Pathol,* **171,** 2012-2020.

Bolmont T, Haiss F, Eicke D, Radde R, Mathis CA, Klunk WE, Kohsaka S, Jucker M, and Calhoun ME (2008) Dynamics of the microglial/amyloid interaction indicate a role in plaque maintenance. *J Neurosci,* **28,** 4283-4292.

Bornemann KD, Wiederhold KH, Pauli C, Ermini F, Stalder M, Schnell L, Sommer B, Jucker M, and Staufenbiel M (2001) Abeta-induced inflammatory processes in microglia cells of APP23 transgenic mice. *Am J Pathol,* **158,** 63-73.

Busciglio J, Gabuzda DH, Matsudaira P, and Yankner BA (1993) Generation of beta-amyloid in the secretory pathway in neuronal and nonneuronal cells. *Proc Natl Acad Sci U S A,* **90,** 2092-2096.

Buxbaum JD, Koo EH, and Greengard P (1993) Protein phosphorylation inhibits production of Alzheimer amyloid beta/A4 peptide. *Proc Natl Acad Sci U S A,* **90,** 9195-9198.

Buxbaum JD, Liu KN, Luo Y, Slack JL, Stocking KL, Peschon JJ, Johnson RS, Castner BJ, Cerretti DP, and Black RA (1998) Evidence that tumor necrosis factor alpha converting enzyme is involved in regulated alpha-secretase cleavage of the Alzheimer amyloid protein precursor. *J Biol Chem,* **273,** 27765-27767.

Cai H, Wang Y, McCarthy D, Wen H, Borchelt DR, Price DL, and Wong PC (2001) BACE1 is the major beta-secretase for generation of Abeta peptides by neurons. *Nat Neurosci,* **4,** 233-234.

Cai Y, Xiong K, Zhang XM, Cai H, Luo XG, Feng JC, Clough RW, Struble RG, Patrylo PR, Chu Y, Kordower JH, and Yan XX (2010) beta-Secretase-1 elevation in aged monkey and Alzheimer's disease human cerebral cortex occurs around the vasculature in partnership with multisystem axon terminal pathogenesis and beta-amyloid accumulation. *Eur J Neurosci,* **32,** 1223-1238.

Calfon M, Zeng H, Urano F, Till JH, Hubbard SR, Harding HP, Clark SG, and Ron D (2002) IRE1 couples endoplasmic reticulum load to secretory capacity by processing the XBP-1 mRNA. *Nature,* **415,** 92-96.

Cao L, Schrank BR, Rodriguez S, Benz EG, Moulia TW, Rickenbacher GT, Gomez AC, Levites Y, Edwards SR, Golde TE, Hyman BT, Barnea G, and Albers MW (2012) Abeta alters the connectivity of olfactory neurons in the absence of amyloid plaques in vivo. *Nat Commun,* **3,** 1009.

Cao X and Südhof TC (2004) Dissection of amyloid-beta precursor protein-dependent transcriptional transactivation. *J Biol Chem,* **279,** 24601-24611.

Carreira S, Dexter TJ, Yavuzer U, Easty DJ, and Goding CR (1998) Brachyury-related transcription factor Tbx2 and repression of the melanocyte-specific TRP-1 promoter. *Mol Cell Biol,* **18,** 5099-5108.

Carter J and Lippa CF (2001) Beta-amyloid, neuronal death and Alzheimer's disease. *Curr Mol Med,* **1,** 733-737.

Casas C, Sergeant N, Itier JM, Blanchard V, Wirths O, van der Kolk N, Vingtdeux V, van de Steeg E, Ret G, Canton T, Drobecq H, Clark A, Bonici B, Delacourte A, Benavides J, Schmitz C, Tremp G, Bayer TA, Benoit P, and Pradier L (2004) Massive CA1/2 neuronal loss with intraneuronal and N-terminal truncated Abeta42 accumulation in a novel Alzheimer transgenic model. *Am J Pathol,* **165,** 1289-1300.

Cavalieri M, Ropele S, Petrovic K, Pluta-Fuerst A, Homayoon N, Enzinger C, Grazer A, Katschnig P, Schwingenschuh P, Berghold A, and Schmidt R (2010) Metabolic syndrome, brain magnetic resonance imaging, and cognition. *Diabetes Care,* **33,** 2489-2495.

Cheng C, Li W, Zhang Z, Yoshimura S, Hao Q, Zhang C, and Wang Z (2013) MicroRNA-144 is regulated by activator protein-1 (AP-1) and decreases expression of Alzheimer disease-related a disintegrin and metalloprotease 10 (ADAM10). *J Biol Chem,* **288,** 13748-13761.

Cheret C, Willem M, Fricker FR, Wende H, Wulf-Goldenberg A, Tahirovic S, Nave KA, Saftig P, Haass C, Garratt AN, Bennett DL, and Birchmeier C (2013) Bace1 and Neuregulin-1 cooperate to control formation and maintenance of muscle spindles. *EMBO J,* **32,** 2015-2028.

Cho HJ, Son SM, Jin SM, Hong HS, Shin DH, Kim SJ, Huh K, and Mook-Jung I (2009) RAGE regulates BACE1 and Abeta generation via NFAT1 activation in Alzheimer's disease animal model. *FASEB J,* **23,** 2639-2649.

Christensen MA, Zhou W, Qing H, Lehman A, Philipsen S, and Song W (2004) Transcriptional regulation of BACE1, the beta-amyloid precursor protein beta-secretase, by Sp1. *Mol Cell Biol,* **24,** 865-874.

Clement AB, Hanstein R, Schroder A, Nagel H, Endres K, Fahrenholz F, and Behl C (2008) Effects of neuron-specific ADAM10 modulation in an in vivo model of acute excitotoxic stress. *Neuroscience,* **152,** 459-468.

Cogswell JP, Ward J, Taylor IA, Waters M, Shi Y, Cannon B, Kelnar K, Kemppainen J, Brown D, Chen C, Prinjha RK, Richardson JC, Saunders AM, Roses AD, and Richards CA (2008) Identification of miRNA changes in Alzheimer's disease brain and CSF yields putative biomarkers and insights into disease pathways. *J Alzheimers Dis,* **14,** 27-41.

Colombo A, Wang H, Kuhn PH, Page R, Kremmer E, Dempsey PJ, Crawford HC, and Lichtenthaler SF (2012) Constitutive alpha- and beta-secretase cleavages of the amyloid precursor protein are partially coupled in neurons, but not in frequently used cell lines. *Neurobiol Dis,* **49C,** 137-147.

Corder EH, Saunders AM, Strittmatter WJ, Schmechel DE, Gaskell PC, Small GW, Roses AD, Haines JL, and Pericak-Vance MA (1993) Gene dose of apolipoprotein E type 4 allele and the risk of Alzheimer's disease in late onset families. *Science,* **261,** 921-923.

Corrigan F, Pham CL, Vink R, Blumbergs PC, Masters CL, van den Heuvel C, and Cappai R (2011) The neuroprotective domains of the amyloid precursor protein, in traumatic brain injury, are located in the two growth factor domains. *Brain Res,* **1378,** 137-143.

Cotman CW, Poon WW, Rissman RA, and Blurton-Jones M (2005) The role of caspase cleavage of tau in Alzheimer disease neuropathology. *J Neuropathol Exp Neurol,* **64,** 104-112.

Craft S (2009) The role of metabolic disorders in Alzheimer disease and vascular dementia: two roads converged. *Arch Neurol,* **66,** 300-305.

Crain BJ, Hu W, Sze CI, Slunt HH, Koo EH, Price DL, Thinakaran G, and Sisodia SS (1996) Expression and distribution of amyloid precursor protein-like protein-2 in Alzheimer's disease and in normal brain. *Am J Pathol,* **149,** 1087-1095.

Crivori P, Cruciani G, Carrupt PA, and Testa B (2000) Predicting blood-brain barrier permeation from three-dimensional molecular structure. *J Med Chem,* **43,** 2204-2216.

de Bruijn RF, Janssen JA, Brugts MP, van Duijn CM, Hofman A, Koudstaal PJ, and Ikram MA (2014) Insulin-Like Growth Factor-I Receptor Stimulating Activity is Associated with Dementia. *J Alzheimers Dis*.

de Felice FG, Wu D, Lambert MP, Fernandez SJ, Velasco PT, Lacor PN, Bigio EH, Jerecic J, Acton PJ, Shughrue PJ, Chen-Dodson E, Kinney GG, and Klein WL (2008) Alzheimer's disease-type neuronal tau hyperphosphorylation induced by A beta oligomers. *Neurobiol Aging,* **29,** 1334-1347.

Deane R, Du YS, Submamaryan RK, LaRue B, Jovanovic S, Hogg E, Welch D, Manness L, Lin C, Yu J, Zhu H, Ghiso J, Frangione B, Stern A, Schmidt AM, Armstrong DL, Arnold B, Liliensiek B, Nawroth P, Hofman F, Kindy M, Stern D, and Zlokovic B (2003) RAGE mediates amyloid-beta peptide transport across the blood-brain barrier and accumulation in brain. *Nat Med,* **9,** 907-913.

Debacq-Chainiaux F, Erusalimsky JD, Campisi J, and Toussaint O (2009) Protocols to detect senescence-associated beta-galactosidase (SA-betagal) activity, a biomarker of senescent cells in culture and in vivo. *Nat Protoc,* **4,** 1798-1806.

Di LA, Linke SP, Clarkin K, and Wahl GM (1994) DNA damage triggers a prolonged p53-dependent G1 arrest and long-term induction of Cip1 in normal human fibroblasts. *Genes Dev,* **8,** 2540-2551.

Dimri GP, Lee X, Basile G, Acosta M, Scott G, Roskelley C, Medrano EE, Linskens M, Rubelj I, Pereira-Smith O, and . (1995) A biomarker that identifies senescent human cells in culture and in aging skin in vivo. *Proc Natl Acad Sci U S A,* **92,** 9363-9367.

Donahue JE, Flaherty SL, Johanson CE, Duncan JA, III, Silverberg GD, Miller MC, Tavares R, Yang W, Wu Q, Sabo E, Hovanesian V, and Stopa EG (2006) RAGE, LRP-1, and amyloid-beta protein in Alzheimer's disease. *Acta Neuropathol,* **112,** 405-415.

Dysken MW, Sano M, Asthana S, Vertrees JE, Pallaki M, Llorente M, Love S, Schellenberg GD, McCarten JR, Malphurs J, Prieto S, Chen P, Loreck DJ, Trapp G, Bakshi RS, Mintzer JE, Heidebrink JL, Vidal-Cardona A, Arroyo LM, Cruz AR, Zachariah S, Kowall NW, Chopra MP, Craft S, Thielke S, Turvey CL, Woodman C, Monnell KA, Gordon K, Tomaska J, Segal Y, Peduzzi PN, and Guarino PD (2014) Effect of vitamin E and memantine on functional decline in Alzheimer disease: the TEAM-AD VA cooperative randomized trial. *JAMA,* **311,** 33-44.

Ehebauer M, Hayward P, and Martinez-Arias A (2006) Notch signaling pathway. *Sci STKE,* **2006,** cm7.

Eisenhardt EU and Bickel MH (1994) Kinetics of tissue distribution and elimination of retinoid drugs in the rat. I. Acitretin. *Drug Metab Dispos,* **22,** 26-30.

Elkabes S, di Cicco-Bloom EM, and Black IB (1996) Brain microglia/macrophages express neurotrophins that selectively regulate microglial proliferation and function. *J Neurosci,* **16,** 2508-2521.

Endres K and Fahrenholz F (2010) Upregulation of the alpha-secretase ADAM10--risk or reason for hope? *FEBS J,* **277,** 1585-1596.

Endres K and Fahrenholz F (2012) Regulation of alpha-secretase ADAM10 expression and activity. *Exp Brain Res,* **217,** 343-352.

Endres K, Mitteregger G, Kojro E, Kretzschmar H, and Fahrenholz F (2009) Influence of ADAM10 on prion protein processing and scrapie infectiosity in vivo. *Neurobiol Dis,* **36,** 233-241.

Endres K, Postina R, Schroeder A, Mueller U, and Fahrenholz F (2005) Shedding of the amyloid precursor protein-like protein APLP2 by disintegrin-metalloproteinases. *FEBS J,* **272,** 5808-5820.

Endres K and Reinhardt S (2013) ER-stress in Alzheimer's disease: turning the scale? *Am J Neurodegener Dis,* **2,** 247-265.

Eriksen JL, Sagi SA, Smith TE, Weggen S, Das P, McLendon DC, Ozols VV, Jessing KW, Zavitz KH, Koo EH, and Golde TE (2003) NSAIDs and enantiomers of flurbiprofen target gamma-secretase and lower Abeta 42 in vivo. *J Clin Invest,* **112,** 440-449.

Escrevente C, Morais VA, Keller S, Soares CM, Altevogt P, and Costa J (2008) Functional role of N-glycosylation from ADAM10 in processing, localization and activity of the enzyme. *Biochim Biophys Acta,* **1780,** 905-913.

Faraci FM (2006) Reactive oxygen species: influence on cerebral vascular tone. *J Appl Physiol (1985),* **100,** 739-743.

Fellgiebel A, Kojro E, Müller MJ, Scheurich A, Schmidt LG, and Fahrenholz F (2009) CSF APPs alpha and phosphorylated tau protein levels in mild cognitive impairment and dementia of Alzheimer's type. *J Geriatr Psychiatry Neurol,* **22,** 3-9.

Ferrer I, Blanco R, Carmona M, Puig B, Ribera R, Rey MJ, and Ribalta T (2001) Prion protein expression in senile plaques in Alzheimer's disease. *Acta Neuropathol,* **101,** 49-56.

Fishel MA, Watson GS, Montine TJ, Wang Q, Green PS, Kulstad JJ, Cook DG, Peskind ER, Baker LD, Goldgaber D, Nie W, Asthana S, Plymate SR, Schwartz MW, and Craft S (2005) Hyperinsulinemia provokes synchronous increases in central inflammation and beta-amyloid in normal adults. *Arch Neurol,* **62,** 1539-1544.

Freese C, Garratt AN, Fahrenholz F, and Endres K (2009) The effects of alpha-secretase ADAM10 on the proteolysis of neuregulin-1. *FEBS J,* **276,** 1568-1580.

Freese C, Reinhardt S, Hefner G, Unger RE, Kirkpatrick CJ, and Endres K (2014) A novel blood-brain barrier co-culture system for drug targeting of Alzheimer's disease: establishment by using acitretin as a model drug. *PLoS One,* **9,** e91003.

Fukumoto J, Fukumoto I, Parthasarathy PT, Cox R, Huynh B, Ramanathan GK, Venugopal RB, Allen-Gipson DS, Lockey RF, and Kolliputi N (2013) NLRP3 deletion protects from hyperoxia-induced acute lung injury. *Am J Physiol Cell Physiol,* **305,** C182-C189.

Gamblin TC, Chen F, Zambrano A, Abraha A, Lagalwar S, Guillozet AL, Lu M, Fu Y, Garcia-Sierra F, LaPointe N, Miller R, Berry RW, Binder LI, and Cryns VL (2003) Caspase cleavage of tau: linking amyloid and neurofibrillary tangles in Alzheimer's disease. *Proc Natl Acad Sci U S A,* **100,** 10032-10037.

Gauthier SG (2005) Alzheimer's disease: the benefits of early treatment. *Eur J Neurol,* **12 Suppl 3,** 11-16.

Ghosh AK, Bilcer G, Harwood C, Kawahama R, Shin D, Hussain KA, Hong L, Loy JA, Nguyen C, Koelsch G, Ermolieff J, and Tang J (2001) Structure-based design: potent inhibitors of human brain memapsin 2 (beta-secretase). *J Med Chem,* **44,** 2865-2868.

Ghosh AK, Brindisi M, and Tang J (2012) Developing beta-secretase inhibitors for treatment of Alzheimer's disease. *J Neurochem,* **120 Suppl 1,** 71-83.

Gidwani M and Singh AV (2014) Nanoparticle Enabled Drug Delivery Across the Blood Brain Barrier: in Vivo and in Vitro Models, Opportunities and Challenges. *Curr Pharm Biotechnol*.

Gkogkas CG, Khoutorsky A, Ran I, Rampakakis E, Nevarko T, Weatherill DB, Vasuta C, Yee S, Truitt M, Dallaire P, Major F, Lasko P, Ruggero D, Nader K, Lacaille JC, and Sonenberg N (2013) Autism-related deficits via dysregulated eIF4E-dependent translational control. *Nature,* **493,** 371-377.

Glenner GG and Wong CW (1984) Alzheimer's disease: initial report of the purification and characterization of a novel cerebrovascular amyloid protein. *Biochem Biophys Res Commun,* **120,** 885-890.

Good PF, Perl DP, Bierer LM, and Schmeidler J (1992) Selective accumulation of aluminum and iron in the neurofibrillary tangles of Alzheimer's disease: a laser microprobe (LAMMA) study. *Ann Neurol,* **31,** 286-292.

Green RC, Schneider LS, Amato DA, Beelen AP, Wilcock G, Swabb EA, and Zavitz KH (2009) Effect of tarenflurbil on cognitive decline and activities of daily living in patients with mild Alzheimer disease: a randomized controlled trial. *JAMA,* **302,** 2557-2564.

Grundke-Iqbal I, Iqbal K, Tung YC, Quinlan M, Wisniewski HM, and Binder LI (1986) Abnormal phosphorylation of the microtubule-associated protein tau (tau) in Alzheimer cytoskeletal pathology. *Proc Natl Acad Sci U S A,* **83,** 4913-4917.

Guo F, Lin EA, Liu P, Lin J, and Liu C (2010) XBP1U inhibits the XBP1S-mediated upregulation of the iNOS gene expression in mammalian ER stress response. *Cell Signal,* **22,** 1818-1828.

Haass C, Schlossmacher MG, Hung AY, Vigo-Pelfrey C, Mellon A, Ostaszewski BL, Lieberburg I, Koo EH, Schenk D, and Teplow DB (1992) Amyloid beta-peptide is produced by cultured cells during normal metabolism. *Nature,* **359,** 322-325.

Halbleib JM and Nelson WJ (2006) Cadherins in development: cell adhesion, sorting, and tissue morphogenesis. *Genes Dev,* **20,** 3199-3214.

Halliday GM, Shepherd CE, McCann H, Reid WG, Grayson DA, Broe GA, and Kril JJ (2000) Effect of anti-inflammatory medications on neuropathological findings in Alzheimer disease. *Arch Neurol,* **57,** 831-836.

Hanzel CE, Pichet-Binette A, Pimentel LS, Iulita MF, Allard S, Ducatenzeiler A, Do CS, and Cuello AC (2014) Neuronal driven pre-plaque inflammation in a transgenic rat model of Alzheimer's disease. *Neurobiol Aging*.

Hardy JA and Higgins GA (1992) Alzheimer's disease: the amyloid cascade hypothesis. *Science,* **256,** 184-185.

Harris B, Pereira I, and Parkin E (2009) Targeting ADAM10 to lipid rafts in neuroblastoma SH-SY5Y cells impairs amyloidogenic processing of the amyloid precursor protein. *Brain Res,* **1296,** 203-215.

Hartmann D, de Strooper B, Serneels L, Craessaerts K, Herreman A, Annaert W, Umans L, Lubke T, Lena Illert A, von Figura K, and Saftig P (2002) The disintegrin/metalloprotease ADAM 10 is essential for Notch signalling but not for alpha-secretase activity in fibroblasts. *Hum Mol Genet,* **11,** 2615-2624.

Hauser WA, Morris ML, Heston LL, and Anderson VE (1986) Seizures and myoclonus in patients with Alzheimer's disease. *Neurology,* **36,** 1226-1230.

He M, Wen L, Campbell CE, Wu JY, and Rao Y (1999) Transcription repression by Xenopus ET and its human ortholog TBX3, a gene involved in ulnar-mammary syndrome. *Proc Natl Acad Sci U S A,* **96,** 10212-10217.

Heber S, Herms J, Gajic V, Hainfellner J, Aguzzi A, Rulicke T, von Kretzschmar H, von Koch C, Sisodia S, Tremml P, Lipp HP, Wolfer DP, and Müller U (2000) Mice with combined gene knock-outs reveal essential and partially redundant functions of amyloid precursor protein family members. *J Neurosci,* **20,** 7951-7963.

Hebert SS, Horre K, Nicolai L, Papadopoulou AS, Mandemakers W, Silahtaroglu AN, Kauppinen S, Delacourte A, and de Strooper B (2008) Loss of microRNA cluster miR-29a/b-1 in sporadic Alzheimer's disease correlates with increased BACE1/beta-secretase expression. *Proc Natl Acad Sci U S A,* **105,** 6415-6420.

Hebert SS, Serneels L, Tolia A, Craessaerts K, Derks C, Filippov MA, Müller U, and de Strooper B (2006) Regulated intramembrane proteolysis of amyloid precursor protein and regulation of expression of putative target genes. *EMBO Rep,* **7,** 739-745.

Hendriks L, van Duijn CM, Cras P, Cruts M, van Hul W, van Harskamp F, Warren A, McInnis MG, Antonarakis SE, Martin JJ, and . (1992) Presenile dementia and cerebral haemorrhage linked to a mutation at codon 692 of the beta-amyloid precursor protein gene. *Nat Genet,* **1,** 218-221.

Heneka MT, Kummer MP, Stutz A, Delekate A, Schwartz S, Vieira-Saecker A, Griep A, Axt D, Remus A, Tzeng TC, Gelpi E, Halle A, Korte M, Latz E, and Golenbock DT (2013) NLRP3 is activated in Alzheimer's disease and contributes to pathology in APP/PS1 mice. *Nature,* **493,** 674-678.

Herms J, Anliker B, Heber S, Ring S, Fuhrmann M, Kretzschmar H, Sisodia S, and Müller U (2004) Cortical dysplasia resembling human type 2 lissencephaly in mice lacking all three APP family members. *EMBO J,* **23,** 4106-4115.

Holmes C, Boche D, Wilkinson D, Yadegarfar G, Hopkins V, Bayer A, Jones RW, Bullock R, Love S, Neal JW, Zotova E, and Nicoll JA (2008) Long-term effects of Abeta42 immunisation in Alzheimer's disease: follow-up of a randomised, placebo-controlled phase I trial. *Lancet,* **372,** 216-223.

Holthoewer D, Endres K, Schuck F, Hiemke C, Schmitt U, and Fahrenholz F (2012) Acitretin, an enhancer of alpha-secretase expression, crosses the blood-brain barrier and is not eliminated by P-glycoprotein. *Neurodegener Dis,* **10,** 224-228.

Holtzman DM (2008) Alzheimer's disease: Moving towards a vaccine. *Nature,* **454,** 418-420.

Hoozemans JJ, van Haastert ES, Nijholt DA, Rozemuller AJ, Eikelenboom P, and Scheper W (2009) The unfolded protein response is activated in pretangle neurons in Alzheimer's disease hippocampus. *Am J Pathol,* **174,** 1241-1251.

Hoozemans JJ, van Haastert ES, Nijholt DA, Rozemuller AJ, and Scheper W (2012) Activation of the unfolded protein response is an early event in Alzheimer's and Parkinson's disease. *Neurodegener Dis,* **10,** 212-215.

Hoozemans JJ, Veerhuis R, van Haastert ES, Rozemuller JM, Baas F, Eikelenboom P, and Scheper W (2005) The unfolded protein response is activated in Alzheimer's disease. *Acta Neuropathol,* **110,** 165-172.

Hu X, Hicks CW, He W, Wong P, Macklin WB, Trapp BD, and Yan R (2006) Bace1 modulates myelination in the central and peripheral nervous system. *Nat Neurosci,* **9,** 1520-1525.

Hung AY and Selkoe DJ (1994) Selective ectodomain phosphorylation and regulated cleavage of beta-amyloid precursor protein. *EMBO J,* **13,** 534-542.

Hussain I, Hawkins J, Harrison D, Hille C, Wayne G, Cutler L, Buck T, Walter D, Demont E, Howes C, Naylor A, Jeffrey P, Gonzalez MI, Dingwall C, Michel A, Redshaw S, and Davis JB (2007) Oral administration of a potent and selective non-peptidic BACE-1 inhibitor decreases beta-cleavage of amyloid precursor protein and amyloid-beta production in vivo. *J Neurochem,* **100,** 802-809.

Hussain I, Powell D, Howlett DR, Tew DG, Meek TD, Chapman C, Gloger IS, Murphy KE, Southan CD, Ryan DM, Smith TS, Simmons DL, Walsh FS, Dingwall C, and Christie G (1999) Identification of a novel aspartic protease (Asp 2) as beta-secretase. *Mol Cell Neurosci,* **14,** 419-427.

Iqbal K and Grundke-Iqbal I (2008) Alzheimer neurofibrillary degeneration: significance, etiopathogenesis, therapeutics and prevention. *J Cell Mol Med,* **12,** 38-55.

Iqbal K, Grundke-Iqbal I, Zaidi T, Merz PA, Wen GY, Shaikh SS, Wisniewski HM, Alafuzoff I, and Winblad B (1986) Defective brain microtubule assembly in Alzheimer's disease. *Lancet,* **2,** 421-426.

Ishida A, Furukawa K, Keller JN, and Mattson MP (1997) Secreted form of beta-amyloid precursor protein shifts the frequency dependency for induction of LTD, and enhances LTP in hippocampal slices. *Neuroreport,* **8,** 2133-2137.

Ishiguro K, Shiratsuchi A, Sato S, Omori A, Arioka M, Kobayashi S, Uchida T, and Imahori K (1993) Glycogen synthase kinase 3 beta is identical to tau protein kinase I generating several epitopes of paired helical filaments. *FEBS Lett,* **325,** 167-172.

Ishiguro K, Takamatsu M, Tomizawa K, Omori A, Takahashi M, Arioka M, Uchida T, and Imahori K (1992) Tau protein kinase I converts normal tau protein into A68-like component of paired helical filaments. *J Biol Chem,* **267,** 10897-10901.

Jacobs JJ, Keblusek P, Robanus-Maandag E, Kristel P, Lingbeek M, Nederlof PM, van Welsem T, van de Vijver MJ, Koh EY, Daley GQ, and van Lohuizen M (2000) Senescence bypass screen identifies TBX2, which represses Cdkn2a (p19(ARF)) and is amplified in a subset of human breast cancers. *Nat Genet,* **26,** 291-299.

Jamain S, Quach H, Betancur C, Rastam M, Colineaux C, Gillberg IC, Soderstrom H, Giros B, Leboyer M, Gillberg C, and Bourgeron T (2003) Mutations of the X-linked genes encoding neuroligins NLGN3 and NLGN4 are associated with autism. *Nat Genet,* **34,** 27-29.

Jicha GA, Berenfeld B, and Davies P (1999a) Sequence requirements for formation of conformational variants of tau similar to those found in Alzheimer's disease. *J Neurosci Res,* **55,** 713-723.

Jicha GA, Lane E, Vincent I, Otvos L, Jr., Hoffmann R, and Davies P (1997) A conformation- and phosphorylation-dependent antibody recognizing the paired helical filaments of Alzheimer's disease. *J Neurochem,* **69,** 2087-2095.

Jicha GA, Rockwood JM, Berenfeld B, Hutton M, and Davies P (1999b) Altered conformation of recombinant frontotemporal dementia-17 mutant tau proteins. *Neurosci Lett,* **260,** 153-156.

Jin M, Shepardson N, Yang T, Chen G, Walsh D, and Selkoe DJ (2011) Soluble amyloid beta-protein dimers isolated from Alzheimer cortex directly induce Tau hyperphosphorylation and neuritic degeneration. *Proc Natl Acad Sci U S A,* **108,** 5819-5824.

Jonsson T, Atwal JK, Steinberg S, Snaedal J, Jonsson PV, Bjornsson S, Stefansson H, Sulem P, Gudbjartsson D, Maloney J, Hoyte K, Gustafson A, Liu Y, Lu Y, Bhangale T, Graham RR, Huttenlocher J, Bjornsdottir G, Andreassen OA, Jonsson EG, Palotie A, Behrens TW, Magnusson OT, Kong A, Thorsteinsdottir U, Watts RJ, and Stefansson K (2012) A mutation in APP protects against Alzheimer's disease and age-related cognitive decline. *Nature,* **488,** 96-99.

Jorissen E, Prox J, Bernreuther C, Weber S, Schwanbeck R, Serneels L, Snellinx A, Craessaerts K, Thathiah A, Tesseur I, Bartsch U, Weskamp G, Blobel CP, Glatzel M, de Strooper B, and Saftig P (2010) The disintegrin/metalloproteinase ADAM10 is essential for the establishment of the brain cortex. *J Neurosci,* **30,** 4833-4844.

Kang DE, Pietrzik CU, Baum L, Chevallier N, Merriam DE, Kounnas MZ, Wagner SL, Troncoso JC, Kawas CH, Katzman R, and Koo EH (2000) Modulation of amyloid beta-protein clearance and Alzheimer's disease susceptibility by the LDL receptor-related protein pathway. *J Clin Invest,* **106,** 1159-1166.

Kang DE, Saitoh T, Chen X, Xia Y, Masliah E, Hansen LA, Thomas RG, Thal LJ, and Katzman R (1997) Genetic association of the low-density lipoprotein receptor-related protein gene (LRP), an apolipoprotein E receptor, with late-onset Alzheimer's disease. *Neurology,* **49,** 56-61.

Kang J, Lemaire HG, Unterbeck A, Salbaum JM, Masters CL, Grzeschik KH, Multhaup G, Beyreuther K, and Müller-Hill B (1987) The precursor of Alzheimer's disease amyloid A4 protein resembles a cell-surface receptor. *Nature,* **325,** 733-736.

Karantzoulis S and Galvin JE (2011) Distinguishing Alzheimer's disease from other major forms of dementia. *Expert Rev Neurother,* **11,** 1579-1591.

Karch A, Manthey H, Ponto C, Hermann P, Heinemann U, Schmidt C, and Zerr I (2013) Investigating the association of ApoE genotypes with blood-brain barrier dysfunction measured by cerebrospinal fluid-serum albumin ratio in a cohort of patients with different types of dementia. *PLoS One,* **8,** e84405.

Kawahara K, Nishi K, Suenobu M, Ohtsuka H, Maeda A, Nagatomo K, Kuniyasu A, Staufenbiel M, Nakagomi M, Shudo K, and Nakayama H (2009) Oral administration of synthetic retinoid Am80 (Tamibarotene) decreases brain beta-amyloid peptides in APP23 mice. *Biol Pharm Bull,* **32,** 1307-1309.

Kelleher RJ and Soiza RL (2013) Evidence of endothelial dysfunction in the development of Alzheimer's disease: Is Alzheimer's a vascular disorder? *Am J Cardiovasc Dis,* **3,** 197-226.

Kitaguchi N, Takahashi Y, Tokushima Y, Shiojiri S, and Ito H (1988) Novel precursor of Alzheimer's disease amyloid protein shows protease inhibitory activity. *Nature,* **331,** 530-532.

Kitaoka K, Shimizu N, Ono K, Chikahisa S, Nakagomi M, Shudo K, Ishimura K, Sei H, and Yoshizaki K (2013) The retinoic acid receptor agonist Am80 increases hippocampal ADAM10 in aged SAMP8 mice. *Neuropharmacology,* **72,** 58-65.

Kojro E, Fuger P, Prinzen C, Kanarek AM, Rat D, Endres K, Fahrenholz F, and Postina R (2010) Statins and the squalene synthase inhibitor zaragozic acid stimulate the non-amyloidogenic pathway of amyloid-beta protein precursor processing by suppression of cholesterol synthesis. *J Alzheimers Dis,* **20,** 1215-1231.

Kojro E, Gimpl G, Lammich S, Marz W, and Fahrenholz F (2001) Low cholesterol stimulates the nonamyloidogenic pathway by its effect on the alpha -secretase ADAM 10. *Proc Natl Acad Sci U S A,* **98,** 5815-5820.

Kojro E and Postina R (2009) Regulated proteolysis of RAGE and AbetaPP as possible link between type 2 diabetes mellitus and Alzheimer's disease. *J Alzheimers Dis,* **16,** 865-878.

Kokubo H, Tomita-Miyagawa S, Hamada Y, and Saga Y (2007) Hesr1 and Hesr2 regulate atrioventricular boundary formation in the developing heart through the repression of Tbx2. *Development,* **134,** 747-755.

Kolliputi N, Galam L, Parthasarathy PT, Tipparaju SM, and Lockey RF (2012) NALP-3 inflammasome silencing attenuates ceramide-induced transepithelial permeability. *J Cell Physiol,* **227,** 3310-3316.

Kolliputi N, Shaik RS, and Waxman AB (2010) The inflammasome mediates hyperoxia-induced alveolar cell permeability. *J Immunol,* **184,** 5819-5826.

Korenberg JR, Pulst SM, Neve RL, and West R (1989) The Alzheimer amyloid precursor protein maps to human chromosome 21 bands q21.105-q21.05. *Genomics,* **5,** 124-127.

Korennykh AV, Korostelev AA, Egea PF, Finer-Moore J, Stroud RM, Zhang C, Shokat KM, and Walter P (2011) Structural and functional basis for RNA cleavage by Ire1. *BMC Biol,* **9,** 47.

Kuhn PH, Koroniak K, Hogl S, Colombo A, Zeitschel U, Willem M, Volbracht C, Schepers U, Imhof A, Hoffmeister A, Haass C, Rossner S, Brase S, and Lichtenthaler SF (2012) Secretome protein enrichment identifies physiological BACE1 protease substrates in neurons. *EMBO J,* **31,** 3157-3168.

Kuhn PH, Wang H, Dislich B, Colombo A, Zeitschel U, Ellwart JW, Kremmer E, Rossner S, and Lichtenthaler SF (2010) ADAM10 is the physiologically relevant, constitutive alpha-secretase of the amyloid precursor protein in primary neurons. *EMBO J,* **29,** 3020-3032.

Lahiri DK, Ge YW, Rogers JT, Sambamurti K, Greig NH, and Maloney B (2006) Taking down the unindicted co-conspirators of amyloid beta-peptide-mediated neuronal death: shared gene regulation of BACE1 and APP genes interacting with CREB, Fe65 and YY1 transcription factors. *Curr Alzheimer Res,* **3,** 475-483.

Lammich S, Buell D, Zilow S, Ludwig AK, Nuscher B, Lichtenthaler SF, Prinzen C, Fahrenholz F, and Haass C (2010) Expression of the anti-amyloidogenic secretase ADAM10 is suppressed by its 5'-untranslated region. *J Biol Chem,* **285,** 15753-15760.

Lammich S, Kamp F, Wagner J, Nuscher B, Zilow S, Ludwig AK, Willem M, and Haass C (2011) Translational repression of the disintegrin and metalloprotease ADAM10 by a stable G-quadruplex secondary structure in its 5'-untranslated region. *J Biol Chem,* **286,** 45063-45072.

Lammich S, Kojro E, Postina R, Gilbert S, Pfeiffer R, Jasionowski M, Haass C, and Fahrenholz F (1999) Constitutive and regulated alpha-secretase cleavage of Alzheimer's amyloid precursor protein by a disintegrin metalloprotease. *Proc Natl Acad Sci U S A,* **96,** 3922-3927.

Lammich S, Schobel S, Zimmer AK, Lichtenthaler SF, and Haass C (2004) Expression of the Alzheimer protease BACE1 is suppressed via its 5'-untranslated region. *EMBO Rep,* **5,** 620-625.

Laumonnier F, Bonnet-Brilhault F, Gomot M, Blanc R, David A, Moizard MP, Raynaud M, Ronce N, Lemonnier E, Calvas P, Laudier B, Chelly J, Fryns JP, Ropers HH, Hamel BC, Andres C, Barthelemy C, Moraine C, and Briault S (2004) X-linked mental retardation and autism are associated with a mutation in the NLGN4 gene, a member of the neuroligin family. *Am J Hum Genet,* **74,** 552-557.

le Blanc AC, Koutroumanis M, and Goodyer CG (1998) Protein kinase C activation increases release of secreted amyloid precursor protein without decreasing Abeta production in human primary neuron cultures. *J Neurosci,* **18,** 2907-2913.

Lee AH, Iwakoshi NN, and Glimcher LH (2003) XBP-1 regulates a subset of endoplasmic reticulum resident chaperone genes in the unfolded protein response. *Mol Cell Biol,* **23,** 7448-7459.

Lichtenthaler SF and Haass C (2004) Amyloid at the cutting edge: activation of alpha-secretase prevents amyloidogenesis in an Alzheimer disease mouse model. *J Clin Invest,* **113,** 1384-1387.

Liu CY, Schröder M, and Kaufman RJ (2000) Ligand-independent dimerization activates the stress response kinases IRE1 and PERK in the lumen of the endoplasmic reticulum. *J Biol Chem,* **275,** 24881-24885.

Liu F, Grundke-Iqbal I, Iqbal K, and Gong CX (2005) Contributions of protein phosphatases PP1, PP2A, PP2B and PP5 to the regulation of tau phosphorylation. *Eur J Neurosci,* **22,** 1942-1950.

Luo X, Prior M, He W, Hu X, Tang X, Shen W, Yadav S, Kiryu-Seo S, Miller R, Trapp BD, and Yan R (2011) Cleavage of neuregulin-1 by BACE1 or ADAM10 protein produces differential effects on myelination. *J Biol Chem,* **286,** 23967-23974.

Luo X and Yan R (2010) Inhibition of BACE1 for therapeutic use in Alzheimer's disease. *Int J Clin Exp Pathol,* **3,** 618-628.

Luo Y, Bolon B, Kahn S, Bennett BD, Babu-Khan S, Denis P, Fan W, Kha H, Zhang J, Gong Y, Martin L, Louis JC, Yan Q, Richards WG, Citron M, and Vassar R (2001) Mice deficient in BACE1, the Alzheimer's beta-secretase, have normal phenotype and abolished beta-amyloid generation. *Nat Neurosci,* **4,** 231-232.

Mann DM, Royston MC, and Ravindra CR (1990) Some morphometric observations on the brains of patients with Down's syndrome: their relationship to age and dementia. *J Neurol Sci,* **99,** 153-164.

Marcinkiewicz M and Seidah NG (2000) Coordinated expression of beta-amyloid precursor protein and the putative beta-secretase BACE and alpha-secretase ADAM10 in mouse and human brain. *J Neurochem,* **75,** 2133-2143.

Maretzky T, Reiss K, Ludwig A, Buchholz J, Scholz F, Proksch E, de Strooper B, Hartmann D, and Saftig P (2005) ADAM10 mediates E-cadherin shedding and regulates epithelial cell-cell adhesion, migration, and beta-catenin translocation. *Proc Natl Acad Sci U S A,* **102,** 9182-9187.

Masters CL, Multhaup G, Simms G, Pottgiesser J, Martins RN, and Beyreuther K (1985a) Neuronal origin of a cerebral amyloid: neurofibrillary tangles of Alzheimer's disease contain the same protein as the amyloid of plaque cores and blood vessels. *EMBO J,* **4,** 2757-2763.

Masters CL, Simms G, Weinman NA, Multhaup G, McDonald BL, and Beyreuther K (1985b) Amyloid plaque core protein in Alzheimer disease and Down syndrome. *Proc Natl Acad Sci U S A,* **82,** 4245-4249.

Matthews V, Schuster B, Schutze S, Bussmeyer I, Ludwig A, Hundhausen C, Sadowski T, Saftig P, Hartmann D, Kallen KJ, and Rose-John S (2003) Cellular cholesterol depletion triggers shedding of the human interleukin-6 receptor by ADAM10 and ADAM17 (TACE). *J Biol Chem,* **278,** 38829-38839.

McDaneld TG (2009) MicroRNA: mechanism of gene regulation and application to livestock. *J Anim Sci,* **87,** E21-E28.

McGuinness B and Passmore P (2010) Can statins prevent or help treat Alzheimer's disease? *J Alzheimers Dis,* **20,** 925-933.

Mechtersheimer S, Gutwein P, Agmon-Levin N, Stoeck A, Oleszewski M, Riedle S, Postina R, Fahrenholz F, Fogel M, Lemmon V, and Altevogt P (2001) Ectodomain shedding of L1 adhesion molecule promotes cell migration by autocrine binding to integrins. *J Cell Biol,* **155,** 661-673.

Meister S, Zlatev I, Stab J, Docter D, Baches S, Stauber RH, Deutsch M, Schmidt R, Ropele S, Windisch M, Langer K, Wagner S, von Briesen H, Weggen S, and Pietrzik CU (2013) Nanoparticulate flurbiprofen reduces amyloid-beta42 generation in an in vitro blood-brain barrier model. *Alzheimers Res Ther,* **5,** 51.

Meredith JE, Jr., Thompson LA, Toyn JH, Marcin L, Barten DM, Marcinkeviciene J, Kopcho L, Kim Y, Lin A, Guss V, Burton C, Iben L, Polson C, Cantone J, Ford M, Drexler D, Fiedler T, Lentz KA, Grace JE, Jr., Kolb J, Corsa J, Pierdomenico M, Jones K, Olson RE, Macor JE, and Albright CF (2008) P-glycoprotein efflux and other factors limit brain amyloid beta reduction by beta-site amyloid precursor protein-cleaving enzyme 1 inhibitors in mice. *J Pharmacol Exp Ther,* **326,** 502-513.

Messing L, Decker JM, Joseph M, Mandelkow E, and Mandelkow EM (2013) Cascade of tau toxicity in inducible hippocampal brain slices and prevention by aggregation inhibitors. *Neurobiol Aging,* **34,** 1343-1354.

Metz VV, Kojro E, Rat D, and Postina R (2012) Induction of RAGE shedding by activation of G protein-coupled receptors. *PLoS One,* **7,** e41823.

Miners JS, van HZ, Kehoe PG, and Love S (2010) Changes with age in the activities of beta-secretase and the Abeta-degrading enzymes neprilysin, insulin-degrading enzyme and angiotensin-converting enzyme. *Brain Pathol,* **20,** 794-802.

Miyata M and Smith JD (1996) Apolipoprotein E allele-specific antioxidant activity and effects on cytotoxicity by oxidative insults and beta-amyloid peptides. *Nat Genet,* **14,** 55-61.

Monro OR, Mackic JB, Yamada S, Segal MB, Ghiso J, Maurer C, Calero M, Frangione B, and Zlokovic BV (2002) Substitution at codon 22 reduces clearance of Alzheimer's amyloid-beta peptide from the cerebrospinal fluid and prevents its transport from the central nervous system into blood. *Neurobiol Aging,* **23,** 405-412.

Montine TJ, Huang DY, Valentine WM, Amarnath V, Saunders A, Weisgraber KH, Graham DG, and Strittmatter WJ (1996) Crosslinking of apolipoprotein E by products of lipid peroxidation. *J Neuropathol Exp Neurol,* **55,** 202-210.

Morris MC, Schneider JA, Li H, Tangney CC, Nag S, Bennett DA, Honer WG, and Barnes LL (2014) Brain tocopherols related to Alzheimer's disease neuropathology in humans. *Alzheimers Dement*.

Munro J, Steeghs K, Morrison V, Ireland H, and Parkinson EK (2001) Human fibroblast replicative senescence can occur in the absence of extensive cell division and short telomeres. *Oncogene,* **20,** 3541-3552.

Nagashima Y, Mishiba K, Suzuki E, Shimada Y, Iwata Y, and Koizumi N (2011) Arabidopsis IRE1 catalyses unconventional splicing of bZIP60 mRNA to produce the active transcription factor. *Sci Rep,* **1,** 29.

Nilsberth C, Westlind-Danielsson A, Eckman CB, Condron MM, Axelman K, Forsell C, Stenh C, Luthman J, Teplow DB, Younkin SG, Naslund J, and Lannfelt L (2001) The 'Arctic' APP mutation (E693G) causes Alzheimer's disease by enhanced Abeta protofibril formation. *Nat Neurosci,* **4,** 887-893.

Nitsch RM, Slack BE, Wurtman RJ, and Growdon JH (1992) Release of Alzheimer amyloid precursor derivatives stimulated by activation of muscarinic acetylcholine receptors. *Science,* **258,** 304-307.

Novak M, Jakes R, Edwards PC, Milstein C, and Wischik CM (1991) Difference between the tau protein of Alzheimer paired helical filament core and normal tau revealed by epitope analysis of monoclonal antibodies 423 and 7.51. *Proc Natl Acad Sci U S A,* **88,** 5837-5841.

Oakley H, Cole SL, Logan S, Maus E, Shao P, Craft J, Guillozet-Bongaarts A, Ohno M, Disterhoft J, van Eldik L, Berry R, and Vassar R (2006) Intraneuronal beta-amyloid aggregates, neurodegeneration, and neuron loss in transgenic mice with five familial Alzheimer's disease mutations: potential factors in amyloid plaque formation. *J Neurosci,* **26,** 10129-10140.

Ogryzko VV, Hirai TH, Russanova VR, Barbie DA, and Howard BH (1996) Human fibroblast commitment to a senescence-like state in response to histone deacetylase inhibitors is cell cycle dependent. *Mol Cell Biol,* **16,** 5210-5218.

Papaioannou VE and Silver LM (1998) The T-box gene family. *Bioessays,* **20,** 9-19.

Paresce DM, Chung H, and Maxfield FR (1997) Slow degradation of aggregates of the Alzheimer's disease amyloid beta-protein by microglial cells. *J Biol Chem,* **272,** 29390-29397.

Parihar MS and Brewer GJ (2010) Amyloid-beta as a modulator of synaptic plasticity. *J Alzheimers Dis,* **22,** 741-763.

Park SW, Zhou Y, Lee J, Lu A, Sun C, Chung J, Ueki K, and Ozcan U (2010) The regulatory subunits of PI3K, p85alpha and p85beta, interact with XBP-1 and increase its nuclear translocation. *Nat Med,* **16,** 429-437.

Pei JJ, Braak E, Braak H, Grundke-Iqbal I, Iqbal K, Winblad B, and Cowburn RF (1999) Distribution of active glycogen synthase kinase 3beta (GSK-3beta) in brains staged for Alzheimer disease neurofibrillary changes. *J Neuropathol Exp Neurol,* **58,** 1010-1019.

Pei JJ, Grundke-Iqbal I, Iqbal K, Bogdanovic N, Winblad B, and Cowburn RF (1998) Accumulation of cyclin-dependent kinase 5 (cdk5) in neurons with early stages of Alzheimer's disease neurofibrillary degeneration. *Brain Res,* **797,** 267-277.

Poduslo JF, Curran GL, Kumar A, Frangione B, and Soto C (1999) Beta-sheet breaker peptide inhibitor of Alzheimer's amyloidogenesis with increased blood-brain barrier permeability and resistance to proteolytic degradation in plasma. *J Neurobiol,* **39,** 371-382.

Postina R (2012) Activation of alpha-secretase cleavage. *J Neurochem,* **120 Suppl 1,** 46-54.

Postina R, Schroeder A, Dewachter I, Bohl J, Schmitt U, Kojro E, Prinzen C, Endres K, Hiemke C, Blessing M, Flamez P, Dequenne A, Godaux E, van Leuven F, and Fahrenholz F (2004) A disintegrin-metalloproteinase prevents amyloid plaque formation and hippocampal defects in an Alzheimer disease mouse model. *J Clin Invest,* **113,** 1456-1464.

Prince S, Carreira S, Vance KW, Abrahams A, and Goding CR (2004) Tbx2 directly represses the expression of the p21(WAF1) cyclin-dependent kinase inhibitor. *Cancer Res,* **64,** 1669-1674.

Prinz M, Priller J, Sisodia S, and Ransohoff RM (2011) Heterogeneity of CNS myeloid cells and their roles in neurodegeneration. *Nat Neurosci,* **14,** 1227-1235.

Prinzen C, Müller U, Endres K, Fahrenholz F, and Postina R (2005) Genomic structure and functional characterization of the human ADAM10 promoter. *FASEB J,* **19,** 1522-1524.

Prinzen C, Trümbach D, Wurst W, Endres K, Postina R, and Fahrenholz F (2009) Differential gene expression in ADAM10 and mutant ADAM10 transgenic mice. *BMC Genomics,* **10,** 66.

Pruessmeyer J and Ludwig A (2009) The good, the bad and the ugly substrates for ADAM10 and ADAM17 in brain pathology, inflammation and cancer. *Semin Cell Dev Biol,* **20,** 164-174.

Qazi O, Parthasarathy PT, Lockey R, and Kolliputi N (2013) Can microRNAs keep inflammasomes in check? *Front Genet,* **4,** 30.

Rajapaksha TW, Eimer WA, Bozza TC, and Vassar R (2011) The Alzheimer's beta-secretase enzyme BACE1 is required for accurate axon guidance of olfactory sensory neurons and normal glomerulus formation in the olfactory bulb. *Mol Neurodegener,* **6,** 88.

Raucci A, Cugusi S, Antonelli A, Barabino SM, Monti L, Bierhaus A, Reiss K, Saftig P, and Bianchi ME (2008) A soluble form of the receptor for advanced glycation endproducts (RAGE) is produced by proteolytic cleavage of the membrane-bound form by the sheddase a disintegrin and metalloprotease 10 (ADAM10). *FASEB J,* **22,** 3716-3727.

Reger MA, Watson GS, Green PS, Baker LD, Cholerton B, Fishel MA, Plymate SR, Cherrier MM, Schellenberg GD, Frey WH, and Craft S (2008) Intranasal insulin administration dose-dependently modulates verbal memory and plasma amyloid-beta in memory-impaired older adults. *J Alzheimers Dis,* **13,** 323-331.

Reim I, Lee HH, and Frasch M (2003) The T-box-encoding Dorsocross genes function in amnioserosa development and the patterning of the dorsolateral germ band downstream of Dpp. *Development,* **130,** 3187-3204.

Reinhardt S, Schuck F, Grösgen S, Riemenschneider M, Hartmann T, Postina R, Grimm M, and Endres K (2014) Unfolded protein response signaling by transcription factor XBP-1 regulates ADAM10 and is affected in Alzheimer's disease. *FASEB J,* **28,** 978-997.

Reiss K, Maretzky T, Ludwig A, Tousseyn T, de Strooper B, Hartmann D, and Saftig P (2005) ADAM10 cleavage of N-cadherin and regulation of cell-cell adhesion and beta-catenin nuclear signalling. *EMBO J,* **24,** 742-752.

Roberds SL, Anderson J, Basi G, Bienkowski MJ, Branstetter DG, Chen KS, Freedman SB, Frigon NL, Games D, Hu K, Johnson-Wood K, Kappenman KE, Kawabe TT, Kola I, Kuehn R, Lee M, Liu W, Motter R, Nichols NF, Power M, Robertson DW, Schenk D, Schoor M, Shopp GM, Shuck ME, Sinha S, Svensson KA, Tatsuno G, Tintrup H, Wijsman J, Wright S, and McConlogue L (2001) BACE knockout mice are healthy despite lacking the primary beta-secretase activity in brain: implications for Alzheimer's disease therapeutics. *Hum Mol Genet,* **10,** 1317-1324.

Rodriguez M, Aladowicz E, Lanfrancone L, and Goding CR (2008) Tbx3 represses E-cadherin expression and enhances melanoma invasiveness. *Cancer Res,* **68,** 7872-7881.

Roncarati R, Sestan N, Scheinfeld MH, Berechid BE, Lopez PA, Meucci O, McGlade JC, Rakic P, and D'Adamio L (2002) The gamma-secretase-generated intracellular domain of beta-amyloid precursor protein binds Numb and inhibits Notch signaling. *Proc Natl Acad Sci U S A,* **99,** 7102-7107.

Rutenberg JB, Fischer A, Jia H, Gessler M, Zhong TP, and Mercola M (2006) Developmental patterning of the cardiac atrioventricular canal by Notch and Hairy-related transcription factors. *Development,* **133,** 4381-4390.

Saftig P and Reiss K (2011) The "A Disintegrin And Metalloproteases" ADAM10 and ADAM17: novel drug targets with therapeutic potential? *Eur J Cell Biol,* **90,** 527-535.

Sandbrink R, Masters CL, and Beyreuther K (1994) Beta A4-amyloid protein precursor mRNA isoforms without exon 15 are ubiquitously expressed in rat tissues including brain, but not in neurons. *J Biol Chem,* **269,** 1510-1517.

Sano F, Tsuji K, Kunika N, Takeuchi T, Oyama K, Hasegawa S, Koike M, Takahashi M, and Ishida M (1998) Pseudotumor cerebri in a patient with acute promyelocytic leukemia during treatment with all-trans retinoic acid. *Intern Med,* **37,** 546-549.

Sauder JM, Arthur JW, and Dunbrack RL, Jr. (2000) Modeling of substrate specificity of the Alzheimer's disease amyloid precursor protein beta-secretase. *J Mol Biol,* **300,** 241-248.

Sayre LM, Perry G, Harris PL, Liu Y, Schubert KA, and Smith MA (2000) In situ oxidative catalysis by neurofibrillary tangles and senile plaques in Alzheimer's disease: a central role for bound transition metals. *J Neurochem,* **74,** 270-279.

Schmitt U, Hiemke C, Fahrenholz F, and Schroeder A (2006) Over-expression of two different forms of the alpha-secretase ADAM10 affects learning and memory in mice. *Behav Brain Res,* **175,** 278-284.

Schröder M and Kaufman RJ (2005) The mammalian unfolded protein response. *Annu Rev Biochem,* **74,** 739-789.

Selkoe DJ (1994) Alzheimer's disease: a central role for amyloid. *J Neuropathol Exp Neurol,* **53,** 438-447.

Selkoe DJ (2001) Clearing the brain's amyloid cobwebs. *Neuron,* **32,** 177-180.

Seubert P, Oltersdorf T, Lee MG, Barbour R, Blomquist C, Davis DL, Bryant K, Fritz LC, Galasko D, Thal LJ, and . (1993) Secretion of beta-amyloid precursor protein cleaved at the amino terminus of the beta-amyloid peptide. *Nature,* **361,** 260-263.

Shibata M, Yamada S, Kumar SR, Calero M, Bading J, Frangione B, Holtzman DM, Miller CA, Strickland DK, Ghiso J, and Zlokovic BV (2000) Clearance of Alzheimer's amyloid-ss(1-40) peptide from brain by LDL receptor-related protein-1 at the blood-brain barrier. *J Clin Invest,* **106,** 1489-1499.

Shoji M, Golde TE, Ghiso J, Cheung TT, Estus S, Shaffer LM, Cai XD, McKay DM, Tintner R, and Frangione B (1992) Production of the Alzheimer amyloid beta protein by normal proteolytic processing. *Science,* **258,** 126-129.

Showell C, Binder O, and Conlon FL (2004) T-box genes in early embryogenesis. *Dev Dyn,* **229,** 201-218.

Shudo K, Fukasawa H, Nakagomi M, and Yamagata N (2009) Towards retinoid therapy for Alzheimer's disease. *Curr Alzheimer Res,* **6,** 302-311.

Simmons LK, May PC, Tomaselli KJ, Rydel RE, Fuson KS, Brigham EF, Wright S, Lieberburg I, Becker GW, and Brems DN (1994) Secondary structure of amyloid beta peptide correlates with neurotoxic activity in vitro. *Mol Pharmacol,* **45,** 373-379.

Simons M, de Strooper B, Multhaup G, Tienari PJ, Dotti CG, and Beyreuther K (1996) Amyloidogenic processing of the human amyloid precursor protein in primary cultures of rat hippocampal neurons. *J Neurosci,* **16,** 899-908.

Simpson JE, Wharton SB, Cooper J, Gelsthorpe C, Baxter L, Forster G, Shaw PJ, Savva G, Matthews FE, Brayne C, and Ince PG (2010) Alterations of the blood-brain barrier in cerebral white matter lesions in the ageing brain. *Neurosci Lett,* **486,** 246-251.

Sinha S, Anderson JP, Barbour R, Basi GS, Caccavello R, Davis D, Doan M, Dovey HF, Frigon N, Hong J, Jacobson-Croak K, Jewett N, Keim P, Knops J, Lieberburg I, Power M, Tan H, Tatsuno G, Tung J, Schenk D, Seubert P, Suomensaari SM, Wang S, Walker D, Zhao J, McConlogue L, and John V (1999) Purification and cloning of amyloid precursor protein beta-secretase from human brain. *Nature,* **402,** 537-540.

Slack BE, Ma LK, and Seah CC (2001) Constitutive shedding of the amyloid precursor protein ectodomain is up-regulated by tumour necrosis factor-alpha converting enzyme. *Biochem J,* **357,** 787-794.

Slunt HH, Thinakaran G, von KC, Lo AC, Tanzi RE, and Sisodia SS (1994) Expression of a ubiquitous, cross-reactive homologue of the mouse beta-amyloid precursor protein (APP). *J Biol Chem,* **269,** 2637-2644.

Smith MA, Harris PL, Sayre LM, and Perry G (1997) Iron accumulation in Alzheimer disease is a source of redox-generated free radicals. *Proc Natl Acad Sci U S A,* **94,** 9866-9868.

Smith MA, Rottkamp CA, Nunomura A, Raina AK, and Perry G (2000) Oxidative stress in Alzheimer's disease. *Biochim Biophys Acta,* **1502,** 139-144.

Smith MA, Taneda S, Richey PL, Miyata S, Yan SD, Stern D, Sayre LM, Monnier VM, and Perry G (1994) Advanced Maillard reaction end products are associated with Alzheimer disease pathology. *Proc Natl Acad Sci U S A,* **91,** 5710-5714.

Solano DC, Sironi M, Bonfini C, Solerte SB, Govoni S, and Racchi M (2000) Insulin regulates soluble amyloid precursor protein release via phosphatidyl inositol 3 kinase-dependent pathway. *FASEB J,* **14,** 1015-1022.

Song JY, Ichtchenko K, Sudhof TC, and Brose N (1999) Neuroligin 1 is a postsynaptic cell-adhesion molecule of excitatory synapses. *Proc Natl Acad Sci U S A,* **96,** 1100-1105.

Stewart PA, Hayakawa K, Akers MA, and Vinters HV (1992) A morphometric study of the blood-brain barrier in Alzheimer's disease. *Lab Invest,* **67,** 734-742.

Sun X, He G, Qing H, Zhou W, Dobie F, Cai F, Staufenbiel M, Huang LE, and Song W (2006) Hypoxia facilitates Alzheimer's disease pathogenesis by up-regulating BACE1 gene expression. *Proc Natl Acad Sci U S A,* **103,** 18727-18732.

Sutton ET, Hellermann GR, and Thomas T (1997) beta-amyloid-induced endothelial necrosis and inhibition of nitric oxide production. *Exp Cell Res,* **230,** 368-376.

Suzuki K, Hayashi Y, Nakahara S, Kumazaki H, Prox J, Horiuchi K, Zeng M, Tanimura S, Nishiyama Y, Osawa S, Sehara-Fujisawa A, Saftig P, Yokoshima S, Fukuyama T, Matsuki N, Koyama R, Tomita T, and Iwatsubo T (2012) Activity-dependent proteolytic cleavage of neuroligin-1. *Neuron,* **76,** 410-422.

Suzuki T, Ando K, Isohara T, Oishi M, Lim GS, Satoh Y, Wasco W, Tanzi RE, Nairn AC, Greengard P, Gandy SE, and Kirino Y (1997) Phosphorylation of Alzheimer beta-amyloid precursor-like proteins. *Biochemistry,* **36,** 4643-4649.

Tanzi RE, McClatchey AI, Lamperti ED, Villa-Komaroff L, Gusella JF, and Neve RL (1988) Protease inhibitor domain encoded by an amyloid protein precursor mRNA associated with Alzheimer's disease. *Nature,* **331,** 528-530.

Tanzi RE, Moir RD, and Wagner SL (2004) Clearance of Alzheimer's Abeta peptide: the many roads to perdition. *Neuron,* **43,** 605-608.

Teske BF, Fusakio ME, Zhou D, Shan J, McClintick JN, Kilberg MS, and Wek RC (2013) CHOP induces activating transcription factor 5 (ATF5) to trigger apoptosis in response to perturbations in protein homeostasis. *Mol Biol Cell,* **24,** 2477-2490.

Thomas T, Thomas G, McLendon C, Sutton T, and Mullan M (1996) beta-Amyloid-mediated vasoactivity and vascular endothelial damage. *Nature,* **380,** 168-171.

Thornton E, Vink R, Blumbergs PC, and Van Den Heuvel C (2006) Soluble amyloid precursor protein alpha reduces neuronal injury and improves functional outcome following diffuse traumatic brain injury in rats. *Brain Res,* **1094,** 38-46.

Tippmann F, Hundt J, Schneider A, Endres K, and Fahrenholz F (2009) Up-regulation of the alpha-secretase ADAM10 by retinoic acid receptors and acitretin. *FASEB J,* **23,** 1643-1654.

Tirasophon W, Lee K, Callaghan B, Welihinda A, and Kaufman RJ (2000) The endoribonuclease activity of mammalian IRE1 autoregulates its mRNA and is required for the unfolded protein response. *Genes Dev,* **14,** 2725-2736.

Tyler SJ, Dawbarn D, Wilcock GK, and Allen SJ (2002) alpha- and beta-secretase: profound changes in Alzheimer's disease. *Biochem Biophys Res Commun,* **299,** 373-376.

Ueki K and Kadowaki T (2011) The other sweet face of XBP-1. *Nat Med,* **17,** 246-248.

Vance KW, Carreira S, Brosch G, and Goding CR (2005) Tbx2 is overexpressed and plays an important role in maintaining proliferation and suppression of senescence in melanomas. *Cancer Res,* **65,** 2260-2268.

Vance KW, Shaw HM, Rodriguez M, Ott S, and Goding CR (2010) The retinoblastoma protein modulates Tbx2 functional specificity. *Mol Biol Cell,* **21,** 2770-2779.

Vassar R, Bennett BD, Babu-Khan S, Kahn S, Mendiaz EA, Denis P, Teplow DB, Ross S, Amarante P, Loeloff R, Luo Y, Fisher S, Fuller J, Edenson S, Lile J, Jarosinski MA, Biere AL, Curran E, Burgess T, Louis JC, Collins F, Treanor J, Rogers G, and Citron M (1999) Beta-secretase cleavage of Alzheimer's amyloid precursor protein by the transmembrane aspartic protease BACE. *Science,* **286,** 735-741.

Verkhratsky A, Olabarria M, Noristani HN, Yeh CY, and Rodriguez JJ (2010) Astrocytes in Alzheimer's disease. *Neurotherapeutics,* **7,** 399-412.

Vincent B, Paitel E, Frobert Y, Lehmann S, Grassi J, and Checler F (2000) Phorbol ester-regulated cleavage of normal prion protein in HEK293 human cells and murine neurons. *J Biol Chem,* **275,** 35612-35616.

Vincent B, Paitel E, Saftig P, Frobert Y, Hartmann D, de Strooper B, Grassi J, Lopez-Perez E, and Checler F (2001) The disintegrins ADAM10 and TACE contribute to the constitutive and phorbol ester-regulated normal cleavage of the cellular prion protein. *J Biol Chem,* **276,** 37743-37746.

Vos SJ, Xiong C, Visser PJ, Jasielec MS, Hassenstab J, Grant EA, Cairns NJ, Morris JC, Holtzman DM, and Fagan AM (2013) Preclinical Alzheimer's disease and its outcome: a longitudinal cohort study. *Lancet Neurol,* **12,** 957-965.

Wang B, Lindley LE, Fernandez-Vega V, Rieger ME, Sims AH, and Briegel KJ (2012) The T box transcription factor TBX2 promotes epithelial-mesenchymal transition and invasion of normal and malignant breast epithelial cells. *PLoS One,* **7,** e41355.

Wang P, Yang G, Mosier DR, Chang P, Zaidi T, Gong YD, Zhao NM, Dominguez B, Lee KF, Gan WB, and Zheng H (2005) Defective neuromuscular synapses in mice lacking amyloid precursor protein (APP) and APP-Like protein 2. *J Neurosci,* **25,** 1219-1225.

Wansley DL, Yin Y, and Prussin C (2013) The retinoic acid receptor-alpha modulators ATRA and Ro415253 reciprocally regulate human IL-5+ Th2 cell proliferation and cytokine expression. *Clin Mol Allergy,* **11,** 4.

Waterhouse RN (2003) Determination of lipophilicity and its use as a predictor of blood-brain barrier penetration of molecular imaging agents. *Mol Imaging Biol,* **5,** 376-389.

Weggen S, Eriksen JL, Das P, Sagi SA, Wang R, Pietrzik CU, Findlay KA, Smith TE, Murphy MP, Bulter T, Kang DE, Marquez-Sterling N, Golde TE, and Koo EH (2001) A subset of NSAIDs lower amyloidogenic Abeta42 independently of cyclooxygenase activity. *Nature,* **414,** 212-216.

Weidemann A, König G, Bunke D, Fischer P, Salbaum JM, Masters CL, and Beyreuther K (1989) Identification, biogenesis, and localization of precursors of Alzheimer's disease A4 amyloid protein. *Cell,* **57,** 115-126.

Weyer SW, Klevanski M, Delekate A, Voikar V, Aydin D, Hick M, Filippov M, Drost N, Schaller KL, Saar M, Vogt MA, Gass P, Samanta A, Jaschke A, Korte M, Wolfer DP, Caldwell JH, and Müller UC (2011) APP and APLP2 are essential at PNS and CNS synapses for transmission, spatial learning and LTP. *EMBO J,* **30,** 2266-2280.

Wienholds E and Plasterk RH (2005) MicroRNA function in animal development. *FEBS Lett,* **579,** 5911-5922.

Willem M, Dewachter I, Smyth N, van Dooren T, Borghgraef P, Haass C, and van Leuven F (2004) beta-site amyloid precursor protein cleaving enzyme 1 increases amyloid deposition in brain parenchyma but reduces cerebrovascular amyloid angiopathy in aging BACE x APP[V717I] double-transgenic mice. *Am J Pathol,* **165,** 1621-1631.

Willem M, Garratt AN, Novak B, Citron M, Kaufmann S, Rittger A, de Strooper B, Saftig P, Birchmeier C, and Haass C (2006) Control of peripheral nerve myelination by the beta-secretase BACE1. *Science,* **314,** 664-666.

Winnay JN, Boucher J, Mori MA, Ueki K, and Kahn CR (2010) A regulatory subunit of phosphoinositide 3-kinase increases the nuclear accumulation of X-box-binding protein-1 to modulate the unfolded protein response. *Nat Med,* **16,** 438-445.

Yan R and Vassar R (2014) Targeting the beta secretase BACE1 for Alzheimer's disease therapy. *Lancet Neurol,* **13,** 319-329.

Yanagitani K, Imagawa Y, Iwawaki T, Hosoda A, Saito M, Kimata Y, and Kohno K (2009) Cotranslational targeting of XBP1 protein to the membrane promotes cytoplasmic splicing of its own mRNA. *Mol Cell,* **34,** 191-200.

Yankner BA, Dawes LR, Fisher S, Villa-Komaroff L, Oster-Granite ML, and Neve RL (1989) Neurotoxicity of a fragment of the amyloid precursor associated with Alzheimer's disease. *Science,* **245,** 417-420.

Yoshida H, Matsui T, Yamamoto A, Okada T, and Mori K (2001) XBP1 mRNA is induced by ATF6 and spliced by IRE1 in response to ER stress to produce a highly active transcription factor. *Cell,* **107,** 881-891.

Yoshida H, Oku M, Suzuki M, and Mori K (2006) pXBP1(U) encoded in XBP1 pre-mRNA negatively regulates unfolded protein response activator pXBP1(S) in mammalian ER stress response. *J Cell Biol,* **172,** 565-575.

Young SE, Mainous AG III, and Carnemolla M (2006) Hyperinsulinemia and cognitive decline in a middle-aged cohort. *Diabetes Care,* **29,** 2688-2693.

Zhang L, Bukulin M, Kojro E, Roth A, Metz VV, Fahrenholz F, Nawroth PP, Bierhaus A, and Postina R (2008) Receptor for advanced glycation end products is subjected to protein ectodomain shedding by metalloproteinases. *J Biol Chem,* **283,** 35507-35516.

Zipser BD, Johanson CE, Gonzalez L, Berzin TM, Tavares R, Hulette CM, Vitek MP, Hovanesian V, and Stopa EG (2007) Microvascular injury and blood-brain barrier leakage in Alzheimer's disease. *Neurobiol Aging,* **28,** 977-986.

Zlokovic BV (2004) Clearing amyloid through the blood-brain barrier. *J Neurochem,* **89,** 807-811.

Zoghbi HY (2003) Postnatal neurodevelopmental disorders: meeting at the synapse? *Science,* **302,** 826-830.

6. Liste der Veröffentlichungen und eigener Beitrag

Die Anfertigung dieser Dissertation erfolgte in kumulativer Form. Die erhaltenen Ergebnisse wurden großteils in den nachfolgend aufgeführten Publikationen veröffentlicht. Zudem wird der wissenschaftliche Beitrag zu jeder aufgeführten Veröffentlichung aufgezeigt. In Kapitel 3 werden die Ergebnisse dieser Arbeiten erörtert und zusammen mit bisher unveröffentlichten Daten diskutiert. Die entsprechenden Manuskripte befinden sich im Anhang (Kapitel 7.1).

6.1 Originalarbeiten

(A) Augustin R, Endres K, Reinhardt S, Kuhn PH, Lichtenthaler SF, Hansen J, Wurst W, Trümbach D. Computational identification and experimental validation of microRNAs binding to the Alzheimer-related gene ADAM10. *BMC Med Genet.* 2012 May 17;13:35.

Die experimentelle Validierung der bioinformatisch evaluierten miRNAs erfolgte durch mich. Die Transfektion der miRNAs zusammen mit dem ADAM10 3'UTR Reporter Vektor in neuronale SH-SY5Y Zellen, den Luziferase Reporter Assay sowie die Analyse der entsprechenden Daten führte ich durch. Des Weiteren trug ich zu dem entsprechenden Material und Methoden Teil bei.

(B) Reinhardt S, Schuck F, Grösgen S, Riemenschneider M, Hartmann T, Postina R, Grimm M, Endres K. Unfolded protein response signaling by transcription factor XBP-1 regulates ADAM10 and is affected in Alzheimer's disease. *FASEB J.* 2014 Feb;28(2):978-97. doi: 10.1096/fj.13-234864. Epub 2013 Oct 28.

Mein Beitrag zu dieser Arbeit bestand in der Konzeption der Methode zum Nachweis der XBP-1 Spleißformen. Des Weiteren führte ich alle Experimente sowie die Datenanalyse aller *in vitro* Studien, Zellkulturexperimente (mit Ausnahme des Fluoreszenz-basierten alpha-Sekretase Assays) sowie Versuche mit murinem Gewebe durch. Kristina Endres und ich verfassten das Manuskript. Darüber hinaus wurden alle Tabellen und Abbildungen von mir erstellt.

(C) Freese C*, Reinhardt S*, Hefner G, Unger RE, Kirkpatrick CJ, Endres K. A novel blood-brain barrier co-culture system for drug targeting of Alzheimer's disease: establishment by using acitretin as a model drug. *PLoS ONE* 2014 9(3): e91003. doi:10.1371/journal.pone.0091003 (* authors contributed equally)

Ich trug zu dieser Veröffentlichung durch die Planung des Nachweises der aktiven Form der GSK3-beta bei. Zudem erarbeitete ich das Konzept für die Etablierung des Nachweises von APPs-alpha per *Dot blot*. Ebenso war ich für die Planung und Durchführung der Transfektion neuronaler SH-SY5Y Zellen und der Schweine Hirn Endothel Zellen verantwortlich. Darüber hinaus führte ich alle Messungen von Luziferase Reporter Assays, Messungen der Zell-Viabilität und Induktion von Apoptose sowie alle Protein-Nachweise für beide Zelllinien durch und analysierte die entsprechenden Daten. Das Manuskript wurde von Christian Freese, Kristina Endres, Ronald E. Unger, Charles J. Kirkpatrick und mir verfasst.

6.2 Übersichtsarbeiten

(D) Endres K, Reinhardt S. ER-stress in Alzheimer's disease: turning the scale? *Am J Neurodegener Dis*. 2013 Nov 29;2(4):247-265. eCollection 2013. Review.

Mein Beitrag zu dieser Veröffentlichung war die Gestaltung des Textes und der entsprechenden Tabelle des Abschnitts „*ER-stress signaling in animal models of AD and human patients*".

6.3 Weitere Veröffentlichungen

a) Vorträge:

Reinhardt S. (2012) Regulation of ADAM10 gene expression and neuroprotection *NGFN Meeting AD-IG,Frankfurt*.

b) Posterpräsentationen

Reinhardt S., Salg A., Postina R., Endres K. (2010) Balancing Alzheimer's disease related genes ADAM10 and BACE1. *1st Rhine-Main-Neuroscience (rmn2) meeting, Oberwesel*.

Reinhardt S., Endres K. (2010) Examination of Transcription Factors balancing Gene-Expression of Alzheimer`s Disease related proteinases ADAM10 and BACE1. *10th International Conference on Alzheimer's & Parkinson's Diseases, Barcelona*.

Salg A., Reinhardt S., Kühn R., Wurst W., Endres K. (2010) Light up the mouse. *Internationales Begegnungszentrum der Wissenschaft, Bielefeld*

Reinhardt S., Endres K. (2011) Modulating gene-expression of Alzheimer`s disease related proteinases ADAM10 and BACE1 - a screening approach – *4th Annual Meeting of NGFN-Plus and NGFN-Transfer, Berlin*
(Annemarie Poustka Poster Preis)

Augustin R., Lichtenthaler SF., Endres K., Reinhardt S., Kuhn PH., Greeff M., Hansen J., Wurst W., Trümbach D. (2011) Bioinformatics approach: Regulation of Alzheimer's disease-related genes by modules of TFBSs and microRNAs. *Internes Meeting der Helmholtz Association, München*

Sakry D. & Reinhardt S., Postina R., Endres K & Trotter J. (2011) Shedding and signaling of the oligodendrocyte precursor protein NG2. *11th annual FTN/IAK symposium – Molecular And Cellular Neuroscience, Mainz*

Schuck F., Reinhardt S., Efferth T., Endres K. (2011) Evaluation of Korean Medical Plant Extracts for their Potential in Alzheimer's Disease Therapy. *11th annual FTN/IAK symposium – Molecular and Cellular Neuroscience, Mainz*

Augustin R., Endres K., Reinhardt S., Kuhn PH., Lichtenthaler SF, Hansen J., Wurst W., Trümbach D. (2012) Computational identification and experimental validation of microRNAs binding to the Alzheimer-related gene ADAM10. *2nd Rhine-Main-Neuroscience (rmn2) meeting, Oberwesel; 1st FTN Status Meeting, Mainz; 5th Annual Meeting of NGFN-Plus and NGFN-Transfer, Heidelberg*

Sakry D., Kaiser N., Karram K., Reinhardt S., Postina R., Endres K., Lutz B., Trotter J. (2012) Neuromodulatory potential of oligodendrocyte precursor cells: role of the NG2 protein? *2nd Rhine-Main-Neuroscience (rmn2) meeting, Oberwesel*

Löffler S., Reinhardt S., Schuck F., Endres K. (2012) A dual mdr1a/b promoter assay as a novel tool for identification of gene expression inducers. *Transporter und Barriere Tage, Bad Herrenalb*

Reinhardt S., Schuck F., Grösgen S., Riemenschneider M., Grimm M., Postina R., Hartmann T., Endres K. (2013) Unfolded protein response signalling by transcription factor XBP-1 regulates ADAM10 and is impaired in Alzheimer's disease. *11th International Conference on Alzheimer's & Parkinson's Diseases, Florence*

Freese C., Reinhardt S., Endres K., Hefner G., Unger R. E., Kirkpatrick C. J. (2013) Development of an in vitro co-culture model of the blood-brain barrier: A potential system to study the transport of Alzheimer drugs coupled to nanoparticles? *International Conference for Nanoparticles and nanotechnologies in medicine, Milan*

Schuck F., Reinhardt S., Freese C., Schmitt U., Efferth T, Endres K. (2013) Evaluation of Korean Plant Extracts for their Potential in Alzheimer's Diseaase Therapy. *12th Annual FTN/IAK Symposium in Molecular and Cellular Neuroscience, Mainz*

Duckro K., Schuck F., Reinhardt S., Endres K. (2013) Development of an ex vivo Alzheimer's Disease Cell Model. *12th Annual FTN/IAK Symposium in Molecular and Cellular Neuroscience, Mainz.*

7. Anhang

7.1 Veröffentlichungen

Augustin R, Endres K, Reinhardt S, Kuhn PH, Lichtenthaler SF, Hansen J, Wurst W, Trümbach D. Computational identification and experimental validation of microRNAs binding to the Alzheimer-related gene ADAM10. *BMC Med Genet.* 2012 May 17;13:35.

Reinhardt S, Schuck F, Grösgen S, Riemenschneider M, Hartmann T, Postina R, Grimm M, Endres K. Unfolded protein response signaling by transcription factor XBP-1 regulates ADAM10 and is affected in Alzheimer's disease. *FASEB J.* 2014 Feb;28(2):978-97. doi: 10.1096/fj.13-234864. Epub 2013 Oct 28.

Endres K, Reinhardt S. ER-stress in Alzheimer's disease: turning the scale? *Am J Neurodegener Dis*. 2013 Nov 29;2(4):247-265. eCollection 2013. Review.

Freese C*, Reinhardt S*, Hefner G, Unger RE, Kirkpatrick CJ, Endres K. A novel blood-brain barrier co-culture system for drug targeting of Alzheimer's disease: establishment by using acitretin as a model drug. *PLoS ONE* 2014 9(3): e91003. doi:10.1371/journal.pone.0091003 (* authors contributed equally)

BMC Medical Genetics

RESEARCH ARTICLE Open Access

Computational identification and experimental validation of microRNAs binding to the Alzheimer-related gene ADAM10

Regina Augustin[1], Kristina Endres[2], Sven Reinhardt[2], Peer-Hendrik Kuhn[3], Stefan F Lichtenthaler[3], Jens Hansen[1], Wolfgang Wurst[1,3,4*] and Dietrich Trümbach[1,4*]

Abstract

Background: MicroRNAs (miRNAs) are post-transcriptional regulators involved in numerous biological processes including the pathogenesis of Alzheimer's disease (AD). A key gene of AD, *ADAM10*, controls the proteolytic processing of *APP* and the formation of the amyloid plaques and is known to be regulated by miRNA in hepatic cancer cell lines. To predict miRNAs regulating *ADAM10* expression concerning AD, we developed a computational approach.

Methods: MiRNA binding sites in the human *ADAM10* 3' untranslated region were predicted using the RNA22, RNAhybrid and miRanda programs and ranked by specific selection criteria with respect to AD such as differential regulation in AD patients and tissue-specific expression. Furthermore, target genes of *miR-103*, *miR-107* and *miR-1306* were derived from six publicly available miRNA target site prediction databases. Only target genes predicted in at least four out of six databases in the case of *miR-103* and *miR-107* were compared to genes listed in the AlzGene database including genes possibly involved in AD. In addition, the target genes were used for Gene Ontology analysis and literature mining. Finally, we used a luciferase assay to verify the potential effect of these three miRNAs on *ADAM10* 3'UTR in SH-SY5Y cells.

Results: Eleven miRNAs were selected, which have evolutionary conserved binding sites. Three of them (*miR-103*, *miR-107*, *miR-1306*) were further analysed as they are linked to AD and most strictly conserved between different species. Predicted target genes of *miR-103* (p-value = 0.0065) and *miR-107* (p-value = 0.0009) showed significant overlap with the AlzGene database except for *miR-1306*. Interactions between *miR-103* and *miR-107* to genes were revealed playing a role in processes leading to AD. *ADAM10* expression in the reporter assay was reduced by *miR-1306* (28%), *miR-103* (45%) and *miR-107* (52%).

Conclusions: Our approach shows the requirement of incorporating specific, disease-associated selection criteria into the prediction process to reduce the amount of false positive predictions. In summary, our method identified three miRNAs strongly suggested to be involved in AD, which possibly regulate *ADAM10* expression and hence offer possibilities for the development of therapeutic treatments of AD.

* Correspondence: wurst@helmholtz-muenchen.de; dietrich.truembach@helmholtz-muenchen.de
[1]Helmholtz Centre Munich, German Research Centre for Environmental Health (GmbH) and Technical University Munich, Institute of Developmental Genetics, Ingolstädter Landstraße. 1, 85764 Munich-Neuherberg, Germany
[3]DZNE-German Center for Neurodegenerative Diseases, Schillerstrasse 44, 80336 Munich, Germany
Full list of author information is available at the end of the article

Background

MicroRNAs (miRNAs) are on average 22 nucleotides long and play a pivotal role in gene regulation. These small RNAs regulate the gene expression post-transcriptionally by suppression of mRNA translation, stimulation of mRNA deadenylation and degradation or induction of target mRNA cleavage, but have also the potential to activate translation [1,2]. Over half of the mammalian protein coding-genes are regulated by miRNAs and most human mRNAs have binding sites for miRNAs [3]. The interaction of miRNA and target mRNA requires base pairing between the seed sequence (positions 2–8) of the miRNA at the 5′ end and a sequence most frequently found in the 3′ untranslated region (UTR) of the target mRNA [4]. MiRNAs are involved in neuronal functions like neurite outgrowth and brain development. They were recently described to play a role in human neurodegenerative diseases. Changes in miRNA expression profiles or miRNA target sequences could contribute to the development of Parkinson's disease and Alzheimer's disease (AD) [5,6].

Characteristics of AD are insoluble plaques of amyloid β (Aβ) peptides emerging from the cleavage of the amyloid beta precursor protein (*APP*) and neuro-fibrillary tangles in the brains of AD patients [7,8]. The alpha-secretase "a disintegrin and metalloproteinase 10" (*ADAM10*) [9-11] generates soluble secreted amyloid precursor protein-alpha (sAPPα) and avoids formation of plaques, because it cleaves *APP* inside the Aβ sequence [12].

Numerous available computational methods predict a large number of genes targeted by miRNAs regulating gene expression, but only few have been validated experimentally. Many computational predictions are false positives and therefore have to be filtered out [13]. The requirement of target-site conservation in different species including far related species would be a potential way to reduce the false positive rate [14].

In this study we established an approach to identify miRNAs regulating *ADAM10* expression which therefore might influence the progression of AD. The three programs RNA22, RNAhybrid and miRanda predicted potential miRNA binding sites to *ADAM10*. We sought to identify the most interesting miRNAs possibly binding to *ADAM10* with additional selection criteria in particular whether they play a role in AD. Additionally, the most interesting miRNAs were experimentally verified by a luciferase assay. Our results show that *miR-103*, *miR-107* and *miR-1306* influence the expression of *ADAM10* at least in the reporter assay system. These miRNAs could play a role in AD and therefore are interesting candidates to be further analysed concerning their biological function and relation to AD.

Methods

miRNA target site prediction databases

MiRNA binding sites to target genes were downloaded from seven different databases: miRBase, 5-Nov-2007, http://www.mirbase.org/ [15]; microRNA, September 2008 Release, http://www.microrna.org/microrna/home.do [16]; PicTar via UCSC Table Browser, assembly = May 2004 (NCBI35/hg17), group = Regulation, track = PicTar miRNA, http://genome.ucsc.edu/ [17]; PITA, version 6 (31-Aug-2008), http://genie.weizmann.ac.il/pubs/mir07/index.html [18]; RNA22, March 2007, http://cbcsrv.watson.ibm.com/rna22.html [19]; TarBase, June 2008, http://diana.cslab.ece.ntua.gr/tarbase/ [20]; TargetScan, Release 5, http://www.targetscan.org/ [3]. We established a workflow considering all miRNA target site predictions downloaded.

miRNA target prediction

We used three prediction programs RNA22, RNAhybrid, miRanda and predicted all binding sites of the miRNA sequences to the 3'UTR sequence of human *ADAM10*.

RNA22 is a pattern-based method for the identification of miRNA-target sites. The method has high sensitivity, is resilient to noise, can be applied to the analysis of any genome without requiring genome-specific retraining and does not rely upon cross-species conservation. Focusing on novel features of miRNA-mRNA interaction RNA22 first finds putative miRNA binding sites in the sequence of interest then identifies the targeting miRNA and hence allows to identify sites targeted by yet-undiscovered miRNAs. An implementation of RNA22 (19-May-2008) is available online at http://cbcsrv.watson.ibm.com/rna22.html [19,21].

The second program RNAhybrid is an extension of the classical RNA secondary structure prediction algorithm from Zuker and Stiegler [22]. It finds the energetically most favorable hybridization sites of a small RNA in a large RNA incorporating 'seed-match speed-up', which first searches for seed matches in the candidate targets and only upon finding such matches the complete hybridization around the seed-match is calculated. The user can define the position and length of the seed region with the option to allow for G:U wobble base pairs in the seed pairing. Intramolecular base pairings and branching structures are forbidden and statistical significance of predicted targets is assessed with an extreme value statistics of length normalized minimum free energies, a Poisson approximation of multiple binding sites, and the calculation of effective numbers of orthologous targets in comparative studies of multiple organisms. RNAhybrid, Version 2.1, is available online at http://bibiserv.techfak.uni-bielefeld.de/rnahybrid/ [23,24].

The miRanda algorithm is similar to the Smith-Waterman algorithm, but scores based on the complementarity of nucleotides (A = U or G ≡ C) and one G:U wobble pair is allowed in the seed region but has to be compensated by matches in the 3′ end of miRNA. In order to estimate the thermodynamic properties of a predicted pairing between miRNA and 3′UTR sequence, the algorithm uses folding routines from the Vienna 1.3 RNA secondary structure programming library (RNAlib) [25]. A conservation filter is used and optionally some rudimentary statistics about each target site can be generated. MiRanda, September 2008 Release, is available online at http://www.microrna.org/microrna/home.do [21,26].

The parameter setting for RNA22 is: maximum number of "UN-paired" bases within the extent of the seed = 0, extent of seed in nucleotides = 6, minimum number of paired-up bases that you want to see in any reported heteroduplex = 14, maximum value for the folding energy in any reported heteroduplex = −25 kcal/mol. The parameter setting for RNAhybrid is: "-s 3utr_human" ("-s" tells RNAhybrid to quickly estimate statistical parameters from "minimal duplex energies" under the assumption that the target sequences are human 3′UTR sequences). The parameter setting for miRanda is the default parameter setting: gap open penalty = −8, gap extend = −2, score threshold = 50, energy threshold = −20 kcal/mol, scaling parameter = 4.

We retrieved the 3′UTR sequence of *ADAM10* (human *ADAM10* 3′UTR based on transcript NM_001110 (chr15:58888510–58889745)) from NCBI http://www.ncbi.nlm.nih.gov/. We downloaded 703 mature miRNA sequences for *Homo sapiens* from miRBase, version 13.0 http://www.mirbase.org/ [15].

Extraction of best miRNA predictions

The extraction of miRNAs was applied according to the following selection criteria. We checked for each miRNA how many programs predicted the miRNA to bind to human *ADAM10* 3′UTR. The regulation of miRNAs in AD was verified by the publication of Cogswell et al. [27], which provides a list of miRNAs expressed in the tissues hippocampus, cerebellum and medial frontal gyrus. Another possibility to check the expression of miRNAs in the brain is the Mouse Genome Informatics (MGI) database (Mouse Genome Database, The Jackson Laboratory, Bar Harbor, Maine; http://www.informatics.jax.org/) [28]. Literature search by PubMed was done as an additional approval, to search for already described target genes of the miRNAs, especially for target genes involved in AD. Mouse ADAM10 3′UTR based on transcript NM_007399 (chr9:70625902–70628036) from NCBI http://www.ncbi.nlm.nih.gov/ was used for binding site search of mouse miRNAs from miRBase, version 13.0 http://www.mirbase.org/ [15]. The parameter setting for RNA22 and miRanda is the same as for human miRNA binding site prediction at the human ADAM10 3′UTR. The parameter setting for RNAhybrid is "-d 1.9,0.28" (1.9 is the location parameter and 0.28 the shape parameter of the assumed extreme value distribution). Additionally, we searched by TargetScan database http://www.targetscan.org/ [3] and microRNA database http://www.microrna.org/microrna/home.do [16] for miRNAs binding to human *ADAM10* 3′UTR and compared the TargetScan and microRNA predictions to our list of miRNAs for equal miRNAs. We identified the number of binding sites of a miRNA in the human *ADAM10* 3′UTR predicted by each program. *ADAM10* 3′UTR sequences from ten different species were analysed for conserved regions. The following sequences where taken: human *ADAM10* 3′UTR from transcript NM_001110 (chr15:58888510–58889745), mouse *ADAM10* 3′UTR from transcript NM_007399 (chr9:70625902–70628036), horse *ADAM10* 3′UTR from transcript XM_001498169.1 (chr1:132875124–132876868), dog *ADAM10* 3′UTR from transcript XM_858910 (chr30:26596273–26598436), chimp *ADAM10* 3′UTR from transcript XM_001172393.1 (chr15:55942343–55944774), chicken *ADAM10* 3′UTR from transcript ENSGALT00000034458 (chr10:7949768–7951846), rhesus monkey *ADAM10* 3′UTR from transcript XM_001096908 (chr7:36929437–36932008), zebra fish *ADAM10* 3′UTR from transcript NM_001159314 (chr7:31745579–31747655), opossum *ADAM10* 3′UTR from transcript ENSMODT00000011088 (chr1:162230000–162230183), zebra finch *ADAM10* 3′UTR from transcript XR_054746 (chr10:6638729–6639273). For multiple sequence alignment of the ten *ADAM10* 3′UTR sequences we applied ClustalW Version 2.1 from the European Bioinformatics Institute (EBI) http://www.ebi.ac.uk/ [29,30]. We used default parameters except: DNA Weight Matrix = 'ClustalW', Clustering = 'UPGMA'. After extraction of the conserved regions between at least seven species we looked for miRNA binding sites localized in these conserved regions. Additionally, we determined the conservation (given in percentage) of the miRNA binding site sequence from human to each species.

Statistical analysis

Statistical analysis was performed with R statistical software (R 2.8.0, http://www.r-project.org/). The *p*-value was computed by the R function fisher.test with default settings. The Fisher's exact test is used to examine the significance of the association (contingency) between the two kinds of classification. Significantly regulated genes were considered, if the *p*-value is equal or below 0.05. We generated Venn diagrams to see the overlap between target genes of *miR-103* and *miR-107* common in 4 out

of 6 databases as well as genes in the AlzGene database (http://www.alzgene.org/; Version: 20.06.2011) [31]. Each set of target genes of *miR-103* and *miR-107* common in 4 out of 6 databases as well as the set of target genes of *miR-1306* in the database PITA was explored for enrichment in Gene Ontology [32] by the software Pathway Studio 8.0 (Ariadne Genomics) based on database ResNet 8.0.

Literature mining and pathway analysis

Literature search by PubMed was done to extract information about the target genes of the miRNAs resulting from Pathway Studio analysis and their relation to AD. To verify the miRNAs searches were performed for miRNA interactions in all PubMed abstracts with the help of the text mining program Pathway Studio 8.0 (Ariadne Genomics) based on the Natural Language Processing (NLP) Technology. Pathway analysis was done with the software Ingenuity Systems IPA 9.0 (http://www.ingenuity.com/) especially with the Path Designer.

Material

Mature miRNAs and the inactive negative control were from Invitrogen (No. PM11012, PM13206, PM10632, PM10056). All RNA species were dissolved to 5 pmol/μl in nuclease-free water upon arrival, aliquoted and stored at −20°C.

Cloning of the ADAM10 3′UTR luciferase reporter construct

The 3′UTR of human *ADAM10* was amplified from THP-1 chromosomal DNA using the FailSafe PCR kit (Epicentre) and the following primers:

AD10_3UTR_for 5′GCGGCCGCGCCCATTCAGCA ACCCCAG 3′
AD10_3UTR_rev 5′GCGGCCGCCACTTGTGCCCG TAGCAGCC 3′.

The obtained DNA fragment was verified by restriction digestion and sequencing. The 3′UTR was subsequently cloned into the *Not*I site of the pCMV-GLuc vector (NEB), which allows to monitor regulated Gaussia luciferase expression in the cell supernatant.

Cell culture

SH-SY5Y cells were cultivated in phenol red-free DMEM/F12, supplemented with 10% FCS and 1% glutamine at 37°C, 95% air moisture, 5% CO_2 and passaged twice a week with a splitting rate of ½ to ¼.

3′UTR luciferase reporter assay

Retro-transfection was performed using 0.005 μl Lipofectamine 2000 (Invitrogen) per μl OptiMEM-medium and 0.1 pmol/μl miRNA (Invitrogen) or negative control. For combination of miRNA 1306 together with miRNA 103 or 107 a concentration of 0.05 pmol/μl each was used. 2 ng/μl endotoxin-free plasmid DNA of the 3′UTR-reporter vector were added to 45.000 cells per well in 96 well format. Control cells were mock-treated with nuclease-free water instead of RNA molecules.

5 hrs after transfection, the cell supernatant was exchanged to 200 μl culture medium per well. In a preliminary experiment, 10 μl cell supernatant were collected at various time points over a 72 hour period; 48 hours were determined to be the optimal incubation time (data not shown). Therefore, 10 μl cell supernatant were aspirated 48 hours after transfection and stored at −20°C until samples were measured. Secreted Gaussia luciferase was quantitatively analyzed (Renilla-Luciferase assay, Promega) using the FluostarOptima luminometer (BMG). Cell densities were checked by quantitation of protein content in the cell lysate by NanoQuant assay (Roth).

Results and discussion

MiRNA prediction

We established a workflow (Figure 1) to obtain miRNAs possibly binding to the human *ADAM10* 3′UTR. Instead of looking up miRNA target sites of *ADAM10* in the miRNA target site prediction databases, we predicted the binding sites of human miRNAs to human *ADAM10* 3′UTR by the three programs, RNA22, RNAhybrid and miRanda, with the aim to yield a more accurate miRNA target site prediction. Due to the fact that the three prediction programs focus on different aspects for miRNA target site prediction (pattern-based search, seed matching, conservation, energy or structure) various properties of the target sequence are covered (see Methods: "miRNA target prediction").

122 miRNAs are predicted by at least two programs to bind to human *ADAM10* 3′UTR sequence and 52 of them are significant according to expression and selection criteria described in the following. To consider different aspects of the distinct prediction algorithms at least two programs should predict a miRNA binding site. Important is also the expression of the miRNA in brain provided by the MGI database or the regulation of the miRNA in AD as described by Cogswell and colleagues (2008) in the tissues hippocampus, cerebellum and medial frontal gyrus [27]. An additional confirmation of miRNA being involved in AD is a binding site to a target gene, which is involved in AD, described in the literature and thus the miRNA might regulate also other AD key genes such as ADAM10. Furthermore, the miRNA

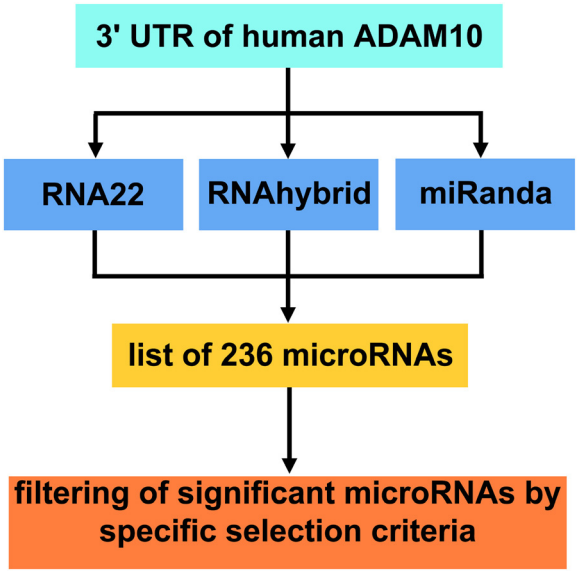

Figure 1 Computational prediction of miRNAs binding to ADAM10 3'UTR. Three programs RNA22, RNAhybrid and miRanda are used for the prediction of miRNAs binding to the human *ADAM10* 3'UTR. After retrieving a list of 236 miRNAs by RNA22, RNAhybrid or miRanda we extracted the relevant miRNAs according to selection criteria: prediction by at least two programs, differential regulation in AD patients (Cogswell et al. 2008), tissue-specific expression (MGI), binding to AD key genes, corresponding mouse miRNA binding to the mouse ADAM10 3'UTR sequence predicted by at least two of the three programs, additional prediction by TargetScan and microRNA, occurrence of multiple binding sites and evolutionary conservation.

prediction is strengthened by the corresponding mouse miRNA binding to the mouse ADAM10 3′UTR sequence predicted by at least two of the three miRNA prediction programs RNA22, RNAhybrid and miRanda. Prediction of the miRNA by other webtools such as TargetScan and microRNA is also a confirmation of the miRNA. Multiple binding sites of a single miRNA in the 3′UTR verify the prediction [33].

The list of 52 miRNAs incorporates not conserved as well as conserved miRNAs or rather miRNA binding sites. Filtering according to conservation helps to reduce the number of miRNAs and improves the selection of candidates for further experimental validations. Consideration of conservation across species, including those not developing AD, was chosen as a filter criterion because a correlation between miRNA conservation and disease susceptibility has in general been suggested by Lu et al. [34]. Our selection procedure therefore excludes non-conserved miRNA binding sites, which also might be relevant for development of the disease but are not lost by being included in the list of 52 miRNAs. In regard to AD being a human disease, future analysis of non-conserved miRNAs might also represent a valuable approach which we did not follow in the context of this manuscript. In our analysis eleven miRNA binding sites are conserved across at least seven species, at which four of these miRNAs are also conserved in the far related species zebra fish. The only miRNA binding site *miR-1306* in the human *ADAM10* 3′UTR predicted by all three programs is also conserved in the far related zebra fish as well as in mouse, horse, dog, chimp, chicken, rhesus monkey and zebra finch (Figure 2A). This binding site is located on chromosome 15 positions 58889309–58889324 and the programs RNA22, RNAhybrid and miRanda predicted the binding energy −32.29, -25.7 and −22.55 kcal/mol, respectively. The conservation of the miRNA binding site sequence between human and the species mouse, horse, dog, chimp as well as rhesus monkey is 100%. The conservation of chicken, zebra finch and zebra fish to human in this binding region is 94%, 88% and 75%, respectively. The second most interesting miRNAs possibly binding to human *ADAM10* 3′UTR are *miR-103* as well as *miR-107* both having the same binding site located on chromosome 15 positions 58889443–58889468. This site is predicted by the two programs RNAhybrid and miRanda with binding energy −27.9 and −23.66 kcal/mol for *miR-103*, respectively, as well as −26.2 and −22.28 kcal/mol for *miR-107*, respectively. The conservation of the miRNA binding site sequence between human and the species mouse, horse, dog and chimp is 96%, while the conservation of chicken, rhesus monkey and finch to human is 65%, 100% and 73%, respectively (Figure 2B–C). Additionally, *miR-202*, *miR-423-5p*, *miR-503*, *miR-184* and *miR-922* bind also to the conserved binding region chromosome 15 positions 58889443–5889473 and *miR-330-5p* (chr15:58889149–58889178), *miR-671-5p* (chr15:58889720–58889745) and *miR-432* (chr15:58889688–58889718) bind to a region with good conservation also to the far related species zebra fish, but these eight miRNAs have no indication to be involved in AD (Table 1). Table 1 shows a ranked list of the best miRNA binding site predictions according to the specific selection criteria. We chose the three most interesting miRNAs 1306, 107 and 103 and performed analyses with the AlzGene database, further miRNA target site prediction databases, Gene Ontology, literature mining and validation experiments to identify the involvement in AD. *MiR-107* and *miR-103* are downregulated with age [35] as well as in AD gray matter [36] and repress the translation of cofilin. In brains of a transgenic mouse model of AD the level of *miR-103* and *miR-107* is decreased while the cofilin protein level is increased which results in the formation of rod-like structures [37]. Furthermore, *miR-107* expression is decreased even in the earliest stages of AD. As *miR-107* regulates beta-site APP-cleaving enzyme 1 (*BACE1*) it might be involved in accelerated disease progression

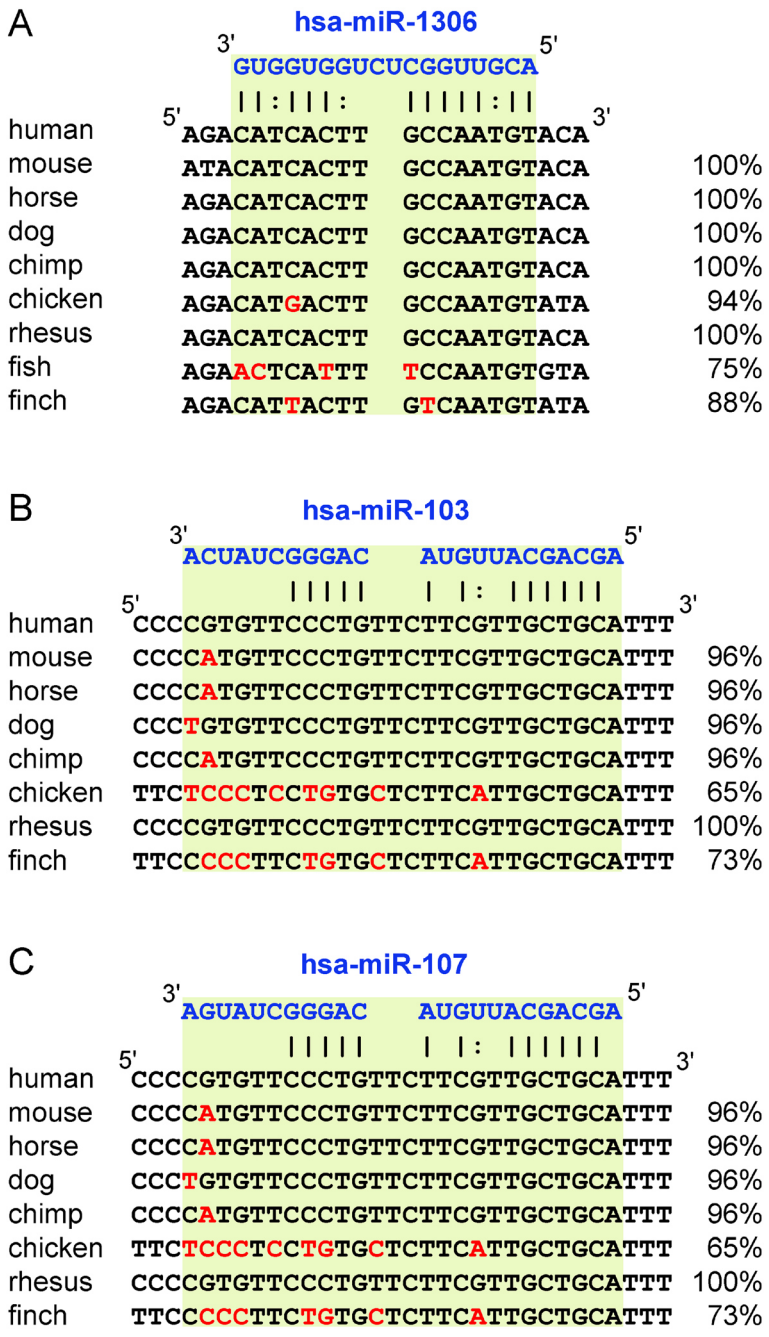

Figure 2 Conservation of the three miRNA binding sites within the ADAM10 3′UTR. The figure shows the conservation of the *miR-1306* (**A**), *miR-103* (**B**) and *miR-107* (**C**) binding region (light green) between different species. The blue sequence represents the miRNA binding to the DNA of different species as listed on the left side. On the right side the conservation of the miRNA binding region (light green) from different species to human sequence is given. Nucleotide mismatches in the binding region to human binding region are marked in red. The lines and colons below the miRNA sequence show perfect nucleotide matches and G:U/T wobble pairs, respectively.

[38]. The downregulation of miR-103 and miR-107 with age could concern a protective effect against plaque formation because reduced levels of these miRNAs would lead to an increased level of the predicted target ADAM10 and its neuroprotective product sAPPα in brains of AD patients. Our observations of strong inhibition (> 40%) of ADAM10 expression in the reporter assay upon application of miR-103 and miR-107 would coincide with such a possible protective influence on amyloid pathology (see "Experimental validation of bioinformatically predicted miRNAs"). According to the publication from Cogswell et al. [27] *miR-103* is

Table 1 List of predicted miRNAs binding to a conserved region of human ADAM10 3'UTR

miRNA	∅ kcal/mol	Confirmations	Differential regulated in AD	Conservation zebra fish
1306	−26.85	predicted by 3 programs, mouse ADAM10		+
107	−24.24	targets BACE1, predicted by TargetScan, literature for AD, mouse ADAM10		
103	−25.78	predicted by TargetScan, literature for AD, mouse ADAM10	hippocampus, cerebellum	
330-5p	−27.20	predicted by microRNA, mouse ADAM10	hippocampus	+
432	−22.81	predicted by microRNA	cerebellum	+
423-5p	−22.1	mouse ADAM10	hippocampus, medial frontal gyrus	
671-5p	−27.61	mouse ADAM10		+
922	−27.99	predicted by microRNA		
503	−25.41	predicted by microRNA, mouse ADAM10		
202	−25.33	predicted by microRNA, mouse ADAM10		
184	−23.33	mouse ADAM10		

The best eleven predicted miRNAs, which bind to a conserved region of human *ADAM10* 3'UTR, are shown with additional information like the average predicted binding energy in kcal/mol (column 2), verifications of the miRNAs from literature, by additional mouse ADAM10 prediction or other prediction programs (column 3), the regulation of miRNAs in AD according to Cogswell et al. (column 4) and the conservation of the binding region in zebra fish marked with + in the last column.

differentially expressed in hippocampus and cerebellum in AD. In addition, the program TargetScan verifies the same binding site of *miR-103* and *miR-107* to human *ADAM10*. *MiR-1306* is further analysed due to its good conservation to the far related species zebra fish with only one mismatch in the seed region. It is the only miRNA whose binding site to human *ADAM10* is predicted by all three programs RNA22, RNAhybrid and miRanda, which strengthens the assumption that this binding site is functionally active. Additionally as shown in Figure 3 the hypothesis is verified that *miR-1306* is associated to AD: Twelve predicted target genes of *miR-1306* are involved in processes and functions playing a role in AD, the nervous system and other neurodegenerative diseases. The predictions rely on TargetScan while the dedicated functions are Ingenuity Expert Findings or from Gene Ontology. *MiR-1306* possibly regulates genes like the cholinergic receptor, nicotinic, alpha 4 (*CHRNA4*), tumor necrosis factor receptor superfamily member 1B (*TNFRSF1B*) and mitogen-activated protein kinase kinase 4 (*MAP2K4*), which are associated to AD by the functions frontotemporal dementia, demyelination of neurons and Huntington's disease, respectively. *MAP2K4* has been found to be involved in AD and is putatively regulated by modules of transcription factor binding sites [39]. Furthermore, miR-1306 is located on chromosome 22 within the second exon of DiGeorge syndrome critical region gene

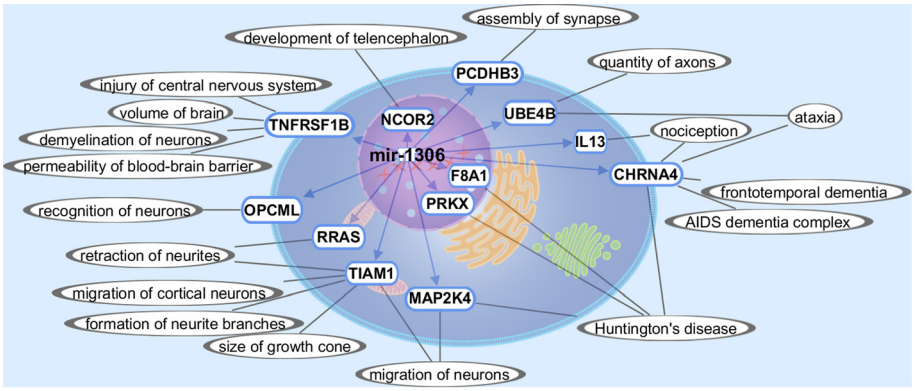

Figure 3 Target gene predictions for miR-1306. Twelve target genes of *miR-1306* were predicted by TargetScan concerning their function in AD, brain, nervous system or other neurodegenerative diseases and graphically interrelated by Path Designer (Ingenuity). The miRNA is located in the nucleus and the predicted target genes indicated by blue arrows and blue framed ellipses are located according to their Gene Ontology either in the nucleus, cytoplasm or membrane. The functions of the target genes are denoted by grey lines and grey framed ellipses and derived from Gene Ontology or Ingenuity Expert Findings, which are substantiated by literature.

8 (DGCR8), which is essential for miRNA biogenesis by being a subunit of the microprocessor complex [40]. Evers et al. presents a case of a DiGeorge syndrome patient with the typical deletion in chromosome band 22q11.2, which contains DGCR8, suffering from dementia [41].

Prediction of miRNA target genes and their relation to AD

To confirm the relationship of the three miRNAs to AD we searched for target gene predictions of these miRNAs in the six databases miRBase, microRNA, PicTar, PITA, RNA22, as well as TargetScan (Figure 4). The combination of different miRNA target site prediction databases and the restriction of the output to four out of six databases in the case of *miR-103* and *miR-107* are important to reduce the amount of false positive miRNA target sites in the end. In the case of *miR-1306* there is no restriction of the output, because only the database PITA incorporates predictions for this miRNA. Additionally, Tarbase can be included in the analysis. The database Tarbase has a special position, because in contrast to the other six databases Tarbase contains experimentally supported miRNA targets and not in-silico predicted miRNA binding sites. All miRNA target sites from Tarbase are automatically included in the output of the analysis. In contrast to the other six databases Tarbase doesn't contain false positive miRNA target sites. In our case Tarbase doesn't contain target genes for the miRNAs: *miR-103*, *miR-107* and *miR-1306*. The six miRNA target site prediction databases miRBase, microRNA, PicTar, PITA, RNA22, and TargetScan contain altogether 18915 different (according to EntrezGene) human genes at which PITA alone contains 16819 genes. After the analysis we got 156 and 157 target genes for *miR-103* and *miR-107*, respectively, common in four out of six databases, and 890 target genes for *miR-1306* of database PITA. As we focus on miRNAs playing a role in AD, we used the AlzGene database to see which target genes of the miRNAs have a genetic association with AD. AlzGene database is a regularly updated aggregation of all published genetic association studies including GWAS (genome-wide association studies) performed on AD phenotypes. 636 and 591 genes of AlzGene database overlap with 18915 genes of the six miRNA target site prediction databases and 16819 genes of database PITA, respectively. The overlap between AlzGene database genes and the target genes of *miR-103*, *miR-107* as well as *miR-1306* are 12, 14 (Figure 5) and 24 genes, respectively (Additional file 1). *MiR-103* and *miR-107* have 130 target genes in common (Figure 5, Additional file 1). Applying a Fisher's exact test we got a *p*-value of 0.0065, 0.0009 and 0.1904 for the overlap of *miR-103*, *miR-107* and *miR-1306*, respectively, with the AlzGene database, which shows that 12 and 14 are significant high numbers of overlapping genes between the target genes and the AlzGene database. This result suggests that *miR-103* and *miR-107* might play a role in AD. It is not remarkable that the *p*-value for the overlap of *miR-1306* with the AlzGene database is not significant as the restriction to four out of six databases was not possible, which consequentially leads to the inclusion of a lot of false positive target genes in the 890 target genes of *miR-1306*.

Gene ontology

Additionally, we did a Gene Ontology analysis with the predicted target genes of the three miRNAs to validate the functionality of the miRNAs and their involvement

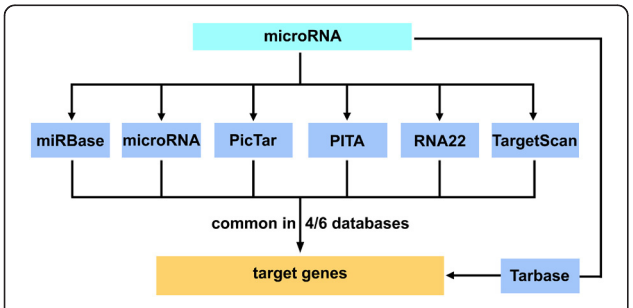

Figure 4 Workflow for miRNA target site prediction. Seven databases miRBase, microRNA, PicTar, PITA, RNA22, TargetScan and Tarbase, which is experimentally supported by miRNA targets, are incorporated in the prediction of miRNA target sites. The input is a miRNA and the output is a set of target genes common to four out of six databases. Tarbase contains experimentally supported miRNA targets and not in-silico predicted miRNA binding sites: all miRNA target genes from Tarbase are automatically included in the output of the analysis.

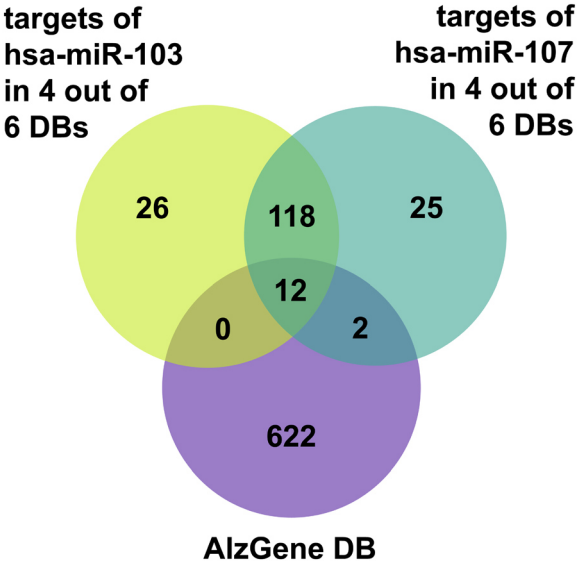

Figure 5 Venn Diagram. The Venn diagram shows the significant overlap of the target genes of *miR-103* and *miR-107* common in four out of six databases as well as the genes of AlzGene database.

to AD. With the help of the literature mining tool Pathway Studio we searched for molecular functions and biological processes common to the target genes of the three miRNAs. The molecular function calcium ion binding is significant in all three miRNA analyses (*miR-103*: p-value = 0.0011; *miR-107*: p-value = 0.0025; *miR-1306*: p-value = 2.1×10^{-5}) and is considered to be involved in AD. Calcium ions are found in an elevated level in tangle-bearing neurons of AD patients compared to healthier neurons [42]. Further, an abnormal increase of intracellular Calcium ion levels in neurites associated with Aβ deposits was demonstrated in a mouse model of AD [43]. An additional evidence is given by the significant biological processes learning (*miR-103*: p-value = 0.0008; *miR-107*: p-value = 3.3×10^{-5}; *miR-1306*: p-value = 0.0003), brain development (*miR-103*: p-value = 0.0023; *miR-107*: p-value = 0.0004; *miR-1306*: p-value = 7.1×10^{-6}) and nervous system development (*miR-103*: p-value = 0.0004; *miR-107*: p-value = 0.0004; *miR-1306*: p-value = 6.9×10^{-8}) that the three miRNAs are involved in AD. Mouse models with an overexpression of *ADAM10* showed a positive effect of the α-secretase on learning and memory and mice with a dominant negative mutant form of *ADAM10* had learning deficiencies [12]. Environmental influences occurring during brain development predefine the expression and regulation of APP. As a consequence levels of APP and Aβ are increased causing AD later in life [44]. The Aβ fragments forming plaques are of varying length depending on the site of cleavage. The $A\beta_{42}$ fragment is a ligand for the cellular prion protein, which is important for nervous system development [45]. (See Additional files 2, 3 and 4: List of enriched target genes of miR-103/107/1306 in Gene Ontology).

Literature mining

Furthermore, a network (Figure 6) containing already published interactions of *miR-103* and *miR-107* with genes involved in AD or included in the AlzGene database was established using the literature mining tool Pathway Studio. This network allowed confirming the relation of the two miRNAs to AD by their respective target genes. The genes dicer 1, ribonuclease type III (*Dicer*) and TAR (HIV-1) RNA binding protein 2 (*TARBP2*) targeted by *miRNA-103* and *miRNA-107* are components of the miRNA-processing complex [46]. Besides those two genes, a link between the two miRNAs is provided by linoleic acid [47], which probably affects AD by increasing the expression of Presenilin1 (*PSEN1*) and Aβ [48]. Another target gene in the network, Granulin (*GRN*), is regulated by *miR-107* [49] which regulates *BACE1* as well [38]. Therefore both genes might be involved in neurodegenerative diseases especially AD. The tumor suppressors *TP53* as well as *TP73* appear to regulate the processing of *miR-107* [46]. M*iR-103* increases the expression level of fatty acid binding protein 4 (*FABP4*) while its expression is reduced by tumor necrosis factor (*TNF*) [50]. All six target genes of the miRNAs 103 and 107 *GRN*, *BACE1*, *TP53*, *TP73*, *FABP4* and *TNF* are included in the AlzGene database, hence putatively playing a role in AD. The four remaining target genes cyclin-dependent kinase 2 (*CDK2*), cAMP responsive element binding protein 1 (*CREB1*), nuclear factor I/A (*NFIA*) and vascular endothelial growth factor A (*VEGFA*) of the network are mentioned in literature to be involved directly or in processes developing AD. *miR-103* directly binds and represses *CDK2* and *CREB1* through 3′UTR binding [51]. *CDK2* is a key regulator in neuronal differentiation with the downregulation of *CDK2* as crucial event [52] and neuronal differentiation is regulated by *PSEN1*, a major key gene of AD [53]. The transcription factor *CREB1* is involved in several types of learning and memory. A direct involvement in AD is seen in some mouse models, where its activity is impaired [54]. *NFIA* is negatively regulated by *miR-107* [55] and plays an important role in the formation of the corpus callosum in the developing brain. The disruption of *NFIA* results in agenesis of the corpus callosum [56], whereas the size of the corpus callosum is significantly reduced in AD patients [57]. The expression of the hypoxia-regulated gene *VEGFA* is decreased by *miR-107* [58]. Additionally, it is known, that polymorphisms within the *VEGFA* promoter region are associated with increased risk for AD, by reducing the neuroprotective effect of *VEGFA* [59]. These findings of the literature and AlzGene database confirm the biological role of the target genes in neurodegenerative processes and hence the involvement of *miR-103* and *miR-107* in AD.

Experimental validation of bioinformatically predicted miRNAs

To demonstrate that the selected miRNAs 1306, 103 and 107 directly regulate *ADAM10* expression by interaction with the 3′UTR of the human gene, we performed cotransfection experiments with a Gaussia reporter vector harbouring the 3′UTR of *ADAM10* downstream of the luciferase coding sequence together with the respective miRNAs. As a positive control we used *miR-122* which has been identified and validated as an important regulator of *ADAM10* in hepatocellular carcinoma by an experimental approach [60]. The programs RNA22, RNAhybrid and miRanda predicted a miR-122 binding site to human *ADAM10* 3′UTR with binding energy −31.2, -25.6 and −21.84 kcal/mol (on average: −26.21 kcal/mol), respectively, comparable to the miR-1306 binding site prediction (see Results and Discussion: “miRNA prediction”). Time resolved measurement revealed that 48 hrs incubation period resulted

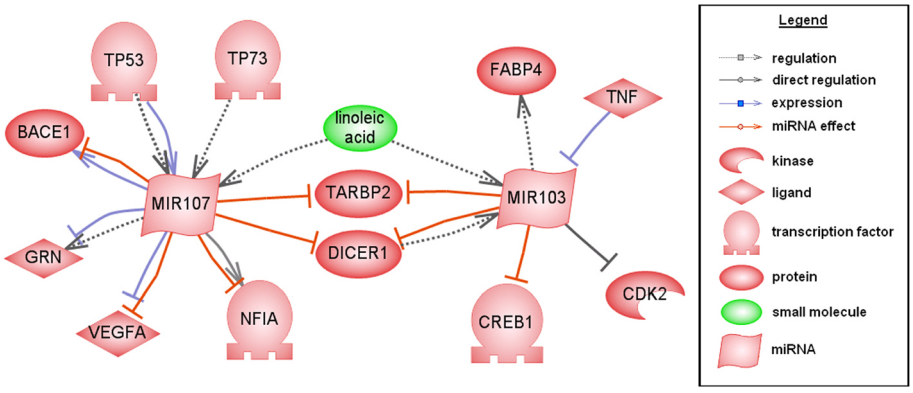

Figure 6 Interaction network of miR-103 and miR-107. The network (established by Pathway Studio) shows already published interactions between *miR-103* as well as *miR-107* and genes known to be involved in AD or neurodegenerative processes. The different types of proteins or small molecules are indicated by different symbols and the various interactions like regulation, expression and miRNA effect are also displayed by various arrows.

in maximal effects of the miRNAs in SH-SY5Y cells (data not shown): while the negative control miRNA had no impact on luciferase activity measured in the cell supernatant, *miR-122* reduced the luminescent signal to 57% as compared to water treated control cells (Figure 7). This effect is even higher than the one observed in the initial publication from Bai et al. (2009) [60] but might be due to the different reporter enzymes or cell lines used. The three miRNAs identified by bioinformatical approaches and integration of literature mining all showed a significant decreasing effect on the *ADAM10* 3′UTR-reporter construct: *miR-1306* lowered the luminescent signal to 72%, *miR-103* to 55% and *miR-107* to 48% of control. While *miR-103* and *miR-107* target the same DNA sequence within the *ADAM10* 3′UTR (see Figure 2), *miR-1306* has a binding site in closer proximity to the Stop codon. We therefore combined *miR-1306* and *miR-103* or *miR-107*, respectively, but observed no distinct significant synergistic effect (*miR-1306* vs. *miR-1306/103* $p < 0.001$; *miR-1306* vs. *miR-1306/107* $p < 0.001$). This might be due to the applied concentration which was reduced to 50% in the combinations (see methods "3′UTR luciferase reporter assay"). These experimental results suggest an influence of *miR-103*, *miR-107* and *miR-1306* on *ADAM10* expression. Nevertheless, the biological impact of either miRNA has to be elucidated further, e.g. by mRNA and protein measurements. Assessing the effect of the selected miRNAs on pathological features in AD mouse models would also help to understand their distinct role in pathogenesis. However, this study shows that the computational workflow consisting of prediction programs and specific selection criteria is a suitable tool for the identification of miRNAs influencing key genes of diseases such as Alzheimer's disease.

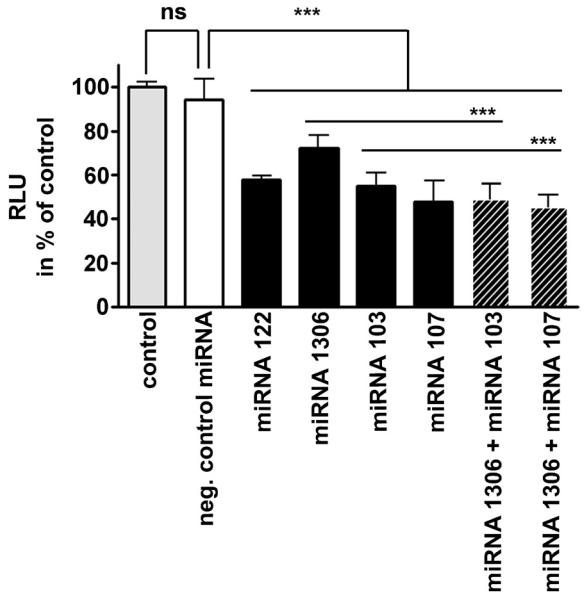

Figure 7 Experimental validation of selected miRNAs. SH-SY5Y cells were transiently cotransfected with the Gaussia reporter vector harbouring the 3'UTR of ADAM10 downstream of the luciferase coding sequence together with the respective miRNAs. *MiR-122*, which has been described by Bai et al. [60] to target *ADAM10*, served as a positive control. After 48 hrs of incubation, luminescence was measured in the cell supernatant. Values obtained for control (water) treated cells were set to 100%, data represent mean ± SD of three independent experiments performed in triplicate. *** $P < 0.001$, ns = not significant, RLU = Relative Light Units.

Conclusions

We established a computational approach for the identification of miRNAs putatively influencing the expression of *ADAM10*. A potential functionality of selected miRNAs 103, 107 and 1306 was confirmed by 3′UTR luciferase reporter assay. These results show that the evolutionary conservation of the target gene binding site

facilitates miRNA candidate selection independently from the disease for further experimental validation. Moreover, these experiments underline the reliability of our computational approach, which is a combination of characteristics of the prediction software and specific selection criteria for filtering out false positive predictions: disease relevance, specificity of expression, evolutionary conservation of binding sites and occurrence of multiple binding sites. This workflow can also be applied to key genes of other diseases with adjustment of the selection criteria according to the scientific research interest. Our approach provides a new selection tool for identification and ranking of AD-related miRNAs, but to elucidate a profound pathological role of selected candidates, further experiments have to be done.

Additional files

Additional file 1: List of predicted target genes common in 4 out of 6 DBs. The table shows a list of predicted target genes of miR-103, miR-107, miR-1306. These target genes are either listed in AlzGene DB and target gene of at least one miRNA or target gene of at least two miRNAs (column 3). Beside the gene symbol the Entrez GeneID is given.

Additional file 2: List of enriched target genes of miR-103 in Gene Ontology. The table shows the Gene Ontology entities with enrichment of predicted target genes of miR-103. Additionally a *p*-value and FDR value is given.

Additional file 3: List of enriched target genes of miR-107 in Gene Ontology. The table shows the Gene Ontology entities with enrichment of predicted target genes of miR-107. Additionally a *p*-value and FDR value is given.

Additional file 4: List of enriched target genes of miR-1306 in Gene Ontology. The table shows the Gene Ontology entities with enrichment of predicted target genes of miR-1306. Additionally a *p*-value and FDR value is given.

Abbreviations

Chr: Chromosome; Human: Homo sapiens; Mouse: Mus musculus; Horse: Equus caballus; Dog: Canis lupus familiaris; Chimp: Pan troglodytes; Chicken: Gallus gallus; Rhesus monkey: Macaca mulatta; Zebra fish: Danio rerio; Opossum: Monodelphis domestica; Zebra finch: Taeniopygia guttata.

Competing interests

The authors declare that they have no competing interests.

Authors' contributions

RA performed the bioinformatic analyses and wrote the manuscript. RA and DT designed the computational workflow. KE designed the experimental system. SR performed transfection and luciferase reporter assay experiments. SFL and PHK contributed to the planning of the whole project. JH participated in the conception of this work. WW directed the work. DT planed and coordinated the entire project. All authors read and approved the final manuscript.

Acknowledgements

We thank Bernd Lentes for technical assistance. This work was supported by the Federal Ministry of Education and Research (BMBF) in the framework of the National Genome Research Network (NGFN), Förderkennzeichen FKZ01GS08130, by the BMBF Project "Kompetenznetzwerk Demenzen - Neurodegeneration" (KNDD, FKZ 01 G1 704) to SFL and WW, by the BMBF Project "Helmholtz Alliance for Mental Health in an Ageing Society" (HelMA, HA215), by the Deutsche Forschungsgemeinschaft (DFG) Project SFB 596 TP A 12 and by the NGFN Project (FKZ 01GS08133).

Author details

[1]Helmholtz Centre Munich, German Research Centre for Environmental Health (GmbH) and Technical University Munich, Institute of Developmental Genetics, Ingolstädter Landstraße. 1, 85764 Munich-Neuherberg, Germany. [2]Department of Psychiatry and Psychotherapy, University Medical Centre of the Johannes Gutenberg-University Mainz, Untere Zahlbacher Str. 8, 55131 Mainz, Germany. [3]DZNE-German Center for Neurodegenerative Diseases, Schillerstrasse 44, 80336 Munich, Germany. [4]Max Planck Institute of Psychiatry, Kraepelinstr. 2-10, 80804 Munich, Germany.

Received: 22 December 2011 Accepted: 19 April 2012
Published: 17 May 2012

References

1. Chekulaeva M, Filipowicz W: **Mechanisms of miRNA-mediated post-transcriptional regulation in animal cells.** *Curr Opin Cell Biol* 2009, **21:**452–460.
2. Vasudevan S, Steitz JA: **AU-rich-element-mediated upregulation of translation by FXR1 and Argonaute 2.** *Cell* 2007, **128:**1105–1118.
3. Friedman RC, Farh KK-H, Burge CB, Bartel DP: **Most mammalian mRNAs are conserved targets of microRNAs.** *Genome Res* 2009, **19:**92–105.
4. Fabian MR, Sonenberg N, Filipowicz W: **Regulation of mRNA translation and stability by microRNAs.** *Annu Rev Biochem* 2010, **79:**351–379.
5. Hébert SS, De Strooper B: **Alterations of the microRNA network cause neurodegenerative disease.** *Trends Neurosci* 2009, **32:**199–206.
6. Satoh J: **MicroRNAs and their therapeutic potential for human diseases: aberrant microRNA expression in Alzheimer's disease brains.** *J Pharmacol Sci* 2010, **114:**269–275.
7. Crews L, Rockenstein E, Masliah E: **APP transgenic modeling of Alzheimer's disease: mechanisms of neurodegeneration and aberrant neurogenesis.** *Brain Struct Funct* 2010, **214:**111–126.
8. Cole SL, Vassar R: **The role of amyloid precursor protein processing by BACE1, the beta-secretase, in Alzheimer disease pathophysiology.** *J Biol Chem* 2008, **283:**29621–29625.
9. Lammich S, Kojro E, Postina R, Gilbert S, Pfeiffer R, Jasionowski M, Haass C, Fahrenholz F: **Constitutive and regulated alpha-secretase cleavage of Alzheimer's amyloid precursor protein by a disintegrin metalloprotease.** *Proc Natl Acad Sci* 1999, **96:**3922–3927.
10. Kuhn PH, Wang H, Dislich B, Colombo A, Zeitschel U, Ellwart JW, Kremmer E, Rossner S, Lichtenthaler SF: **ADAM10 is the physiologically relevant, constitutive alpha-secretase of the amyloid precursor protein in primary neurons.** *EMBO J* 2010, **29:**3020–3032.
11. Lichtenthaler SF, Haass C, Steiner H: **Regulated intramembrane proteolysis – lessons from amyloid precursor protein processing.** *J Neurochem* 2011, **117:**779–796.
12. Postina R, Schroeder A, Dewachter I, Bohl J, Schmitt U, Kojro E, Prinzen C, Endres K, Hiemke C, Blessing M, Flamez P, Dequenne A, Godaux E, van Leuven F, Fahrenholz F: **A disintegrin-metalloproteinase prevents amyloid plaque formation and hippocampal defects in an Alzheimer disease mouse model.** *J Clin Invest* 2004, **113:**1456–1464.
13. Watanabe Y, Tomita M, Kanai A: **Computational methods for microRNA target prediction.** *Methods Enzymol* 2007, **427:**65–86.
14. Lewis BP, Burge CB, Bartel DP: **Conserved seed pairing, often flanked by adenosines, indicates that thousands of human genes are microRNA targets.** *Cell* 2005, **120:**15–20.
15. Griffiths-Jones S, Saini HK, van Dongen S, Enright AJ: **miRBase: tools for microRNA genomics.** *Nucleic Acids Res* 2008, **36:**D154–D158.
16. Betel D, Wilson M, Gabow A, Marks DS, Sander C: **The microRNA.org resource: targets and expression.** *Nucleic Acids Res* 2008, **36:**D149–D153.
17. Krek A, Grün D, Poy MN, Wolf R, Rosenberg L, Epstein EJ, MacMenamin P, da Piedade I, Gunsalus KC, Stoffel M, Rajewsky N: **Combinatorial microRNA target predictions.** *Nat Genet* 2005, **37:**495–500.
18. Kertesz M, Iovino N, Unnerstall U, Gaul U, Segal E: **The role of site accessibility in microRNA target recognition.** *Nat Genet* 2007, **39:**1278–1284.
19. Miranda KC, Huynh T, Tay Y, Ang Y-S, Tam W-L, Thomson AM, Lim B, Rigoutsos I: **A pattern-based method for the identification of MicroRNA binding sites and their corresponding heteroduplexes.** *Cell* 2006, **126:**1203–1217.
20. Papadopoulos GL, Reczko M, Simossis VA, Sethupathy P, Hatzigeorgiou AG: **The database of experimentally supported targets: a functional update of TarBase.** *Nucleic Acids Res* 2009, **37:**D155–D158.

21. Witkos TM, Koscianska E, Krzyzosiak WJ: **Practical Aspects of microRNA Target Prediction.** *Curr Mol Med* 2011, **11:**93–109.
22. Zuker M, Stiegler P: **Optimal computer folding of large RNA sequences using thermodynamics and auxiliary information.** *Nucleic Acids Res* 1981, **9:**133–148.
23. Rehmsmeier M, Steffen P, Hochsmann M, Giegerich R: **Fast and effective prediction of microRNA/target duplexes.** *RNA* 2004, **10:**1507–1517.
24. Krüger J, Rehmsmeier M: **RNAhybrid: microRNA target prediction easy, fast and flexible.** *Nucleic Acids Res* 2006, **34:**W451–W454.
25. Wuchty S, Fontana W, Hofacker IL, Schuster P: **Complete suboptimal folding of RNA and the stability of secondary structures.** *Biopolymers* 1999, **49:**145–165.
26. Enright AJ, John B, Gaul U, Tuschl T, Sander C, Marks DS: **MicroRNA targets in Drosophila.** *Genome Biol* 2003, **5:**R1.
27. Cogswell JP, Ward J, Taylor IA, Waters M, Shi Y, Cannon B, Kelnar K, Kemppainen J, Brown D, Chen C, Prinjha RK, Richardson JC, Saunders AM, Roses AD, Richards CA: **Identification of miRNA changes in Alzheimer's disease brain and CSF yields putative biomarkers and insights into disease pathways.** *J Alzheimers Dis* 2008, **14:**27–41.
28. Bult CJ, Eppig JT, Kadin JA, Richardson JE, Blake JA, Mouse Genome Database Group: **The Mouse Genome Database (MGD): mouse biology and model systems.** *Nucleic Acids Res* 2008, **36:**D724–D728.
29. Larkin MA, Blackshields G, Brown NP, Chenna R, McGettigan PA, McWilliam H, Valentin F, Wallace IM, Wilm A, Lopez R, Thompson JD, Gibson TJ, Higgins DG: **Clustal W and Clustal X version 2.0.** *Bioinformatics* 2007, **23:**2947–2948.
30. Goujon M, McWilliam H, Li W, Valentin F, Squizzato S, Paern J, Lopez R: **A new bioinformatics analysis tools framework at EMBL-EBI.** *Nucleic Acids Res* 2010, **38:**W695–W699.
31. Bertram L, McQueen MB, Mullin K, Blacker D, Tanzi RE: **Systematic meta-analyses of Alzheimer disease genetic association studies: the AlzGene database.** *Nat Genet* 2007, **39:**17–23.
32. Ashburner M, Ball CA, Blake JA, Botstein D, Butler H, Cherry JM, Davis AP, Dolinski K, Dwight SS, Eppig JT, Harris MA, Hill DP, Issel-Tarver L, Kasarskis A, Lewis S, Matese JC, Richardson JE, Ringwald M, Rubin GM, Sherlock G: **Gene Ontology: tool for the unification of biology.** *Nat Genet* 2000, **25:**25–29.
33. Sethupathy P, Megraw M, Hatzigeorgiou AG: **A guide through present computational approaches for the identification of mammalian microRNA targets.** *Nat Meth* 2006, **3:**881–886.
34. Lu M, Zhang Q, Deng M, Miao J, Guo Y, Gao W, Cui Q: **An analysis of human microRNA and disease associations.** *PLoS One* 2008, **3:**e3420.
35. Noren Hooten N, Abdelmohsen K, Gorospe M, Ejiogu N, Zonderman AB, Evans MK: **microRNA expression patterns reveal differential expression of target genes with age.** *PLoS One* 2010, **5:**e10724.
36. Wang WX, Huang Q, Hu Y, Stromberg AJ, Nelson PT: **Patterns of microRNA expression in normal and early Alzheimer's disease human temporal cortex: white matter versus gray matter.** *Acta Neuropathol* 2011, **121:**193–205.
37. Yao J, Hennessey T, Flynt A, Lai E, Beal MF, Lin MT: **MicroRNA-related cofilin abnormality in Alzheimer's disease.** *PLoS One* 2010, **5:**e15546.
38. Wang WX, Rajeev BW, Stromberg AJ, Ren N, Tang G, Huang Q, Rigoutsos I, Nelson PT: **The expression of microRNA miR-107 decreases early in Alzheimer's disease and may accelerate disease progression through regulation of beta-site amyloid precursor protein-cleaving enzyme 1.** *J Neurosci* 2008, **28:**1213–1223.
39. Augustin R, Lichtenthaler SF, Greeff M, Hansen J, Wurst W, Trümbach D: **Bioinformatics identification of modules of transcription factor binding sites in Alzheimer's disease-related genes by in silico promoter analysis and microarrays.** *International Journal of Alzheimer's Disease* 2011, **2011:**154325.
40. Wang Y, Medvid R, Melton C, Jaenisch R, Blelloch R: **DGCR8 is essential for microRNA biogenesis and silencing of embryonic stem cell self-renewal.** *Nat Genet* 2007, **39:**380–385.
41. Evers LJ, Vermaak MP, Engelen JJ, Curfs LM: **The velocardiofacial syndrome in older age: dementia and autistic features.** *Genet Couns* 2006, **17:**333–340.
42. Nixon RA, Saito KI, Grynspan F, Griffin WR, Katayama S, Honda T, Mohan PS, Shea TB, Beermann M: **Calcium-activated neutral proteinase (calpain) system in aging and Alzheimer's disease.** *Ann N Y Acad Sci* 1994, **747:**77–91.
43. Mattson MP: **ER calcium and Alzheimer's disease: in a state of flux.** *Sci Signal* 2010, **3:**pe10.
44. Zawia NH, Lahiri DK, Cardozo-Pelaez F: **Epigenetics, oxidative stress, and Alzheimer disease.** *Free Radic Biol Med* 2009, **46:**1241–1249.
45. Kim D, Tsai LH: **Bridging physiology and pathology in AD.** *Cell* 2009, **137:**997–1000.
46. Boominathan L: **The tumor suppressors p53, p63, and p73 are regulators of microRNA processing complex.** *PLoS One* 2010, **5:**e10615.
47. Parra P, Serra F, Palou A: **Expression of adipose microRNAs is sensitive to dietary conjugated linoleic acid treatment in mice.** *PLoS One* 2010, **5:**e13005.
48. Liu Y, Yang L, Conde-Knape K, Beher D, Shearman MS, Shachter NS: **Fatty acids increase presenilin-1 levels and gamma-secretase activity in PSwt-1 cells.** *J Lipid Res* 2004, **45:**2368–2376.
49. Wang WX, Wilfred BR, Madathil SK, Tang G, Hu Y, Dimayuga J, Stromberg AJ, Huang Q, Saatman KE, Nelson PT: **miR-107 regulates granulin/progranulin with implications for traumatic brain injury and neurodegenerative disease.** *Am J Pathol* 2010, **177:**334–345.
50. Xie H, Lim B, Lodish HF: **MicroRNAs induced during adipogenesis that accelerate fat cell development are downregulated in obesity.** *Diabetes* 2009, **58:**1050–1057.
51. Liao Y, Lönnerdal B: **Global microRNA characterization reveals that miR-103 is involved in IGF-1 stimulated mouse intestinal cell proliferation.** *PLoS One* 2010, **5:**e12976.
52. Dobashi Y, Kudoh T, Matsumine A, Toyoshima K, Akiyama T: **Constitutive overexpression of CDK2 inhibits neuronal differentiation of rat pheochromocytoma PC12 cells.** *J Biol Chem* 1995, **270:**23031–23037.
53. Wines-Samuelson M, Handler M, Shen J: **Role of presenilin-1 in cortical lamination and survival of Cajal-Retzius neurons.** *Dev Biol* 2005, **277:**332–346.
54. Puzzo D, Vitolo O, Trinchese F, Jacob JP, Palmeri A, Arancio O: **Amyloid-beta peptide inhibits activation of the nitric oxide/cGMP/cAMP-responsive element-binding protein pathway during hippocampal synaptic plasticity.** *J Neurosci* 2005, **25:**6887–6897.
55. Garzon R, Pichiorri F, Palumbo T, Visentini M, Aqeilan R, Cimmino A, Wang H, Sun H, Volinia S, Alder H, Calin GA, Liu CG, Andreeff M, Croce CM: **MicroRNA gene expression during retinoic acid-induced differentiation of human acute promyelocytic leukemia.** *Oncogene* 2007, **26:**4148–4157.
56. Das Neves L, Duchala CS, Godinho F, Haxhiu MA, Colmenares C, Macklin WB, Campbell CE, Butz KG, Gronostajski RM: **Disruption of the murine nuclear factor I-A gene (Nfia) results in perinatal lethality, hydrocephalus, and agenesis of the corpus callosum.** *Proc Natl Acad Sci* 1999, **96:**11946–11951.
57. Teipel SJ, Bayer W, Alexander GE, Zebuhr Y, Teichberg D, Kulic L, Schapiro MB, Moller H-J, Rapoport SI, Hampel H: **Progression of corpus callosum atrophy in Alzheimer disease.** *Arch Neurol* 2002, **59:**243–248.
58. Yamakuchi M, Lotterman CD, Bao C, Hruban RH, Karim B, Mendell JT, Huso D, Lowenstein CJ: **P53-induced microRNA-107 inhibits HIF-1 and tumor angiogenesis.** *Proc Natl Acad Sci* 2010, **107:**6334–6339.
59. Del Bo R, Scarlato M, Ghezzi S, Martinelli Boneschi F, Fenoglio C, Galbiati S, Virgilio R, Galimberti D, Galimberti G, Crimi M, Ferrarese C, Scarpini E, Bresolin N, Comi GP: **Vascular endothelial growth factor gene variability is associated with increased risk for AD.** *Ann Neurol* 2005, **57:**373–380.
60. Bai S, Nasser MW, Wang B, Hsu SH, Datta J, Kutay H, Yadav A, Nuovo G, Kumar P, Ghoshal K: **MicroRNA-122 inhibits tumorigenic properties of pepatocellular carcinoma cells and sensitizes these cells to sorafenib.** *J Biol Chem* 2009, **284:**32015–32027.

doi:10.1186/1471-2350-13-35
Cite this article as: Augustin *et al.*: Computational identification and experimental validation of microRNAs binding to the Alzheimer-related gene ADAM10. *BMC Medical Genetics* 2012 **13**:35.

Unfolded protein response signaling by transcription factor XBP-1 regulates ADAM10 and is affected in Alzheimer's disease

Sven Reinhardt,* Florian Schuck,* Sven Grösgen,[‡] Matthias Riemenschneider,[§] Tobias Hartmann,[‡,‖] Rolf Postina,[†] Marcus Grimm,[‡,‖] and Kristina Endres*,[1]

*Clinical Research Group, Department of Psychiatry and Psychotherapy, and [†]Institute of Pharmacy and Biochemistry, Johannes Gutenberg University Mainz, Mainz, Germany; and [‡]Department of Neurodegeneration and Neurobiology, Deutsches Institut für DemenzPrävention (DIDP), [§]Clinic of Psychiatry and Psychotherapy, and [‖]Department of Experimental Neurology, Saarland University, Homburg/Saar, Germany

ABSTRACT **In Alzheimer's disease (AD), disturbed homeostasis of the proteases competing for amyloid precursor protein processing has been reported: a disintegrin and metalloproteinase 10 (ADAM10), the physiological α-secretase, is decreased in favor of the amyloid-β-generating enzyme BACE-1. To identify transcription factors that modulate the expression of either protease, we performed a screening approach: 48 transcription factors significantly interfered with ADAM10/BACE-1-promoter activity. One selective inducer of *ADAM10* gene expression is the X-box binding protein-1 (XBP-1). This protein regulates the unfolded protein-response pathway. We demonstrate that particularly the spliced XBP-1 variant dose dependently regulates ADAM10 expression, which can be synergistically enhanced by 100 nM insulin. Analysis of 2 different transgenic mouse models (APP/PS1 and 5xFAD) revealed that at early time points in pathology XBP-1 metabolism is induced. This is accompanied by a 2-fold augmented ADAM10 amount as compared with non-transgenic littermates (P=0.011). Along with aging of the mice, the system is counterregulated, and XBP-1 together with ADAM10 expression level decreased to ~50% as compared with control animals. Analyses of expression levels in human AD brains showed that ADAM10 mRNA correlated with active XBP-1 (r=0.3120), but expression did not reach levels of healthy age-matched controls, suggesting deregulation of XBP-1 signaling. Our results demonstrate that XBP-1 is a driver of *ADAM10* gene expression and that disturbance of this pathway might contribute to development or progression of AD.—Reinhardt, S., Schuck, F., Grösgen, S., Riemenschneider, M., Hartmann, T., Postina, R., Grimm, M., Endres, K. Unfolded protein response signaling by transcription factor XBP-1 regulates ADAM10 and is affected in Alzheimer's disease. *FASEB J.* 28, 978–997 (2014). www.fasebj.org**

Key Words: APP processing · insulin signaling · ER stress · stress response · α-secretase

Alzheimer's disease (AD) is the most prevalent type of dementia, with a steadily growing number of patients. Albeit the pathological hallmarks of this disease were described more than 100 yr ago, the pathomechanistically relevant elicitors in sporadic AD have not yet been clearly delineated. Inflammatory events, metabolic disbalance, and altered enzymatic activity have been intensely discussed in this concern. For example, it has been reported that in patients with dementia, insulin resistance develops within the brain, accompanied by reduction of insulin itself and insulin receptor (IR) expression (1). Moreover, amyloid β (Aβ) peptides might be able to block the IR, which consequently contributes to a persistent insulin resistance in the brain in patients with dementia and therefore resem-

Abbreviations: Aβ, amyloid β; AD, Alzheimer's disease; ADAM10, a disintegrin and metalloproteinase 10; AP1, activator protein 1; APP, amyloid precursor protein; ATF, activating transcription factor; BACE-1, β-site APP-cleaving enzyme 1; EMSA, electrophoretic mobility shift assay; ER, endoplasmic reticulum; ERSE, endoplasmic reticulum-stress-responsive element; EST, expressed sequence tag; HEK, human embryonic kidney; HRP, horseradish peroxidase; HSF-1, heat-shock factor 1; IR, insulin receptor; IRE1-α, inositol requiring enzyme 1-α; IRS-1, insulin receptor substrate 1; LPS, lipopolysaccharide; ns, not splicable (vector sequence); PS1, presenilin 1; PSEN1, presenilin 1; s, spliced (vector sequence); SEAP, secreted embryonic alkaline phosphatase; TF, transcription factor; TLR4, toll-like receptor 4; u, unspliced (vector sequence); UPR, unfolded protein response; UPRE, unfolded protein response element; UPRE_del, unfolded protein response element deletion mutant; USF, upstream stimulatory factor; UTR, untranslated region; UV, ultraviolet; XBP-1, X box binding protein 1; WT, wild type; YY-1, Yin Yang 1

[1] Correspondence: Department of Psychiatry and Psychotherapy, University Medical Center of the Johannes Gutenberg University Mainz, Untere Zahlbacher Strasse 8, 55131 Mainz, Germany. E-mail: kristina.endres@unimedizin-mainz.de

doi: 10.1096/fj.13-234864

This article includes supplemental data. Please visit *http://www.fasebj.org* to obtain this information.

0892-6638/14/0028-0978 © FASEB

bles an even more complex picture of the disease (reviewed in ref. 2). There is discordance in the research field about the identity of the toxic Aβ species: intracellular monomeric peptides, certain kinds of oligomers, or modified Aβ; but the central role of Aβ in development of the disease is generally accepted (3). In accordance with this, a variety of studies reported a misbalance in the expression and/or activity of central proteases that are responsible for production of Aβ in the human brain. Two main pathways exist in amyloid precursor protein (APP) cleavage: in the amyloidogenic pathway, the β-secretase BACE-1 (β-site APP-cleaving enzyme 1) delivers the prerequisite shedding event for γ-secretase-derived A-β generation. Contrarily, the α-secretase prevents formation of Aβ peptides and leads to secretion of the neurotrophic and neuroprotective APP-processing product APPs-α. Analyses in mouse models have revealed that the major α-secretase within at least the murine brain is the metalloprotease ADAM10 (a disintegrin and metalloproteinase 10). Overexpression of this enzyme in transgenic mice impressively reduced the Aβ plaque load and soluble Aβ and additionally restored learning deficits in double-transgenic Alzheimer model mice (4). RNAi-mediated reduction of ADAM10 in primary hippocampal neurons nearly abolished APP-α generation (5), and animals with a conditional ADAM10 knockdown showed largely reduced α-secretase activity in neurons (6). Overexpression of BACE-1 in animal models. in contrast. increased Aβ plaque load and led to an exacerbated phenotype (7, 8).

Enhanced BACE-1 protein level and activity have been observed in the cerebrospinal fluid (CSF) of patients with mild cognitive impairment and mostly an increased expression as well as enhanced amounts of protein and activity in CNS tissue of humans affected by AD have been reported (*e.g.*, 9; reviewed in ref. 10). ADAM10 amount or activity, in contrast, was mainly found to be decreased in moderate to severe AD (11). Moreover, several publications reported a reduction of APPs-α in the CSF of patients with AD (12–14), which probably is linked to reduced amount and/or activity of the ADAM10 protease itself. Therefore, elucidating endogenous factors that balance expression of either protease (ADAM10 or BACE-1) might lead to a deeper understanding of AD pathogenesis and disclose new therapeutic approaches. Common regulatory networks for AD genes have been identified by a combination of *in silico* promoter and multivariate analysis (15) and outlined 2 significant modules composed of 3 transcription factor (TF) families: CCCTC binding factor (CTCF), GC-box factors SP1/GC (SP1F), and EGR/nerve growth factor-induced protein C and related factors (EGRF)/zinc-binding protein factors (ZBPF; ref. 15). Our approach, on the contrary, aims at differentiation of TFs that specifically regulate either BACE-1 or ADAM10.

Therefore, we established a dual-promoter assay for simultaneous assessment of transcriptional activity of BACE-1 and ADAM10 to identify TFs balancing the gene expression of these opponent enzymes in the human neuroblastoma cell line SH-SY5Y. Within our novel reporter gene assay, the signals derived from either promoter emerge from one vector, which makes normalization for transfection efficiency dispensable. We filtered candidate hits regarding to expression in the adult human brain by expressed sequence tag (EST) analysis. One of the newly identified, physiologically relevant selective inducers of *ADAM10* gene expression is the X-box binding protein 1 (XBP-1). XBP-1 is a transcriptional regulator activated by inositol-requiring enzyme 1-α (IRE1-α), one of the 3 endoplasmic reticulum (ER)-stress sensors, and specifically regulates the unfolded protein response (UPR). This transcription factor displayed a strong effect on the ratio of ADAM10- to BACE-1-promoter activity in our screening approach, and UPR has already been correlated to neurodegenerative disease in recently rising numbers of publications (reviewed in ref. 16). We investigated the underlying mechanism of ADAM10 regulation by XBP-1 in cell culture and demonstrate the consistency of our findings by quantitative analysis of mRNA from 2 AD mouse models and cortical tissue of AD postmortem samples.

MATERIALS AND METHODS

Generation of luciferase-reporter and expression vectors

ADAM10-*promoter luciferase-reporter vector*

The human *ADAM10*-promoter sequence comprising −2179 to +1 bp upstream of the translation initiation codon of the *ADAM10* gene (chromosome 15, NC_000015.9) was obtained by digestion with *Nhe*I and *Bgl*II from the previously described plasmid pCP53 AB.1 (17) and subcloned into the *Nhe*I and *Bgl*II site of the pGL 4.76 vector (Promega, Madison, WI, USA).

ADAM10-*promoter UPR element (UPRE) deletion mutant (UPRE_del)*

The consensus sequence of the UPRE has been described by Wang *et al.* (18). A potential UPRE was identified within the *ADAM10*-promoter sequence at −308 bp. The UPRE_del was generated as follows: a UPRE_del fragment lacking the 3′ part of the UPRE sequence (5′ TCACGTGG3′; deleted part is underscored) was amplified from pGL4.76 ADAM10-promoter reporter vector using the primers UPRE_for (5′-TGAGGAAGGAGGCGGAGG-3′) and pGL4.76_rev (5′-GAGGCCCAGTGATCATGCG-3′). The obtained amplicon was digested with *Bgl*II and inserted as a replacement for the *Pml*I and *Bgl*II site flanked sequence of the pGL 4.76 ADAM10-promoter reporter vector.

BACE-1-*promoter luciferase-reporter vector*

The human *BACE-1*-promoter sequence (−2644 bp to +1 of 5′ flanking region of the *BACE-1* gene, described by ref. 19) was amplified from chromosomal DNA of U373 cells and subsequently cloned in the *EcoICR*I and *Bgl*II site of the pGL 4.76 vector (Promega).

Dual luciferase-reporter vector

To determine the ADAM10- and BACE-1-promoter activity simultaneously and to circumvent differences in transfection efficiency, we established a dual-promoter construct with a *Renilla reniformis* luciferase cDNA dependent on the activity of the human *BACE-1* promoter and a firefly (*Photinus pyralis*) luciferase cDNA under the control of the human *ADAM10* promoter. The *ADAM10* promoter and firefly luciferase cDNA sequences were obtained by cleaving the pGL3 ADAM10-promoter construct CP53 AB.1 (17) with *Nhe*I and *Sal*I and inserted into the *Bam*HI and *Sal*I restriction sites of the pGL4.76 vector (Promega). The *BACE-1*-promoter sequence was obtained by digestion of the *BACE-1*-promoter luciferase-reporter vector (described above) with *Kpn*I and *Bgl*II and subsequently integrated upstream of the *Renilla* luciferase coding sequence into the *Kpn*I and *Bgl*II sites of the pGL 4.76 ADAM10-promoter construct.

APP-*promoter luciferase-reporter vector*

A reporter vector expressing a *Renilla* luciferase under the control of the human *APP* promoter (−2980 bp to+1 bp of translation initiation site; ref. 20) was generated by amplification of the promoter sequence from chromosomal DNA of SKNMC cells. The amplicon was ligated into the restriction sites *Nhe*I and *Bgl*II of the luciferase expression vector pGL4.76 (Promega).

Spliced XBP-1 expression vector

To generate an expression vector for the active spliced (s) form of XBP-1, the 26-bp intron in the sequence of the unspliced (u) XBP-1 expression vector (Origene, Rockville, MD, USA) was removed. PCRs were performed using the following primers: PCR1: XBP1s_for1, 5′-TACGGTGGGAGGTCTATATAAGCAG-3′, XBP1s_rev1, 5′-GTGACAACTGGGCCTGCACCTGCTGCG-GACTCAGCAGACC-3′; and PCR2: XBP1s_for 2, 5′-GGTCTGCTGAGTCCGCAGCAGGTGCAGGCCCAGTTGTCAC-3′, XBP1s_rev2, 5′-GGTCCTTCTGGGTAGACCTGTG-3′.

Amplicons from PCR1 and PCR2 with overlapping sequences (underscored) were fused *via* a second PCR with primers XBP1s_for1 und XBP1s_rev2, resulting in an 817-bp fragment, which was digested with *Sac*I and subsequently inserted instead of the 26-nt-containing sequence of the cDNA encoding the u form of *XBP-1* into the *Sac*I site of XBP-1 expression vector.

Not splicable XBP-1 expression vector

The u XBP-1 mRNA forms 2 distinct hairpin loops (previously described in ref. 21), which contain splice donor and splice acceptor sites for the unconventional splicing by IRE1-α. We inserted 6 silent mutations to weaken base pairing in the second loop, which results in inhibition of the splicing process (see **Fig. 2*A***); initially, the *u XBP-1* expression vector was digested with *Sac*I, and the *XBP-1* sequence containing cDNA-fragment was subcloned into the pUC19 vector (Clontech, Mountain View, CA, USA). The wild-type (WT) sequence of the second loop was replaced by an oligonucleotide adapter, which was inserted into the *BsaA*I/*Nco*I site of the WT cDNA. The mutated sequence [not splicable (ns) *XBP-1*] was inserted into the pCMV6-XL5 vector (Origene) by *Sac*I digestion. The following oligonucleotides were used to generate the oligonucleotide adapter: ns_XBP1_for, 5′-GCGCACCCCTCCAACAAGTACAGGCCCAGTTGTCACCCCTC-CAGAACATCTCCC-3′, and ns_XBP1_rev, 5′-CATGGG-GAGATGTTCTGGAGGGGTGACAACTGGGCCTGTACTTGT-TGGAGGGGTGCGC-3′.

All PCR-derived sequences were verified by restriction analysis and sequencing (SRD, Bad Homburg, Germany).

Electrophoretic mobility shift assay (EMSA)

For EMSA, the LightShift Chemiluminecent EMSA Kit (Thermo Scientific, Waltham, MA, USA) was used as recommended by the manufacturer. Oligonucleotides were biotinylated using the Biotin 3′ End DNA Labeling Kit (Thermo Scientific). The sequences of oligonucleotides including potential UPRE and ER-stress-responsive element (ERSE)-like within the human ADAM10 promoter are as follows: UPRE, 5′-AACCTCTGTTACTTGTGACGTTAAGAAGTCGA-3′ and 5′-TCGACTTCTTAACGTCACAAGTAACAGAGGTT-3′; and ERSE-like, 5′-GCCTCCCAAGCCCAATCCCAGCTCTCCGCCG-3′ and 5′-CGGCGGAGAGCTGGGATTGGGCTTGGGAGGC-3′ (potential binding sites are underscored). Nuclear protein extracts from s XBP-1-overexpressing human embryonic kidney (HEK) 293 cells were obtained using the NE-PER nuclear and cytoplasmic extraction reagents (Thermo Scientific). Protein-DNA complexes were separated on native 6% polyacrylamide gels containing 0.5× TBE buffer (50 mM Tris, 45 mM boric acid, and 0.5 mM Na_2-EDTA, pH 8.3). As gel running buffer, 0.5× TBE was used. After electrophoresis, nucleic acids and proteins were blotted onto Biodyne precut nylon membranes (Thermo Scientific) and fixed by ultraviolet (UV) irradiation using a Stratalinker (Stratagene, La Jolla, CA, USA). Chemiluminescent signals of biotinylated molecules were captured using a CCD camera imaging system (Raytest, Straubenhardt, Germany).

Cell culture

Cell lines were maintained at humidified air (95%), 5% CO_2, and 37°C. The human neuroblastoma cell line SH-SY5Y was cultured in DMEM/F12 (Life Technologies, Darmstadt, Germany) supplemented with 10% FCS and 1% glutamine (both GE Healthcare, Piscataway, NJ, USA). THP-1 Blue cells [human monocyte-progenitor cells stably transfected with an NFκB-dependent secreted embryoinic alkaline phosphatase (SEAP) reporter; Invivogen, San Diego, CA, USA] were cultivated in RPMI medium (GE Healthcare) supplemented with 10% heat-inactivated FCS, 1% glutamine, 1% pen/strep, and 1% sodium pyruvate (GE Healthcare). Zeocin (300 μg/ml; Invivogen) was applied for THP-1 passage. The human astroglioma cell line U373, the HEK 293 cells, and the human neuroblastoma cell line IMR-32 were cultured in DMEM (GE Healthcare) supplemented with 10% FCS, 1% glutamine, and 1% sodium pyruvate. SH-SY5Y and U373 cells were passaged 2×/wk, 1:2–1:4; IMR-32 and HEK 293 cells were passaged 1:10–11:12; and THP-1 Blue cells were cultivated at a density of 2.4×10^5 cells/ml.

Screening of the transcription factor library

To identify potential modulators of ADAM10 and BACE-1 gene expression, we realized a screening approach including 704 expression vectors for human TFs (TF GFC transfection array; Origene). We performed a transient retrotransfection of dual luciferase reporter plasmid in combination with one of the 704 expression vectors or the empty vector pCMV6-XL5, respectively, in SH-SY5Y cells. Briefly, to each well of a 96-well plate containing 100 ng of TF expression vector, 20 μl Opti-MEM containing 75 ng of the dual luciferase vector was added. The DNA mixture was incubated for 20 min at room temperature. Opti-MEM (20 μl) containing 0.3 μl transfection reagent (Lipofectamine2000; Life Technologies, Darm-

stadt, Germany) was added to each well and incubated for 45 min at room temperature. Then, 1.5×10^5 cells/cm^2 surface area of the dish were seeded, and transfected cells were cultivated for 48 h. Cells were lysed in 20 μl passive lysis buffer (Promega) per well, and lysis was promoted by freezing overnight at −20°C. *Renilla* and firefly luciferase activity was assessed using a reporter assay kit (Dual-Luciferase Reporter Assay; Promega) and the Fluostar Optima luminometer (BMG Labtech, Cary, NC, USA). The ratio of ADAM10-promoter activity (firefly luciferase) to BACE-1-promoter activity (*Renilla* luciferase) was calculated, and the transcriptional activity of empty vector (pCMV6-XL5; Origene)-transfected cells was set to 100%. Hits were considered as follows: values > mean + SD (130%) or < mean − SD (70%) of control transfected cells.

Transfection and luciferase assay

Cotransfections of XBP-1 expression plasmids (u XBP-1, s XBP-1, or ns XBP-1) together with respective reporter constructs were performed as described above. Luciferase activity was measured with *Renilla* or firefly luciferase assay kit (Promega) following the manufacturer's protocol. Relative light unit (RLU) values were normalized to protein content in the cell lysate, quantified by Bradford Nanoquant reagent (Roth, Karlsruhe, Germany) and a BSA standard curve. For time-resolved measurements of promoter activities, either ADAM10- or BACE-1-promoter reporter plasmid together with XBP-1 expression vector was transfected in SH-SY5Y cells. After 5 h, cell supernatant was replaced by medium containing 30 μM EnduRen live cell substrate (Promega). Luminescence was measured at indicated time points within the living cells.

sRNAi transfection

SH-SY5Y cells were transfected with 50 ng XBP-1 expression plasmid or empty vector together with 50 ng luciferase reporter vector or a promoterless control construct. This was combined with 1 pmol XBP-1-specific sRNAi (HSS111392; Life Technologies) or scrambled control RNAi with medium GC content (Life Technologies). Cells were transfected using 0.5 μl Lipofectamine2000 (Life Technologies) per well. Cells were harvested 48 h post-transfection and subsequently analyzed *via* luciferase-based assay as described above.

Stimulation and cell treatment

To induce ER stress, SH-SY5Y cells were treated with 10 μM tunicamycin (Sigma-Aldrich, Steinheim, Germany) or 1 μM thapsigargin (Enzo Life Sciences, Lörrach, Germany) for the indicated time points. To inhibit proteasomal activity, cells were incubated with 5 μM MG132 (Merck Chemicals, Darmstadt, Germany) for 5 h. Splicing of u XBP-1 by IRE1-α was inhibited using 100 μM STF083010 (Axon Medchem, Groningen, The Netherlands) for 6 h. For stimulation of THP-1 Blue cells with lipopolysaccharide (LPS; Sigma-Aldrich), a concentration of 1 μg/ml was used for indicated intervals. Additive effects of insulin on s XBP-1-evoked regulation of the ADAM10 promoter were analyzed by incubation of cells with 0.1 or 1 μM human insulin (Sigma-Aldrich) for 48 h. Corresponding solvents were used for control treatment.

RNA isolation and quantitative real-time RT-PCR

Total RNA from SH-SY5Y cells grown on 6-well plates was extracted using the RNA II Kit (Macherey&Nagel, Düren, Germany) following the manufacturer's protocol. Samples were stored at −80°C and freshly diluted for application. RNA (100 ng) was subjected to real-time RT-PCR analysis, performed with the StepOne Plus thermocycler (Life Technologies) and QuantiTect SYBR Green RT-PCR kit (Qiagen, Valencia, CA, USA). QuantiTect primer assays (Qiagen) were used for detection of the following genes: *ADAM10* (Hs_ADAM10_1 _SG), *ADAM17* (Hs_ADAM17_1_SG), *BACE-1* (Hs_BACE1_1_SG), *APP* (Hs_APP2_SG), *Tubulin* (Hs_TUBB_1_SG), and *18 S rRNA* (Hs_RRN18S_1_SG). Obtained mRNA quantities of each reaction were calculated from calibration curve and normalized to those of the respective housekeeping gene (Tubulin, 18S rRNA). Normalized data were set in relation to control (empty vector-transfected cells or solvent treated control).

Preparation of whole-cell lysates and immunoblotting

SH-SY5Y cells were transiently transfected with the respective XBP-1 expression plasmid as described above. Cells were seeded on 12-well plates at a density of 5×10^5 cells/well. After the respective incubation time, cells were lysed in LDS sample buffer (Life Technologies) containing 10% DTT (1 M) and 1× protease inhibitor cocktail (Roche, Basel, Switzerland). Samples were incubated for 10 min at 95°C and stored at −20°C. Lysates were assayed for protein content using the Nanoquant reagent (Roth, Karlsruhe, Germany). Protein of whole-cell lysate (20 μg), protein of mouse tissue homogenate (whole brain or pancreas; 50 μg), or nuclear hippocampal extract (5 μg; BioCat, Heidelberg, Germany) was separated on 10–14% SDS-polyacrylamide gels and blotted onto nitrocellulose membrane at 100 V for 2 h. Immunodetection was carried out by blocking the membranes for 1 h in blocking solution and incubating overnight at 4°C with the appropriate primary antibody at a dilution of 1:1000. Antibodies were as follows: XBP-1 rabbit polyclonal antibody (ab37152; Abcam, Cambridge, UK), histone deacetylase 1 (HDAC1) rabbit polyclonal antibody (PA1-860; Thermo Scientific), β-actin rabbit polyclonal antibody (A2066; Sigma-Aldrich), ADAM10 rabbit polyclonal antibody (Merck, Darmstadt, Germany), ADAM17 rabbit polyclonal antibody (Chemicon, Temecula, CA, USA), phospho-IRE1-α (pSer724) rabbit polyclonal antibody (PA1-16927; Thermo Scientific), and APP N-terminal mouse monoclonal antibody (6E10; Covance, Madison, WI, USA) or APP C-terminal antibody (described previously; ref. 22). Blots were incubated with respective secondary antibody coupled with horseradish peroxidase (HRP; Thermo Scientific), and signals were obtained by applying SuperSignal West Femto chemiluminescent substrate (Thermo Scientific) were captured using a CCD camera imaging system (Raytest). Quantitative analysis was carried out with AIDA image analyzer 4.26 software (Raytest).

ELISA measurements

SH-SY5Y cells were transfected with s XBP-1 expression plasmid or empty vector as described above. After 32 h, transfection medium was exchanged, followed by a secretion period of 16 h. Conditioned medium was collected and centrifuged for 5 min at 1500 rpm. For the detection of human Aβ peptides, an ELISA kit was used as recommended by the manufacturer [human Aβ 1-x Assay Kit (L); IBL, Hamburg, Germany]. The concentration of Aβ peptides was determined using 100 μl of cell supernatant, and obtained values were normalized to protein content of respective whole-cell lysates.

α-Secretase activity assay

Pelleted SH-SY5Y cells were resuspended in 1 ml HEPES buffer (pH 7.5). For solubilization, samples were passed

through needles (BD, Franklin Lakes, NJ, USA) with decreasing diameters. Samples were dispended in triplicate onto a black 96-well plate using 100 μl/well, corresponding to 100 μg protein content. After addition of 3 μM α-secretase substrate (Calbiochem, Darmstadt, Germany), fluorescence was detected with excitation wavelength at 340 nm and emission wavelength at 490 nm using a Safire2 fluorometer (Tecan, Männedorf, Switzerland) as described previously (23).

PhosTag gels for detection of phosphorylated IRE1-α

To examine the induction of ER stress due to incubation of SH-SY5Y cells with tunicamycin, we applied the Phos-tag gel system as previously described (24). For detection of IRE1-α (phosphorylated and unphosphorylated), we used a specific rabbit polyclonal antibody (14C10; Cell Signaling, Danvers, MA, USA).

SEAP assay

In THP-1 Blue cells, LPS-mediated signaling *via* Toll-like receptor 4 (TLR4) can be detected by measuring the activity of a SEAP, the secretion of which is controlled by a NF-κB- and AP1-dependent promoter reporter vector. Cells were incubated with LPS as described above. Quanti Blue substrate (Invivogen) was used for detection of SEAP production according to the manufacturer's protocol, using 20 μl cell supernatant and 180 μl Quanti Blue substrate incubated for 16 h at 37°C and 300 rpm. Absorbance was measured at 620 nm, and values of control (water)-treated cells were set to 100%.

Detection of XBP-1 splicing forms

Total RNA (1 μg) extracted from SH-SY5Y cells was reverse transcribed using the MMLV kit (Epicenter, Madison, WI, USA). The resulting cDNA was digested with either *Bgl*II or *Pst*I overnight and precipitated by ethanol and 3 M sodium acetate (pH 4.8). Dried DNA was dissolved in water, and 100 ng cDNA was subjected to PCR using the SYBR Green kit (Qiagen). Primers for detection of total *XBP-1* were 5′-CCTTGTAGTTGAGAACCAGG-3′ and 5′-CCACATATATAC-CAAGCCCC-3′. *Pst*I cleaves the u *XBP-1* sequence within the 26-bp intron. Therefore, in *Pst*I-treated samples, the s form of *XBP-1* (416 bp) will mainly be detected. *Bgl*II cleaves within the *XBP-1* sequence outside of the primer binding sites. Consequently, *Bgl*II digestion allows the detection of both u and *s XBP-1* (amplicons of 442 and 416 bp). The respective PCR sample (2 μl) was separated on 8% acrylamide gels. Gels were stained with ethidium bromide and detected with UV light using the Bio Doc-It imaging system (UVP, Upland, CA, USA).

Evaluation of the XBP-1 metabolism in AD mode mice

Brains of APP/presenilin 1(PS1) mice (2, 6, or 9 mo of age) or 5xFAD mice (1, 2, or 9 mo of age) and those of respective nontransgenic littermates were stored in RNA-later (Qiagen) at −80°C, and total RNA from brain tissue was isolated using the RNeasy Lipid Tissue Minikit (Qiagen) following the manufacturer's protocol. Samples were freshly diluted for application, and 100 ng of RNA was subsequently subjected to real-time RT-PCR analysis using the StepOne Plus thermocycler (Life Technologies) and QuantiTect SYBR Green RT-PCR kit (Qiagen). The following primers were used for analysis: QuantiTect primer assay (Qiagen) *Adam10* (Mm_Adam10_1_SG), *18S rRNA* (Mm_Rrn18s_1_SG), *Adam17* (Mm_Adam17_1_SG); *u Xbp-1*: 5′-GCACTCAGACTATGTGCACCT-3′ and 5′-GCCTCTTCAGATTCTGAGTCTG-3′; *s Xbp-1*: 5′-TCTGCTGAGTCCGCAGCAGG-3′ and 5′-GCCTCTTCA-GATTCTGAGTCTG-3′; *Ire1*-α: 5′-CCTGCAACCTTGACT-GTTTCC-3′ and 5′-GCTATGGATCCCCAGCAGC-3′. Obtained mRNA quantities of each reaction were calculated from calibration curve and normalized to those of 18 S rRNA. Normalized data were set in relation to controls (nontransgenic littermates).

Evaluation of the XBP-1 metabolism in AD postmortem brains

Total RNA of frozen cortex tissue (BrainNet, Munich, Germany) was extracted using Trizol (Life Technologies) following the manufacturer's protocol. RNA (2 μg) was reverse transcribed with the High Capacity cDNA Reverse Transcription Kit (Life Technologies) and subsequently subjected to PCR analysis performed with the thermocycler 7500 Fast real-time PCR system (Life Technologies) and Fast SYBR Green Master Mix (Life Technologies). Primers were used as follows: β-*actin*: previously described (25); *ADAM10*: 5′-GCAAACTGAAACCTG GGAAA-3′ and 5′-TTCCTTCCCTTGCA-CAGTCT-3′; *ADAM17*: 5′-ACCTGAAGAGCTTGTTCATCG-3′ and 5′-CCCTCTGCCCATGTATCTGT-3′; total *XBP-1*: 5′-GGGTTCGCGACAGAATTGAG-3′ and 5′-TACCTAAGACCGC-CATAACT-3′; *u XBP-1*: 5′-GACGTCTCCACGTGCATCAGA-3′ and 5′-TCTAAGTCTCAGACTATAGG-3′; *s XBP-1*: 5′-GGACGTGGAC-GACGCCTGAG-3′ and 5′-TCTAAGTCTCAGACTATAGG-3′; *IRE1*-α: 5′-ACCGACGGGAGTCTCTAATG-3′ and 5′-TGGGTCTCTTCGTGCTTCTG-3′. The mRNA level for the respective gene was quantified using the $2^{-\Delta\Delta C_t}$ method (26); data were normalized to β-actin mRNA levels, and the mean value of healthy controls was set to 100%.

In silico analysis

For further evaluation, candidate TFs identified with the dual-promoter assay were classified according to their expression levels in the CNS of adults by using databank information on EST profiles (http://www.ncbi.nlm.nih.gov/unigene). TFs were ranked by relative expression in the human brain compared with other tissues and, additionally, in adults in contrast to other developmental stages.

Conservation of UPRE binding element in the ADAM10 promoter

Promoter regions of human and murine *ADAM10* were extracted from the Transcriptional Regulatory Element Database (http://rulai.cshl.edu/cgibin/TRED/tred.cgi?process=home) as follows: *ADAM10*: chr15: 56621111 [−700.299] (−) [human, *Homo sapiens*], and *Adam10*: chr9: 70908083 [−700.299] (+) [mouse, *Mus musculus*]. Sequence alignment was performed using ClustalX2 software (UCD, Dublin, Ireland).

Secondary structure prediction of u and ns XBP-1 mRNA

Prediction of mRNA secondary structure was performed with the online-tool GeneBee (http://www.gene bee.msu.su/services/rna2_reduced.html).

Statistical analysis

Testing of statistical significance was performed using 1-way ANOVA followed by Bonferroni posttest or by unpaired Student's *t* test. For correlation analysis, the Pearson's correlation coefficient (r) was used. Values of $P < 0.05$ were considered statistically significant.

RESULTS

Identification of transcriptional regulators of human ADAM10 and BACE-1 by a dual-reporter screening approach

To identify potential modifiers of the AD-relevant proteases ADAM10 and BACE-1 on the transcriptional level, a library containing 704 expression plasmids encoding for human TFs was analyzed. SH-SY5Y cells were cotransfected with respective TF plasmids and a novel vector, which allows simultaneous measurement of both promoter activities. Factors that influenced both ADAM10 and BACE-1 expression activity due to their general mode of action, such as GTF2I (general transcription factor 2 I) or the RNA-modulating enzyme PARN [poly(A)-specific ribonuclease] were excluded from ensuing analyses. The screening revealed 48 TFs, which display a specific modulation of ADAM10- to BACE-1-promoter activity relation (**Fig. 1*A***). For a further classification, the identified TFs were ranked according to their relative expression levels in the adult human brain (Fig. 1*B*): 23 of the 48 TFs show a relatively high expression in the adult (>50 transcripts/10^6) as compared with embryonic state and also in brain tissue (>20 transcripts/10^6). Therefore, they represent the most probable factors potentially being involved in pathogenesis of AD (see Supplemental Table S1).

Within these 23 transcription factors, 4 are closely related to cellular stress responses: p53, which becomes activated by DNA damage; heat-shock factor 1 (HSF1) which transduces heat shock; activating transcription factor 4 (ATF4); and XBP-1. The latter 2 TFs are components of the signaling network of the UPR, which is activated on ER stress (27). All stress-related factors, except XBP-1, decreased the ratio of ADAM10- to BACE-1-promoter activity by their influence on one (HSF1) or both promoters (ATF4, p53). On the contrary, XBP-1 strongly enhanced ADAM10 transcriptional activity while not affecting the BACE-1 promoter (Fig. 1*C*).

Spliced XBP-1 isoform is responsible for the increase of ADAM10 gene expression in neuronal cells

The mRNA of XBP-1 is unconventionally spliced by the endonuclease IRE1-α due to ER stress signals, such as unfolded proteins (see **Fig. 10** and refs. 28, 29). Loss of the 26-nt intron (Fig. 2*A*) leads to a shift in the open reading frame and subsequently leads to the synthesis of a protein with a higher molecular mass (54 kDa, s XBP-1). The weight gain is the result of the insertion of a transcriptional activation domain and the loss of a nuclear exclusion signal (30). The u mRNA gives rise to a smaller protein of ~33 kDa (u XBP-1) under nonstress conditions. While u XBP-1 revealed only a comparably slight

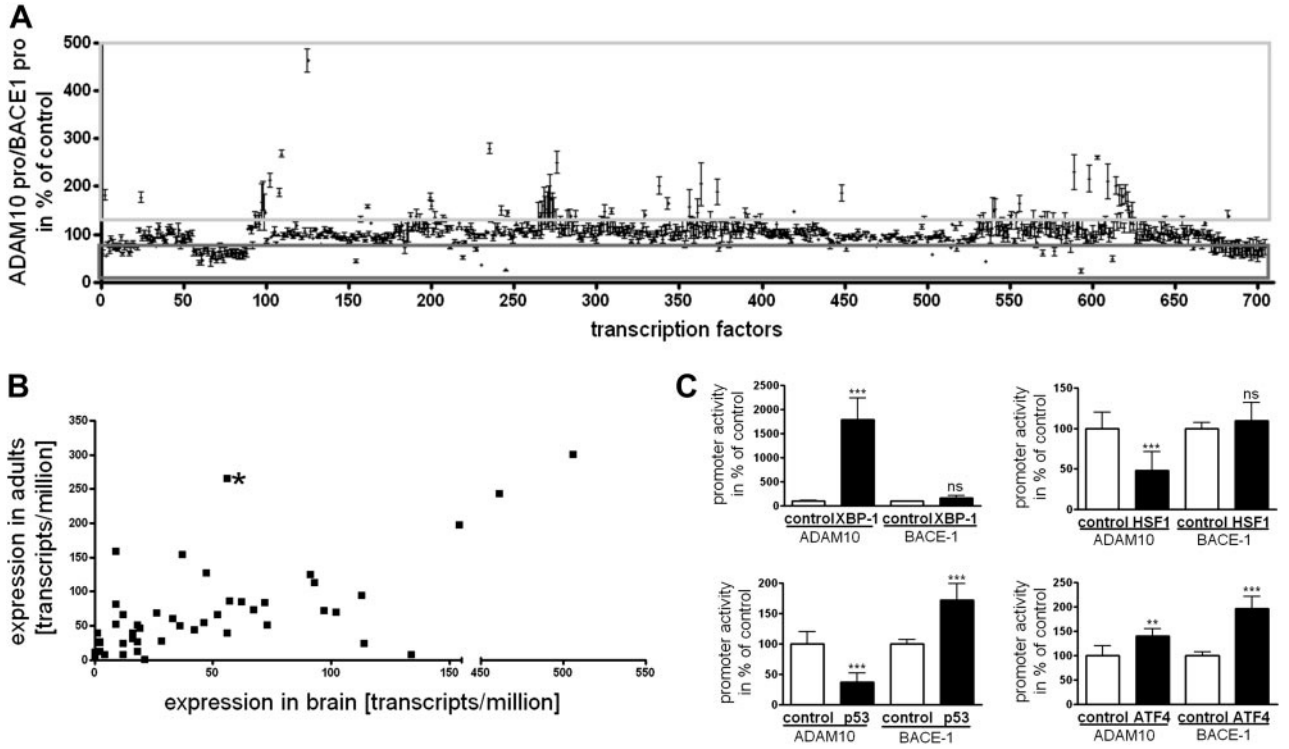

Figure 1. Identification of TFs modulating the ratio of ADAM10- to BACE-1-promoter activity in SH-SY5Y cells. *A*) Screening of the TF cDNA library analyzed with a dual-luciferase assay. Hits were considered as follows: calculated quotient > 130% (light gray box); or < 70% (dark gray box). *B*) EST profile analysis of selected TFs. Candidate TFs were ranked according to relative expression level in the adult brain, indicated in transcripts/10^6. Asterisk indicates XBP-1, a central constituent of the UPR. *C*) Influence of selected stress-related TFs on ADAM10- or BACE-1-promoter activity: XBP-1, p53, HSF1, and ATF4. Ratios of ADAM10- to BACE-1-promoter activities were as follows: XBP-1, 899 ± 177 (P<0.001); p53, 33 ± 11 (P<0.001); HSF1, 76 ± 6 (P<0.001); ATF4, 72 ± 8 (P<0.01). Bars represent means ± SD from 3 independent experiments. ns, not significant (P>0.05). **P<0.01, ***P<0.001; Bonferroni posttest.

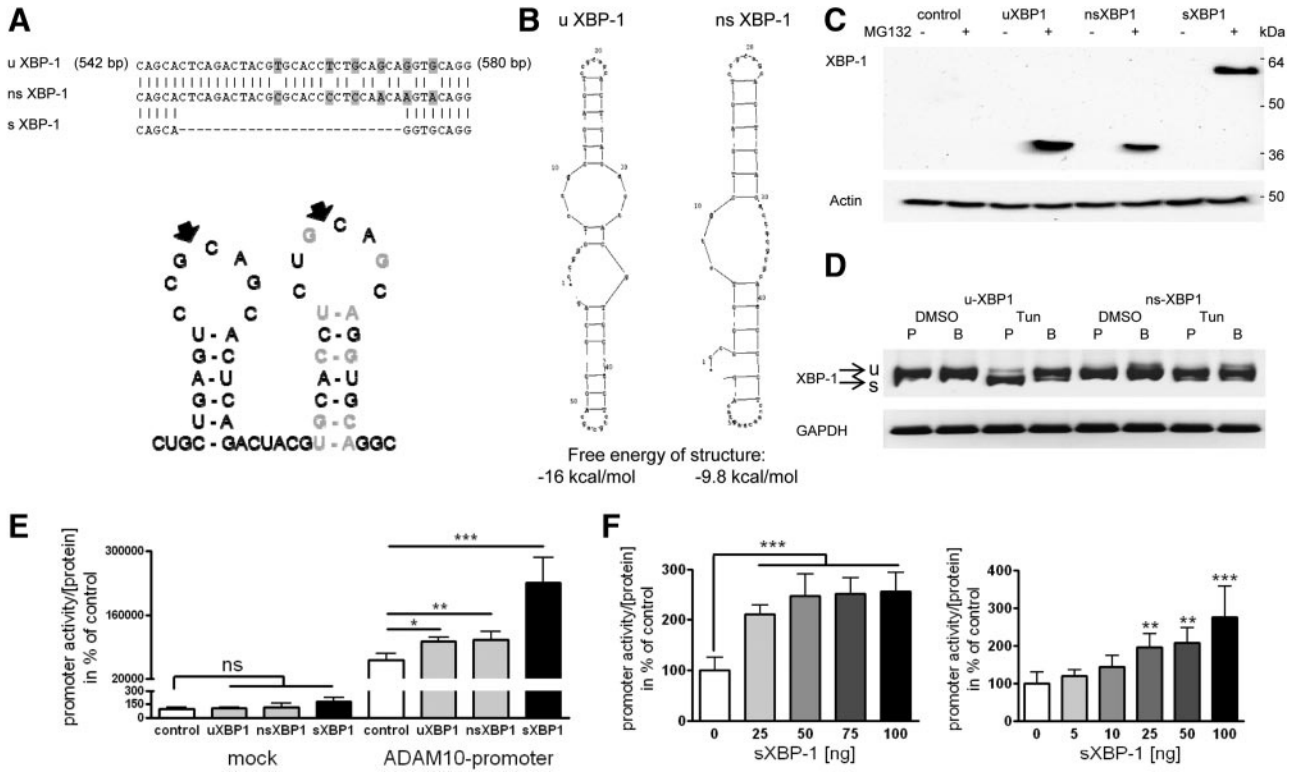

Figure 2. Characterization of XBP-1 variants and experimental validation regarding ADAM10-promoter activity. *A*) Sequence comparison of spliced and mutated XBP-1 mRNA with WT sequence of u XBP-1. s XBP-1 lacks the 26-nt intron. uXBP-1 mRNA forms 2 distinct hairpin loops, which contain splice donor and splice acceptor sites (indicated by arrowheads). Gray highlighted nucleotides indicate silent mutations in the ns XBP-1 sequence. *B*) Predicted mRNA secondary structures of u and ns XBP-1. *C*) Immunodetection of XBP-1 protein forms in transiently transfected SH-SY5Y cells. *D*) Demonstration of splice defect of ns XBP-1. SH-SY5Y cells (transfected with u and ns XBP-1 expression vectors) were treated with 10 μM tunicamycin to induce ER stress. Samples were analyzed *via* splice-variant-specific RT-PCR (P, *Pst*I cleavage; B, *Bgl*II cleavage; see also Materials and Methods). *E*) Effect of the XBP-1 variants on ADAM10-promoter activity. Transcriptional activity was assessed in cells transfected with either the ADAM10-promoter reporter vector or a promoterless control (mock) vector together with respective XBP-1 expression plasmid or empty vector. *F*) Dose-dependent effect of s XBP-1 on the human ADAM10 promoter. s XBP-1 was reverse titrated with the u XBP-1 variant (left panel) or empty vector (right panel) up to a total amount of 100 ng DNA in the transfection experiment, and ADAM10-promoter activity was measured (respective amount of s XBP-1 plasmid is indicated). *E*, *F*) Experiments were performed 3 times independently in triplicate. Bars represent means ± SD. ns, not significant ($P>0.05$). $^*P < 0.05$, $^{**}P < 0.01$, $^{***}P < 0.001$; Bonferroni posttest.

effect of ~65% on ADAM10-promoter activity, s XBP1 strongly enhanced reporter expression up to 376% of mock-transfected cells after 48 h (Fig. 2*E*). Both u and s XBP-1 are rapidly degraded by proteolysis (see Fig. 2*C*, overexpressed proteins are only visible on inhibition of the proteasome by MG132 preincubation). Therefore, we cannot exclude the possibility that a small proportion of u XBP-1 might have been converted to s XBP-1 due to experimental conditions, such as stress evoked by the transfection procedure. However, cotransfection of an unsplicable XBP-1 variant (ns XBP-1) derived by silent mutations in the XBP-1 cDNA (Fig. 2*A*) led to comparable values as measured for u XBP-1-transfected cells (Fig. 2*E*). Splice deficiency of ns XBP-1 was verified by variant-specific RT-PCR on tunicamycin-induced ER stress (Fig. 2*D*). The lack of splicing is probably due to the loss of the second hairpin loop in the mutated mRNA structure, which contains the splice acceptor site, as predicted by *in silico* analysis (Fig. 2*B*).

Dose dependency of s XBP-1-mediated ADAM10-promoter activation was demonstrated by titration with empty vector (Fig. 2*F*, right panel): 25 ng s XBP-1 coding plasmid was sufficient to result in a significant enhancement of the ADAM10-reporter activity. As u XBP-1 has been suggested as a counterbalance for s XBP-1-evoked transcriptional function (30), we also measured ADAM10-promoter activity in cells transfected with reverse gradients of u and s XBP-1. None of the applied amounts of u XBP-1 expression plasmid was able to impair the s XBP-1-induced ADAM10-promoter activity (Fig. 2*F*, left panel). This is in accordance with our finding that u XBP-1 and ns XBP-1 both slightly enhance the ADAM10 promoter despite having a functional transcriptional activation domain.

Validation of the gene expression enhancement of the APP-sheddase ADAM10 by XBP-1

For further examination of XBP-1-induced ADAM10-promoter activity, we performed a time-resolved measurement of both promoter activities, ADAM10 and BACE-1, by a single reporter assay using a life cell substrate (**Fig. 3*A***). For all investigated time points, we

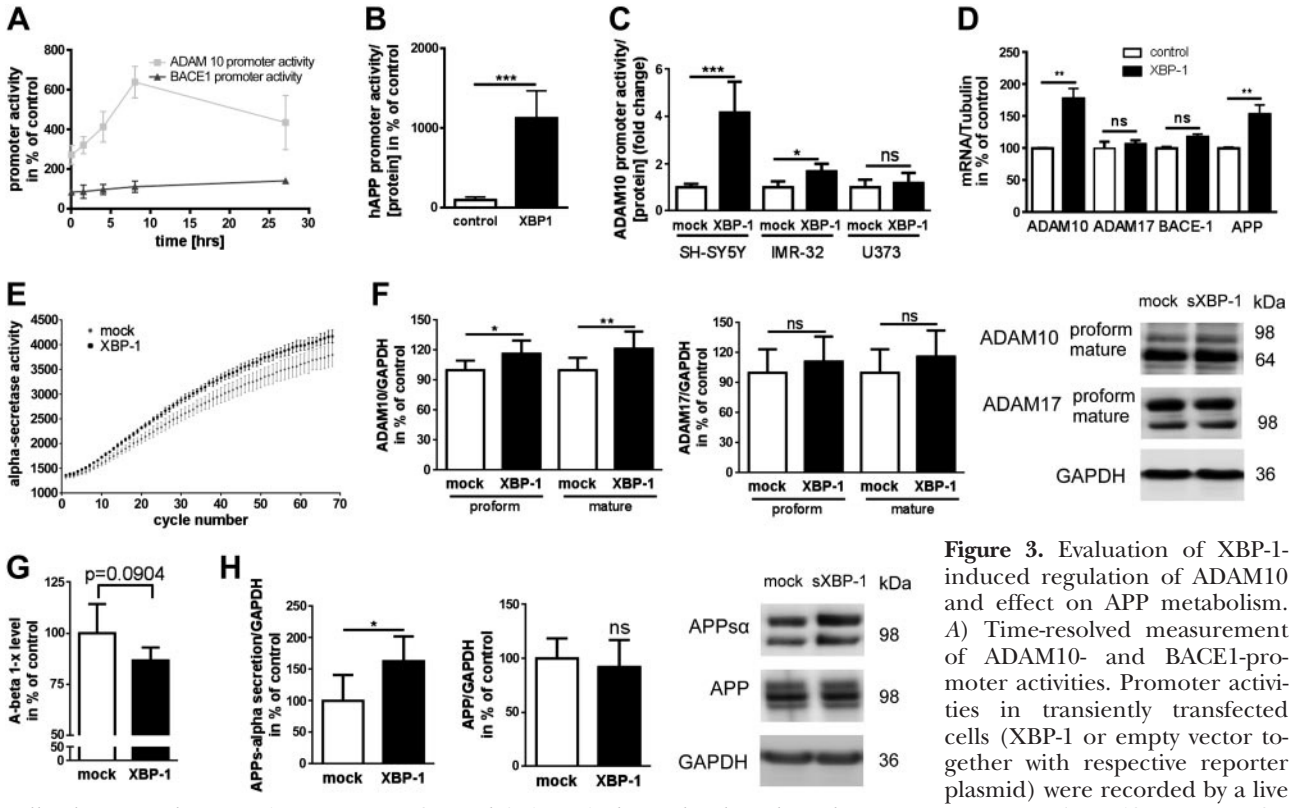

Figure 3. Evaluation of XBP-1-induced regulation of ADAM10 and effect on APP metabolism. *A*) Time-resolved measurement of ADAM10- and BACE1-promoter activities. Promoter activities in transiently transfected cells (XBP-1 or empty vector together with respective reporter plasmid) were recorded by a live cell substrate. The experiment was performed 3 times independently; values denote means ± SD. *B*) Luciferase assay for human APP-promoter activity in XBP-1-overexpressing SH-SY5Y cells. Bars represent values of 3 independent experiments performed in triplicate. *C*) Evaluation of the XBP-1-mediated effect on ADAM10 transcriptional activity in different cell lines. Human neuroblastoma cells (SH-SY5Y, IMR-32) or astroglioma cells (U373) were transiently transfected with s XBP-1 expression plasmid or empty vector together with luciferase-based reporter plasmid for the human ADAM10 promoter. Bars represent mean values of 2 independent experiments performed in triplicate. *D*) Evaluation of the effect of XBP-1 on ADAM10, ADAM17, BACE-1, and APP mRNA levels in SH-SY5Y cells using real time RT-PCR. Values represent means ± SD from 2 independent experiments performed in duplicate. *E*) Assessment of α-secretase activity on s XBP-1 overexpression in SH-SY5Y cells *via* fluorescent *in vitro* assay. *F*) Analysis of the effect of s XBP-1 overexpression on ADAM10 and ADAM17 protein levels. Cells were transfected with XBP-1 expression vector or empty vector, and samples were subjected to Western blot method using specific antibodies for human ADAM10 and ADAM17. GAPDH was used for loading control. *G*) Determination of Aβ levels. Conditioned medium from s XBP-1-overexpressing cells was subjected to ELISA measurement; protein content of cell lysates served as normalization. *H*) Evaluation of s XBP-1 overexpression on APP protein level and secretion of APPs-α in SH-SY5Y cells. Samples for analysis of APP protein level were the same as described in *F*. For detection, a specific APP C-terminal antibody was used. For determination of secreted APPs-α, supernatants of s XBP-1 or empty vector-transfected cells were collected, and samples of secreted proteins were subjected to Western blot using an APP N-terminal antibody. *F–H*) Bars represent means ± SD of 3 independent experiments conducted in triplicates. ns, not significant ($P>0.05$). *$P < 0.05$, **$P < 0.01$, ***$P < 0.001$; Bonferroni posttest.

obtained enhanced ADAM10-promoter-driven luciferase expression in XBP-1-cotransfected cells as compared with mock-transfected cells, peaking at 8 h after transfection. The BACE-1 promoter did not respond to the overexpressed TF during the whole observation period.

Retinoic acid, an enhancer of ADAM10 expression (17), led to a combined up-regulation of ADAM10 and its substrate APP (31). To identify such a potential common regulation for the UPR mediator XBP-1, a luciferase assay with an APP-promoter-driven reporter was conducted: XBP-1 overexpression resulted in strongly enhanced APP-promoter activity of 1127% as compared with mock-transfected cells (Fig. 3*B*). Moreover, s XBP-1-overexpressing SH-SY5Y cells showed a significant increase of APP mRNA levels of 154% as compared with empty vector-transfected cells (Fig. 3*D*). However, the effect could not be confirmed on the protein level (Fig. 3*H*). This might indicate that while APP gene transcription is influenced by s XBP-1, a post-translational regulatory mechanism counterbalances the induction.

To further analyze the specificity of the XBP-1-mediated effect on ADAM10 transcriptional activity, we performed luciferase reporter experiments in different cell types. Both neuroblastoma cell lines (SH-SY5Y and IMR-32) responded to XBP-1 overexpression by an increase of ADAM10-promoter activity to 4.2- and 1.7-fold, respectively. On the contrary, ADAM10 transcriptional activity was not elevated in the astroglioma cell line U373 (Fig. 3*C*).

Results obtained by reporter gene assays were verified by quantitative real-time RT-PCR of SH-SY5Y cells transiently transfected with XBP-1: ADAM10 mRNA levels significantly increased to 178% as compared with

mock-transfected cells (Fig. 3*D*). Regarding protein level, both the proform and the mature ADAM10 reached statistically significance at 117 and 122%, respectively, compared with mock-transfected cells (Fig. 3*F*). In addition, we analyzed ADAM17 protein level; overexpression of s XBP-1 showed no significant effect on both the proform and the mature ADAM17 (Fig. 3*F*). The increase of ADAM10 expression was substantiated by detection of the α-secretase-dependent APP proteolysis product APPs-α; its secretion was increased to 163% in XBP-1-overexpressing cells compared with empty vector-transfected cells (Fig. 3*H*). s XBP-1 overexpression in SH-SY5Y cells resulted in a slight reduction of secreted Aβ peptides, which did not reach statistical significance (Fig. 3*G*). However, when α-secretase activity was measured by a fluorescent *in vitro* assay, signals were significantly enhanced using membrane fractions derived from XBP-1-transfected cells as compared with mock-transfected cells (Fig. 3*E*).

Contribution of UPR and ERS elements in s XBP-1-induced ADAM10 up-regulation

In silico analysis of the human *ADAM10*-promoter sequence revealed 4 TF binding sites (**Table 1**) potentially being involved in UPR-related activation of *ADAM10* gene expression; we identified 2 potential UPREs (18, 32) located at −308 and −626 bp upstream of the translation initiation start site. XBP-1 binds to the TGACGTGG/A sequence of the UPRE as a homodimer without the involvement of the cofactor nuclear transcription factor-Y (NF-Y; ref. 29). Both identified binding sites are conserved, with only 1 nt deviating from the described consensus sequence. Furthermore, one ERSE-like sequence (33, 34) at −464 bp and an ERSE II-like sequence (35) at −591 bp were identified within the *ADAM10*-promoter sequence. Theoretically, the ERSE site has the conserved sequence CCAAT-N_9-CCACG. The 9-nt spacing between both consensus motifs has been demonstrated to be quite important for their functionality. Therefore, the identified binding site within the *ADAM10* promoter is not well conserved by having only 1 nt located between both binding motifs. The ER-stress-related TF ATF6 specifically binds to the CCACG sequence of the ERSE motif, if the general TF NF-Y has bound to the CCAAT part of the sequence (36). However, XBP-1 is also able to bind to this sequence instead of ATF6 (29, 33). The ERSE II has been shown to be occupied NF-Y dependently by ATF6 (35) or NF-Y independently by XBP-1 (37). The half site of the motif ATTGG is not well conserved within the human *ADAM10*-promoter sequence, while the CCACG is fully conserved.

As a first step to identify DNA sequences relevant for s XBP-1 binding to the human *ADAM10* promoter, we deleted the 3′ half site of the well-conserved UPRE, positioned within the core promoter region (−308 bp, **Fig. 4*A***). We chose especially this specific UPRE site for deletion, because the majority of XBP-1 recognition motifs are located within the 500 bp 5′ to the transcription start site of the target genes, with the greatest enrichment within the first 200 bp (38). The luciferase-based promoter assay revealed that this mutated ADAM10 promoter still was inducible by s XBP-1 (UPRE_del; Fig. 4*B*). Basal and induced activity of the mutated ADAM10-promoter sequence compared with the vector with the WT-promoter sequence was generally lowered. This might be due to the functional upstream stimulatory factor (USF) binding site in proximity to the mutated sequence (−317 bp; ref. 17), which probably has been affected by deletion of the respective nucleotides. Subsequently, we analyzed the contribution of both ERSE-like sequences and the remaining UPRE by cotransfection of reporter plasmids with truncated versions of the ADAM10 promoter (previously described in ref. 17) with s XBP-1 expression vector; the reporter vector comprising the complete promoter sequence (−2179 to +1 bp) was generally less active than the constructs starting at −433 bp correlating to the translational repressor identified in the 5′ untranslated region (UTR; ref. 39). The XBP-1-evoked ADAM10-promoter activity was significantly decreased in the promoter constructs lacking the UPRE at −626 bp revealed by fold-induction analysis (Fig. 4*C*). Nevertheless, the effect of the overexpressed TF was still present if the ERSE-like sequence at −464 bp was included in the promoter sequence. Thus, the UPRE at position −626 bp and also the ERSE-like element at position −464 bp might be involved in transduction of XBP-1 transcriptional activation of the *ADAM10* gene. To further analyze the contribution of either binding

TABLE 1. *Characterization of potential XBP-1 binding sites within the human ADAM10-promoter sequence*

		ADAM10 promoter		
Binding site	Theoretical sequence	Sequence	Position	Present in reporter plasmid
UPRE	TGACGTGG/A	TCACGTGG	−308 to −316	CP53 AB.1
ERSE	CCAAT-N_9-CCACG	CCAATCCCAGC	−464 to −475	CP53 AB.1, CP 30.1, CP 31.3, CP 34.1
ERSE II	ATTGG-N-CCACG	ATCTTCCACG	−591 to −601	CP53 AB.1, CP 30.1, CP 31.3
UPRE	TGACGTGG/A	TGACGTTA	−626 to −634	CP53 AB.1, CP 30.1

Four potential binding sites for XBP-1 were identified within the human ADAM10-promoter sequence. Two UPREs and 2 ERSE-like sites are located in the range from −634 to −308 bp upstream of the translation initiation site. However, since the spacing between the ERSE sites is important for their activity, the ERS-like element is not well conserved within the ADAM10-promoter sequence, and the ERS II-like element lacks conservation in the consensus motif ATTGG. Table displays the theoretical sequences compared with the sequences identified within the human promoter. In addition, the respective reporter vectors harboring one or more potential binding sites are denoted (see Fig. 4).

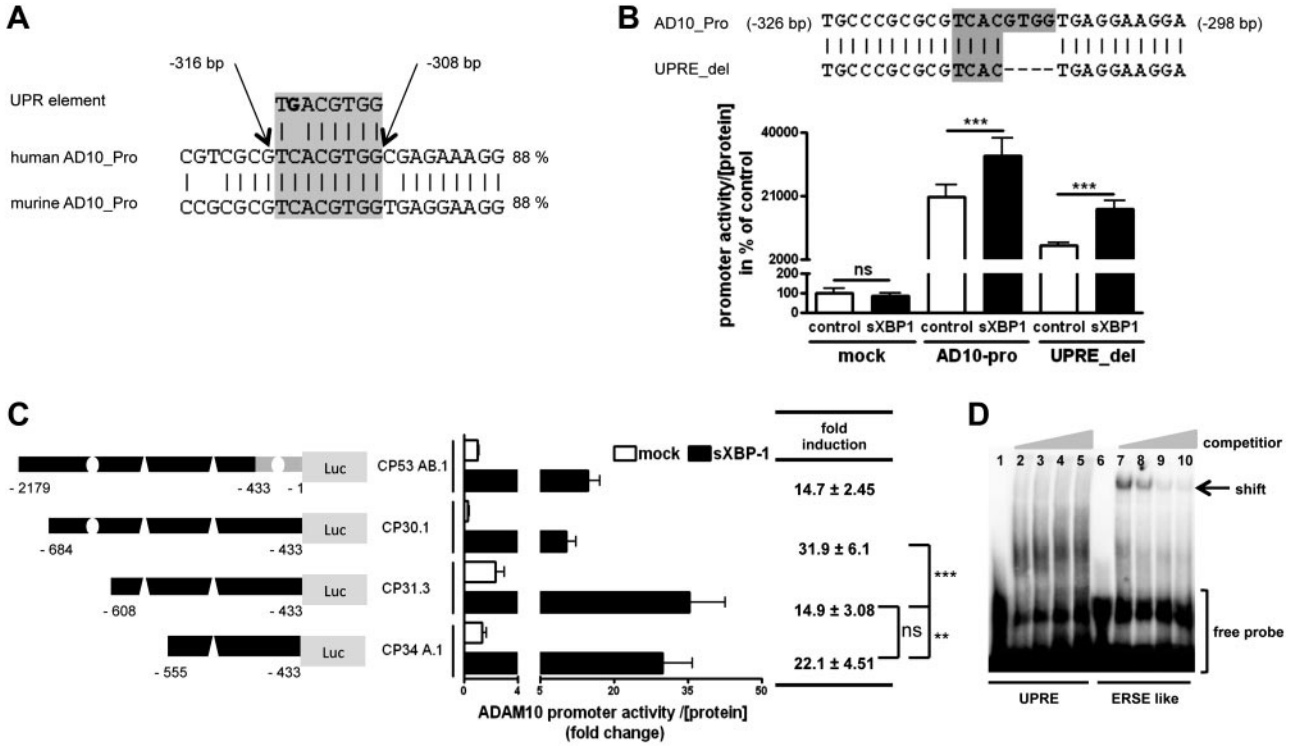

Figure 4. Identification and characterization of putative XBP-1 binding sites within the human *ADAM10*-promoter sequence. *A*) A putative UPRE is conserved in the range of the human and murine *ADAM10* core-promoter sequence (−308 bp upstream of the translation initiation site). *B*) Contribution of the conserved UPRE to the s XBP-1-mediated effect on the *ADAM10* promoter. The reporter vector with the mutated UPRE, lacking the 3′ part of the UPRE (UPRE_del), together with s XBP-1 plasmid or empty vector, was transiently transfected in SH-SY5Y cells. Samples were assayed for luminescence *via* luciferase-reporter assay. *C*) Luciferase-reporter assay for truncated ADAM10-promoter reporter plasmids. Four potential binding sites for XBP-1 or related UPRE-mediating transcription factors were identified (see Table 1; blank oval, UPRE; blank wedge, ERSE- or ERSE II-like). *B, C*) Values represent means ± SD of 2 independent experiments performed in triplicate. ns, not significant ($P>0.05$). $^{**}P < 0.01$, $^{***}P < 0.001$; Bonferroni posttest. *D*) EMSA for the potential XBP-1 binding sites UPRE and ERSE-like within the human *ADAM10*-promoter sequence. Respective biotinylated double-stranded oligonucleotides were incubated with nuclear fraction of s XBP-1-overexpressing HEK 293 cells in the absence (lanes 1 and 6) or presence of increasing amounts of respective unlabeled oligonucleotides as competitor (20-, 200-, and 400-fold molar ratio; UPRE, lanes 2–5; ERSE-like, lanes 7–10). Protein-DNA complexes were separated from the free DNA probe by electrophoresis in a native polyacrylamide gel, and chemiluminecent signals were visualized by HRP-coupled streptavidin conjugate.

site, we performed EMSA. Incubation of biotinylated oligonucleotides including the potential UPRE or ERSE-like sequence together with nuclear extracts of s XBP-1-overexpressing cells revealed a shift due to DNA-protein binding for the ERSE-like sequence. This binding was dose-dependently attenuated with increasing amounts of respective unlabeled oligonucleotide (Fig. 4*D*).

Effect of ER stress on ADAM10 mRNA level

ER stress can be provoked in cells by different approaches. Tunicamycin, for example, inhibits N-glycosylation and leads to accumulation of proteins in the ER. Thapsigargin interferes with the calcium ion release from the ER and leads subsequently to ER-stress response. Both pharmacologically induced ER-stress conditions led to a transient generation of s XBP-1 in SH-SY5Y cells as demonstrated by RT-PCR (see **Fig. 5*A***). The active form of XBP-1 occurs on incubation with thapsigargin or tunicamycin after 1 and 2 h, respectively. Both ER-stress inducers significantly enhanced the ADAM10 mRNA level 1.5- or 1.4-fold at early time points (2 h for tunicamycin, 6 h for thapsigargin). The effect was reversible, and mRNA amounts returned to unstimulated levels within 18 h after beginning of treatment. This coincides with the loss of detectable levels of s XBP-1 mRNA amounts after prolonged incubation with tunicamycin (Fig. 5*A*). In thapsigargin-treated cells, s XBP-1 was still detectable after 18 h; nevertheless, ADAM10 mRNA was comparable to control-treated cells at this time point. When STF083010, a specific IRE1-α inhibitor, was added to cells in which ER stress was evoked by thapsigargin, the maturation of u XBP-1 mRNA into its active form was blocked (Fig. 5*B*). Under these conditions, the effect of XBP-1 on *ADAM10* gene expression was completely inhibited.

The effect of ER-stress induction on ADAM10 transcriptional level was also confirmed on the protein level. The determination of the active, phosphorylated enzyme IRE1-α (Fig. 5*D*) verified the successful activation of the ER-stress pathway by Tunicamycin. Under

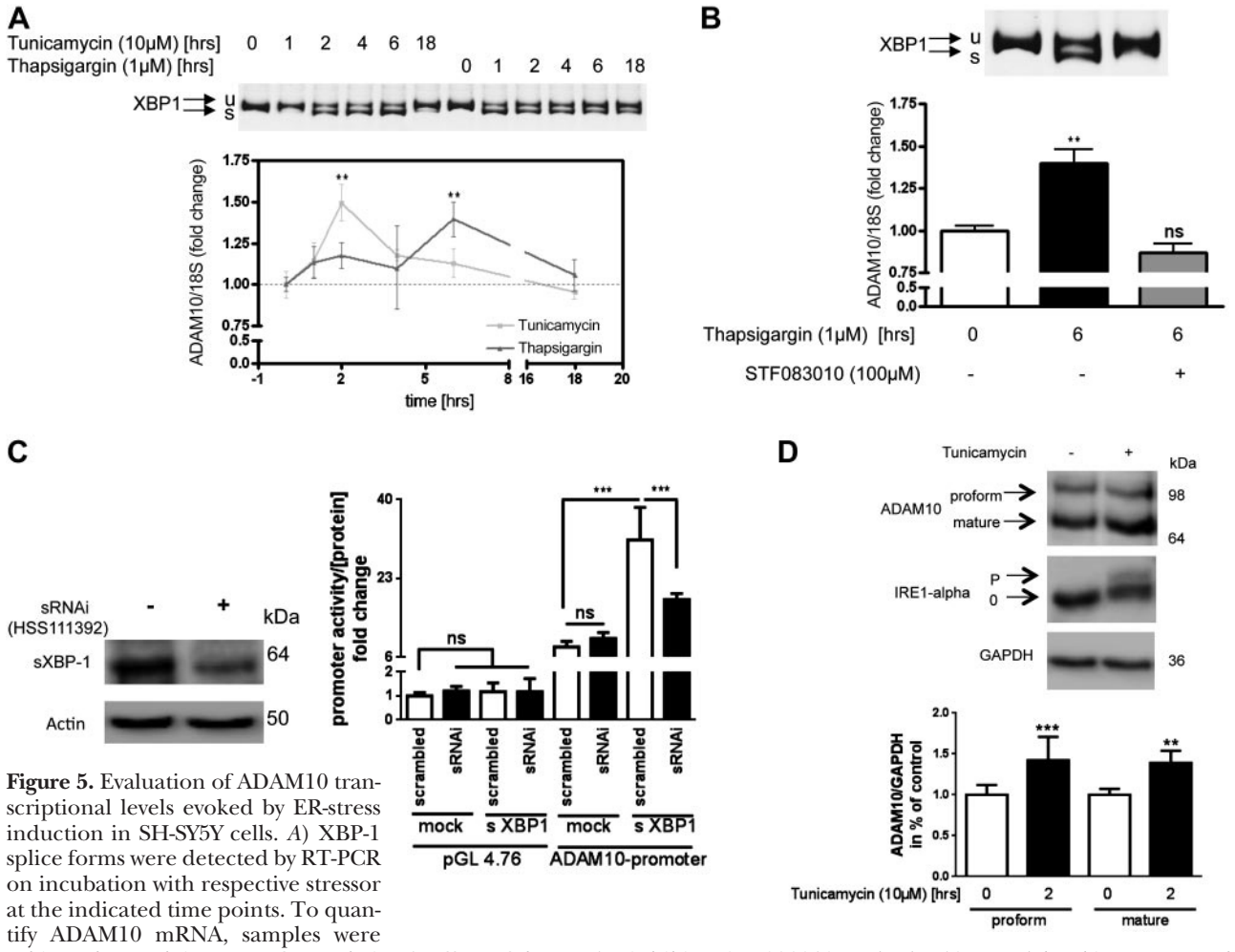

Figure 5. Evaluation of ADAM10 transcriptional levels evoked by ER-stress induction in SH-SY5Y cells. *A*) XBP-1 splice forms were detected by RT-PCR on incubation with respective stressor at the indicated time points. To quantify ADAM10 mRNA, samples were subjected to real-time RT-PCR analysis. *B*) Effect of the IRE1-α inhibitor STF083010 on ADAM10 mRNA level in ER-stressed SH-SY5Y cells. u and s XBP-1 mRNAs were detected as described above. *A*, *B*) Bars represent means ± SE of 2 independent experiments performed in duplicate. *C*) Effect of sRNAi-mediated knockdown of XBP-1 on ADAM10-promoter activity. Knockdown was verified by Western blot using a specific XBP-1 antibody. Detection of actin served as loading control. s XBP-1 expression plasmid or empty vector was transfected together with ADAM10-promoter reporter construct or respective promoterless plasmid in combination with sRNAi (HSS111392; Invitrogen) or scrambled control sRNAi. Samples were analyzed *via* luciferase-based measurement. *D*) Evaluation of the effect of ER-stress induction on ADAM10 protein level. SH-SY5Y cell were incubated with tunicamycin or solvent control for 2 h. ADAM10 protein level was assessed by immunoblot method using a specific antibody for human ADAM10. For verification of successful ER-stress induction, active, phosphorylated IRE1-α was detected using Phos-tag gel system (P, phosphorylated; 0, unphosphorylated). *C*, *D*) Bars represent values of 2 independent experiments performed in triplicate. ns, not significant ($P>0.05$). $^{**}P < 0.01$, $^{***}P < 0.001$; Bonferroni posttest.

these conditions, the proform and mature ADAM10 level were increased to 142 and 139% as compared with solvent-treated cells. To further substantiate these findings, we performed XBP-1-knockdown experiments: ADAM10-promoter activity was induced ~4-fold on s XBP-1 overexpression, while the effect was significantly diminished ~0.6-fold when active XBP-1 was knocked down with specific siRNA (Fig. 5*C*).

Synergistic regulation of ADAM10-promoter activity by insulin signaling and s XBP-1

Besides unfolded proteins themselves, different signal transduction pathways, such as LPS-TLR4 or insulin signaling, have been described to contribute to the UPR. LPS-derived stimulation of TLR4 was reported to interfere with components of the ER-stress signal transduction: LPS activates IRE1-α and consequently the splicing of XBP-1 in J774 cells (ref. 40; see Fig. 9). This effect is based on the successive recruitment of tumor necrosis factor receptor-associated factor 6 (*TRAF6*), NADH-oxidase 2 (NOX2), and reactive oxygen species (ROS) to TLR4, as demonstrated in MyD88-knockout mice (40). To investigate a potential implication of TLR4 signaling in XBP-1-regulated *ADAM10* gene expression, we treated the monocyte precursor cell line THP-1 with LPS for 4 and 24 h, respectively. LPS-induced signal transduction was confirmed by a NF-κB-dependent SEAP reporter assay (**Fig. 6*A***). Instead of elevated ADAM10 mRNA amounts, we rather observed

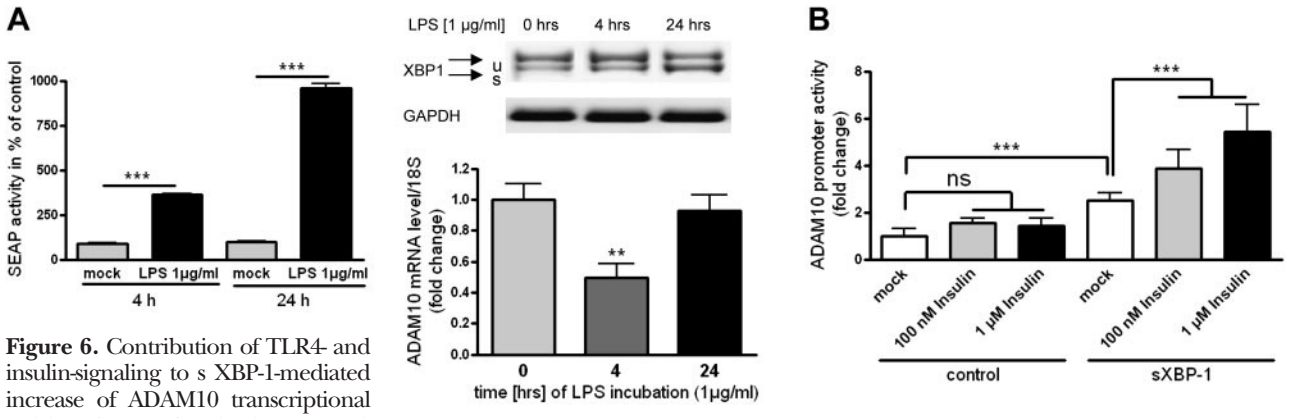

Figure 6. Contribution of TLR4- and insulin-signaling to s XBP-1-mediated increase of ADAM10 transcriptional activity. *A*) TLR 4 activation *via* LPS was verified by a SEAP assay in THP-1 cells. ADAM10 mRNA levels were detected in cells treated with 1 μg/ml LPS for indicated time points using real-time RT-PCR analysis. *B*) Influence of insulin treatment on s XBP-1-induced ADAM10-promoter stimulation. SH-SY5Y cells were transfected with ADAM10-promoter reporter and s XBP-1 or empty vector (mock) and subsequently treated with insulin for 48 h. To circumvent a saturation-effect on ADAM10-promoter activity 25 ng s XBP-1 expression vector were used in these experiments. Results are represented as means ± SD. ns, not significant ($P>0.05$). $^{**}P < 0.01$, $^{***}P < 0.001$; Bonferroni posttest.

a decrease on 4 h incubation with LPS, which returned to levels of solvent-treated controls on prolonged incubation of 24 h. When analyzing s XBP-1-specific RT-PCR amplificates in LPS-treated cells, it became obvious that THP1 cells contain detectable amounts of the active XBP-1 splice form already at $i = 0$ h (Fig. 6*A*). In addition, LPS activates several TFs that might mask the s XBP-1 effect on the ADAM10 promoter, for example NFκB and activator protein 1 (AP1), as shown by the activation of the NF-κB- and AP1-dependent SEAP reporter in THP-1 cells (Fig. 6*A*).

Insulin is another physiological coregulator of s XBP-1-evoked gene transcription; on binding of insulin to its receptor, p85 becomes activated and heterodimerizes with s XBP-1 (ref. 41; see Fig. 9). This drives translocation of s XBP-1 to the nucleus and therefore enhances its transcriptional potency. Incubation of cells expressing the ADAM10-promoter reporter solely with insulin did not result in enhanced promoter activity (Fig. 6*B*). On the contrary, combined cotransfection with s XBP-1 expression plasmid and insulin treatment of cells strongly enhanced transcription of the reporter. Insulin contributed synergistically to the s XBP-1-mediated increase of the ADAM10-promoter activity in a dose-dependent manner; induction analysis revealed a 1.5- and 2.2-fold increase of the ADAM10 transcriptional activity for incubation with 100 nM or 1 μM insulin, respectively, compared with solvent-treated cells (Fig. 6*B*).

Analysis of XBP-1 metabolism in AD model mice

To further validate the physiological effect of the cell culture-based data regarding XBP-1-mediated regulation of ADAM10, brain tissue from 2 different AD mouse models (5xFAD, ref. 42; APP/PS1, ref. 43) were analyzed. Due to mutated *APP* and *PS1* genes, mice develop first pathological changes at ~1 mo (5xFAD) and 6 mo (APP/PS1), respectively (42, 44). We analyzed XBP-1 metabolism and ADAM10 as well as ADAM17 expression in brain samples from mice. For our analysis, we chose different ages: 2, 6, and 9 mo for APP/PS1 mice and 1, 2, and 9 mo for 5xFAD mice. Nontransgenic littermates served as controls for appropriate time points. mRNA levels of s and u XBP-1, as well as IRE1-α, were significantly increased as compared with nontransgenic mice at 6 mo of age for APP/PS1 mice (**Fig. 7*A, D, E***). Analysis of s XBP-1 level in 5xFAD mice at 1 mo of age confirmed an early induction of UPR (Fig. 7*F*). At this time point, the amount of ADAM10 mRNA was also significantly enhanced ~2-fold (APP/PS1) and 3-fold (5xFAD) as compared with nontransgenic littermates (Fig. 7*D*, *G*). Elevation of ADAM17 expression level did not reach statistical significance in 6-mo-old APP/PS1 mice, but was strongly induced (5-fold) in 5xFAD mice at 1 mo of age. Analysis of brain samples derived from 2-mo-old APP/PS1 mice revealed that ADAM10, ADAM17, and XBP-1 metabolism was unaffected at this early stage (Fig. 7*A–E*). s XBP-1, ADAM10, and ADAM17 mRNA levels in 5xFAD mice at 2 mo of age were comparable to WT (Fig. 7*F–H*); analysis of older 5xFAD mice (9 mo of age) showed a significant reduction of s XBP-1 and ADAM10 mRNA level. The ADAM17 expression level in the transgenic mice reached basal levels of WT littermates (Fig. 7*F–H*). A significant reduction of s and u XBP-1 in 9-mo-old APP/PS1 mice occurred as compared with control animals. ADAM10, ADAM17 and IRE1-α levels were revised to WT levels at this age (Fig. 7*A–E*). In accordance with early increase in s XBP-1, we also observed an increase of phosphorylated IRE1-α in 5xFAD transgenic mice as compared with WT at the age of 1 mo (1.7-fold, Fig. 7*I*). This enhanced activation was clearly attenuated at an advanced age (0.7-fold, 9 mo).

Our results indicate that XBP-1 metabolism, together with ADAM10 mRNA amount, is elevated in brain tissue from transgenic mice compared with nontransgenic littermates at early time points of pathological changes.

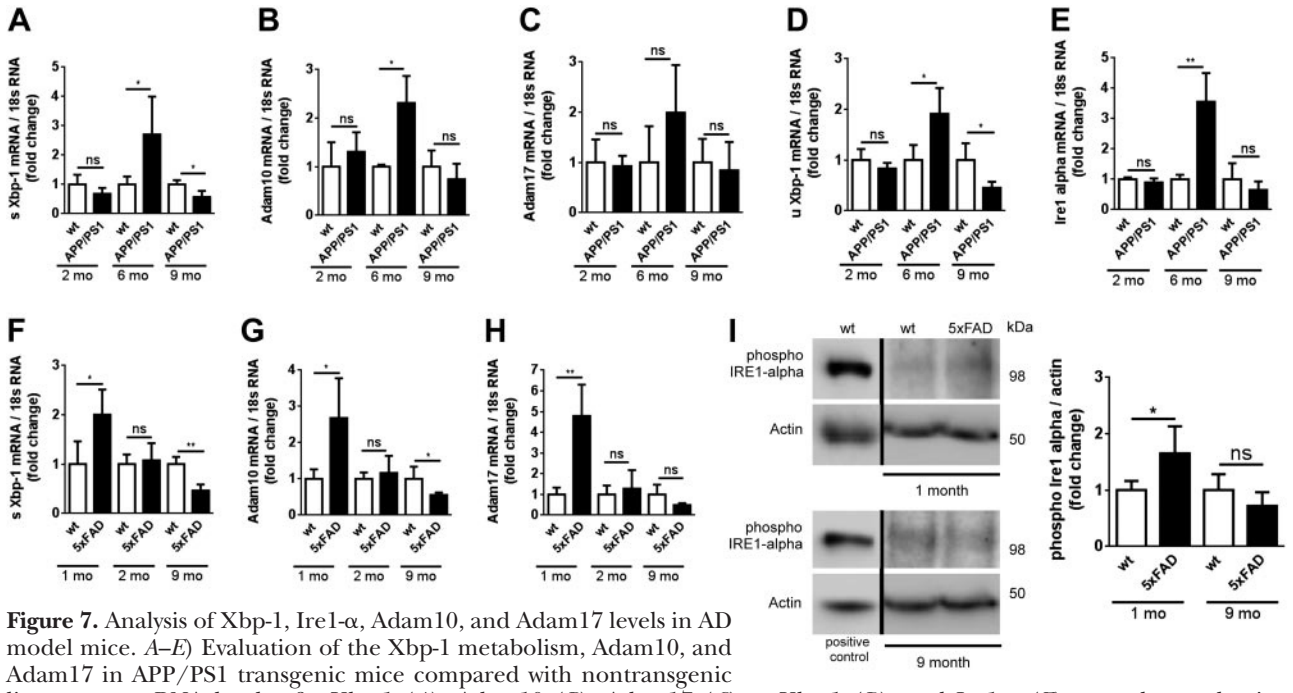

Figure 7. Analysis of Xbp-1, Ire1-α, Adam10, and Adam17 levels in AD model mice. *A–E*) Evaluation of the Xbp-1 metabolism, Adam10, and Adam17 in APP/PS1 transgenic mice compared with nontransgenic littermates. mRNA levels of s Xbp-1 (*A*), Adam10 (*B*), Adam17 (*C*), u Xbp-1 (*D*), and Ire1-α (*E*) were detected using real-time RT-PCR. Obtained values were normalized to those of 18 S rRNA and set in relation to nontransgenic littermates. *F–H*) Analysis of s Xbp-1 (*F*), Adam10 (*G*), and Adam17 (*H*) mRNA levels in 5xFAD mice. *I*) Determination of active IRE1-α in 5xFAD mice. Brain samples were subjected to immunoblot analysis using phospho-IRE1-α antibody. Pancreatic tissue served as a positive control for antibody specificity (24); the respective signal was visualized using shorter exposure time than for brain. Age of the respective animals is indicated. Transgenity was confirmed by PCR. Values are given as means ± SD with $n = 4$ for each group of animals. ns, not significant ($P > 0.05$). $^*P < 0.05$, $^{**}P < 0.01$; Bonferroni posttest.

During prolonged AD-like pathology, the system is counterregulated; consequently, mRNA levels of s XBP-1 and ADAM10 decreased in mice at 9 mo of age in both models.

XBP-1 correlates with ADAM10 expression, and its metabolism is affected in AD postmortem brain tissue

Active XBP-1-induced ADAM10-promoter activity in neuronal cell lines and parallel enhancement of ADAM10 and XBP-1 signaling was obtained in AD model mice at early disease stages. We therefore compared expression levels of active XBP-1 and ADAM10 in samples derived from postmortem cortical tissue of patients with AD and healthy control subjects. Both sample groups were matched according to age and gender; the postmortem delay period revealed no statistically significant differences (**Table 2**). In addition, cortical samples were characterized regarding AD pathology by Braak stages (control group: 71% stage 0–II; AD group: 93% stage V–VI; Table 2) and Consortium to Establish a Registry for Alzheimer's Disease (CERAD) scores (control group: 64% scores 0 or A; AD group: 100% scores B or C; **Fig. 8*A***). In frontal as well as temporal cortex tissue of patients with AD, a significant decrease of ADAM10 mRNA level, as compared with controls, was observed, which is in accordance with previous reports (11, 45), whereas ADAM17 level was unaffected in both tissues (Fig. 8*B*). In the control group, we found no correlation of ADAM10 mRNA and s XBP1 expression (Fig. 9*B*, Pearson's coefficient of $r=0.0932$), but in AD samples, a moderate but significant correlation was observed (Pearson's coefficient of $r=0.3120$). Regarding IRE1-α, which splices XBP-1, in both groups, healthy control subjects and patients with AD, a significant correlation with ADAM10 amount was found (Fig. 9*B*). This coincides with an up-regulation of IRE1-α in temporal as well as frontal cortical tissue samples from patients with AD patients in comparison to control samples (Fig. 9*A*). Interestingly, albeit IRE1-α-coding mRNA was induced 3- to 4-fold, s XBP-1 mRNA, as measured by splice-variant-specific RT-PCR, was reduced in both tissue types in patients with AD patients. In the temporal cortex, a reduction of ~28%, which did not reach statistical significance, was obtained. In the frontal cortex, s XBP-1 was reduced significantly to 75% as compared with controls (Fig.

TABLE 2. *Characterization of cortical brain tissues*

Parameter	Control	AD	*P*
n	14	30	
Age (yr)	77 ± 8.27	78 ± 6.90	0.68
Postmortem delay (h)	25.2 ± 8.05	27.5 ± 14.62	0.68
Male:female ratio	0.75	0.76	—
Braak stage			
0–II	10	0	—
III–IV	4	2	—
V–VI	0	28	—

See Fig. 8*A*.

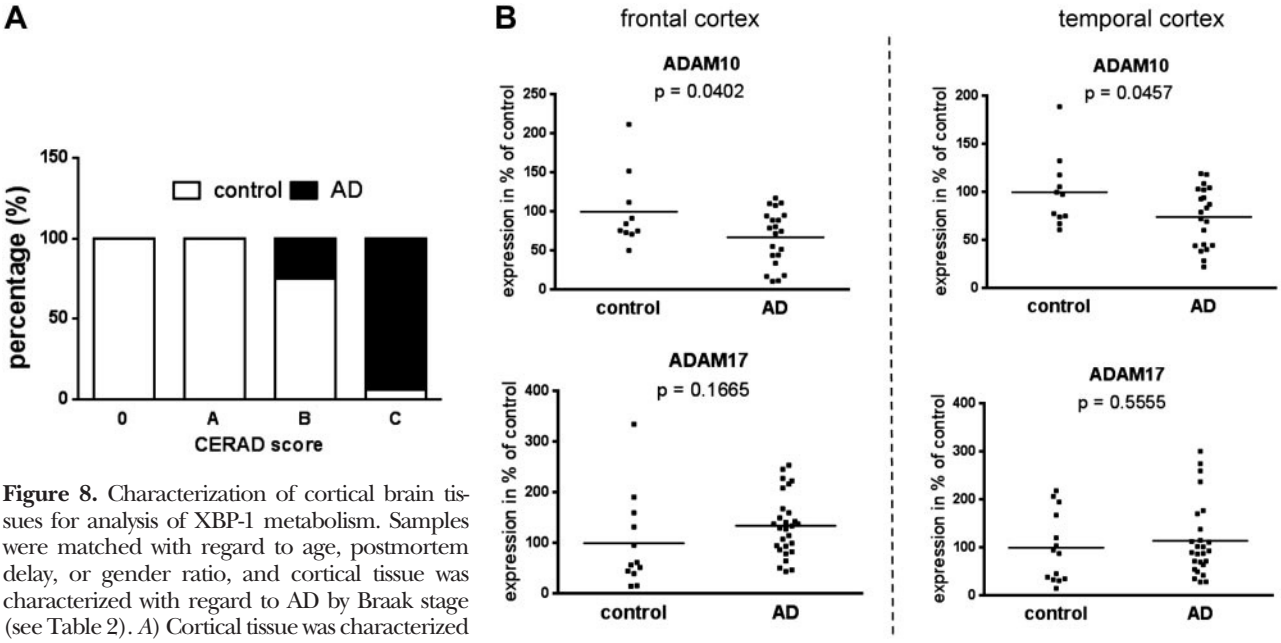

Figure 8. Characterization of cortical brain tissues for analysis of XBP-1 metabolism. Samples were matched with regard to age, postmortem delay, or gender ratio, and cortical tissue was characterized with regard to AD by Braak stage (see Table 2). *A*) Cortical tissue was characterized with regard to AD by Consortium to Establish a Registry for Alzheimer's Disease (CERAD) score. *B*) Evaluation of ADAM10 and ADAM17 mRNA levels in cortical brain tissue of patients with AD compared with healthy control subjects.

9*A*). The amount of total XBP-1 (u and s) was unaffected in the frontal cortex area of patients with AD as compared with healthy controls; for temporal tissue, an increase to 165% was observed.

In samples of hippocampal nuclear extracts, we analyzed the XBP-1 protein amount; the XBP-1 antibody, which binds to an epitope included in both splice forms of XBP-1, detected a protein of ~36 kDa (Fig.

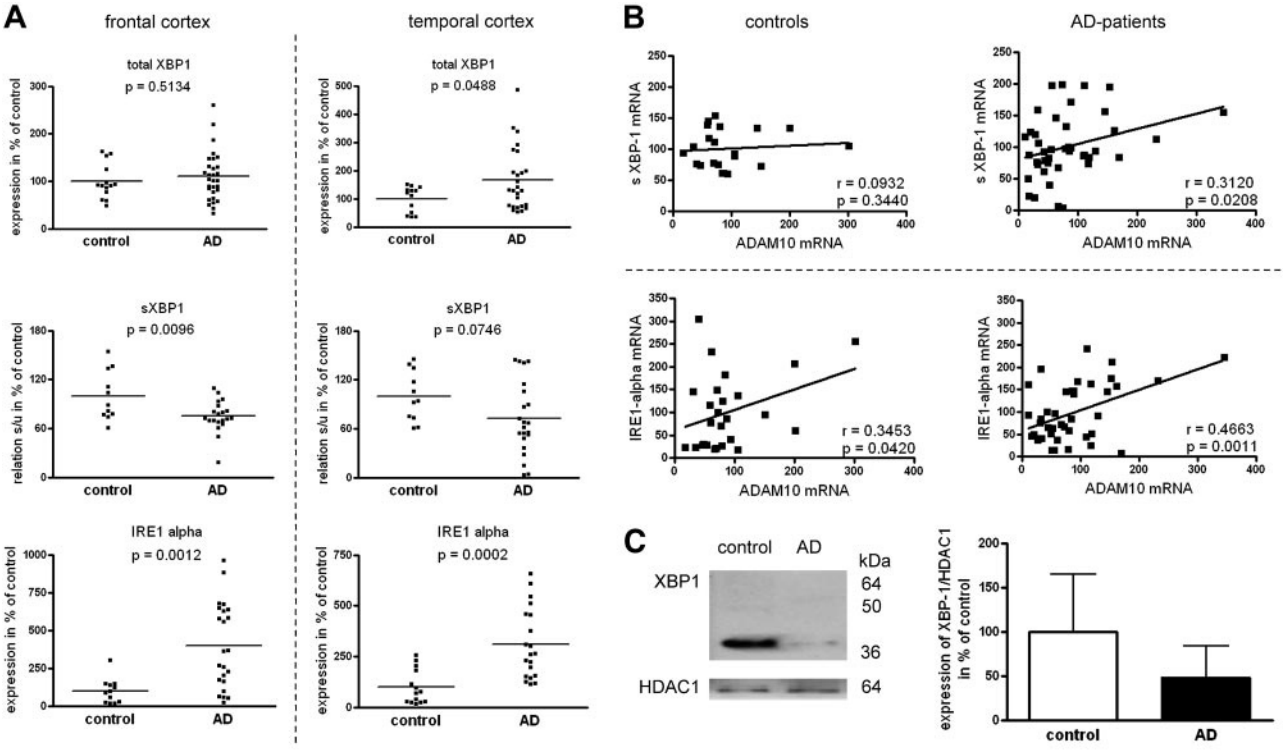

Figure 9. XBP-1 metabolism in AD postmortem brain tissue. *A*) Analysis of XBP-1 and IRE1-α mRNA level in frontal and temporal cortex tissue of patients with AD compared with healthy control subjects (for characterization of samples, see Table 2 and Fig. 8). *B*) Correlation between ADAM10 mRNA and s XBP-1 or IRE1-α mRNA, respectively, in AD postmortem brains. *r* indicates Pearson's correlation coefficient. *C*) XBP-1 quantitation in nuclear hippocampal protein extracts of patients with AD compared with healthy, age-matched controls (n=2 each). Left panel; representative blot. Right panel: quantitative analysis. Bars represent means ± SD.

9*C*). This protein band was reduced in both AD samples analyzed in comparison to the age-matched controls even if not reaching statistical significance ($P=0.424$) due to the lack of further samples. s XBP-1 has a theoretical molecular mass of 54 kDa and u XBP-1 of 33 kDa (Fig. 3*C*). Both protein species are degraded on ubiquitinylation, but s XBP-1 reveals a higher half-life time (28). However, the detected protein displays a similar molecular mass as observed for the overexpressed u XBP-1 (Fig. 3*D*) and therefore probably represents the unspliced protein. Nevertheless, these results in addition indicate a deregulation of XBP-1-mediated UPR in AD brains and its potential contribution to failure in ADAM10 up-regulation under pathological conditions.

DISCUSSION

In patients with prodromal or manifested AD, a decrease in the amount or catalytic activity of ADAM10 has repeatedly been reported (reviewed in ref. 10). As BACE-1 activity or protein amount seems to increase, this potentially leads to a misbalance within the proteolytical processing of APP and augmented release of Aβ peptides. In our study, we unraveled 48 TFs by screening a library of 704 expression vectors that significantly modulate the ratio of ADAM10- to BACE-1-promoter activity (see Results).

Single regulatory effectors for gene expression of both enzymes have been investigated before; for example, miRNAs that regulate the translational level of BACE-1 (46, 47) and ADAM10 (48, 49) were identified, and sequences interfering with translational capacity have additionally been characterized within the respective 5′-UTR sequences (39, 50). Previously, we investigated binding of retinoic acid receptor heterodimers within the ADAM10 promoter (31, 51), and several other TFs, such as USF-1 and SP1, were determined to function as expression enhancers (17). For BACE-1, Yin Yang 1 (YY-1) and SP1 have been shown to induce its transcription (19, 52). In addition, the ER-stress-related factor eukaryotic translation initiation factor 2-α (*eIF-2-α*), which activates ATF4 signaling, revealed enhancing properties in regard to the BACE-1 promoter (53). Sp1 and YY-1, as well as ATF4, were reidentified in our screening approach as BACE-1-promoter stimuli (2.5-fold induction by YY-1; 3.4 fold induction for SP1, data not shown explicitly), verifying the approach we used.

While other stress mediators, such as p53, HSF1, or ATF4, resulted in shifting the ratio in favor of BACE-1, we identified XBP-1 as a selective inducer of ADAM10 transcriptional activity. This effect was reproducible in another neuronal cell line (IMR-32), whereas the XBP-1-mediated increase in ADAM10-promoter activity was not present in the human astroglioma cell line U373. The difference in the observed effect size between both neuroblastoma cell lines (SH-SY5Y: 4.2-fold; IMR-32: 1.7-fold) might be caused by using different neuronal cell types (SH-SY5Y: neuronal-type; SKNMC: intermediate type). These findings might indicate a neuron-specific regulation of ADAM10 by active XBP-1 but have to be elucidated further.

A genome-wide approach to identify targets of XBP-1 in myotubular, plasma, and pancreatic cells revealed that XBP-1 is able to bind the promoters of several genes involved in APP trafficking and processing, such as *nicastrin* or *presenilin 1* (*PSEN1*) (38). XBP-1 has a relatively high expression in the human adult brain, as shown by EST analysis. Moreover, it has been demonstrated in mice of all developmental stages to be expressed prominently in the hippocampus (54), a region with high vulnerability in AD progression in humans. In addition, synthesis of active s XBP-1 has been shown to be induced by brain-derived neurotrophic factor (BDNF) in neurons and to contribute to neurite outgrowth (54), albeit the molecular downstream, targets of neuronal XBP-1 signaling have not been investigated in detail. We show here that ADAM10-promoter activity and mRNA synthesis are induced by active s XBP-1 in a time-dependent manner. These results were consolidated by significant increase of both the proform and mature form of ADAM10 protein on s XBP-1 overexpression, whereas ADAM17 protein levels remained unaffected. As a consequence, the secretion of the ADAM10-dependent APP proteolysis product APPs-α together with enzyme activity was significantly increased in XBP-1-overexpressing cells. However, measurement of secreted Aβ levels showed only a slight tendency of decrease, which did not reach statistical significance ($P=0.09$). This might be caused by a regulating effect of active XBP-1 on components of γ-secretase complex, such as PSEN1 (38). Nevertheless, analysis of APP protein levels in s XBP-1 overexpressing cells revealed that increased APPs-α release is not due to elevated APP protein expression but rather is derived from regulation of α-secretase. Chemically evoked ER stress mimicked the effect of s XBP-1 on the transcription of the α-secretase ADAM10. The up-regulation of *ADAM10* gene expression was specifically blocked by an IRE1-α inhibitor, as well as an XBP-1-targeting siRNA.

Interestingly, u XBP-1 and an unsplicable mutant had a weak but statistically significant enhancing effect on the ADAM10-promoter activity, too. u XBP-1 signal transduction has been suggested as a negative regulator of UPR signaling (30, 55, 56). When we titrated s with u XBP-1, we observed a similar result as obtained for titration with empty vector, meaning that u XBP-1 has no negative effect on transcriptional activity of ADAM10. Tirosh *et al.* (57) reported that the expression of a specific target of XBP-1, ER-localized DnaJ (Erdj4), was fully restored by reconstitution of XBP-1-knockout mouse embryonic fibroblasts with WT XBP-1, and stabilized u XBP-1 accounts for the transcription of most of the 324 constitutive UPR targets (58). This indicates that u XBP-1 might contribute to target gene expression under certain circumstances. u XBP-1 protein and, in particular, its hydrophobic region are involved in the anchoring of its own mRNA to the ER membrane (59). As a result, the pre-mRNA can be

spliced considerably more easily, leading to a higher amount of transcriptionally active XBP-1, which might be a very rapid response to ER stress. This could explain the slight increase of ADAM10 transcriptional activity by overexpressing the u XBP-1 and even the unspliceable construct in our experiments.

Four potential XBP-1 binding sites were identified within the human ADAM10-promoter sequence (2 UPREs, 1 ERSE II-like, and 1 ERSE-like; see Table 1). By deletion of the half site of the UPRE located at −308 bp in the core promoter sequence of *ADAM10*, we were able to exclude a possible contribution of this binding site. Furthermore, we were able to identify 2 potential responsive elements (UPRE at −626 bp and ERSE-like at −464 bp) potentially playing a role in mediating the XBP-1-specific effect on ADAM10 transcriptional activation by analyzing reporter constructs with truncated forms of the *ADAM10*-promoter sequence. EMSA confirmed that the ERSE-like sequence within the human *ADAM10* promoter is occasionally involved in binding a protein derived from s XBP-1-overexpressing HEK 293 nuclear fractions. The ERSE site has the conserved consensus sequence CCAAT-N_9-CCACG, and the spacing of 9 nt has been reported to be mandatory for activation by ATF6 and NF-Y (29). Recently, a novel ERSE sequence has been reported, which is regulated by XBP-1 and comprises a spacing of 26 nt between binding responsive elements CCAAT and CCACG (60). Therefore, although the ERSE-like sequence within the ADAM10 promoter is lacking 8 bp from the usual spacer, it might be responsible for the s XBP-1-specific effect on *ADAM10* gene expression.

Our finding that ADAM10 is targeted by s XBP-1 signaling is consistent with the reported decrease in production of Aβ peptides under ER stress (61) and the enhanced amounts of α-secretase-derived C83 membrane stub of APP (62). It has been shown that binding of LPS to TLR4 triggers XBP-1 splicing (40); however, this does not lead to typical target gene activation within ER-stress signaling but induces cytokine production in macrophages (63). In this concern, it is of note that LPS did not lead to enhanced *ADAM10* gene expression in monocyte precursors, although we were able to detect s XBP-1. These results are consistent with the finding that overnight incubation of primary human keratinocytes with LPS also resulted in unchanged ADAM10 mRNA levels (64).

Another pathway that interferes with the transcriptional enhancer function of s XBP-1 is the insulin signaling cascade; binding of insulin to its receptor leads to the formation of a XBP-1/p85 complex, which facilitates entry into the nuclear compartment and therefore increases the transcription of XBP-1 target genes (65, 66). In addition, insulin enhances XBP-1 expression by induction of transient ER stress (65). By a combinatory treatment of neuronal cells with insulin and s XBP-1 overexpression, we identified a synergistic effect of both on *ADAM10* gene expression. This is of special interest, because type 2 diabetes mellitus (T2DM) has been defined as a risk factor for developing AD (2, 67). Insulin as well as insulin-like growth factor 1 (IGF-1) resistance and insulin receptor substrate 1 (IRS-1) deregulation were demonstrated in AD brains (1). Aβ itself was recently shown to inhibit the physiological phosphorylation of IRS-1 and therefore to impair insulin signaling (68). The up-regulation of ADAM10 by XBP-1 in the context of insulin signaling might therefore represent a physiological response to transient stress situations integrated into induction of ER capacity enlargement (reviewed in ref. 41).

It has been reported that the neurotoxic Aβ peptides activate ER-stress response *via* active s XBP-1, which facilitates neuroprotective effects in transgenic flies and cultured neurons (69). The protective nature of s XBP-1 in these models is due to the prevention of calcium accumulation in the cytosol. In general, the ER-stress response is activated to protect the neuron from damage by a disturbed cellular homeostasis (70). Our results indicate that at early points of pathological changes, s XBP-1 levels were significantly increased in the brain of 2 different transgenic mouse lines (APP/PS1 and 5xFAD) in comparison to WT mice. This, in consequence, was accompanied by increased ADAM10 mRNA and might indicate a functional interplay of XBP-1-mediated signaling with the α-secretase at an early stage of the disease. In contrast, we observed in a prolonged stage of AD-like pathology (mice at 9 mo of age), that s XBP-1 level was significantly decreased as compared with nontransgenic littermates. This consequently led to a return of ADAM10 expression to basal levels in APP/PS1 mice, whereas ADAM10 amounts were even decreased in the 5xFAD mouse line. These findings are consistent with an activation of the UPR as an early event regarding neurodegenerative processes, as depicted in human postmortem brain tissue (reviewed in ref. 71). In addition, we analyzed ADAM17 mRNA amounts in mouse brain; ADAM17 expression partially mimicked the expression of ADAM10, at least in 5xFAD mice at 1 mo of age. This might be caused by other regulatory factors within this mouse model, which influence the amount of ADAM17. For example, it has been previously reported that induction of ADAM17 is regulated by the ATF4, which belongs to one of the 3 ER-stress pathways but different from XBP-1 pathway (72). Data obtained from cell culture experiments indicate that ADAM17 is at least not regulated by s XBP-1. The changes obtained for s XBP-1 levels were paralleled by changes in IRE1-α mRNA levels in total mouse brain. It is noteworthy that examination of IRE1-α mRNA level is no direct indicator for enzyme activity even if a feedback mechanism exists whereby IRE1-α cleaves its own mRNA (73). Nevertheless, in 5xFAD mice, quantitation of phospho-IRE1-α directly mirrored the amount of its target s XBP-1.

Pronounced and sustained activation of stress signals in the brain in patients with AD has been reported. Concerning ER stress, it has been noted that intraneuronal Aβ oligomers cause cell death *via* ER-stress induction (74) and that ER-stress-induced apoptosis is potentiated by the intracellular soluble domain of APP (75).

Moreover, it has been reported that the ER-stress-related enzyme protein disulfide isomerase (PDI) is upregulated in patients with patients (76). It has been previously reported that the α-secretase ADAM10 is decreased in its expression and activity in patients with AD (11, 45). Coincident with this, we obtained a decreased amount of ADAM10 mRNA in human temporal and frontal cortex tissue from patients with AD, while ADAM17 expression was not affected. To investigate the role of XBP-1 signaling in the brain in dementia, we analyzed cortical mRNA samples of patients with AD in comparison to healthy control subjects; the effect of s XBP-1 on the human *ADAM10* promoter revealed from cell culture experiments was consolidated by a moderate correlation of s XBP-1 and IRE1-α mRNA with ADAM10 mRNA in the AD samples. For healthy controls, only a weak correlation of IRE1-α and ADAM10 mRNA was observed. We suggest that in dementia, ER stress in the brain is pathologically increased and the correlation is strengthened.

This coincides with the strong up-regulation of IRE1-α expression we obtained in frontal and temporal cortex for AD samples as compared with age-matched healthy control samples. Nevertheless, the relative amount of active XBP-1 is rather decreased in both tissue types in patients with AD in comparison to healthy subjects. This result obtained from human brain samples is in accordance with our results obtained from samples of old mice with prolonged disease-like pathology. Obviously, despite up-regulation of IRE1-α expression, the pathologically disturbed brain is no more able to respond appropriately to ER stress. It has been reported that prolonged ER stress leads to a counterregulation of XBP-1 splicing (77), resulting in a diminution of s XBP-1 production and a decrease in target gene expression. This consequently leads to induction of apoptotic cell death (reviewed in ref. 78) instead of protection from stress-mediated triggers such as Aβ peptides.

It is of great interest that recently a C/G polymorphism at position −116 of the *XBP-1* promoter has been identified, which shifts the consensus motif ACGT to AGGT. This consequently results in an aberrant transcriptional activity and in reduced XBP-1 expres-

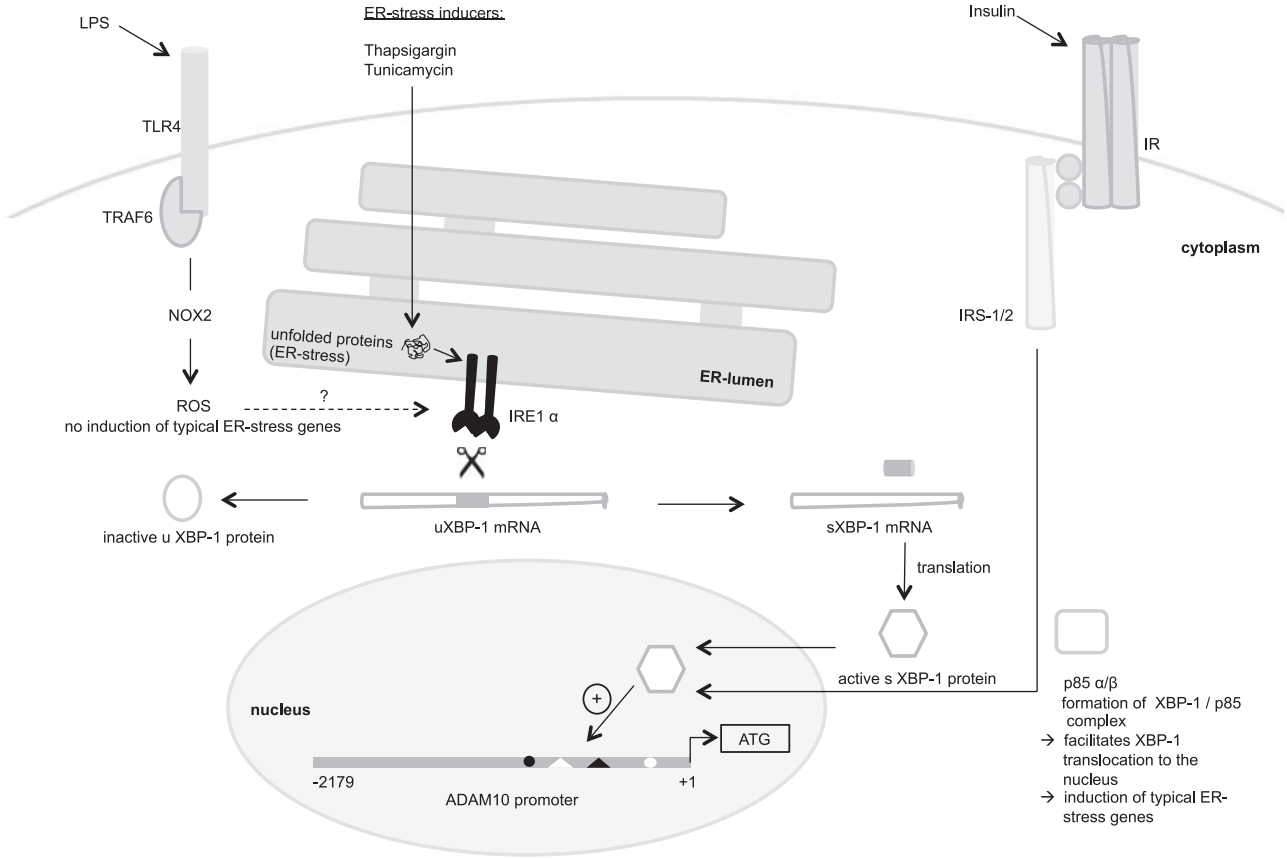

Figure 10. Schematic view of ADAM10-promoter activation by XBP-1. During ER stress, the occurrence of unfolded proteins in the ER lumen activates IRE1-α, thus catalyzing the unconventional splicing of u XBP-1 by removing a 26-nt intron. The resulting mRNA is translated into the active protein, which possesses transcriptional activity. Besides known target genes coding for ERAD proteins, we here report a yet unidentified target, ADAM10, which has a protective capability with regard to AD. We identified 2 potential binding sites (marked in black) probably playing a role in promoter activation by s XBP-1. LPS can mediate the formation of active XBP-1 *via* TLR4, TRAF6, NOX2, and ROS, which finally activate IRE1-α. However, the LPS-dependent pathway does not lead to the up-regulation of ADAM10 gene expression within the typical XBP-1 pathway. Insulin-dependent signaling promotes the formation of an s XBP-1/p85 complex, which facilitates nucleus import of s XBP-1. Consistent with this, insulin-triggered signaling is able to augment the effect of s XBP-1 on the human ADAM10 promoter.

sion (79). A recent publication by Liu *et al.* (80) reported an increased susceptibility for development of AD for carriers of the −116 C/G polymorphism in a Chinese population cohort. Cellular and animal models of other diseases evoked by amyloidogenic processes, such as Huntington's disease or Parkinson's disease (PD) have also been associated with activation of XBP-1 signaling (81–83). Sado *et al.* (84) demonstrated a protective effect of XBP-1 activation against PD-related insults.

In summary, our data demonstrate reliability of our newly applied dual-promoter reporter assay by recapitulation of already known regulators. In addition, we were able to identify XBP-1 as a physiological relevant TF by insulin-driven synergistic coregulation of the ADAM10-promoter activity *in vitro* (see Fig. 10) and by correlation of ADAM10 mRNA with components of XBP-1 signaling in human cortical tissue. We suggest that ER-stress-induced generation of s XBP-1, probably at early pathological stages, results in a short-term up-regulation of ADAM10. This might be interpreted as an attempt to counterbalance deregulation of APP processing, as Aβ peptides are one trigger of the UPR (74, 85). In future studies, it might be interesting to analyze patients with mild cognitive impairment for XBP-1 metabolism with regard to regulation of ADAM10. At this early stage of cognitive deficits and potential conversion to AD, an up-regulation of s XBP-1 and, consequently, ADAM10 would represent a possible protective mechanism that might delay disease. Integration of data obtained by our dual-promoter assay with bioinformatics resources and further evaluation of single identified TFs will help to understand what might lead to loss of proteolytic homeostasis in AD. Whether our findings open up a novel therapeutic strategy in AD needs further investigation due to concerted up-regulation of APP or other components of APP processing and trafficking. FJ

This work was supported by the German Federal Ministry of Education and Research (BMBF) in the framework of the National Genome Research Network (NGFN) and FKZ01GS08130, 01GS08125, and 01GS08129-5. The authors kindly thank C. Haass (Ludwig Maximilian University, Munich, Germany) for providing APP antibody 6687 and C. Pietrzik (Johannes Gutenberg University Mainz, Mainz, Germany) for putting 5xFAD brain samples at their disposal. Author contributions: K.E. conceived the project and wrote the manuscript; S.R. performed cell culture experiments and analysis of mouse tissue and *in vitro* studies, analyzed the data, wrote the manuscript, and prepared the figures; M.G., T.H., and M.R. coordinated and designed the experiments with human samples; S.G. performed experiments with human samples and the fluorescent enzyme assay; S.G. and M.G. analyzed the respective data; F.S. and R.P. provided a critical evaluation of the experimental design and of the manuscript. The authors declare no conflicts of interest.

REFERENCES

1. Talbot, K., Wang, H. Y., Kazi, H., Han, L. Y., Bakshi, K. P., Stucky, A., Fuino, R. L., Kawaguchi, K. R., Samoyedny, A. J., Wilson, R. S., Arvanitakis, Z., Schneider, J. A., Wolf, B. A., Bennett, D. A., Trojanowski, J. Q., and Arnold, S. E. (2012) Demonstrated brain insulin resistance in Alzheimer's disease patients is associated with IGF-1 resistance, IRS-1 dysregulation, and cognitive decline. *J. Clin. Invest.* **122,** 1316–1338
2. De la Monte, S. M. (2012) Brain insulin resistance and deficiency as therapeutic targets in Alzheimer's disease. *Curr. Alzheimer Res.* **9,** 35–66
3. Benilova, I., Karran, E., and De Strooper, B. (2012) The toxic Abeta oligomer and Alzheimer's disease: an emperor in need of clothes. *Nat. Neurosci.* **15,** 349–357
4. Postina, R., Schroeder, A., Dewachter, I., Bohl, J., Schmitt, U., Kojro, E., Prinzen, C., Endres, K., Hiemke, C., Blessing, M., Flamez, P., Dequenne, A., Godaux, E., Van Leuven, F., and Fahrenholz, F. (2004) A disintegrin-metalloproteinase prevents amyloid plaque formation and hippocampal defects in an Alzheimer disease mouse model. *J. Clin. Invest.* **113,** 1456–1464
5. Kuhn, P. H., Wang, H., Dislich, B., Colombo, A., Zeitschel, U., Ellwart, J. W., Kremmer, E., Rossner, S., and Lichtenthaler, S. F. (2010) ADAM10 is the physiologically relevant, constitutive alpha-secretase of the amyloid precursor protein in primary neurons. *EMBO J.* **29,** 3020–3032
6. Jorissen, E., Prox, J., Bernreuther, C., Weber, S., Schwanbeck, R., Serneels, L., Snellinx, A., Craessaerts, K., Thathiah, A., Tesseur, I., Bartsch, U., Weskamp, G., Blobel, C. P., Glatzel, M., De Strooper, B., and Saftig, P. (2010) The disintegrin/metalloproteinase ADAM10 is essential for the establishment of the brain cortex. *J. Neurosci.* **30,** 4833–4844
7. Ozmen, L., Woolley, M., Albientz, A., Miss, M. T., Nelboeck, P., Malherbe, P., Czech, C., Gruninger-Leitch, F., Brockhaus, M., Ballard, T., and Jacobsen, H. (2005) BACE/APPV717F double-transgenic mice develop cerebral amyloidosis and inflammation. *Neurodegener. Dis.* **2,** 284–298
8. Mohajeri, M. H., Saini, K. D., and Nitsch, R. M. (2004) Transgenic BACE expression in mouse neurons accelerates amyloid plaque pathology. *J. Neural. Transm.* **111,** 413–425
9. Li, R., Lindholm, K., Yang, L. B., Yue, X., Citron, M., Yan, R., Beach, T., Sue, L., Sabbagh, M., Cai, H., Wong, P., Price, D., and Shen, Y. (2004) Amyloid beta peptide load is correlated with increased beta-secretase activity in sporadic Alzheimer's disease patients. *Proc. Natl. Acad. Sci. U. S. A.* **101,** 3632–3637
10. Endres, K., and Fahrenholz, F. (2012) Regulation of alpha-secretase ADAM10 expression and activity. *Exp. Brain Res.* **217,** 343–352
11. Bernstein, H. G., Bukowska, A., Krell, D., Bogerts, B., Ansorge, S., and Lendeckel, U. (2003) Comparative localization of ADAMs 10 and 15 in human cerebral cortex normal aging, Alzheimer disease and Down syndrome. *J. Neurocytol.* **32,** 153–160
12. Colciaghi, F., Borroni, B., Pastorino, L., Marcello, E., Zimmermann, M., Cattabeni, F., Padovani, A., and Di Luca, M. (2002) α-Secretase ADAM10 as well as αAPPs is reduced in platelets and CSF of Alzheimer disease patients. *Mol. Med.* **8,** 67–74
13. Olsson, A., Höglund, K., Sjögren, M., Andreasen, N., Minthon, L., Lannfelt, L., Buerger, K., Möller, H. J., Hampel, H., Davidsson, P., and Blennow, K. (2003) Measurement of alpha- and beta-secretase cleaved amyloid precursor protein in cerebrospinal fluid from Alzheimer patients. *Exp. Neurol.* **183,** 74–80
14. Fellgiebel, A., Kojro, E., Müller, M. J., Scheurich, A., Schmidt, L. G., and Fahrenholz, F. (2009) CSF APPs alpha and phosphorylated tau protein levels in mild cognitive impairment and dementia of Alzheimer's type. *J. Geriatr. Psychiatry Neurol.* **22,** 3–9
15. Augustin, R., Lichtenthaler, S. F., Greeff, M., Hansen, J., Wurst, W., and Trümbach, D. (2011) Bioinformatics identification of modules of transcription factor binding sites in Alzheimer's disease-related genes by in silico promoter analysis and microarrays. *Int. J. Alzheimers Dis.* **2011,** 154325
16. Bernales, S., Soto, M. M., and McCullagh, E. (2012) Unfolded protein stress in the endoplasmic reticulum and mitochondria: a role in neurodegeneration. *Front. Aging Neurosci.* **4,** 5
17. Prinzen, C., Müller, U., Endres, K., Fahrenholz, F., and Postina, R. (2005) Genomic structure and functional characterization of the human ADAM10 promoter. *FASEB J.* **19,** 1522–1524
18. Wang, Y., Shen, J., Arenzana, N., Tirasophon, W., Kaufman, R. J., and Prywes, R. (2000) Activation of ATF6 and an ATF6 DNA binding site by the endoplasmic reticulum stress response. *J. Biol. Chem.* **275,** 27013–27020

19. Christensen, M. A., Zhou, W., Qing, H., Lehman, A., Philipsen, S., and Song, W. (2004) Transcriptional regulation of BACE1, the beta-amyloid precursor protein beta-secretase, by Sp1. *Mol. Cell. Biol.* **24,** 865–874
20. Lahiri, D. K., and Ge, Y. W. (2004) Role of the APP promoter in Alzheimer's disease: cell type-specific expression of the beta-amyloid precursor protein. *Ann. N. Y. Acad. Sci.* **1030,** 310–316
21. Nagashima, Y., Mishiba, K., Suzuki, E., Shimada, Y., Iwata, Y., and Koizumi, N. (2011) Arabidopsis IRE1 catalyses unconventional splicing of bZIP60 mRNA to produce the active transcription factor. *Sci. Rep.* **1,** 29
22. Steiner, H., Kostka, M., Romig, H., Basset, G., Pesold, B., Hardy, J., Capell, A., Meyn, L., Grim, M. L., Baumeister, R., Fechteler, K., and Haass, C. (2000) Glycine 384 is required for presenilin-1 function and is conserved in bacterial polytopic aspartyl proteases. *Nat. Cell Biol.* **2,** 848–851
23. Grimm, M. O., Haupenthal, V. J., Rothhaar, T. L., Zimmer, V. C., Grösgen, S., Hundsdörfer, B., Lehmann, J., Grimm, H. S., and Hartmann, T. (2013) Effect of different phospholipids on alpha-secretase activity in the non-amyloidogenic pathway of Alzheimer's disease. *Int. J. Mol. Sci.* **14,** 5879–5898
24. Qi, L., Yang, L., and Chen, H. (2011) Detecting and quantitating physiological endoplasmic reticulum stress. *Methods Enzymol.* **490,** 137–146
25. Grimm, M. O., Grösgen, S., Rothhaar, T. L., Burg, V. K., Hundsdörfer, B., Haupenthal, V. J., Friess, P., Müller, U., Fassbender, K., Riemenschneider, M., Grimm, H. S., and Hartmann, T. (2011) Intracellular APP domain regulates serine-palmitoyl-CoA transferase expression and is affected in Alzheimer's disease. *Int. J. Alzheimers Dis.* **2011,** 695413
26. Livak, K. J., and Schmittgen, T. D. (2001) Analysis of relative gene expression data using real-time quantitative PCR and the 2[-Delta Delta C(T)] method. *Methods* **25,** 402–408
27. Schröder, M., and Kaufman, R. J. (2005) The mammalian unfolded protein response. *Annu. Rev. Biochem.* **74,** 739–789
28. Calfon, M., Zeng, H., Urano, F., Till, J. H., Hubbard, S. R., Harding, H. P., Clark, S. G., and Ron, D. (2002) IRE1 couples endoplasmic reticulum load to secretory capacity by processing the XBP-1 mRNA. *Nature* **415,** 92–96
29. Yoshida, H., Matsui, T., Yamamoto, A., Okada, T., and Mori, K. (2001) XBP1 mRNA is induced by ATF6 and spliced by IRE1 in response to ER stress to produce a highly active transcription factor. *Cell* **107,** 881–891
30. Yoshida, H., Oku, M., Suzuki, M., and Mori, K. (2006) pXBP1(U) encoded in XBP1 pre-mRNA negatively regulates unfolded protein response activator pXBP1(S) in mammalian ER stress response. *J. Cell Biol.* **172,** 565–575
31. Endres, K., Postina, R., Schroeder, A., Mueller, U., and Fahrenholz, F. (2005) Shedding of the amyloid precursor protein-like protein APLP2 by disintegrin-metalloproteinases. *FEBS J.* **272,** 5808–5820
32. Yoshida, H., Matsui, T., Hosokawa, N., Kaufman, R. J., Nagata, K., and Mori, K. (2003) A time-dependent phase shift in the mammalian unfolded protein response. *Dev. Cell* **4,** 265–271
33. Yoshida, H., Haze, K., Yanagi, H., Yura, T., and Mori, K. (1998) Identification of the cis-acting endoplasmic reticulum stress response element responsible for transcriptional induction of mammalian glucose-regulated proteins. Involvement of basic leucine zipper transcription factors. *J. Biol. Chem.* **273,** 33741–33749
34. Roy, B., and Lee, A. S. (1999) The mammalian endoplasmic reticulum stress response element consists of an evolutionarily conserved tripartite structure and interacts with a novel stress-inducible complex. *Nucleic Acids Res.* **27,** 1437–1443
35. Kokame, K., Kato, H., and Miyata, T. (2001) Identification of ERSE-II, a new cis-acting element responsible for the ATF6-dependent mammalian unfolded protein response. *J. Biol. Chem.* **276,** 9199–9205
36. Yoshida, H., Okada, T., Haze, K., Yanagi, H., Yura, T., Negishi, M., and Mori, K. (2000) ATF6 activated by proteolysis binds in the presence of NF-Y (CBF) directly to the cis-acting element responsible for the mammalian unfolded protein response. *Mol. Cell. Biol.* **20,** 6755–6767
37. Yamamoto, K., Yoshida, H., Kokame, K., Kaufman, R. J., and Mori, K. (2004) Differential contributions of ATF6 and XBP1 to the activation of endoplasmic reticulum stress-responsive cis-acting elements ERSE, UPRE and ERSE-II. J. *Biochem.* **136,** 343–350
38. Acosta-Alvear, D., Zhou, Y., Blais, A., Tsikitis, M., Lents, N. H., Arias, C., Lennon, C. J., Kluger, Y., and Dynlacht, B. D. (2007) XBP1 controls diverse cell type- and condition-specific transcriptional regulatory networks. *Mol. Cell* **27,** 53–66
39. Lammich, S., Buell, D., Zilow, S., Ludwig, A. K., Nuscher, B., Lichtenthaler, S. F., Prinzen, C., Fahrenholz, F., and Haass, C. (2010) Expression of the anti-amyloidogenic secretase ADAM10 is suppressed by its 5′-untranslated region. *J. Biol. Chem.* **285,** 15753–15760
40. Martinon, F., Chen, X., Lee, A. H., and Glimcher, L. H. (2010) TLR activation of the transcription factor XBP1 regulates innate immune responses in macrophages. *Nat. Immunol.* **11,** 411–418
41. Ueki, K., and Kadowaki, T. (2011) The other sweet face of XBP-1. *Nat. Med.* **17,** 246–248
42. Oakley, H., Cole, S. L., Logan, S., Maus, E., Shao, P., Craft, J., Guillozet-Bongaarts, A., Ohno, M., Disterhoft, J., Van Eldik, L., Berry, R., and Vassar, R. (2006) Intraneuronal beta-amyloid aggregates, neurodegeneration, and neuron loss in transgenic mice with five familial Alzheimer's disease mutations: potential factors in amyloid plaque formation. *J. Neurosci.* **26,** 10129–10140
43. Radde, R., Bolmont, T., Kaeser, S. A., Coomaraswamy, J., Lindau, D., Stoltze, L., Calhoun, M. E., Jäggi, F., Wolburg, H., Gengler, S., Haass, C., Ghetti, B., Czech, C., Hölscher, C., Mathews, P. M., and Jucker, M. (2006) Abeta42-driven cerebral amyloidosis in transgenic mice reveals early and robust pathology. *EMBO Rep.* **7,** 940–946
44. Duyckaerts, C., Potier, M. C., and Delatour, B. (2008) Alzheimer disease models and human neuropathology: similarities and differences. *Acta Neuropathol.* **115,** 5–38
45. Marcinkiewicz, M., and Seidah, N. G. (2000) Coordinated expression of beta-amyloid precursor protein and the putative beta-secretase BACE and alpha-secretase ADAM10 in mouse and human brain. *J. Neurochem.* **75,** 2133–2143
46. Hébert, S. S., Horré, K., Nicolaï, L., Papadopoulou, A. S., Mandemakers, W., Silahtaroglu, A. N., Kauppinen, S., Delacourte, A., and De Strooper, B. (2008) Loss of microRNA cluster miR-29a/b-1 in sporadic Alzheimer's disease correlates with increased BACE1/beta-secretase expression. *Proc. Natl. Acad. Sci. U. S. A.* **105,** 6415–6420
47. Boissonneault, V., Plante, I., Rivest, S., and Provost, P. (2009) MicroRNA-298 and microRNA-328 regulate expression of mouse beta-amyloid precursor protein-converting enzyme 1. *J. Biol. Chem.* **284,** 1971–1981
48. Augustin, R., Endres, K., Reinhardt, S., Kuhn, P. H., Lichtenthaler, S. F., Hansen, J., Wurst, W., and Trümbach, D. (2012) Computational identification and experimental validation of microRNAs binding to the Alzheimerrelated gene ADAM10. *BMC Med. Genet.* **13,** 35
49. Bai, S., Nasser, M. W., Wang, B., Hsu, S. H., Datta, J., Kutay, H., Yadav, A., Nuovo, G., Kumar, P., and Ghoshal, K. (2009) MicroRNA-122 inhibits tumorigenic properties of hepatocellular carcinoma cells and sensitizes these cells to sorafenib. *J. Biol. Chem.* **284,** 32015–32027
50. Mihailovich, M., Thermann, R., Grohovaz, F., Hentze, M. W., and Zacchetti, D. (2007) Complex translational regulation of BACE1 involves upstream AUGs and stimulatory elements within the 5′ untranslated region. *Nucleic Acids Res.* **35,** 2975–2985
51. Tippmann, F., Hundt, J., Schneider, A., Endres, K., and Fahrenholz, F. (2009) Up-regulation of the alpha-secretase ADAM10 by retinoic acid receptors and acitretin. *FASEB J.* **23,** 1643–1654
52. Nowak, K., Lange-Dohna, C., Zeitschel, U., Günther, A., Lüscher, B., Robitzki, A., Perez-Polo, R., and Rossner, S. (2006) The transcription factor Yin Yang 1 is an activator of BACE1 expression. *J. Neurochem.* **96,** 1696–1707
53. O'Connor, T., Sadleir, K. R., Maus, E., Velliquette, R. A., Zhao, J., Cole, S. L., Eimer, W. A., Hitt, B., Bembinster, L. A., Lammich, S., Lichtenthaler, S. F., Hébert, S. S., De Strooper, B., Haass, C., Bennett, D. A., and Vassar, R. (2008) Phosphorylation of the translation initiation factor eIF2alpha increases BACE1 levels and promotes amyloidogenesis. *Neuron* **60,** 988–1009
54. Hayashi, A., Kasahara, T., Iwamoto, K., Ishiwata, M., Kametani, M., Kakiuchi, C., Furuichi, T., and Kato, T. (2007) The role of

brain-derived neurotrophic factor (BDNF)-induced XBP1 splicing during brain development. *J. Biol. Chem.* **282,** 34525–34534
55. Lee, A. H., Iwakoshi, N. N., and Glimcher, L. H. (2003) XBP-1 regulates a subset of endoplasmic reticulum resident chaperone genes in the unfolded protein response. *Mol. Cell. Biol.* **23,** 7448–7459
56. Guo, F., Lin, E. A., Liu, P., Lin, J., and Liu, C. (2010) XBP1U inhibits the XBP1S-mediated upregulation of the iNOS gene expression in mammalian ER stress response. *Cell. Signal.* **22,** 1818–1828
57. Tirosh, B., Iwakoshi, N. N., Glimcher, L. H., and Ploegh, H. L. (2006) Rapid turnover of unspliced Xbp-1 as a factor that modulates the unfolded protein response. *J. Biol. Chem.* **281,** 5852–5860
58. Shen, X., Ellis, R. E., Sakaki, K., and Kaufman, R. J. (2005) Genetic interactions due to constitutive and inducible gene regulation mediated by the unfolded protein response in *C. elegans*. *PLoS Genet.* **1,** e37
59. Yanagitani, K., Imagawa, Y., Iwawaki, T., Hosoda, A., Saito, M., Kimata, Y., and Kohno, K. (2009) Cotranslational targeting of XBP1 protein to the membrane promotes cytoplasmic splicing of its own mRNA. *Mol. Cell* **34,** 191–200
60. Misiewicz, M., Dery, M. A., Foveau, B., Jodoin, J., Ruths, D., and Leblanc, A. C. (2013) Identification of a novel endoplasmic reticulum stress response element regulated by XBP1. *J. Biol. Chem.* **288,** 20378–20391
61. Kaneko, M., Koike, H., Saito, R., Kitamura, Y., Okuma, Y., and Nomura, Y. (2010) Loss of HRD1-mediated protein degradation causes amyloid precursor protein accumulation and amyloid-beta generation. *J. Neurosci.* **30,** 3924–3932
62. Takahashi, K., Niidome, T., Akaike, A., Kihara, T., and Sugimoto, H. (2009) Amyloid precursor protein promotes endoplasmic reticulum stress-induced cell death via C/EBP homologous protein-mediated pathway. *J. Neurochem.* **109,** 1324–1337
63. Zeng, L., Liu, Y. P., Sha, H., Chen, H., Qi, L., and Smith, J. A. (2010) XBP-1 couples endoplasmic reticulum stress to augmented IFN-beta induction via a cis-acting enhancer in macrophages. *J. Immunol.* **185,** 2324–2330
64. Maretzky, T., Scholz, F., Köten, B., Proksch, E., Saftig, P., and Reiss, K. (2008) ADAM10-mediated E-cadherin release is regulated by proinflammatory cytokines and modulates keratinocyte cohesion in eczematous dermatitis. *J. Invest. Dermatol.* **128,** 1737–1746
65. Park, S. W., Zhou, Y., Lee, J., Lu, A., Sun, C., Chung, J., Ueki, K., and Ozcan, U. (2010) The regulatory subunits of PI3K, p85alpha and p85beta, interact with XBP-1 and increase its nuclear translocation. *Nat. Med.* **16,** 429–437
66. Winnay, J. N., Boucher, J., Mori, M. A., Ueki, K., and Kahn, C. R. (2010) A regulatory subunit of phosphoinositide 3-kinase increases the nuclear accumulation of X-box-binding protein-1 to modulate the unfolded protein response. *Nat. Med.* **16,** 438–445
67. Biessels, G. J., Staekenborg, S., Brunner, E., Brayne, C., and Scheltens, P. (2006) Risk of dementia in diabetes mellitus: a systematic review. *Lancet Neurol.* **5,** 64–74
68. Bomfim, T. R., Forny-Germano, L., Sathler, L. B., Brito-Moreira, J., Houzel, J. C., Decker, H., Silverman, M. A., Kazi, H., Melo, H. M., McClean, P. L., Holscher, C., Arnold, S. E., Talbot, K., Klein, W. L., Munoz, D. P., Ferreira, S. T., and De Felice, F. G. (2012) An anti-diabetes agent protects the mouse brain from defective insulin signaling caused by Alzheimer's disease- associated Abeta oligomers. *J. Clin. Invest.* **122,** 1339–1353
69. Casas-Tinto, S., Zhang, Y., Sanchez-Garcia, J., Gomez-Velazquez, M., Rincon-Limas, D. E., and Fernandez-Funez, P. (2011) The ER stress factor XBP1s prevents amyloid-beta neurotoxicity. *Hum. Mol. Genet.* **20,** 2144–2160
70. Castillo-Carranza, D. L., Zhang, Y., Guerrero-Muñoz, M. J., Kayed, R., Rincon-Limas, D. E., and Fernandez-Funez, P. (2012) Differential activation of the ER stress factor XBP1 by oligomeric assemblies. *Neurochem. Res.* **37,** 1707–1717
71. Hoozemans, J. J., van Haastert, E. S., Nijholt, D. A., Rozemuller, A. J., and Scheper, W. (2012) Activation of the unfolded protein response is an early event in Alzheimer's and Parkinson's disease. *Neurodegener. Dis.* **10,** 212–215
72. Rzymski, T., Petry, A., Kracun, D., Riess, F., Pike, L., Harris, A. L., and Gorlach, A. (2012) The unfolded protein response controls induction and activation of ADAM17/TACE by severe hypoxia and ER stress. *Oncogene* **31,** 3621–3634
73. Tirasophon, W., Lee, K., Callaghan, B., Welihinda, A., and Kaufman, R. J. (2000) The endoribonuclease activity of mammalian IRE1 autoregulates its mRNA and is required for the unfolded protein response. *Genes Dev.* **14,** 2725–2736
74. Umeda, T., Tomiyama, T., Sakama, N., Tanaka, S., Lambert, M. P., Klein, W. L., and Mori, H. (2011) Intraneuronal amyloid beta oligomers cause cell death via endoplasmic reticulum stress, endosomal/lysosomal leakage, and mitochondrial dysfunction in vivo. *J. Neurosci. Res.* **89,** 1031–1042
75. Kögel, D., Concannon, C. G., Müller, T., König, H., Bonner, C., Poeschel, S., Chang, S., Egensperger, R., and Prehn, J. H. (2012) The APP intracellular domain (AICD) potentiates ER stress-induced apoptosis. *Neurobiol. Aging* **33,** 2200–2209
76. Uehara, T., Nakamura, T., Yao, D., Shi, Z. Q., Gu, Z., Ma, Y., Masliah, E., Nomura, Y., and Lipton, S. A. (2006) S-nitrosylated protein-disulphide isomerase links protein misfolding to neurodegeneration. *Nature* **441,** 513–517
77. Lin, J. H., Li, H., Yasumura, D., Cohen, H. R., Zhang, C., Panning, B., Shokat, K. M., Lavail, M. M., and Walter, P. (2007) IRE1 signaling affects cell fate during the unfolded protein response. *Science* **318,** 944–949
78. Viana, R. J., Nunes, A. F., and Rodrigues, C. M. (2012) Endoplasmic reticulum enrollment in Alzheimer's disease. *Mol. Neurobiol.* **46,** 522–534
79. Kakiuchi, C., Iwamoto, K., Ishiwata, M., Bundo, M., Kasahara, T., Kusumi, I., Tsujita, T., Okazaki, Y., Nanko, S., Kunugi, H., Sasaki, T., and Kato, T. (2003) Impaired feedback regulation of XBP1 as a genetic risk factor for bipolar disorder. *Nat. Genet.* **35,** 171–175
80. Liu, S. Y., Wang, W., Cai, Z. Y., Yao, L. F., Chen, Z. W., Wang, C. Y., Zhao, B., and Li, K. S. (2013) Polymorphism −116C/G of human X-box-binding protein 1 promoter is associated with risk of Alzheimer's disease. *CNS Neurosci. Ther.* **19,** 229–234
81. Nishitoh, H., Matsuzawa, A., Tobiume, K., Saegusa, K., Takeda, K., Inoue, K., Hori, S., Kakizuka, A., and Ichijo, H. (2002) ASK1 is essential for endoplasmic reticulum stress-induced neuronal cell death triggered by expanded polyglutamine repeats. *Genes Dev.* **16,** 1345–1355
82. Nishitoh, H., Kadowaki, H., Nagai, A., Maruyama, T., Yokota, T., Fukutomi, H., Noguchi, T., Matsuzawa, A., Takeda, K., and Ichijo, H. (2008) ALS-linked mutant SOD1 induces ER stress- and ASK1-dependent motor neuron death by targeting Derlin-1. *Genes Dev.* **22,** 1451–1464
83. Holtz, W. A., and O'Malley, K. L. (2003) Parkinsonian mimetics induce aspects of unfolded protein response in death of dopaminergic neurons. *J. Biol. Chem.* **278,** 19367–19377
84. Sado, M., Yamasaki, Y., Iwanaga, T., Onaka, Y., Ibuki, T., Nishihara, S., Mizuguchi, H., Momota, H., Kishibuchi, R., Hashimoto, T., Wada, D., Kitagawa, H., and Watanabe, T. K. (2009) Protective effect against Parkinson's disease-related insults through the activation of XBP1. *Brain Res.* **1257,** 16–24
85. Kim, H. J., Cho, H. K., and Kwon, Y. H. (2008) Synergistic induction of ER stress by homocysteine and beta-amyloid in SH-SY5Y cells. *J. Nutr. Biochem.* **19,** 754–761

Received for publication May 21, 2013.
Accepted for publication October 15, 2013.

OPEN ACCESS Freely available online

PLOS ONE

A Novel Blood-Brain Barrier Co-Culture System for Drug Targeting of Alzheimer's Disease: Establishment by Using Acitretin as a Model Drug

Christian Freese[1]*[9], Sven Reinhardt[2,9], Gudrun Hefner[2], Ronald E. Unger[1], C. James Kirkpatrick[1], Kristina Endres[2]

1 REPAIR-lab, Institute of Pathology, University Medical Center of the Johannes Gutenberg University Mainz and European Institute of Excellence on Tissue Engineering and Regenerative Medicine, Mainz, Germany, **2** Department of Psychiatry and Psychotherapy, Medical Center of the Johannes Gutenberg University Mainz, Mainz, Germany

Abstract

In the pathogenesis of Alzheimer's disease (AD) the homeostasis of amyloid precursor protein (APP) processing in the brain is impaired. The expression of the competing proteases ADAM10 (a disintegrin and metalloproteinase 10) and BACE-1 (beta site APP cleaving enzyme 1) is shifted in favor of the A-beta generating enzyme BACE-1. Acitretin–a synthetic retinoid–e.g., has been shown to increase ADAM10 gene expression, resulting in a decreased level of A-beta peptides within the brain of AD model mice and thus is of possible value for AD therapy. A striking challenge in evaluating novel therapeutically applicable drugs is the analysis of their potential to overcome the blood-brain barrier (BBB) for central nervous system targeting. In this study, we established a novel cell-based bio-assay model to test ADAM10-inducing drugs for their ability to cross the BBB. We therefore used primary porcine brain endothelial cells (PBECs) and human neuroblastoma cells (SH-SY5Y) transfected with an ADAM10-promoter luciferase reporter vector in an indirect co-culture system. Acitretin served as a model substance that crosses the BBB and induces ADAM10 expression. We ensured that ADAM10-dependent constitutive APP metabolism in the neuronal cells was unaffected under co-cultivation conditions. Barrier properties established by PBECs were augmented by co-cultivation with SH-SY5Y cells and they remained stable during the treatment with acitretin as demonstrated by electrical resistance measurement and permeability-coefficient determination. As a consequence of transcellular acitretin transport measured by HPLC, the activity of the ADAM10-promoter reporter gene was significantly increased in co-cultured neuronal cells as compared to vehicle-treated controls. In the present study, we provide a new bio-assay system relevant for the study of drug targeting of AD. This bio-assay can easily be adapted to analyze other Alzheimer- or CNS disease-relevant targets in neuronal cells, as their therapeutical potential also depends on the ability to penetrate the BBB.

Citation: Freese C, Reinhardt S, Hefner G, Unger RE, Kirkpatrick CJ, et al. (2014) A Novel Blood-Brain Barrier Co-Culture System for Drug Targeting of Alzheimer's Disease: Establishment by Using Acitretin as a Model Drug. PLoS ONE 9(3): e91003. doi:10.1371/journal.pone.0091003

Editor: Koichi M. Iijima, National Center for Geriatrics and Gerontology, Japan

Received September 18, 2013; **Accepted** February 7, 2014; **Published** March 7, 2014

Funding: This work was supported by Federal Ministry of Education and Research (BMBF) grant (FKZ01GS08130; www.bmbf.de). The funders had no role in study design, data collection and analysis, decision to publish, or preparation of the manuscript.

Competing Interests: The authors have declared that no competing interests exist.

* E-mail: freesec@uni-mainz.de

These authors contributed equally to this work.

Introduction

Alzheimer's disease (AD) is a progressive degenerative disorder of the brain. While maximally 5% of all cases of this type of dementia are based on gene mutations [1], the cause of the sporadically occurring cases is still enigmatic. Literature suggests an involvement of processes such as impairment of the blood-brain barrier (BBB), mitochondrial dysfunction and tau-mediated destabilization of microtubules [2,3,4]. Nevertheless, deregulation of the proteolytic processing of a type I transmembrane protein – the amyloid precursor protein (APP) – has been accepted as closely correlated to AD pathology. Therefore, interference with one of the proteinases that cleave APP offers a target for therapeutic strategies (e.g. reviewed in [5,6,7]. In the non-amyloidogenic pathway the alpha-secretase ADAM10 prevents formation of toxic A-beta peptides from APP and alternatively gives rise to a neuroprotective and neurotrophic soluble fragment (APPs-alpha) [8,9,10]. We were able to demonstrate that overexpression of ADAM10 in transgenic mice [11] and acitretin-induced upregulation of ADAM10 gene expression in an AD mouse model [12] leads to a significant reduction of A-beta peptides. Acitretin is an already FDA-approved drug for treatment of psoriasis and has been shown to penetrate into the brain of rats [13]. It does not show P-glycoprotein (P-gp) substrate properties as well as favorable kinetics [14] and therefore was directly applicable for entering a clinical study in humans (NCT01078168). To evaluate novel, potent alpha-secretase enhancers it has to be guaranteed that the drug candidates can cross the BBB and that they can act on central nervous APP processing. Overall, literature is heterogeneous regarding a disturbed BBB permeability in AD pathology [15]. On one hand, microvascular injury has been correlated with progress of disease pathology (Braak stages) and ApoE genotype [16]. On

the other hand, albumin ratio (QAlb), which is an indicator of BBB function, showed no systematic differences compared within different ApoE genotype carriers [17]. However, an early treatment to prevent pathogenesis of AD is an urgent requirement for a drug with therapeutic value. A recent study of Vos and colleagues demonstrated that subjects with preclinical AD had a higher risk for development of AD [18]. Therapeutic intervention at such preclinical stages has to face the challenge of an unimpaired BBB, which basically is a tight barrier and transport of nutrients as well as drugs is highly regulated or even impaired due to cell-cell junctions and efflux transporters such as P-gp [19,20,21]. Primary *in vivo* screening processes for evaluating BBB permeability of drugs are time consuming and expensive. Thus, the establishment of *in vitro* models is under intensive investigation. A few well-characterized *in vitro* blood-brain barrier models have been described within the last years which were developed using primary endothelial cells from the brain of different species [22,23,24,25]. Isolated from rat, bos taurus or pig, and co-cultured with astrocytes, pericytes or even both cell types, brain microvascular endothelial cells were shown to form a tight barrier, generally demonstrated by high transendothelial electrical resistance (TEER) and low permeability coefficients [26,27,28,29]. In addition to primary isolated endothelial cells, immortalized cell lines such as HBMEC or hCMEC/D3 which express brain endothelial markers but exhibit lower TEER have also been used for establishment of such models [30,31,32,33]. In general, the advantages of *in vitro* models are the possibility for high throughput screening, their reproducibility and more importantly, the reduction of animal experiments.

The aim of this study was the development of a post-screening bio-assay model for analyzing the transport properties of anti-AD drug candidates. It combines an *in vitro* BBB model system and a luciferase-based reporter assay to detect drug transported across the BBB model. For this purpose, we co-cultured porcine brain endothelial cells (PBECs) on filter membranes and human neuroblastoma cells (SH-SY5Y) transfected with an ADAM10-promoter-driven reporter gene, seeded on the bottom of the basal well. To make our bio-assay system easily available to other laboratories we also investigated if the cell line hCMEC/D3 can be used as the barrier building unit in this model. To validate the functionality of our bio-assay, the potent alpha-secretase enhancer acitretin was used as a model drug because it was shown to cross the BBB in rats and mice [13,14] and to induce ADAM10 expression *in vivo* [12]. The benefit of such a co-culture system developed in this study is on the one hand the well-characterized BBB model and on the other hand the sensitive reporter gene-based detection of therapeutically active drug transported across the barrier.

Materials and Methods

Materials

Acitretin was purchased from LGC Promochem (Germany), DMSO and butylhydroxytoluol (BHT) from AppliChem (Germany).

Isolation of Porcine Brain Endothelial Cells and Cell Culture

Brain microvascular endothelial cells (PBECs) were isolated from fresh porcine using a modified protocol which was described previously for the isolation of human brain microvascular endothelial cells [34]. Brains were provided by Mr. Wohn (local butcher, Mainz, Germany) and used with his permission. The meninges were carefully removed. The grey matter tissue was minced into small pieces and digested with 0.1% collagenase type IV (Worthington, NJ, USA) and 200 µl DNase I (100 µg/mL; Sigma-Aldrich, USA) for 30 minutes at 37°C. The tissue solution was diluted with PBS containing 20% Percoll Plus (GE Healthcare, Sweden) and centrifuged at 2600 rpm at 4°C for 1 hour. The capillary fragments were washed with PBS and digested with 1 mg/mL collagenase/dispase (Roche, Germany) and 150 µl DNase I at 37°C for 10 minutes. After additional washing with PBS, the cell pellet was resuspended in PBS and loaded on a prepared Percoll gradient [34]. Finally, cells were resuspended in ECBM, supplement mix (both PromoCell, Germany), penicillin/streptomycin (10,000 U/mL/10,000 µg/mL; Gibco, Germany), 3 µg/mL puromycin (Calbiochem, Germany), and seeded on fibronectin-coated HTS Transwell-24 polyester filter membranes (0.4 µm pore size, 6.5 mm in diameter; Corning Costar, USA). Cells were sustained in medium containing 3 µg/ml puromycin for 3 days. Afterwards, medium without puromycin was used and the transendothelial electrical resistance (TEER) was measured, beginning from day 6 of preparation. Cell experiments were started at day 8 with cells which exhibited a resistance of at least 170 $\Omega \times cm^2$.

SH-SY5Y cells (neuroblastoma cell line; ATCC (Manassas, USA); # CRL-2266) were cultivated in DMEM/HamF12 medium (Gibco, Germany) supplemented with 10% FCS and 1% glutamine (both PAA, Germany). The human cerebral microvascular endothelial cell line hCMEC/D3 was kindly provided by Pierre-Olivier Couraud (Department of Cell Biology, Institut Cochin, Paris, France) [33]. hCMEC/D3 were cultivated on fibronectin-coated tissue culture flasks in ECBM, supplement mix and penicillin/streptomycin. The immortalized cell lines were passaged twice a week and maintained under standard conditions (5% CO_2, 95% humidity, 37°C).

Setup of the Co-culture Model System

hCMEC/D3 (10,000 cells/filter) were seeded on fibronectin-coated Transwell filters (Corning Costar, USA; see above) and cultured using ECBM, 15% FCS, 2.5 ng/mL basal fibroblast growth factor, 10 µg/mL sodium heparin (both Sigma-Aldrich, USA) and penicillin/streptomycin. At day 5 after seeding of hCMEC/D3, 250,000 SH-SY5Y cells were placed on the bottom of a 24-well plate compatible with the Corning Transwell filter plate using Opti-MEM (Invitrogen, Germany). For transport experiments with the test substance acitretin, SH-SY5Y cells were transfected with a human ADAM10-promoter luciferase reporter construct [12] as described in the respective section. After 5 hours the medium of SH-SY5Y cells was changed to DMEM/HamF12 medium supplemented with 10% FCS and 1% glutamine. Filters with hCMEC/D3 were put on top of the 24-well plate and cells were grown in co-culture for 2 days.

For the co-culture with PBEC, SH-SY5Y cells were seeded at day 8 after isolation of the primary cells by the same procedure as described for hCMEC/D3.

Treatment of Cells with Acitretin

The co-culture of PBEC and ADAM10-promoter reporter transfected SH-SY5Y cells was set up as described above. For the application of acitretin, 50 µl of the supernatant of the upper compartment were replaced by acitretin diluted in ECBM, 15% FCS, 2.5 ng/ml basal fibroblast growth factor, 10 µg/ml sodium heparin (both Sigma-Aldrich, USA) and penicillin/streptomycin. The final concentration of acitretin in the upper compartment was 12 µM (in whole medium volume: 2 µM) and the cells of the co-culture model were incubated for 48 hrs. Mono-cultures of PBEC were compared to the co-culture. Empty transwell filters coated

with fibronectin were used as controls in mono-cultures of SH-SY5Y cells. Dimethylsulfoxide (DMSO) served as the solvent control. TEER was measured before and after the treatment to ensure the tightness of the endothelial cell barrier. For experiments examining the cellular uptake of acitretin in brain endothelial cells, a final concentration of 2 μM acitretin was applied to the cells seeded in 24 well plates which were subsequently incubated for 48 hours.

Detection of Acitretin by HPLC

To determine acitretin concentrations in the upper and lower compartment of the Transwell system, cell supernatant was collected at the end of the incubation period. The retinoid was stabilized by addition of BHT (50 μg/ml) and quantified by HPLC as described previously [14].

Transfection and Reporter Gene Assays

Analysis of cellular uptake of acitretin into the brain endothelial cells was performed by transfection of a retinoid-response reporter with Lipofectamine LTX (Invitrogen, Germany). Briefly, 45,000 cells were seeded on 96 well plates in OptiMEM (Invitrogen, Germany) and transfected with 100 ng DR5 element reporter vector [12] using 0.5 μl transfection reagent per well as recommended by the manufacturer.

For co-culture experiments 250,000 SH-SY5Y cells were transiently transfected with 800 ng ADAM10-promoter reporter plasmid [12] in 24 well format using Lipofectamine 2000 (Invitrogen, Germany). The transfection procedure was performed as specified by the manufacturer. Cells were lysed after the incubation period with the appropriate lysis buffer (Promega, Germany) and light emission measured upon addition of luciferase substrate (Promega, Germany) using a Fluostar Omega (BMG Labtech). Protein content of the cell lysates from the reporter gene assays was determined with Nanoquant (Roth, Germany) and used for normalization of luciferase activity yielding the parameter, RLU (relative light unit).

Fluorescence Imaging of Tight Junction Proteins

After incubation, endothelial cells attached to the filter membranes were washed with PBS (Gibco, Germany) and fixed with a mixture of methanol/ethanol (2:1) at room temperature for 20 min. Cells were washed and stained with antibodies recognizing different tight junction proteins (zonula occludens protein-1, occludin (both Zymed Laboratories, CA, USA), claudin-5 (Abcam, UK)) and the corresponding secondary antibodies (Alexa fluor 546; Molecular Probes, CA, USA). All antibodies were diluted in 1% bovine serum albumin (Roth, Germany) in PBS. Nuclei were stained with Hoechst 33342 dye (Sigma-Aldrich, USA). The filter membranes were embedded with GelMount (Biomeda, Natutec, Germany) and analyzed via fluorescence microscopy (Olympus IX71 with Delta Vision system, Applied Precision, USA).

Electron Microscopy

For electron microscopy analysis PBECs cultured on filter membranes were fixed with cacodylate-buffered glutaraldehyde (pH 7.2, Serva, Germany) for 20 minutes at room temperature. This was followed by a fixation step in 1% (w/v) osmium tetroxide for 2 hours and dehydration in ethanol. Cells were transferred through propylene oxide, embedded in agar-100 resin (PLANO, Germany) and polymerized at 60°C for 24 hours. Ultrathin sections were cut with an ultramicrotome (Leica Microsystems, Germany), placed onto copper grids and analyzed with a transmission electron microscope (Jem-1400, JOEL, Japan).

Samples for scanning electron microscopy were dried after the fixation step with osmium tetroxide (Sigma-Aldrich, St. Louis, MO; USA). They were transferred to a carbon-coated metal plate, sputtered with gold and analysed with a scanning electron microscope (Zeiss, Modell DSM 962).

Histological Examination of Endothelial Cells Grown on Filter Membranes

PBECs cultured on filter membranes were fixed with 3.7% paraformaldehyde at room temperature for 15 minutes. Afterwards, cells were embedded in paraffin, thin sections were cut and stained with hematoxylin-eosin (Merck, Germany). Light microscopy was performed using a Biorevo BZ-9000 microscope (Keyence, Germany).

Western Blotting

Cells were lysed in LDS sample buffer (Invitrogen, Germany) including 100 mM dithiothreitol (Roth, Germany) and protease inhibitor mix (Roche, Germany). 20 μg proteins of whole cell lysate were separated on 10% SDS-acrylamide gels and transferred to a nitrocellulose membrane. Blots were either blocked with 5% BSA or milk powder and incubated with primary antibodies diluted in respective blocking buffer as follows: anti-APP (previously described: [35]), anti-ADAM10 (Merck, Germany), anti-GSK3-beta (Bioss, Germany), anti-Pgp (Santa Cruz, Germany) anti-Actin (Sigma, Germany), anti-P-ERK and anti-GAPDH (both: Cell Signaling, USA). Detection of APPs-alpha was performed as a dot blot with direct application of cell culture supernatant to the nitrocellulose membrane and 6E10 (Covance, Germany) as primary antibody. Blots were incubated with respective HRP-labeled secondary anti-mouse or anti-rabbit antibodies (Thermo Scientific, Germany) and GAPDH or actin were used as loading controls. Signals were detected with a CCD-camera imaging system and quantitatively analyzed with AIDA image analyzer 4.26 software (Raytest, Germany).

Toxicity Assays

To study the impact of SH-SY5Y cells on PBEC or hCMEC/D3 cells and vice versa, cells in co-culture were investigated for cell viability and activation of initiator caspases 3 and 7 using CellTiterGlo Assay and CaspaseGlo Assay (Promega, Germany) respectively, according to the manufacturer's instructions. Cell viability and cytotoxicity of PBECs after treatment with various concentrations of acitretin were assessed with CellTiter 96 Aqueous non-radioactive assay (MTS reduction assay) and CytoTox 96 non-radioactive cytotoxicity assay (lactate conversion; Promega, Germany) as recommended by the manufacturer. Untreated cells were set to 100% cell viability and cells treated with DMSO were used as control to exclude effects by the solvent. LDH-release cytotoxicity assay was performed for assessing membrane integrity and values obtained for lysed cells were set to 100%.

TEER and Permeability Analyses

Both methodologies have been described previously [36,37]. Briefly, starting at day 6 after isolation of PBEC or at day 3 after seeding of hCMEC/D3, the transendothelial electrical resistance (TEER) was measured with an EVOM voltohmmeter (WorldPrecision Instruments, Germany) equipped with a STX-2 chopstick electrode. Barrier resistance readings were obtained for each well individually calculated by subtracting the resistance of the blank filter membrane coated with fibronectin and multiplied by the membrane area (0.33 cm^2) to give ohm×cm^2.

To measure the permeability of the brain endothelial cell layer, 50 µl of the supernatant of the upper compartment was replaced by sodium fluorescein solution (Sigma Aldrich, USA) diluted in ECBM, 15% FCS, 2.5 ng/mL basal fibroblast growth factor and 10 µg/mL sodium heparin (both Sigma-Aldrich, USA), penicillin/streptomycin. Mono-cultures of PBEC were compared to the co-culture and empty transwell filters coated with fibronectin were used to determine free diffusion of sodium fluorescein through the filter membrane. Permeability coefficients (P_{app}) were calculated using the equation: $P_{app} = (1/(A \times c_0)) \times (dQ/dt)$, where A is the surface area of the filter (0.33 cm^2), c_0 the initial concentration of sodium fluorescein in the donor fluid (10 µg/mL), dQ/dt the amount of sodium fluorescein passing across the cell layer in a defined time period (3 and 24 hrs). Since the treatment with acitretin was performed for 48 hours, P_{app} for sodium fluorescein was calculated for the same time period to exclude a potential paracellular transport during longer treatment periods. 50 µl samples from the lower compartment were diluted with 1 mM NaOH and the fluorescence was measured using a multiplate reader (GeniusPuls, Tecan, Switzerland) with an excitation wavelength of $\lambda = 480$ nm and an emission wavelength of $\lambda = 535$ nm.

The permeability coefficient of acitretin was calculated as described for sodium fluorescein using the concentration of acitretin in the lower compartment determined by HPLC.

Statistical Analyses

T-test and One-way ANOVA with Bonferroni post-test analyses were performed using GraphPad Prism version 5.00 software (Prism, USA).

Results

Characterization of PBECs in the BBB Co-culture Model

The development of the co-culture model system of barrier-building brain endothelial cells with neuronal cells serving as a biological reporter system is schematically shown in Figure 1 A. We initially compared two endothelial cell types for this model: immortalized hCMEC/D3 and primary porcine brain endothelial cells (PBEC). Properties of the barrier such as electrical resistance, expression of tight junction proteins and viability were assessed in mono- as well as in co-culture with SH-SY5Y cells.

After the isolation and seeding of PBECs onto filter membranes, cells formed a dense cell layer and tight junction proteins such as occludin and claudin-5 were highly expressed, as demonstrated by fluorescent staining (Figure 1 B (a–c)). In co-culture with the human neuroblastoma cell line SH-SY5Y the morphology of the PBECs was unaltered and no negative impact regarding the expression of the tight junction proteins was observed (Figure 1 B (d–f)). Cell viability and apoptosis assays confirmed that co-cultivation of PBECs with SH-SY5Y cells did not induce cytotoxicity or the activation of initiator caspases, which might negatively influence the properties of the barrier (Figure 1 D). In contrast, co-cultivation of hCMEC/D3 with SH-SY5Y cells resulted in a significant decrease in viability of endothelial cells to 89% as compared to hCMEC/D3 in mono-culture, although caspase 3 and 7 were not activated (Figure 1 D).

Western Blot analysis indicated an unaltered expression of P-glycoprotein (P-gp), the most important efflux transporter of the BBB [38,39], in both co-culture models compared to the respective monocultures (Figure 1 E). To further characterize the endothelial cells in the co-culture model, scanning and transmission electron microscopic analyses (SEM, TEM) were performed (Figure 1 H (a–b)). Microscopic images displayed a dense monolayer and tight cell-cell contacts of PBECs grown on a filter membrane under co-culture conditions (Figure 1 H, cell-cell contacts are indicated by arrows). These results are in accordance with the strong expression of tight junction proteins as described above (Figure 1 B (a–f)). Hematoxylin-eosin (HE) staining of PBECs cross sections showed that even for a larger section of the filter membrane cells grew in a flat monolayer and continuously covered the filter membrane (Figure 1 G (a)). Although hCMEC/D3 also displayed a flat monolayer (Figure 1 G (b)), the expression of tight junction proteins was less intense and more discontinuous as compared to the primary PBECs (Figure 1 C).

The results obtained for tight junction structure are in accordance with measurement of the electrical resistance and determination of the permeability coefficients (Figure 1 F): a 20-fold higher TEER was observed for PBECs as compared to hCMEC/D3 already at the beginning of the co-cultivation with SH-SY5Y cells (day 8 and 5, respectively). hCMEC/D3 cells in general built a less dense cell layer, which was also demonstrated by the determination of the P_{app}-value for sodium-fluorescein (7.41×10^5 versus 4.3×10^4 cm/min; Figure 1 F). Co-culture of PBECs with SH-SY5Y cells further improved the barrier properties: the mean TEER of PBECs co-cultured for 48 hrs with SH-SY5Y was 331 ± 18 Ohms$\times$$cm^2$ and thus 32% higher than the resistance measured for PBECs in mono-culture at day 10 (Figure 1 F). This is in accordance with the observation that PBECs in co-culture with SH-SY5Y cells also possessed the lowest permeability coefficient after 48 hours of incubation in contrast to all other conditions (Figure 1 F).

In summary, these results demonstrate a continuous tightness and a strong integrity of the barrier generated by PBECs under co-cultivation conditions with SH-SY5Y cells. Therefore, PBECs were used for further analysis of the co-culture model.

Impact of Brain Endothelial Cells on SH-SY5Y Cell Viability and APP Metabolism

To analyze the influence of PBECs on SH-SY5Y cells under co-cultivation conditions, cell viability and potential apoptotic effects were determined. Furthermore, since the newly developed model was established for the evaluation of AD therapeutics, we had to ensure that pivotal cellular pathways, such as APP processing and AD-relevant signal transduction, were not affected by co-cultivation conditions. PBECs demonstrated no significant impact on the viability of SH-SY5Y cells after co-cultivation for 48 hours (Figure 2 A). Moreover, no induction of the initiator caspases 3 and 7 was observed in the neuronal cell line (Figure 2 A). Since glycogen synthase kinase 3-beta (GSK3- beta) is known to play a crucial role in the pathology of AD by hyperphosphorylation of tau protein [40] and by influencing the BACE1-mediated cleavage of APP [41], it is of great importance that the activity of GSK3-beta in SH-SY5Y is not altered during co-cultivation with PBECs as shown in Figure 2 B (109% compared to SH-SY5Y mono-cultures). ERK-1/−2 provide another central signaling pathway contributing to the regulation of AD-relevant proteins such as ADAM10 [42]. In our co-culture model no impact of PBECs on ERK-phosphorylation was observed (105% compared to SH-SY5Y mono-cultures, Figure 2 B). Therefore, it can be concluded that kinase activity is not altered under these conditions. Next, we showed that ADAM10 expression as well as APP expression and metabolism was not disturbed in the presence of the brain endothelial cells: SH-SY5Y cells maintained with PBECs for 48 hours neither displayed a deviating amount or maturation of ADAM10 (Figure 2 C) nor an altered APP expression. In addition, APPs-alpha secretion as well as the amount of the C-terminal

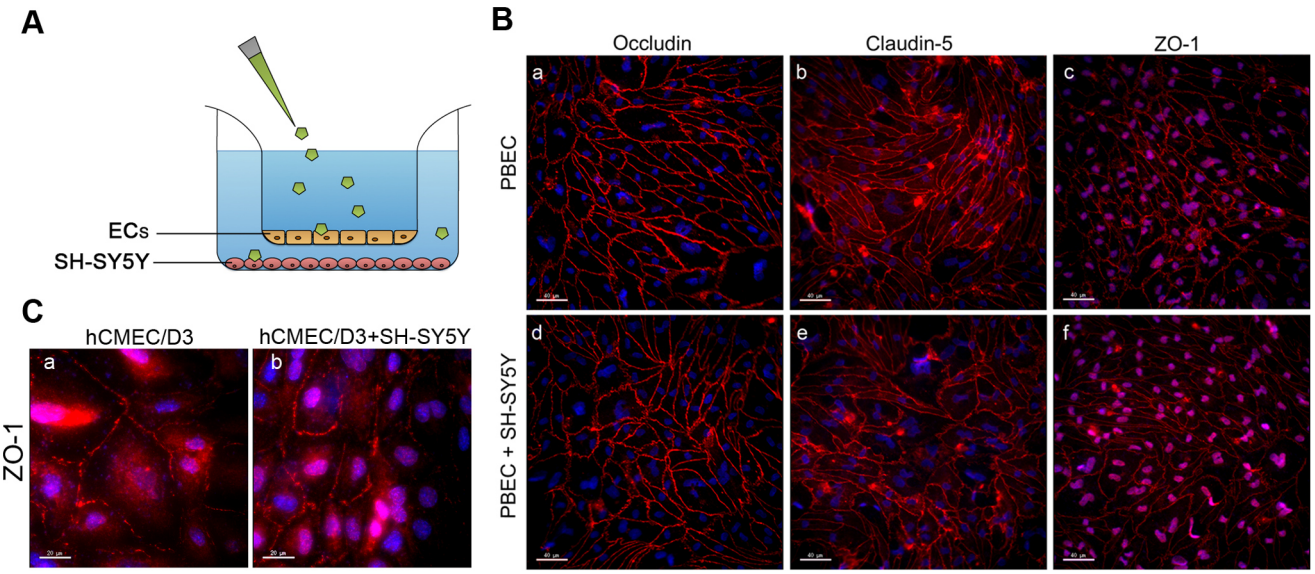

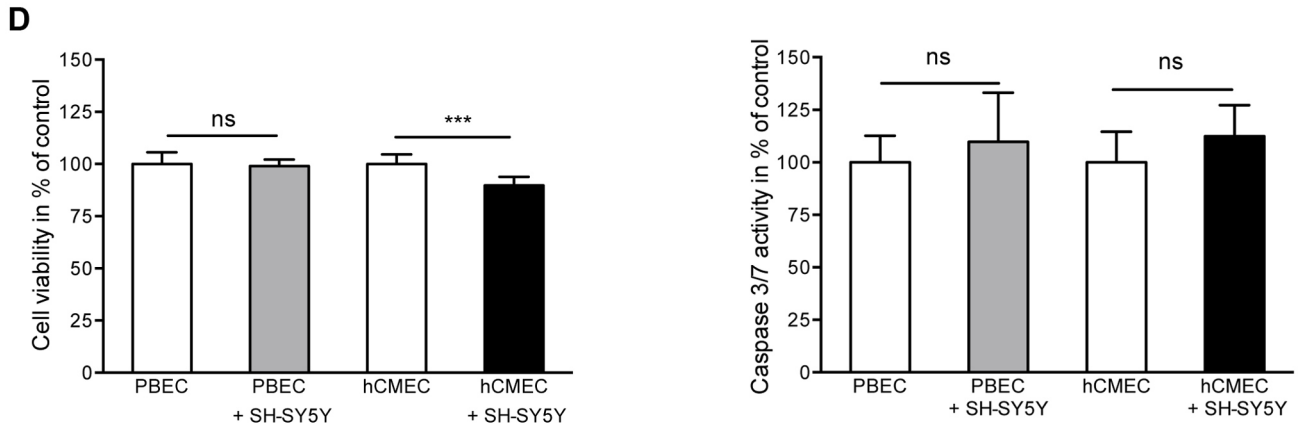

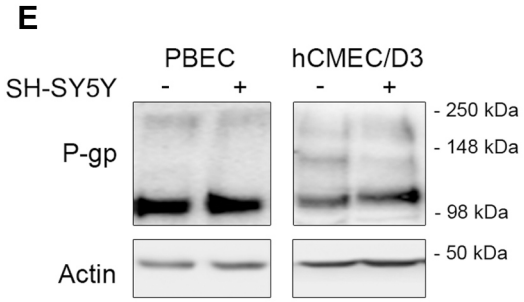

F

		PBEC		hCMEC/D3	
		x	x	x	x
TEER [Ohm x cm²]⁺	day 8	188 (± 33)	165 (± 27)	9 (± 1.4)	8 (± 0.9)
		x	SH-SY5Y	x	SH-SY5Y
	day 10	251 (± 25)	331 (± 18)	7 (± 0.5)	25 (± 18)
P_{app} NaFITC [cm x min⁻¹]*	3 hour	7.60×10^{-5}	6.10×10^{-5}	4.72×10^{-4}	1.52×10^{-4}
	48 hours	7.41×10^{-5}	5.45×10^{-5}	4.30×10^{-4}	1.53×10^{-4}

⁺ ± SEM; * filter: 9.69×10^{-4} cm x min⁻¹; x: no SH-SY5Y

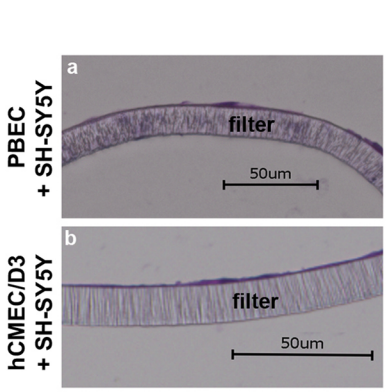

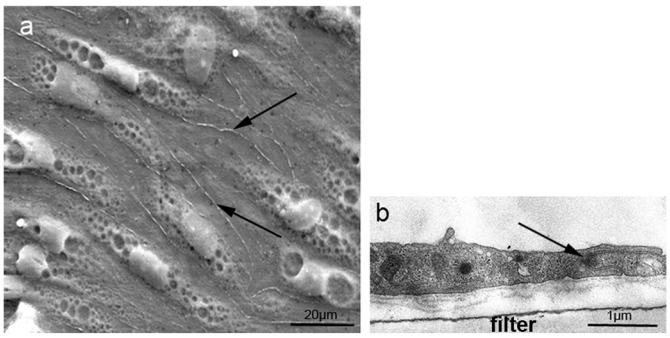

Figure 1. Characterization of the bio-assay model consisting of brain endothelial cells and SH-SY5Y cells. (A) Scheme of the developed bio-assay model system. (B) Immunofluorescence staining of different tight junction proteins expressed in PBEC mono- and co-culture with SH-SY5Y cells. Scale bars: 40 μm. (C) Immunofluorescent staining of zonula occludens protein (ZO-1) in hCMEC/D3 in mono-culture and in co-cultivation with SH-SY5Y cells. Scale bars: 20 μm. (D) Cell viability and caspase 3/7 activity of brain endothelial cells cultured with or without SH-SY5Y cells. Values obtained for mono-cultures were set to 100%, data represent mean ± standard deviation of three experiments (n ≥8; One Way Anova; Bonferroni post-test; ns: $p>0.05$; ***: $p<0.001$). (E) Western Blot analysis of P-gp expressed in brain endothelial cells in mono- and co-culture with SH-SY5Y. (F) Comparison of TEER and permeability coefficients (P_{app}) of hCMEC/D3 and PBECs grown with or without SH-SY5Y cells. At day eight SH-SY5Y cells were seeded on the bottom of the 24-well plate. P_{app} of sodium fluorescein was determined 3 hours and 48 hours after seeding of SH-SY5Y cells. (G) HE-staining of brain endothelial cell monolayers grown on top of the filter membranes. Scale bar: 50 μm. (H) Electron microscopy images (a: SEM; b: TEM) of PBEC grown on top of the filter membranes. Arrows indicate the cell-cell connections. Scale bars: 20 μm (a) and 1 μm (b).
doi:10.1371/journal.pone.0091003.g001

fragments (APP-CTFs) were comparable to the amount found in SH-SY5Y cells kept under mono-culture conditions (Figure 2 C).

The Effect of Acitretin on the BBB Built by PBECs

The aim of the developed *in vitro* BBB model was to determine if a substance with already known therapeutic potential targeting AD can overcome the barrier built by brain endothelial cells. As a model drug we used acitretin, which is known to cross the BBB *in vivo* [13,14] and has therapeutic activity by increasing the expression of the alpha-secretase ADAM10 in AD model mice [12]. To avoid misinterpretation of the *in vitro* transport data the tightness of the barrier has to be guaranteed during the treatment with acitretin. Therefore, we investigated cell viability and cytotoxicity in PBEC after treatment with different acitretin concentrations for 48 hrs. The results obtained by cytotoxicity- and LDH-assay show that acitretin did not significantly affect PBECs in any of the tested concentrations (Figure 3 A). In addition, the expression of representative tight junction proteins such as occludin and ZO-1 revealed that acitretin did not lead to a disruption of cell-cell contacts and thus the endothelial cell barrier in the co-culture model remained intact (Figure 3 B). The distinct transport mechanisms of acitretin across the BBB are not yet known. An uptake of acitretin into endothelial cells would support the assumed transcellular transport mechanism across the barrier. Thus, we transfected PBECs with a reporter plasmid containing a retinoid response element (RARE). Acitretin displaces all-trans retinoic acid from its cellular binding protein (CRABP) due to its higher affinity and therefore enhances effects based on retinoic acid receptors [43]. In response to acitretin treatment the retinoic acid-dependent expression of the reporter luciferase was increased 2-fold in PBECs compared to control cells treated with the solvent (Figure 3 C). Thus, the uptake of acitretin into PBECs was demonstrated and a potential transport across the cells can be assumed.

Transport of Acitretin Across the Endothelial Barrier and Induction of ADAM10-Promoter Activity in Neuronal Cells

It was demonstrated in the experiments described above that acitretin is internalized into the porcine brain endothelial cells and does not negatively influence properties of the cellular barrier. Next, the amount of acitretin transported across the barrier was determined by HPLC after 48 hours of incubation. In parallel, we analyzed the transport properties of sodium fluorescein during acitretin treatment and calculated both, the permeability coefficient of acitretin and sodium fluorescein. The permeability coefficient of sodium fluorescein was not affected during acitretin treatment (Figure 4 A) compared to the untreated control (Figure 1 F). Furthermore, less sodium fluorescein was transported with PBECs as compared to empty filter membranes. The data suggest that under these conditions a superficial paracellular transport can be excluded. Acitretin on the contrary was transported across the brain endothelial cell barrier. The permeability coefficient of acitretin demonstrates that the transport of acitretin across the barrier was comparable to the transport across the filter membrane without PBECs (Figure 4 A). In addition, we determined the amount of transported acitretin into the lower compartment of the transwell system by HPLC. The measured acitretin concentration of 1.77 ± 0.22 μM without endothelial cells on the filter membrane is in accordance with the theoretically obtainable concentration of 2 μM acitretin by assuming an entire substance transport. In comparison, significantly less transported acitretin was obtained in the co-culture model with endothelial cells (1.24 ± 0.29 μM, $p=0.0269$, Figure 4 A). Under these conditions, incubation with acitretin led to induction of ADAM10-promoter driven luciferase expression in SH-SY5Y cells seeded in the lower compartment of the transwell system. Elevation of promoter activity was indistinguishable from that of neuroblastoma cells cultivated without PBECs (148% versus 151%, Figure 4 B) and comparable to a promoter induction of about 150% reported previously [12].

Discussion

Alzheimer's disease (AD) is characterized histopathologically by neurofibrillary tangles, which occur intracellularly in neurons of AD-patients and by senile plaque deposits consisting mainly of A-beta peptides. The latter are generated by amyloidogenic processing of amyloid precursor protein (APP) by beta-secretase activity [44,45,46]. Alternatively APP can be cleaved by the alpha-secretase ADAM10 within the A-beta stretch, consequently preventing the release of toxic A-beta peptides [11,47]. In addition, APP processing by ADAM10 generates a neuroprotective, soluble APP-derived fragment - sAPP-alpha - which is correlated to the survival of neurons [10,48]. Thus, the induction of ADAM10 gene expression provides a promising approach in AD-therapy. The synthetic retinoid, acitretin, is capable of inducing the potentially AD-attenuating enzyme ADAM10 in neuronal cells and AD model mice [12]. This FDA approved drug has been previously used for systematic application in skin disease. Testing such an established drug for the ability to overcome the physiological barrier of the BBB and to potentially reach a CNS target may be a short cut to developing a novel therapy for a brain disease.

Characterization of Brain Endothelial Cells in the BBB Co-culture Model

To make our bio-assay system, consisting of brain endothelial cells and the reporter-transfected SH-SY5Y cells, easily available to other laboratories, we first investigated if the cell line hCMEC/D3 is suitable instead of more physiological primary cells. As demonstrated by different groups the well-characterized hCMEC/D3 display brain endothelial cell characteristics, i.e. expression of brain endothelial cell specific transporters, receptors and tight junction proteins [33,49,50,51]. The development of a BBB *in vitro* model has been described based on these cells [33,52] and it has been suggested that the co-culture with a second cerebral cell type

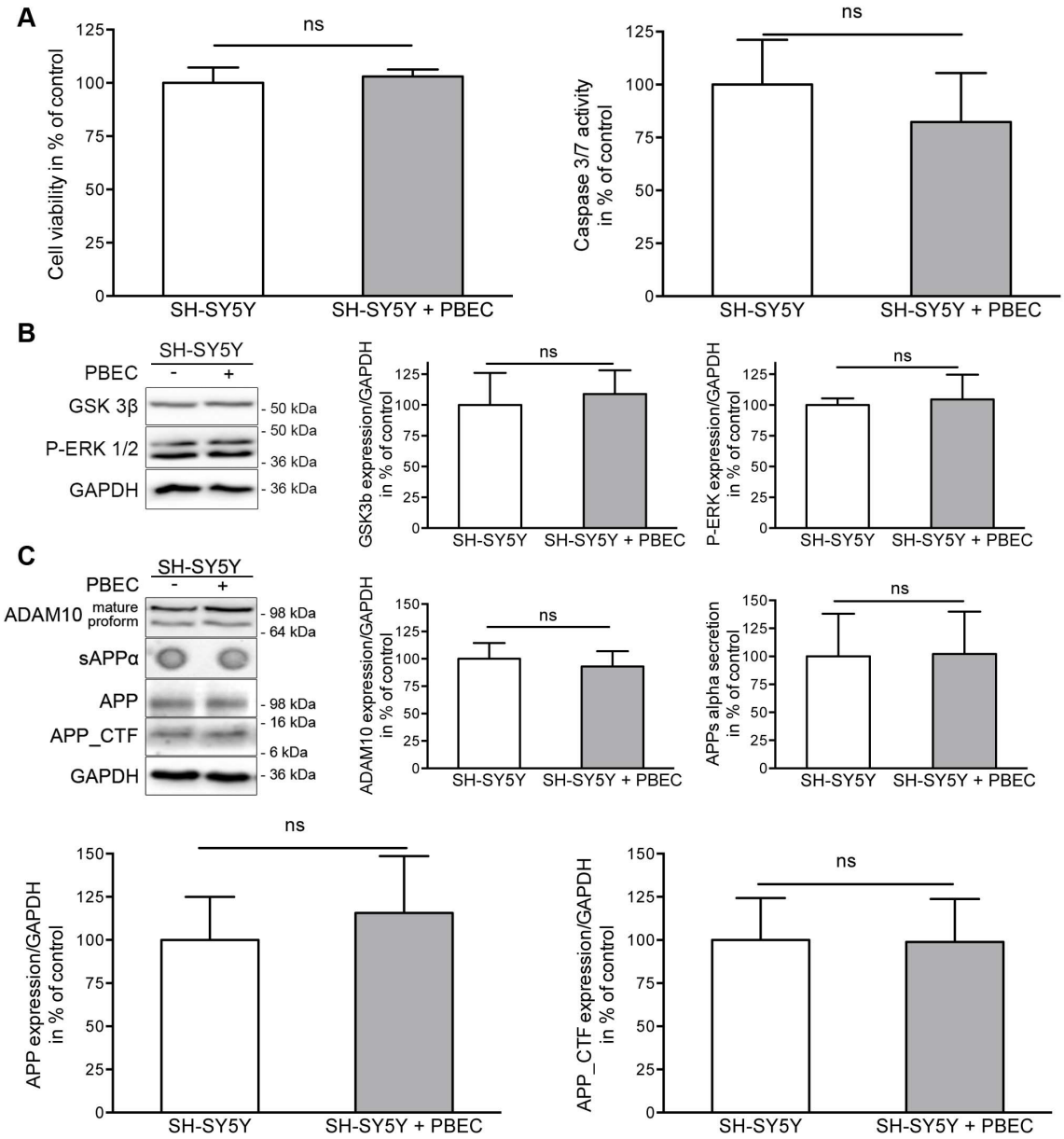

Figure 2. Impact of brain endothelial cells on SH-SY5Y cell viability, signal transduction and APP metabolism. (A) Cell viability and caspase 3/7 activity of SH-SY5Y cultured with or without porcine brain endothelial cells. Respective values for SH-SY5Y mono-cultures were set to 100%. (B) GSK3β and P-ERK-1/2 expression level in SH-SY5Y cells. Cells were grown in mono-cultures or co-cultivated with PBECs for 48 hrs. Protein levels were determined by Western blot and obtained values were normalized to expression of GAPDH. Values measured within mono-cultures were set to 100%. (C) ADAM10-dependent APP metabolism in SH-SY5Y cells under co-cultivation. Expression level of ADAM10, APP and APP C-terminal fragments were determined by Western blot. Values were normalized to GAPDH and set in relation to respective SH-SY5Y mono-cultures. Amount of secreted APPs-alpha was examined by a dot blot method with the specific APP N-terminal antibody (6E10). Values obtained for mono-cultured SH-SY5Y cells were set to 100% for all analysis. (three experiments; n≥6; unpaired two-tailed t-test; ns: $p>0.05$).
doi:10.1371/journal.pone.0091003.g002

is of advantage [51]. Hatherell and colleagues reported an improvement of the barrier properties as measured by transendothelial electrical resistance (TEER) when hCMEC/D3 were co-cultivated with the human cerebral astrocyte cell line SC1810 [30]. In short duration experiments these results were in accordance with our observations, although a neuronal cell line was used instead of astrocytes. However, we aimed at developing an *in vitro* model applicable for long-term treatment. In our investigations only primary endothelial cells were able to maintain a constant and consistent tightness of the barrier during 48 hrs treatment period. Another option to improve the barrier properties of hCMEC/D3 is the use of glucocorticoids, i.e. hydrocortisone [31]. Our model system was set up to study the induction of ADAM10-promoter activity by acitretin as a model substance. Although it has been demonstrated in Tg2576 mice that ADAM10 level did not change after corticosteroid treatment [53], induction of corticoid receptors might carry the risk of potential side effects regarding other neuronal targets. For example, it has been shown in the same study that the amount of soluble A-beta 40 in the brain increased following administra-

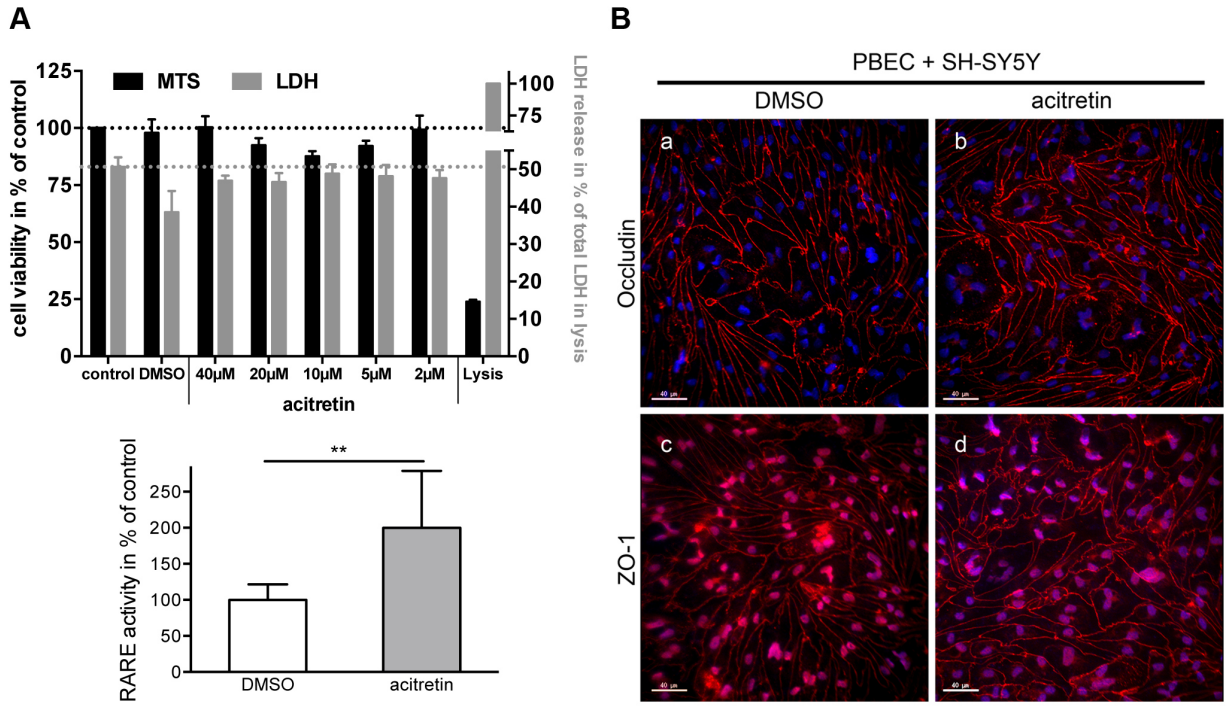

Figure 3. Influence of acitretin on PBEC viability and barrier properties. (A) Cell viability and cytotoxicity was measured after treatment with different concentrations of acitretin. Maximum amount of LDH (lysis) was set to 100% for the cytotoxicity assay whereas the cell viability of untreated cells (control) was set to 100%. DMSO was used as solvent control. (B) Impact of acitretin on the expression of tight junction proteins in PBEC grown on filter membranes and co-cultivated with SH-SY5Y cells. Scale bar: 40 µm. (C) Internalization of acitretin into PBEC. PBEC transfected with a luciferase-based retinoic acid response element (RARE)-containing reporter plasmid were treated with 2 µM acitretin for 48 hours and the retinoic acid dependent expression of luciferase was determined by luminescence measurement (three experiments; n = 10; unpaired two-tailed t-test; **: $p < 0.005$).
doi:10.1371/journal.pone.0091003.g003

tion of glucocorticoids. Moreover, Cury et al. revealed that glucocorticoids induce the expression of several matrix metalloproteinases and alter the activity of glycogen synthase kinase 3-beta (GSK3-beta) protein [54]. Due to the variety of potential interaction sites of hydrocortisone on the amyloid precursor protein (APP) metabolism, hydrocortisone was not applied in our model and as a consequence primary endothelial cells were used for the further experiments, based on the pronounced barrier properties exhibited by these cells.

Several co-culture models of the BBB exist, in which brain endothelial cells were co-cultured with other cell types. An overview of the variety of *in vitro* models is given by Deli et al. [55]. For example, *in vitro* co-culture models have been described consisting of brain endothelial cells and cells that are in close contact *in situ*, e.g. astrocytes or pericytes [30,56]. It has been shown that BBB models using astrocytes improved the barrier properties regarding tightness and expression of TJ proteins [57,58]. To our knowledge, there are only few publications examining the interaction of endothelial cells and neuronal cells, but the improvement of the barrier properties observed in our study is in accordance with those demonstrated under similar co-culture conditions [59,60,61].

We found TEER values of approximately 190 Ohm×cm^2 which were higher than data published by others [55,62,63] and even reached values as high as 331 Ohm×cm^2 in co-culture with SH-SY5Y cells. On the basis of *in vivo* measurements it is estimated that TEER of brain parenchymal microvessels exceeds 1000 Ohm×cm^2 [55,64]. In addition, determination of the permeability coefficient of sodium fluorescein revealed that the barrier built by PBECs was sufficient to prevent a paracellular transport of even small molecules. In further experiments we were able to show that the expression of tight junction proteins was not affected during co-cultivation conditions. Since at the BBB several active transport mechanisms for drug delivery are involved, we analyzed the expression of the most prominent representative of ABC transporters –P-glycoprotein (P-gp) [38,39]. Analysis revealed that expression level of P-gp was not affected during co-culture conditions as compared to mono-cultures of endothelial cells. In addition, transmission electron microscopy (TEM) and hematoxylin-eosin (HE) staining were used to demonstrate that PBECs grew as monolayers during transport experiments.

Impact of Brain Endothelial Cells on SH-SY5Y Cell Viability and APP Metabolism

Together with the characterization of the barrier formed by primary endothelial cells we evaluated if a co-cultivation with neuronal SH-SY5Y cells would influence barrier properties. It was demonstrated that co-cultivation with PBECs does not affect cell viability and also the activity of initiator caspases 3 and 7 in neuronal cells.

It has been postulated that extracellular receptor kinase (ERK) dysregulation plays a critical role in the development of AD. ERK is activated by oxidative stress [65], which is directly correlated to neuronal loss during disease progression. It has been demonstrated that a hyperactivation can be observed in neurons that display oxidative damage and contain hyperphophorylated tau protein [66]. Furthermore, treatment of primary cortical neurons with A-beta peptides in combination with inducers of oxidative stress,

A

	acitretin [µM]*	P_{app} (acitretin) [cm x min^{-1}]	P_{app} ($NaFITC_{acitretin}$) [cm x min^{-1}]
w/o PBEC	1.77 ± 0.22	1.55×10^{-4}	1.48×10^{-4}
PBEC	1.24 ± 0.29	1.09×10^{-4}	6.05×10^{-5}

* concentrations in lower compartment measured by HPLC

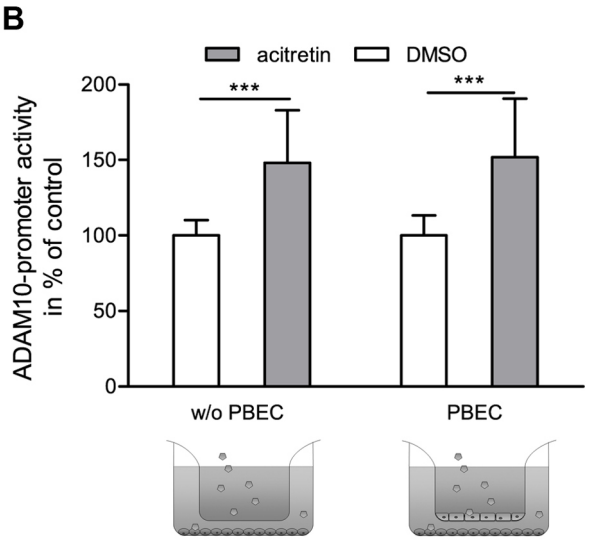

Figure 4. Detection of acitretin transport across the BBB. (A) After 48 hours the amount of acitretin transported across the brain endothelial cell barrier was measured by HPLC. Various concentrations were used to calculate the permeability coefficient of acitretin (P_{app} (acitretin)). To ensure the tightness of the barrier during the treatment with acitretin, the permeability coefficient of sodium fluorescein was simultaneously determined (acitretin (P_{app} ($NaFITC_{acitretin}$)). (B) Induction of ADAM10-promoter activity in SH-SY5Y cells by acitretin transported across endothelial cells. SH-SY5Y cells were transiently transfected with an ADAM10 promoter reporter plasmid and co-cultured with PBECs for 48 hrs. Acitretin was applied to the upper compartment of the transwell system. The induction of ADAM10 promoter activity by acitretin was monitored by measurement of luciferase activity and was normalized to protein content of whole cell lysate. As control, filters without PBEC (w/o PBEC) were used (three experiments; n $\geq$10; One Way Anova; Bonferroni post-test; ***: $p<0.001$).
doi:10.1371/journal.pone.0091003.g004

such as Fe (II), led to a rapid activation of ERK, implicating a strong correlation with AD pathogenesis [67]. In the present studies, quantitation of ERK phosphorylation by Western blot revealed no significant change during co-culture as compared to the respective mono-culture. Another regulatory protein contributing to AD pathology is the glycogen synthase kinase 3-beta (GSK3-beta), which phosphorylates tau [40,68]. It is confirmed by several reports, that the occurrence of the tau protein in its hyperphosphorylated state is paralleled by e.g. a reduction of dendritic spines and alteration of spine morphology [69]. Western blot analysis indicated that the protein level of active GSK3-beta was not affected in co-cultures of PBECs and SH-SY5Y cells as compared to respective mono-cultures of neuronal cells.

Since the developed co-culture model aims at analyzing drugs with therapeutic potential with respect to an enhancement of ADAM10 expression, it is important to assess the endogenous ADAM10-dependent APP metabolism in co-cultivated neuronal cells. Therefore, we quantified protein levels of APP and the respective cleavage products (APP C-terminal fragments and the ADAM10-dependent soluble fragment sAPP-alpha). The amount of the secretase ADAM10– both the pro-form and the mature protein - was not affected under co-cultivation conditions. In addition, the substrate APP was not affected regarding expression and/or cleavage as demonstrated by unchanged sAPP-alpha production and CTFs.

The Effect of Acitretin as Model Substance on the BBB Formed by PBECs

Acitretin, an aromatic retinoid able to overcome the BBB and to induce ADAM10 expression, was used to evaluate the co-culture model. Franke et al. studied the transport of retinoids across an *in vitro* BBB model using PBECs and speculated that retinoids were internalized into the ECs and released to the lower compartment [70]. To exclude a paracellular transport of acitretin in the present model we studied the transport of sodium fluorescein in parallel to the retinoid. Both substances have a similar molecular weight (acitretin: 326 Da and NaFITC: 332 Da) but fluorescein can cross the endothelial cell layer only paracellularly. We obtained a low permeability coefficient for fluorescein but high permeability coefficients for acitretin. This might indicate a transcellular transport of acitretin across the barrier. In addition, the results highlight that acitretin does not negatively influence barrier properties, as demonstrated by detection of representative tight junction protein expression using an immunofluorescence staining method as compared to solvent-treated cells. To further substantiate our results regarding transcellular transport of acitretin, we demonstrated the acitretin-induced response of PBECs transfected with a retinoid-responsive element containing a luciferase reporter vector. Acitretin liberates endogenous retinoic acid from its respective binding protein, which can only be mediated by cellular uptake of acitretin.

Transport of Acitretin Across the Endothelial Barrier and Induction of ADAM10-Promoter Activity in Neuronal Cells

In the presented model acitretin induced ADAM10-promoter activity to 150% compared to mock-treated cells. This was previously described in a similar way without using a BBB-based model [12]. With the described model, drugs which have been demonstrated to enhance the amount of ADAM10 and consequently display therapeutic potential regarding AD can subsequently be examined for their ability to cross the BBB by a sensitive promoter-dependent luciferase assay. This avoids the need for different HPLC applications and also reduces the number of animals for *in vivo* evaluation of BBB permeability. Furthermore, this bio-assay can easily be modified to analyze the influence of unique compounds on other disease relevant proteins by adapting the respective promoter reporter assay. This might consequently be useful to evaluate BBB penetrance of drugs against brain diseases or for investigating modification of drugs to obtain or enhance BBB permeability, such as coating on or attaching to nanoparticles. Moreover, our model might also be useful for unraveling transport mechanism for e.g. acitretin or for analysis of drug-drug interference with already applied AD symptomatic treatments such as Donepezil.

Conclusion

The results presented in this study demonstrate the functionality of a novel bio-assay system. The well-characterized *in vitro* model is suitable for predicting drug passage across the BBB of therapeutically useful drugs applicable for AD. This model uses an easy and

fast reporter assay read-out system present in neuronal co-cultured cells which might also be adapted for drugs with different target genes.

Acknowledgments

The authors are grateful to A. Sartoris for excellent assistance in cell culture. The authors acknowledge the team of C. Brochhausen (Institute of Pathology, University Medical Center Mainz, Germany) for its technical assistance in the TEM/SEM analyses. In addition, we thank P.-O. Couraud (Department of Cell Biology, Institut Cochin, Paris, France) for providing us with the immortalized brain endothelial cell line, hCMEC/D3 and C. Haass (University Munich, Germany) for providing APP C-terminal antibody 6687.

Author Contributions

Conceived and designed the experiments: KE CF SR. Performed the experiments: CF SR GH. Analyzed the data: CF SR GH KE. Contributed reagents/materials/analysis tools: REU CJK KE. Wrote the paper: CF SR KE REU CJK.

References

1. Hendrie HC (1998) Epidemiology of dementia and Alzheimer's disease. Am J Geriatr Psychiatry 6: S3–18.
2. Bowman GL, Quinn JF (2008) Alzheimer's disease and the Blood-Brain Barrier: Past, Present and Future. Aging health 4: 47–55.
3. Maruszak A, Zekanowski C (2011) Mitochondrial dysfunction and Alzheimer's disease. Prog Neuropsychopharmacol Biol Psychiatry 35: 320–330.
4. Iqbal K, Grundke-Iqbal I (2008) Alzheimer neurofibrillary degeneration: significance, etiopathogenesis, therapeutics and prevention. J Cell Mol Med 12: 38–55.
5. Endres K, Fahrenholz F (2010) Upregulation of the alpha-secretase ADAM10–risk or reason for hope? FEBS J 277: 1585–1596.
6. Sathya M, Premkumar P, Karthick C, Moorthi P, Jayachandran KS, et al. (2012) BACE1 in Alzheimer's disease. Clin Chim Acta 414: 171–178.
7. Wolfe MS (2012) gamma-Secretase as a target for Alzheimer's disease. Adv Pharmacol 64: 127–153.
8. Mattson MP (1997) Cellular actions of beta-amyloid precursor protein and its soluble and fibrillogenic derivatives. Physiol Rev 77: 1081–1132.
9. Caille I, Allinquant B, Dupont E, Bouillot C, Langer A, et al. (2004) Soluble form of amyloid precursor protein regulates proliferation of progenitors in the adult subventricular zone. Development 131: 2173–2181.
10. Thornton E, Vink R, Blumbergs PC, Van Den Heuvel C (2006) Soluble amyloid precursor protein alpha reduces neuronal injury and improves functional outcome following diffuse traumatic brain injury in rats. Brain Res 1094: 38–46.
11. Postina R, Schroeder A, Dewachter I, Bohl J, Schmitt U, et al. (2004) A disintegrin-metalloproteinase prevents amyloid plaque formation and hippocampal defects in an Alzheimer disease mouse model. The Journal of clinical investigation 113: 1456–1464.
12. Tippmann F, Hundt J, Schneider A, Endres K, Fahrenholz F (2009) Up-regulation of the alpha-secretase ADAM10 by retinoic acid receptors and acitretin. FASEB J 23: 1643–1654.
13. Eisenhardt EU, Bickel MH (1994) Kinetics of tissue distribution and elimination of retinoid drugs in the rat. I. Acitretin. Drug Metab Dispos 22: 26–30.
14. Holthoewer D, Endres K, Schuck F, Hiemke C, Schmitt U, et al. (2012) Acitretin, an enhancer of alpha-secretase expression, crosses the blood-brain barrier and is not eliminated by P-glycoprotein. Neurodegener Dis 10: 224–228.
15. Kelleher RJ, Soiza RL (2013) Evidence of endothelial dysfunction in the development of Alzheimer's disease: Is Alzheimer's a vascular disorder? Am J Cardiovasc Dis 3: 197–226.
16. Zipser BD, Johanson CE, Gonzalez L, Berzin TM, Tavares R, et al. (2007) Microvascular injury and blood-brain barrier leakage in Alzheimer's disease. Neurobiol Aging 28: 977–986.
17. Karch A, Manthey H, Ponto C, Hermann P, Heinemann U, et al. (2013) Investigating the Association of ApoE Genotypes with Blood-Brain Barrier Dysfunction Measured by Cerebrospinal Fluid-Serum Albumin Ratio in a Cohort of Patients with Different Types of Dementia. PLoS ONE 8: e84405.
18. Vos SJ, Xiong C, Visser PJ, Jasielec MS, Hassenstab J, et al. (2013) Preclinical Alzheimer's disease and its outcome: a longitudinal cohort study. Lancet Neurol 12: 957–965.
19. Hawkins BT, Davis TP (2005) The blood-brain barrier/neurovascular unit in health and disease. Pharmacological reviews 57: 173–185.
20. Löscher W, Potschka H (2005) Role of drug efflux transporters in the brain for drug disposition and treatment of brain diseases. Progress in neurobiology 76: 22–76.
21. Abbott NJ, Patabendige AAK, Dolman DEM, Yusof SR, Begley DJ (2010) Structure and function of the blood-brain barrier. Neurobiology of Disease: 13–25.
22. Dehouck MP, Méresse S, Delorme P, Fruchart JC, Cecchelli R (1990) An easier, reproducible, and mass-production method to study the blood-brain barrier in vitro. Journal of neurochemistry 54: 1798–1801.
23. Franke H, Galla H, Beuckmann CT (2000) Primary cultures of brain microvessel endothelial cells: a valid and flexible model to study drug transport through the blood-brain barrier in vitro. Brain research Brain research protocols 5: 248–256.
24. Culot M, Lundquist S, Vanuxeem D, Nion S, Landry C, et al. (2008) An in vitro blood-brain barrier model for high throughput (HTS) toxicological screening. Toxicology in vitro : an international journal published in association with BIBRA 22: 799–811.
25. Patabendige A, Skinner RA, Abbott NJ (2013) Establishment of a simplified in vitro porcine blood-brain barrier model with high transendothelial electrical resistance. Brain Res 1521: 1–15.
26. Fricker G, Nobmann S, Miller DS (2002) Permeability of porcine blood brain barrier to somatostatin analogues. British journal of pharmacology 135: 1308–1314.
27. Lai C-H, Kuo K-H (2005) The critical component to establish in vitro BBB model: Pericyte. Brain research Brain research reviews 50: 258–265.
28. Kido Y, Tamai I, Nakanishi T, Kagami T, Hirosawa I, et al. (2004) Evaluation of blood-brain barrier transporters by co-culture of brain capillary endothelial cells with astrocytes. Drug metabolism and pharmacokinetics 17: 34–41.
29. Nakagawa S, Deli MA, Nakao S, Honda M, Hayashi K, et al. (2007) Pericytes from brain microvessels strengthen the barrier integrity in primary cultures of rat brain endothelial cells. Cellular and molecular neurobiology 27: 687–694.
30. Hatherell K, Couraud P-O, Romero IA, Weksler B, Pilkington GJ (2011) Development of a three-dimensional, all-human in vitro model of the blood-brain barrier using mono-, co-, and tri-cultivation Transwell models. Journal of neuroscience methods 199: 223–229.
31. Forster C, Burek M, Romero IA, Weksler B, Couraud P-O, et al. (2008) Differential effects of hydrocortisone and TNF{alpha} on tight junction proteins in an in vitro model of the human blood-brain barrier. J Physiol 586: 1937–1949.
32. Stins MF, Badger J, Sik Kim K (2001) Bacterial invasion and transcytosis in transfected human brain microvascular endothelial cells. Microb Pathog 30: 19–28.
33. Weksler BB, Subileau EA, Perrière N, Charneau P, Holloway K, et al. (2005) Blood-brain barrier-specific properties of a human adult brain endothelial cell line. The FASEB journal : official publication of the Federation of American Societies for Experimental Biology 19: 1872–1874.
34. Unger RE, Oltrogge JB, Briesen H, Engelhardt B, Woelki U, et al. (2002) Isolation and molecular characterization of brain microvascular endothelial cells from human brain tumors. In Vitro Cellular & Developmental Biology - Animal 38: 273–281.
35. Steiner H, Kostka M, Romig H, Basset G, Pesold B, et al. (2000) Glycine 384 is required for presenilin-1 function and is conserved in bacterial polytopic aspartyl proteases. Nat Cell Biol 2: 848–851.
36. Hermanns MI, Kasper J, Dubruel P, Pohl C, Uboldi C, et al. (2009) An impaired alveolar-capillary barrier in vitro: effect of proinflammatory cytokines and consequences on nanocarrier interaction. Journal of The Royal Society Interface.
37. Kasper J, Hermanns MI, Bantz C, Maskos M, Stauber R, et al. (2011) Inflammatory and cytotoxic responses of an alveolar-capillary coculture model to silica nanoparticles: comparison with conventional monocultures. Particle and fibre toxicology 8: 6.
38. Cordon-Cardo C, O'Brien JP, Casals D, Rittman-Grauer L, Biedler JL, et al. (1989) Multidrug-resistance gene (P-glycoprotein) is expressed by endothelial cells at blood-brain barrier sites. Proc Natl Acad Sci U S A 86: 695–698.
39. Sharom FJ (2011) The P-glycoprotein multidrug transporter. Essays Biochem 50: 161–178.
40. Ishiguro K, Shiratsuchi A, Sato S, Omori A, Arioka M, et al. (1993) Glycogen synthase kinase 3 beta is identical to tau protein kinase I generating several epitopes of paired helical filaments. FEBS Lett 325: 167–172.
41. Ly PT, Wu Y, Zou H, Wang R, Zhou W, et al. (2013) Inhibition of GSK3beta-mediated BACE1 expression reduces Alzheimer-associated phenotypes. J Clin Invest 123: 224–235.
42. Wan XZ, Li B, Li YC, Yang XL, Zhang W, et al. (2012) Activation of NMDA receptors upregulates a disintegrin and metalloproteinase 10 via a Wnt/MAPK signaling pathway. J Neurosci 32: 3910–3916.
43. Armstrong JL, Redfern CP, Veal GJ (2005) 13-cis retinoic acid and isomerisation in paediatric oncology–is changing shape the key to success? Biochem Pharmacol 69: 1299–1306.
44. Sinha S, Lieberburg I (1999) Cellular mechanisms of beta-amyloid production and secretion. Proc Natl Acad Sci U S A 96: 11049–11053.
45. Vassar R, Bennett BD, Babu-Khan S, Kahn S, Mendiaz EA, et al. (1999) Beta-secretase cleavage of Alzheimer's amyloid precursor protein by the transmembrane aspartic protease BACE. Science 286: 735–741.

46. Hussain I, Powell D, Howlett DR, Tew DG, Meek TD, et al. (1999) Identification of a novel aspartic protease (Asp 2) as beta-secretase. Mol Cell Neurosci 14: 419–427.
47. Lammich S, Kojro E, Postina R, Gilbert S, Pfeiffer R, et al. (1999) Constitutive and regulated alpha-secretase cleavage of Alzheimer's amyloid precursor protein by a disintegrin metalloprotease. Proceedings of the National Academy of Sciences of the United States of America 96: 3922–3927.
48. Ishida A, Furukawa K, Keller JN, Mattson MP (1997) Secreted form of beta-amyloid precursor protein shifts the frequency dependency for induction of LTD, and enhances LTP in hippocampal slices. Neuroreport 8: 2133–2137.
49. Carl SM, Lindley DJ, Couraud PO, Weksler BB, Romero I, et al. (2010) ABC and SLC Transporter Expression and Pot Substrate Characterization across the Human CMEC/D3 Blood-Brain Barrier Cell Line. Molecular Pharmaceutics.
50. Dauchy S, Miller F, Couraud P-O, Weaver RJ, Weksler B, et al. (2009) Expression and transcriptional regulation of ABC transporters and cytochromes P450 in hCMEC/D3 human cerebral microvascular endothelial cells. Biochemical Pharmacology 2009: 897–909.
51. Weksler B, Romero IA, Couraud PO (2013) The hCMEC/D3 cell line as a model of the human blood brain barrier. Fluids Barriers CNS 10: 16.
52. Poller B, Drewe J, Krähenbühl S, Huwyler J, Gutmann H (2010) Regulation of BCRP (ABCG2) and P-glycoprotein (ABCB1) by cytokines in a model of the human blood-brain barrier. Cellular and molecular neurobiology 30: 63–70.
53. Joshi YB, Chu J, Pratico D (2012) Stress hormone leads to memory deficits and altered tau phosphorylation in a model of Alzheimer's disease. J Alzheimers Dis 31: 167–176.
54. Cury PR, Araujo VC, Canavez F, Furuse C, Araujo NS (2007) Hydrocortisone affects the expression of matrix metalloproteinases (MMP-1, -2, -3, -7, and -11) and tissue inhibitor of matrix metalloproteinases (TIMP-1) in human gingival fibroblasts. J Periodontol 78: 1309–1315.
55. Deli MA, Abraham CS, Kataoka Y, Niwa M (2005) Permeability studies on in vitro blood-brain barrier models: physiology, pathology, and pharmacology. Cell Mol Neurobiol 25: 59–127.
56. Zozulya A, Weidenfeller C, Galla H-J (2008) Pericyte-endothelial cell interaction increases MMP-9 secretion at the blood-brain barrier in vitro. Brain research 1189: 1–11.
57. Gaillard PJ, Voorwinden LH, Nielsen JL, Ivanov A, Atsumi R, et al. (2001) Establishment and functional characterization of an in vitro model of the blood-brain barrier, comprising a co-culture of brain capillary endothelial cells and astrocytes. European journal of pharmaceutical sciences : official journal of the European Federation for Pharmaceutical Sciences 12: 215–222.
58. Zhang Y, Li CSW, Ye Y, Johnson K, Poe J, et al. (2006) Porcine brain microvessel endothelial cells as an in vitro model to predict in vivo blood-brain barrier permeability. Drug metabolism and disposition: the biological fate of chemicals 34: 1935–1943.
59. Schiera G, Bono E, Raffa MP, Gallo A, Pitarresi GL, et al. (2003) Synergistic effects of neurons and astrocytes on the differentiation of brain capillary endothelial cells in culture. J Cell Mol Med 7: 165–170.
60. Tontsch U, Bauer HC (1991) Glial cells and neurons induce blood-brain barrier related enzymes in cultured cerebral endothelial cells. Brain Res 539: 247–253.
61. Weidenfeller C, Svendsen CN, Shusta EV (2007) Differentiating embryonic neural progenitor cells induce blood-brain barrier properties. J Neurochem 101: 555–565.
62. Igarashi Y, Utsumi H, Chiba H, Yamada-Sasamori Y, Tobioka H, et al. (1999) Glial cell line-derived neurotrophic factor induces barrier function of endothelial cells forming the blood-brain barrier. Biochem Biophys Res Commun 261: 108–112.
63. Yamagata K, Tagami M, Takenaga F, Yamori Y, Nara Y, et al. (2003) Polyunsaturated fatty acids induce tight junctions to form in brain capillary endothelial cells. Neuroscience 116: 649–656.
64. Gumbleton M, Audus KL (2001) Progress and limitations in the use of in vitro cell cultures to serve as a permeability screen for the blood-brain barrier. J Pharm Sci 90: 1681–1698.
65. McCubrey JA, Lahair MM, Franklin RA (2006) Reactive oxygen species-induced activation of the MAP kinase signaling pathways. Antioxid Redox Signal 8: 1775–1789.
66. Perry G, Roder H, Nunomura A, Takeda A, Friedlich AL, et al. (1999) Activation of neuronal extracellular receptor kinase (ERK) in Alzheimer disease links oxidative stress to abnormal phosphorylation. Neuroreport 10: 2411–2415.
67. Kuperstein F, Yavin E (2002) ERK activation and nuclear translocation in amyloid-beta peptide- and iron-stressed neuronal cell cultures. Eur J Neurosci 16: 44–54.
68. Ishiguro K, Takamatsu M, Tomizawa K, Omori A, Takahashi M, et al. (1992) Tau protein kinase I converts normal tau protein into A68-like component of paired helical filaments. J Biol Chem 267: 10897–10901.
69. Messing L, Decker JM, Joseph M, Mandelkow E, Mandelkow EM (2013) Cascade of tau toxicity in inducible hippocampal brain slices and prevention by aggregation inhibitors. Neurobiol Aging 34: 1343–1354.
70. Franke H, Galla H-J, Beuckmann CT (1999) An improved low-permeability in vitro-model of the blood-brain barrier: transport studies on retinoids, sucrose, haloperidol, caffeine and mannitol. Brain Research 818: 65–71.

Am J Neurodegener Dis 2013;2(4):247-265
www.AJND.us /ISSN:2165-591X/AJND1309005

Review Article

ER-stress in Alzheimer's disease: turning the scale?

Kristina Endres, Sven Reinhardt

Department of Psychiatry and Psychotherapy, Clinical Research Group, University Medical Centre Johannes Gutenberg-University Mainz, Untere Zahlbacher Str. 8, D-55131 Mainz, Germany

Received September 30, 2013; Accepted November 5, 2013; Epub November 29, 2013; Published December 15, 2013

Abstract: Pathogenic mechanisms of Alzheimer's disease (AD) are intensely investigated as it is the most common form of dementia and burdens society by its costs and social demands. While key molecules such as A-beta peptides and tau have been identified decades ago, it is still enigmatic what drives the disease in its sporadic manifestation. Synthesis of A-beta peptides as well as phosphorylation of tau proteins comprise normal cellular functions and occur in principle in the healthy as well as in dementia-affected persons. Dyshomeostasis of Amyloid Precursor Protein (APP) cleavage, energy metabolism or kinase/phosphatase activity due to stressors has been suggested as a trigger of the disease. One way for cells to escape stress based on dysfunction of ER is the unfolded protein response - the UPR. This pathway is composed out of three different routes that differ in proteins involved, targets and consequences for cell fate: activation of transmembrane ER resident kinases IRE1-alpha and PERK or monomerization of membrane-anchored activating transcription factor 6 (ATF6) induce activation of versatile transcription factors (XBP-1, eIF2-alpha/ATF4 and ATF6 P50). These bind to specific DNA sequences on target gene promoters and on one hand attenuate general ER-prone protein synthesis and on the other equip the cell with tools to de-stress. If cells fail in stress compensation, this signaling also is able to evoke apoptosis. In this review we summarized knowledge on how APP processing and phosphorylation of tau might be influenced by ER-stress signaling. In addition, we depicted the effects UPR itself seems to have on molecules closely related to AD and describe what is known about UPR in AD animal models as well as in human patients.

Keywords: Alzheimer's disease, secretases, APP, tau, unfolded protein response, calcium homeostasis, autophagy, apoptosis

Introduction

The term amyloidosis describes a family of diseases that are characterized by abnormal protein deposition within the extracellular space. Examples are the cardiac amyloidosis or Alzheimer's disease (AD). Pathological features of this type of disease are mediated on one hand by direct malfunction of the affected tissue or organ. Amyloid deposits in the ventricles and atria of the heart e.g. result in biventricular wall thickening with an ensuing elevation of pressure in the thin-walled part of the respective atrium [1, 2]. On the other hand, interference of already deposited material or intermediate protein oligomers with cellular function has been described to lead to dysbalance and subsequent pathogenesis. For example, amyloidogenic light chains are able to evoke oxidative stress, cellular dysfunction, and apoptosis in primary cardiomyocyte cultures via MAPK signaling [3]. In case of Alzheimer's disease the scientific landscape was dominated for a long time by the assumption that large aggregates of A-beta peptides (designated as senile plaques) are triggering neuronal degeneration. More recent investigations led to the insight that small oligomers (reviewed e.g. in [4]) or even intraneuronal A-beta peptides are culprit to pathogenic derailment [5, 6]. Tau protein with its microtubule binding properties is another characteristic of the disease and has been suggested to act downstream of neurotoxic A-beta species (reviewed e.g. in [7]).

A-beta peptides derive from proteolytic processing of a large type I transmembrane protein - the amyloid precursor protein (APP). This protein matures within trafficking through ER and the Golgi-apparatus by being cleaved by signal peptidases and being modified in regard of carbohydrate-attachment. Despite having the

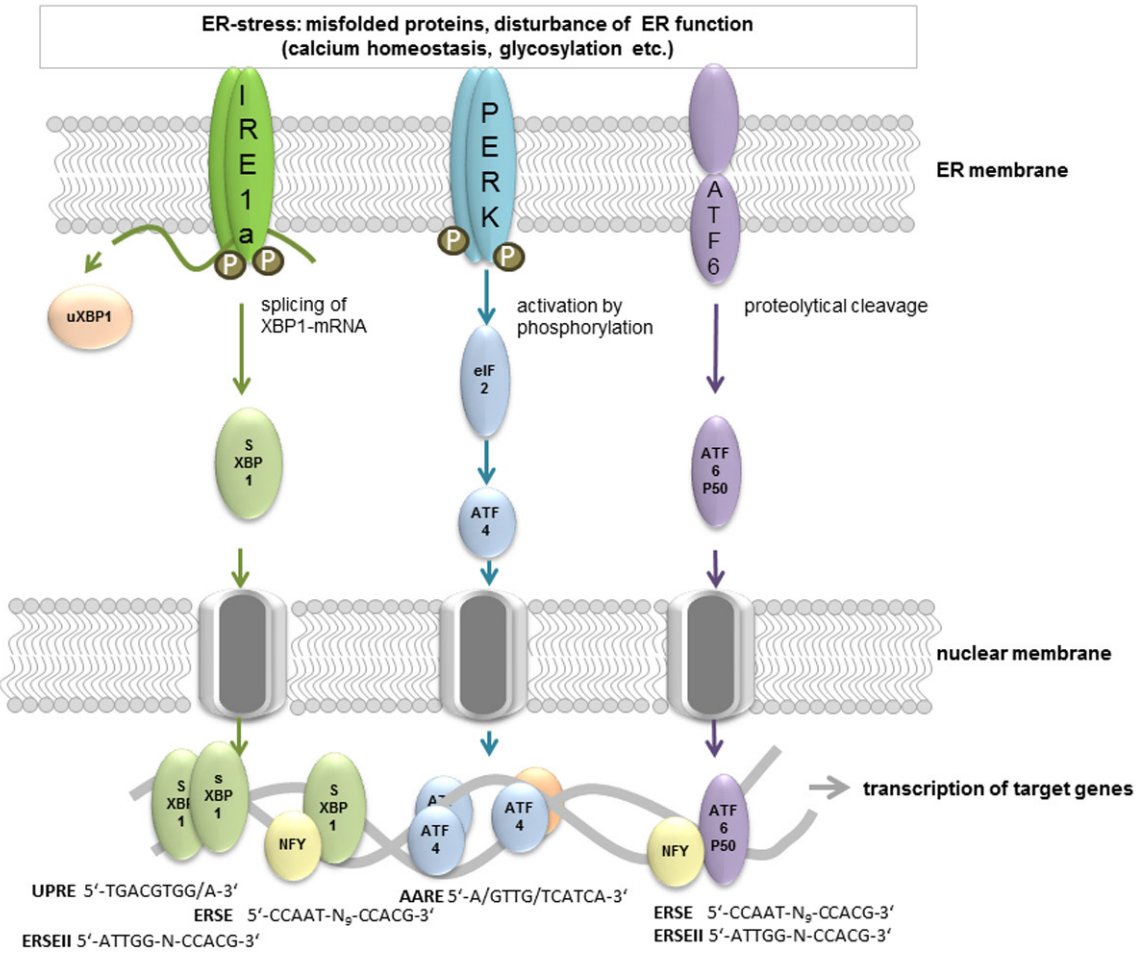

Figure 1. Three different signaling pathways conduct UPR upon ER-stress induction. ER-stress is sensed by the luminal proportion of three distinct transmembrane ER resident proteins: IRE1-alpha, PERK and ATF6. There are several mechanisms that have been proposed for this activation step such as direct binding of unfolded proteins or displacement of GRP78 binding (reviewed in [151]). Activation subsequently leads to changes in oligomerization status and the signal is transmitted via the C-terminus of all three proteins. PERK and IRE1-alpha homodimerize and perform autophosphorylation. PERK also phosphorylates the translation initiation factor eIF2-alpha resulting in a reversible attenuation of translation. Only single translational events such as ATF4 protein biosynthesis are enhanced under these conditions. Delayed reinitiation by reduced amount of eIF2-GTP allows ribosomes to scan through an inhibitory upstream open reading frame of ATF4 mRNA and instead reinitiate at the coding region [152]. ATF4 binds to a consensus motif of target gene promoters (e.g. AARE) as a homodimer or heterodimer with e.g. Fos, Jun [153] or other cofactors such as PCAF [154]. IRE1-alpha conducts its endonuclease function and splices XBP-1 mRNA as well as other mRNAs. This process is termed regulated IRE1-alpha-dependent decay (RIDD; [62]) and may further contribute to limitation of translation. Target genes of the active sXBP-1 (binding to UPRE, ERSE or ERSEII) produced by splicing are proteins involved in protein folding, maturation, secretion, and degradation. ATF6 translocates to the Golgi upon activation where it is cleaved by site-1-and 2 proteases. This generates the b-Zip transcription factor ATF6 P50 which initiates transcription of target genes in combination with NF-Y via ERSE motifs in its target genes.

knowledge about distinct function of each proteolysis product, the proteolytic degradation of this protein has been described in detail: subsequent cleavage by the beta-secretase BACE-1 (beta-site APP cleaving enzyme 1) and the gamma-secretase complex gives rise to the already mentioned A-beta peptides (e.g. [8, 9]). Alternatively, alpha-secretase leads to prevention of A-beta peptide formation and to secretion of the so-called APPs-alpha fragment (for example [10-13]). The latter has been described to conduct neurotrophic and neuroprotective properties (reviewed in e.g. [14]). APP is a ubiquitously expressed protein and A-beta peptides are generated not only under pathological conditions but also in healthy human subjects.

Nevertheless, under certain circumstances, synthesis and/or degradation of A-beta peptides are disturbed and oligomers and fibrils rise that are deposited in brain parenchyma or blood vessel walls. Some human beings seem to cope with these deposits very well and show no signs of cognitive decline despite having high plaque loads while others do not [15]. Understanding the underlying resilience factors might lead to development of new therapeutic approaches since directly inhibiting A-beta production or immunization strategies in the first line failed regarding curing this disease.

An adaptable access to gain resilience might be given by the cellular response to endogenous stressors. One cellular organelle that is related to stress mediation by its multifunctionality is the endoplasmic reticulum (ER, for example [16, 17]): 1) the ER assists and closely monitors quality of nascent proteins. Protein disulfide isomerase (PDI) and ERp57 (thio-oxidoreductases) e.g. catalyze disulfide bond formation using the oxidative capacity provided by ER oxidoreduction 1 (ERO1). Glucose-regulated protein 78 (BiP or GRP78) or 94 (GRP94, calreticulin), stabilize as chaperones of the heat-shock protein family unfolded proteins. 2) Calcium-storage in the ER and regulated release protects the cell from cell death caused by calcium concentration dysbalance. This is driven by calcium import via SERCA (sarcoplasmic/endoplasmic reticulum calcium-ATPase) and ion release via Rhyanodine and IP3 receptors. Calcium binding proteins such as calreticulin and calnexin further buffer the calcium content of the cell.

Disturbance of ER homeostasis is not separated from general cellular function. The peripheral ER is in contact to other cellular organelles and for example forms physical interaction zones with mitochondria. These structures - designated as MAM in mammals (Mitochondrial-associated endoplasmic reticulum Membranes, [18], reviewed in [19]) - are enriched by certain proteins such as Mitofusin-2 or the autocrine motility factor receptor which allow attachment [20, 21]. In case of perturbations regarding ER function these are not only sensed by the ER but also transduced to the cytoplasm and nucleus to evoke an appropriate response. This response includes enhanced expression of chaperones, transiently inhibited translation, increase in ER volume and enhanced degradation of misfolded proteins as well as enhanced autophagy [22, 23]. If this attenuation of stressors and capacity compensation along the unfolded protein response (UPR) is not sufficient within a certain time frame, cells undergo apoptosis (reviewed in [24]).

APP as a central player in Alzheimer's disease matures via bypassing the ER and beta- as well as gamma-secretase cleavage takes place in the Golgi apparatus [25, 26]. In addition, mitochondrial dysfunction, disturbed autophagy and aberrant calcium signaling have been repeatedly connected to Alzheimer's disease (reviewed e.g. in [27-29]). A general role of the UPR in neurodegenerative processes has been summarized previously [30]. Hence, a contribution of activated UPR signaling in the pathology of Parkinson's or in particular Alzheimer's disease has been discussed as an early event of disease progression [31]. Therefore, we focused on known correlations of APP, its processing products and related proteins with ER-stress events in this review.

ER-stress: three routes of UPR signal transduction

Three signal pathways operate in parallel to sense ER-stress and to react as the UPR (**Figure 1**). They have in common that signaling is transduced by a protein with an ER luminal domain, a transmembrane part and a cytoplasmic effector domain: IRE1-alpha (inositol requiring enzyme 1, [32-34]), PERK (double-stranded RNA-activated protein kinase (PKR)-like ER kinase, [35]), and ATF6 (activating transcription factor 6, [36-38]). All three proteins use a specific signal transduction mechanism but end in activation of b-Zip transcription factors that subsequently lead to altered transcription of target genes.

ATF6 and PERK represent evolutionary newer pathways that evolved in metazoans [39]. ATF6 exists partially oligomerized in the absence of stress through intermolecular disulfide bonds [40]. These are reduced upon accumulation of unfolded proteins, subsequently the monomeric form leaves the ER via transport vesicles and is cleaved within the Golgi apparatus by site-1 and site-2 proteases [41]. The cytoplasmic domain then is liberated from its transmembrane anchor and acts as a transcription factor on target genes such as GRP78 or GRP94 [42].

Both are part of the functional ER machinery and therefore might contribute to enhanced ER capacity.

PERK is a transmembrane kinase that oligomerizes during ER-stress and performs trans-autophosphorylation of its C-terminal cytoplasmic kinase domain at multiple residues [43, 44] as well as phosphorylation of the general translation factor eIF2-alpha [45]. This inhibits eIF2-alpha which lowers translation rates regarding a wide variety of mRNAs [46, 47] and consequently reduces protein burden within the ER. Only few mRNAs show increased translation upon eIF2-alpha phosphorylation such as ATF4 which by itself acts as a transcription factor on targets such as CHOP (transcription factor C/EBP homologous protein, [48]) or GADD34 (growth arrest and DNA damage-inducible 34, [49]). CHOP regulates expression of components of the apoptotic pathway (reviewed in [50]) while GADD34 encodes a regulatory subunit of PP1C - the protein phosphatase that dephosphorylates eIF2-alpha [51]. This on one hand indicates that the PERK branch contains both, alleviating strategies and death triggering ones, and that it is strictly regulated.

IRE1-alpha represents the third branch which also exists in lower eukaryotes [39]. By sensing ER-stress this bifunctional enzyme dimerizes and becomes activated [52]. During the dimer assembly trans-autophosphorylation takes place [53] which is discussed to be mandatory for the human enzyme activity or regulation [54, 55]. Formation of the active dimer then evokes endonuclease function and the ER-associated mRNA of the transcription factor XBP-1 (X-box binding protein 1) is spliced to yield the active protein sXBP-1 (for the splicing mechanism see: [56]). In non-yeast organisms unspliced XBP-1-mRNA is translated to uXBP-1 which might act as an inhibitory counterbalance of sXBP1 action [57]. Downstream targets of activated XBP1 include ER chaperones as well as so-called ERAD (ER associated degradation) components such as HRD1 [58], PDI [59] or ER-localized DnaJ (Erdj4) [60]. Besides specifically activating XBP-1, IRE1-alpha is involved in activation of JNK [61] and degradation of other ER-associated mRNAs (e.g. its own mRNA: [53]; regulated IRE1-alpha-dependent decay (RIDD): [62]) further contributing to relief of ER machinery by decreasing translation into the ER lumen. In secretory cells such as B-cells IRE1-alpha also mediates UPR-independent enhancement of secretion [63, 64].

The three signaling pathways are not fully isolated but also comprise cross-linkage. For example PERK facilitates synthesis and trafficking of ATF6 from ER to the Golgi [65] and IRE1-alpha activity also steers ATF6 activation [66].

Target genes of the UPR contain conserved binding sequences (**Figure 1**) designated as UPRE (UPR element, [67]) or ERSE (ER-stress element, [68]) or ERSEII [69]). ERSE sites consist of the conserved sequence CCAAT-N_9-CCACG; the 9 nucleotide spacing between both half site motifs has been suggested to be quiet important for their functionality [70]. A recent report nevertheless described a functional XBP-1-responsive element with a 26 nt spacer [71]. ATF6 binds e.g. to the CCACG sequence of the ERSE motif, if the general transcription factor NF-Y has bound to the CCAAT part of the sequence. Active XBP-1 also binds to this sequence instead of ATF6 [70, 72]. The ERSEII (ATTGG-N-CCACG) might be occupied by ATF6 NF-Y-dependent [69] or by XBP-1 without further binding of NF-Y [67]. To the UPRE (TGACGTGG/A) sXBP-1 binds as a homodimer [70].

A genome wide approach to identify targets of XBP-1 in myotubular, plasma and pancreatic cells by Acosta-Alvear and colleagues [73] revealed that XBP-1 is able to bind the promoters of a wide variety of target genes whereof 40% are not directly linked to ER-stress compensation. One of the unexpected GO categories contained disease-associated genes, including genes connected to Alzheimer's disease. In cell culture studies UPR as indicated by eIF2-alpha phosphorylation is evoked by compounds such as Tunicamycin, Thapsigargin or DTT (e.g. [74]) which impair N-glycosylation of proteins, calcium homeostasis or formation of disulfide bonds. In addition, brefeldin A, 2-deoxy-glucose or eeyarestatin function as UPR inducers. These compounds seem to belong to two different clusters of drugs as shown by analysis of expression patterns of nine typical UPR target genes by [75]. Endogenous provokers of ER-stress are under intensive investigation and several molecules

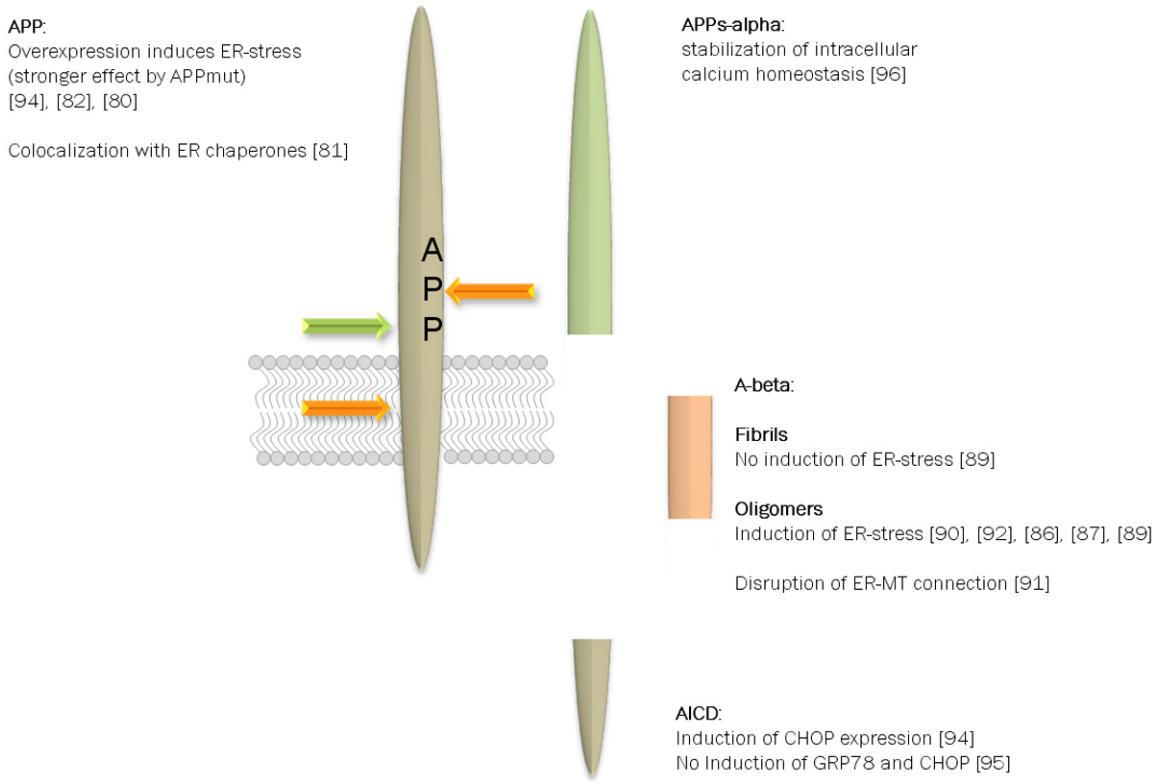

Figure 2. APP processing products and their potential role in UPR. APP is subject to a wide variety of posttranslational modifications such as phosphorylation and glycosylation (e.g. [62, 155]). In addition, the type I transmembrane protein is cleaved by several proteases yielding protein fragments of different size and function [14]. In regard of ER-stress not all protein fragments have been analyzed but for the full length protein, A-beta peptides and the alpha-secretase derived soluble ectodomain correlation to subsequent signaling events have been reported. In this scheme only the most prominent facts are included but one has to consider that contradictory results have been published.

associated with Alzheimer's disease are under suspicion.

Influence of APP-cleavage products on ER-stress

Shortly after cloning of the mammalian PERK and IRE1-alpha [43, 32], first investigations indicated a potential link to Alzheimer dementia: Katayama et al. [76] described that mutations in Presenilin 1 (PS1), the catalytic component of the gamma-secretase complex, decreased GRP78 expression by interfering with IRE1-alpha function in cell culture experiments. Moreover, they already assessed reduced amount of GRP78 and GRP94 within temporal cortex tissue from sporadic and familiar Alzheimer patients. A potential role of PS1 in UPR was further confirmed by Niwa et al. [77], where a reduced nuclear translocation and attenuated UPR was reported for PS1 knockout fibroblasts. A direct cleavage of IRE1-alpha has been suggested but could not be confirmed for human fibroblasts due to technical problems [77]. In addition, cleavage of ATF6 has been analyzed but no influence of gamma-secretase inhibitor or dominant negative PS1 could be demonstrated [78]. Gamma-secretase is a very promiscuous endoproteolytic complex that cleaves a wide variety of substrates (e.g. reviewed in [79]) such as APP. Therefore, regulation of UPR by several proteolysis products could be assumed.

For APP as a substrate of gamma-secretase, there have been reports about correlation with ER-stress and subsequent UPR signaling: APP overexpression led for example to an enhanced upregulation of CHOP in PC12 cells upon Thapsigargin administration [80]. For other typical ER-stress associated chaperones such as GRP94 this was not confirmed in this cell line. However, colocalization of APP with ER chaperones calnexin, calreticulin, GRP94, GRP78, and

ERp72 has been demonstrated in sporadic inclusion body myositis (s-IBM) muscle biopsies with APP containing aggregation products [81]. This was also confirmed for APP overexpressing human muscle fibers. While basal expression of UPR-related proteins in another report did not differ in APP overexpressing cells from wild type cells, UPR induction by ER-stress was augmented [82]. This was even higher in cells with overexpression of mutant APP. In contrast, elevated but comparable GRP78 mRNA levels were measured in B103 cells expressing either mutated or wild type APP after UPR induction with Tunicamycin [83]. In PC12 cells, APP has been reported to be protective against ER-stress evoked by brefeldin A application while GRP78 or CHOP expression remained unaffected. In sum, there is a rather inhomogeneous picture of how APP might interfere with ER-stress and subsequent signaling. This might be explained by different types of cells used in either investigation which might be characterized by differential APP processing activities since for proteolytic fragments of APP there is growing evidence for interfering with UPR and ER-stress (**Figure 2**). Mostly, reduction of A-beta is correlated with attenuated ER-stress and vice versa. For example, aged PS2 mutant mice revealed inhibited BACE-1 activity and C99 amount in brain tissue upon treadmill exercise [84]. This was accompanied by a down-regulation of GRP78 and PDI enzymes as well as an inhibited activation status of PERK, eIF2-alpha, ATF6 and sXBP-1. In GNE myopathy that is characterized by A-beta deposition, muscle biopsies showed enhanced expression of molecular chaperones such as GRP78 [85]. This might be interpreted as mere coincidence but direct application of A-beta also has been demonstrated to lead to ER-stress signaling: GRP78 and XBP-1 protein levels increased for example in neurons treated with A-beta [86] which could be further augmented by mitochondrial dysfunction. SK-S-SH cells displayed activation of the PERK pathway as well as increase in CHOP upon A-beta administration [87]. Another publication on the contrary found triggering of eIF2-alpha phosphorylation and calcium depletion from the ER, but no activation of UPR (as shown e.g. by splicing of XBP-1 mRNA, amount of XBP-1 mRNA and PERK phosphorylation) in primary cortical neurons [88]. The A-beta1-42 peptide used in this study comprised both, oligomeric and fibril forms and this might be the cause of observing no induction of UPR. Chafekar and colleagues demonstrated mild induction of the signaling pathway only by oligomers and not by fibrils [89]. A very recent report on human iPSC derived neurons from familial and sporadic Alzheimer cases confirmed that A-beta oligomer accumulation leads to ER as well as oxidative stress [90]. The mechanism behind this is still not fully understood: low molecular A-beta peptides have been described to interrupt mitochondria-ER anchoring and thereby to evoke ER collapse [91]. Yoon *et al* reported an AMPK-mediated translational block upon application of A-beta 42 oligomers [92]. This subsequently inhibited mTOR signaling and resulted in activated ER-stress as shown by eIF2-alpha phosphorylation in rat hippocampal neurons [92]. Interestingly, monomeric A-beta peptides as well as fibrils here failed to activate AMPK.

Not only A-beta peptides are thought to interfere with ER-stress but single reports also exist on other cleavage products - the APP intracellular domain (AICD) and the fragment produced by alpha-secretase-cleavage (APPs-alpha). The AICD is discussed to act as a transcription factor in analogy to the Notch C-terminal domain [93]. Regarding this, infliction in signal transduction to the nucleus by the UPR-prone transcription factors ATF6, 4 and sXBP-1 seems plausible. Takahashi and coworkers found increased CHOP mRNA and protein level in APP overexpressing cells. This could be attenuated by treatment with DAPT (a potent gamma-secretase inhibitor) and occurred also upon transfection with a tagged AICD variant [94]. CHIP assays in AICD transfected HEK293 cells additionally indicated a physical interaction of the AICD with the CHOP promoter region. Nevertheless, another group reported that AICD overexpression in SHEP neuroblastoma cells did not enhance GRP78 and CHOP expression but led to potentiation of ER-stress driven apoptosis [95]. This would rather indicate that AICD might act downstream or independently from UPR. APPs-alpha, which is released via alpha-secretase activity on APP, seems to provide protection against ER-stress: Guo et al. [96] described an NF-kappa B-dependent stabilization of intracellular calcium homeostasis in differentiated PC12 cells by APPs-alpha. In addition, enhancement of APPs-alpha secretion via DHA-treatment was observed to be protective against apoptosis induced by ER Ca(2+)

store depletion via Thapsigargin in HEK293-APP cells [97]. This protective potential could be transferred to untransfected HEK293 or PC12 cells using the supernatant of DHA-treated cells.

For other cleavage products of APP such as APPs-beta, C99 and C83 as wells as p3 to our knowledge no literature exist so far that describes entangling in ER-stress and downstream signaling.

Influence of tau and APP-modifying molecules on ER-stress

A-beta peptides are just one component that triggers or induces AD pathology: a growing number of molecules has been correlated to this type of dementia, which makes it difficult to reflect a complete picture of interference with ER-stress. Therefore, we here focus on tau as the second central player and proteins, directly acting on APP.

An investigation by Unterberger [98] indicated the importance for tau proteins in ER-stress response by demonstrating that in human prion diseases activated PERK and eIF2-alpha only occurred concomitantly to neurofibrillary pathology. In contrast, phosphorylated PERK correlated with hyperphosphorylated forms of tau protein in AD. This connection of UPR activation and the microtubule-associated protein tau has been confirmed in a wide range of publications within the last years. Hoozemans and colleagues described that phospho-PERK was absent from neurofibrillary tangles but abundantly detectable in neurons with hyperphosphorylated tau [99]. The percentage of affected neurons thereby increased with the Braak stage for neurofibrillary changes. In frontotemporal lobar degeneration with Tau pathology (FTLD-tau) phospho-PERK and phospho-IRE1-alpha were increased in a similar way while FTLD without tau pathology or non-neurological control cases showed no signs of UPR activation in neurons and glia [100]. The implication of tau in UPR has also been shown in animal models of tau-pathology such as in [101] where high levels of activated PERK and eIF2-alpha were identified in the hippocampus of aged tau-transgenic mice (P301L). This is contradicted by a paper from Spatara and colleague [102]: they were not able to demonstrate activation of UPR in a mouse line where the P301S variant of tau was expressed (aged 6 and 11 months). They investigated XBP-1 splicing by splice variant specific PCR which might be difficult in tissue with low abundance of sXBP-1. No significant changes as compared to tissue of wild-type mice in calreticulin and GRP78 mRNA levels were found; unfortunately it is not clear whether those samples were from 6 month or 11 month old mice, which impairs a direct comparison with the data from Ho et al. [101]. In 9 month old rTg4510 mice (advanced stage of disease) phospho-PERK was significantly increased in comparison to non-transgenic control mice [103]. This was accompanied by an increase in GRP78 and occurred in the hippocampus and cortex of the mice, regions severely affected by tau pathology in this disease model. Suppression of the transgene by the TET-off-system for one month revised the phospho-PERK elevation as did the acute suppression for 4 days: decrease of phospho-PERK and GRP78 strongly suggests reversibility of ER-stress induction by tau protein [103].

Besides the colocalization of phospho-PERK and phospho-tau, Ho et al. [101] described a direct influence of ER-stress on tau metabolism: Thapsigargin stimulated phosphorylation of tau (Thr231, Ser262 and Ser396) as well as its cleavage [101]. This "vicious cycle" was also shown for neuronal and non-neuronal cell lines SH-SY5Y and HEK293 and rat brain preparations [104]. Recently, in addition an increase of total endogenous tau protein in cultured neurons and primary cultured neurons has been described due to a reduction in the degradation rate of tau under ER-stress [105].

Interestingly, UPR here directly links A-beta and tau pathology via ER-stress signaling: oligomeric A-beta peptides have repeatedly been linked to ER-stress (see **Figure 2**) and release of calcium from the ER leads to activation of GSK3-beta, a major tau-kinase, in primary rat embryonic cortical neurons [106]. Moreover, ventricular infusion of ER-stressors in rats resulted in GSK3-beta activation and tau hyperphosphorylation [107]. In addition, GRP78 was elevated and an enhanced binding of GSK3-beta and tau to this chaperone was demonstrated in brain tissue from Tunicamycin-treated animals. In HEK293 cells with overexpression of GRP78 and tau this increase in binding levels occurred in a similar manner. siRNA-mediated knock down of GRP78 in HEK/

Table 1. Changes in ER-stress signaling in AD and AD animal models

AD (human patients)	Severity of disease/tissue	Components of ER-stress pathway	Reference
	Stage 5 to 6	Accumulation of CD3-delta (ERAD substrate)	[103]
		Correlation of toxic turn A-beta with GRP78	[133]
		Reduced HRD1 protein levels, increased mRNA (function in ERAD)	[140]
		Increase in p-eIF2-alpha, ATF4, CHOP, and PERK	[92]
		Pro-apoptotic ER-stress pathway molecules increase with AD severity Pro-homeostatic ER-stress molecules mainly upregulated in the intermediate stage of AD	[137]
	Hippocampus and frontal lobe	PDI immuno-positive inclusions (NFTs)	[139]
	Stage 1 to 6 Temporal cortex	Increased XBP-1 splicing and PDI expression CHOP activation	[87]
	Temporal cortex	Reduction in GRP78 and 94	[76]
	Frontal cortex	Phosphorylation of eIF2-alpha upregulated	[110]
	Temporal cortex	Phosphorylation of eIF2-alpha upregulated	[113]
	Hippocampus CA1 region	Phospho-PERK immunopositive neurons	[99]
	Hippocampus and temporal cortex	Phosphorylation of eIF2-alpha upregulated	[131]
	Stage 3 to 6 Temporal and frontal cortex	sXBP-1 mRNA level downregulated	[120]
AD models	Model		
	rTg4510 mice (tauopathy) 9 months	Activation of PERK Accumulation of CD3-delta (ERAD substrate)	[103]
	3x Tg-AD mice 2 months	Increased GRP78	[133]
	APP(E693Δ) mice 18 months	up-regulation of GRP78 and HRD1	[135]
	A-beta transgenic flies	suppression of neurotoxicity by sXBP-1	[138]
	Tg2576 mice 17 months	No activation of UPR or apoptosis	[87]
	5xFAD 6 months	Phosphorylation of eIF2-alpha upregulated	[110]
	APP/PS1 9 months	Phosphorylation of eIF2-alpha upregulated	[113]
	5xFAD 1 and 9 month APP/PS1 6 and 9 month	sXBP-1 mRNA level increased (1 and 6 month) sXBP-1 mRNA level decreased (9 month)	[120]

tau cells revised tau hyperphosphorylation upon Thapsigargin-application while GSK3-beta was still activated [107]. This in sum reflects the ambivalence of ER-stress driven signaling: once induced, it might even worsen degenerative processes, but activation of ER-stress induced UPR - e.g. via tau hyperphosphorylation - might also contribute to protection against apoptosis. HEK cells that overexpress tau for example revealed attenuated apoptosis in response to treatment with ER-stress inducers such as staurosporine or camptothecin [107].

For involvement of APP-modifying proteinases in ER-stress signaling, only scattered reports exist: for instance increased production of BACE-1 mRNA and non-coding antisense transcript has been reported in sporadic inclusion-body myositis muscle fibers [108] which have been correlated with increased ER-stress signaling [81]. Both transcripts were also elevated by experimentally evoked ER-stress via Tunicamycin or Thapsigargin in cultured human muscle cells [108]. In the APP/PS1 AD mouse model at 3, 6 and 12 months of age hippocampal neurons showed increased staining for PERK phosphorylation [109]. At 3 month also phospho-eI2Fa levels were elevated in brain tissue homogenates in comparison to wild type mice. Salubrinal, an inhibitor of eIF2-alpha

phosphatase PP1c, increased BACE1 and subsequently A-beta production in primary neurons [110]. HSV1 transfection of SH-SY5Y cells which leads to activation of PRK - an alternative kinase that phosphorylates eI2F-alpha - strongly increased BACE-1 protein amounts [111]. Moreover, inhibition of eIF2-alpha phosphatase de-repressed the signal from a BACE1-5'UTR-luciferase reporter in HeLa cells, indicating that this is an important pathway regulating BACE1 translational repression [112]. If PKR or PERK both contribute in a similar manner to the regulation has to be investigated. However, CSF levels of PKR and phospho-PKR were found to be elevated in AD and amnestic mild cognitive impairment subjects [113] and the latter was also linked to cognitive decline measured by longitudinal MMSE changes [114].

Regarding gamma-secretase, very early on correlation to ER-stress has been suggested (see above) by the observation that PS1 knock-out fibroblasts revealed a reduction in nuclear translocation and lowered UPR signaling [77]. But again, the influence seems to be a mutual one: Tunicamycin application *in vivo* enhanced PS1 expression in mouse kidney [115]. Furthermore, it has been demonstrated that ATF4 binds to the amino acid response element (AARE) regulatory region of human PS1 gene. Quercetin, which induces XBP-1 splicing but suppresses ATF4 activation, prevented the Tunicamycin-evoked increase in PS1 and subsequently production of A-beta peptides in HEK293 cells [116].

Takahashi et al. described in 2009 that Tunicamycin not only induces AICD production in HEK293 but also C83, the C-terminal fragment derived by cleavage of APP by alpha-secretase [94]. Treatment of retinal pigment epithelia cells (ARPE19) with Tunicamycin or Thapsigargin for 24hrs revealed enhanced amounts of TACE-mRNA [117]. TACE (tumour necrosis factor alpha converting enzyme, ADAM17) is widely accepted as the regulated alpha-secretase (for a comparison of ADAM10 and 17 physiological roles see [118]). The TACE-induction by ER-stress was also observed for several tumor cell lines such as HeLa or MCF7 [119]. By applying siRNA targeted against central players of the three arms of UPR - ATF4, XBP-1 and ATF6 - it was demonstrated that only ATF4 and 6 are able to act as regulators of TACE expression. ATF4 had the most prominent effect and was shown to bind at least to one of the three predicted binding sites of the TACE promoter by CHIP analysis [119]. This has been confirmed by overexpression of active XBP-1 in SH-SY5Y human neuroblastoma cells where TACE mRNA as well as protein was not elevated [120]. Interestingly, despite the failure of XBP-1 in enhancing TACE expression, secretion of APPs-alpha was induced. This has been shown to be based on upregulation of ADAM10 expression, the major alpha-secretase in neuronal tissue [11, 121, 122]. Mice with B-cells deleted in Adam10 contained normal numbers of plasma cells but were impaired in antibody responses [123]. This was accompanied by reduced amounts of transcription factors implicated in plasma cell function such as XBP-1.

In sum, different parts of ER-stress and UPR signaling are involved in a multimodal manner in APP processing as well as tau metabolism and players of AD pathogenesis by themselves affect ER-stress and adequate response of the cell due to stress.

ER-stress signaling in animal models of AD and human patients

Most transgenic models of AD are based on the amyloid hypothesis and therefore are predicated on genetic mutations of human AD-relevant genes such as APP or PS1, which have been identified in familial AD cases. These models mimic in part AD-like pathological features indicated e.g. by increased A-beta peptide generation, tau fibrillization or even cognitive impairment (reviewed in [124]). In this section we summarize the regulation of crucial ER-stress components belonging to one of the three branches (PERK, ATF6 or IRE1-alpha) in AD animal models and compare them to knowledge obtained by brain samples derived from human AD-patients (for an overview see **Table 1**).

Regarding the PERK pathway, in the rTg4510 tau-based Alzheimer mouse model a significant increase in activated phosphorylated PERK was observed at 9 month of age [103]. This is a rather aggressive model, where pathological features such as tangle formation, deficits in neuronal function or cognitive decline occur as early as 3 or 5.5 months of age [125, 126]. Tissues severely affected by tau fibrillization such as hippocampus and cortex displayed a 2.4-fold increase in phospho-PERK [103].

These findings are consistent with analyses regarding AD brain samples: immunopositive phospho-PERK neurons were found in hippocampal CA1 region and the amount was significantly increased as compared to non-demented [99]. Furthermore, activation of PERK was positively correlated with advanced Braak scores and consequently with severity of disease. Longitudinal study of tau pathology and accumulation of phospho-PERK revealed also a correlation in the rTg4510 mouse model as early as 6 month of age (first time point investigated: 3 month) [103]. The influence of tau on ER-stress might be rather indirect because pathological tau did not colocalize with an ER-marker. Human cortical sections of advanced Braak stages (5-6) which also display robust accumulation of hyperphosphorylated tau confirmed that aberrant tau and the-ER marker calnexin are not colocalized. As tau was shown to co-immunoprecipitated with the ERAD protein complex members VCP and HRD1 this might explain triggering of ER-stress by tau.

In whole brain lysates of Tg2576 mice, which overexpress the Swedish mutant of human APP [127] activation/phosphorylation of the PERK downstream target eIF2-alpha was demonstrated and positively correlated with an increased expression of BACE-1 [110]. For this analysis 9 month old mice which already exhibit maximum plaque formation were further challenged by energy deprivation, therefore activation of PERK signaling might be due to the specific experimental paradigms. However, the induction of ER-stress in an APP-based mouse model was further substantiated by analysis using an aggressive amyloid deposition mouse model - 5xFAD, which display detectable A-beta peptide generation already at 1 month of age [128]. In 6 month old 5xFAD mice with a severe amyloid pathology the BACE-1 expression level was increased 1.7-fold as compared to non-transgenic littermates [110]. This was accompanied by an increased ratio of phospho-eIF2-alpha to total eIF2-alpha. The regulation of the BACE-1 expression by active eIF2-alpha could be mechanistically elucidated by Mouton-Liger and colleagues: in 9 month old APP/PS1 mice, which already show neuronal loss (detectable at 6 month of age [129]) the expression of BACE-1 was regulated by active eIF2-alpha under the control of PKR [113]. On the contrary, analysis of cortical samples of aged Tg2576 mice (17 month of age) with massive plaque formation revealed no significant change in CHOP expression, which is the most prominent downstream target of the PERK pathway [49]. These contradictory results might be explained by the different ages of animals used in the studies. ER-stress is known to be a transient process with the IRE1-alpha-branch being down-regulated with prolonged exposure to respective signals [130]. As CHOP induction was reported to maintain due to sustained stress at least in human cells, counter-regulation in old mice is to be debatable. Nevertheless, immunoblot analysis of human post-mortem frontal cortex tissue of AD-patients revealed a positive correlation of active eIF2-alpha with BACE-1 protein level and also with amyloid load of AD brain samples [110]. Increased levels of active eIF2-alpha have also been described in temporal cortex [113, 131] and hippocampal tissue [131] of AD-patients. Moreover, CHOP has been reported to be increased in temporal [87] and frontal [92] cortex tissue as compared to age-matched controls.

In sum, literature is almost consistent with an overall upregulation of single PERK-pathway components e.g. PERK, eIF2-alpha and CHOP in AD or aggressive disease models. CHOP is responsible for the regulation of apoptosis under ER-stress conditions e.g. by ATF5 induction [132]. Therefore neuronal cell death in AD might be partially understood as a consequence of long lasting ER-stress in the brain.

For the most prominent ATF6-mediated ER-stress marker GRP78 the field of literature is more heterogeneous: for example it has been demonstrated that GRP78 is significantly upregulated in two different AD mouse models. In neurons of 3xTg AD mice aged 2 month an increase in GRP78 expression was detected [133]. Mice at this age are cognitively unimpaired und consequently are representative for a pre-pathological stage [134]. Umeda and colleagues described an increase of GRP78 expression in hippocampal neurons and cerebral cortex of APP (E693Δ) mice aged 18 month [135]. These mice display impaired hippocampal synaptic plasticity at an age of 8 month and even neuronal loss detectable at 24 month of age [136]. In addition, no expression changes of GRP78 were found in in the brain of 17 month old Tg2576 mice [87]. Comparably, analysis of human post mortem samples of AD-patients are characterized by contradictory

results: a positive correlation of intraneuronal A-beta peptides with the expression of GRP78 has been reported by double-label immunostaining of AD brain sections as compared to those of healthy controls [133]. Consistent with this, the GRP78 protein level was significantly increased in cortical tissue derived from AD brains as compared to samples from non-demented [131]. On the contrary, Katayama and colleagues have shown that expression level of this protein was slightly reduced in temporal cortex samples derived from sporadic AD cases and even more reduced in the brain of patients with familial AD linked to PS1 mutations [76].

Existing literature does not allow a final appraisal of GRP78 expression in brain tissue of AD-patients due to missing characterization of samples regarding e.g. Braak stages. However, one possible attempt to explain these heterogeneous results might be the two-sited direction of ER-stress signaling dependent on the intensity and the duration of stress signals. Expression of molecules ensuring recovery of ER function and homeostasis were rather induced at intermediate disease stages while for progressed disease severity pro-apoptotic mediators were predominant in an investigation from de la Monte and colleagues [137].

Concerning the IRE1-alpha pathway, a *Drosophila* model with human A-beta expression underlined a potential neuroprotective function of XBP-1, the main downstream target of IRE1-alpha [138]. Those flies show a strong A-beta-dependent phenotype in the eye regarding structure and size of the organ. These pathological changes were alleviated by introducing XBP-1. Such a protective effect of XBP-1 regarding neurodegenerative processes has been further substantiated by a sXBP-1-mediated induction of ADAM10 gene expression [120]. Within two different AD mouse models (APP/PS1 and 5xFAD) sXBP-1 mRNA level were significantly increased in whole brain samples as compared to non-transgenic littermates at early time points of pathological changes (APP/PS1: 6 month; 5xFAD: 1 month). This was accompanied by an increase of ADAM10 expression [120]. Analyzing more advanced stages (9 month of age for both models), XBP-1 returned to wild type levels or was even decreased [120]. However, mRNA level of spliced/active XBP-1 has been reported to be increased in temporal cortex tissue of AD-patients as compared to healthy controls (Braak scores ranged from 1 to 6 for AD samples, [87]). Our own study with a more defined stage of disease (Braak scores 3-6) demonstrated a significant decrease of sXBP-1 in temporal as well as frontal cortex tissue of AD-patients in a larger cohort of individuals [120]. Analyzing the same samples, a significant reduction of ADAM10 as a novel downstream target of XBP-1 in both tissue types was observed. Another downstream target of the transcription factor XBP-1 is the protein disulfide isomerase (PDI) for which Lee and colleagues revealed an unaltered expression level as demonstrated by immunoblot analysis in 17 month old Tg2576 mice (advanced stage of AD-like pathology [87]). However, in the same report this enzyme was found to be upregulated in cortical AD brain tissue and PDI immune-positive neurofibrillary tangles (NFTs) were described in slices from hippocampus and frontal lobe of AD-patients [139]. On the contrary, PDI protein level was unaffected in cerebral cortex samples derived from AD-patients as compared to healthy controls [140]. HRD-1, which is an ERAD-associated E3 ubiquitin ligase acting downstream of XBP-1 [58], was investigated immunohistochemically in 18 month old APP (E693Δ) mice with severe amyloid pathology [135]. Analysis revealed an intense immunoreactivity in hippocampal neurons and cerebral cortex tissue of the animals. However, Kaneko and colleagues showed that HRD1 is downregulated in the cerebral cortex of AD-patients [140]. This is in accordance with an increase of a subunit of the T-cell antigen receptor - CD3-delta, which is a well characterized substrate for ERAD driven proteolysis, in hippocampus of 9 month old rTg4510 mice [103]. Increased accumulation of CD3-delta was also described in temporal brain tissue from AD-patients (Braak scores: 5-6) as compared to non-demented controls (Braak scores: 1-2) and would rather support a defect in XBP-1 evoked ERAD in AD.

Conclusions

Literature predominantly hints at an early but transient induction of XBP-1 signaling in the AD context and an activation of the PERK-dominated pathway throughout to late stages of disease. This suggests ER-stress functioning as a scale in AD pathogenesis, balancing cells between coping with protein misfolding associ-

ated stress and undergoing cell death. Double-edged properties of ER-stress signaling comes clear e.g. in a recent investigation of a *C. elegans* model of Alzheimer's disease: basal activity of the UPR was beneficial under normal conditions, but repression of the signaling delayed toxicity evoked by inducible A-beta peptide expression [141]. Age-onset loss of ER proteostasis could be reversed by neuronal expression of sXBP-1 in *C. elegans* and enhanced longevity [142], pointing at a potential role of UPR in age-related changes which will be interesting to investigate in humans.

All these observations lead to the rather alluring prospect that interfering with ER-stress might bear novel therapeutic approaches regarding neurodegenerative diseases such as AD and has been presented in previous reviews (e.g. [143-145]). For example, administration of CNB-001, a pyrazole-inhibitor of 5-lipoxygenase, was able to induce PERK signaling and improve memory in AD model mice [146]. Nevertheless, several uncertainties and open questions regarding the role of ER-stress in AD remain: 1) Animal models used for investigation of ER-stress signaling under pathological conditions are differing in time of onset of pathological features and no real scaling exists for comparison of "severity of disease" at the investigated age of animals. Only a minority of reports give a longitudinal picture on evolvement of stress which would allow estimating the role of single components in pathology. Investigations using human tissue partly miss characterization of disease stages and data concerning MCI patients and normal aging are missing - at least to our knowledge. 2) The actors of the three signaling branches are phosphorylated proteins and transcription factors and per se are rather unstable or regulated by further posttranslational processing, translocation events or protein interactions (e.g. interplay of ATF4 with p300 acetyltransferase, [147] or SUMO-conjugase UBC9 with sXBP-1, [148]). This might explain why a wide variety of investigations are based on mRNA quantitation which might distort the underlying scenario. 3) Crosstalk of the ER-stress signaling pathways among themselves and with other signal transduction pathways such as insulin signaling [149, 150] further complicate entangling ER-stress involvement in AD. Nevertheless, elucidating ER-stress function or failure in AD might help turning the scale in therapeutic considerations or for evolvement of new highly diagnostic biomarkers.

Acknowledgements

The authors' own work was supported by the Federal Ministry of Education and Research (BMBF) in the framework of the National Genome Research Network (NGFN, FKZ01-GS08130) and by the Alfons Geib Stiftung of the University Medical Centre Mainz.

Disclosure of conflict of interest

The authors declare that they have no conflicts of interest.

Address correspondence to: Dr. Kristina Endres, Department of Psychiatry and Psychotherapy, Clinical Research Group, University Medical Centre Johannes Gutenberg-University Mainz, Untere Zahlbacher Str. 8, D-55131 Mainz, Germany. Tel: 49-06131-172133; Fax: 49-06131-176690; E-mail: kristina.endres@unimedizin-mainz.de

References

[1] Falk RH. Diagnosis and management of the cardiac amyloidoses. Circulation 2005; 112: 2047-2060.

[2] Rapezzi C, Quarta CC, Riva L, Longhi S, Gallelli I, Lorenzini M, Ciliberti P, Biagini E, Salvi F and Branzi A. Transthyretin-related amyloidoses and the heart: a clinical overview. Nat Rev Cardiol 2010; 7: 398-408.

[3] Shi J, Guan J, Jiang B, Brenner DA, del Monte F, Ward JE, Connors LH, Sawyer DB, Semigran MJ, Macgillivray TE, Seldin DC, Falk R and Liao R. Amyloidogenic light chains induce cardiomyocyte contractile dysfunction and apoptosis via a non-canonical p38alpha MAPK pathway. Proc Natl Acad Sci U S A 2010; 107: 4188-4193.

[4] Kayed R and Lasagna-Reeves CA. Molecular mechanisms of amyloid oligomers toxicity. J Alzheimers Dis 2013; 33 Suppl 1: S67-S78.

[5] Cuello AC, Allard S and Ferretti MT. Evidence for the accumulation of Abeta immunoreactive material in the human brain and in transgenic animal models. Life Sci 2012; 91: 1141-1147.

[6] Laferla FM, Green KN and Oddo S. Intracellular amyloid-beta in Alzheimer's disease. Nat Rev Neurosci 2007; 8: 499-509.

[7] Krstic D and Knuesel I. Deciphering the mechanism underlying late-onset Alzheimer disease. Nat Rev Neurol 2013; 9: 25-34.

[8] Vassar R, Bennett BD, Babu-Khan S, Kahn S, Mendiaz EA, Denis P, Teplow DB, Ross S, Ama-

rante P, Loeloff R, Luo Y, Fisher S, Fuller J, Edenson S, Lile J, Jarosinski MA, Biere AL, Curran E, Burgess T, Louis JC, Collins F, Treanor J, Rogers G and Citron M. Beta-secretase cleavage of Alzheimer's amyloid precursor protein by the transmembrane aspartic protease BACE. Science 1999; 286: 735-741.

[9] Anderson JP, Chen Y, Kim KS and Robakis NK. An alternative secretase cleavage produces soluble Alzheimer amyloid precursor protein containing a potentially amyloidogenic sequence. J Neurochem 1992; 59: 2328-2331.

[10] Lammich S, Kojro E, Postina R, Gilbert S, Pfeiffer R, Jasionowski M, Haass C and Fahrenholz F. Constitutive and regulated alpha-secretase cleavage of Alzheimer's amyloid precursor protein by a disintegrin metalloprotease. Proc Natl Acad Sci U S A 1999; 96: 3922-3927.

[11] Postina R, Schroeder A, Dewachter I, Bohl J, Schmitt U, Kojro E, Prinzen C, Endres K, Hiemke C, Blessing M, Flamez P, Dequenne A, Godaux E, van Leuven F and Fahrenholz F. A disintegrin-metalloproteinase prevents amyloid plaque formation and hippocampal defects in an Alzheimer disease mouse model. J Clin Invest 2004; 113: 1456-1464.

[12] Buxbaum JD, Liu KN, Luo Y, Slack JL, Stocking KL, Peschon JJ, Johnson RS, Castner BJ, Cerretti DP and Black RA. Evidence that tumor necrosis factor alpha converting enzyme is involved in regulated alpha-secretase cleavage of the Alzheimer amyloid protein precursor. J Biol Chem 1998; 273: 27765-27767.

[13] Skovronsky DM, Moore DB, Milla ME, Doms RW and Lee VM. Protein kinase C-dependent alpha-secretase competes with beta-secretase for cleavage of amyloid-beta precursor protein in the trans-golgi network. J Biol Chem 2000; 275: 2568-2575.

[14] Chasseigneaux S and Allinquant B. Functions of Abeta, sAPPalpha and sAPPbeta : similarities and differences. J Neurochem 2012; 120 Suppl 1: 99-108.

[15] Rodrigue KM, Kennedy KM and Park DC. Beta-amyloid deposition and the aging brain. Neuropsychol Rev 2009; 19: 436-450.

[16] Araki K and Nagata K. Protein folding and quality control in the ER. Cold Spring Harb Perspect Biol 2012; 4: a015438

[17] Benham AM. Protein secretion and the endoplasmic reticulum. Cold Spring Harb Perspect Biol 2012; 4: a012872

[18] Vance JE. Phospholipid synthesis in a membrane fraction associated with mitochondria. J Biol Chem 1990; 265: 7248-7256.

[19] Raturi A and Simmen T. Where the endoplasmic reticulum and the mitochondrion tie the knot: the mitochondria-associated membrane (MAM). Biochim Biophys Acta 2013; 1833: 213-224.

[20] de Brito OM and Scorrano L. Mitofusin 2 tethers endoplasmic reticulum to mitochondria. Nature 2008; 456: 605-610.

[21] Registre M, Goetz JG, St Pierre P, Pang H, Lagacé M, Bouvier M, Le PU and Nabi IR. The gene product of the gp78/AMFR ubiquitin E3 ligase cDNA is selectively recognized by the 3F3A antibody within a subdomain of the endoplasmic reticulum. Biochem Biophys Res Commun 2004; 320: 1316-1322.

[22] Ogata M, Hino S, Saito A, Morikawa K, Kondo S, Kanemoto S, Murakami T, Taniguchi M, Tanii I, Yoshinaga K, Shiosaka S, Hammarback JA, Urano F and Imaizumi K. Autophagy is activated for cell survival after endoplasmic reticulum stress. Mol Cell Biol 2006; 26: 9220-9231.

[23] Pankiv S, Clausen TH, Lamark T, Brech A, Bruun JA, Outzen H, Øvervatn A, Bjørkøy G and Johansen T. p62/SQSTM1 binds directly to Atg8/LC3 to facilitate degradation of ubiquitinated protein aggregates by autophagy. J Biol Chem 2007; 282: 24131-24145.

[24] Walter P and Ron D. The unfolded protein response: from stress pathway to homeostatic regulation. Science 2011; 334: 1081-1086.

[25] Dyrks T, Dyrks E, Mönning U, Urmoneit B, Turner J and Beyreuther K. Generation of beta A4 from the amyloid protein precursor and fragments thereof. FEBS Lett 1993; 335: 89-93.

[26] Sambamurti K, Shioi J, Anderson JP, Pappolla MA and Robakis NK. Evidence for intracellular cleavage of the Alzheimer's amyloid precursor in PC12 cells. J Neurosci Res 1992; 33: 319-329.

[27] Selfridge JE, E L, Lu J and Swerdlow RH. Role of mitochondrial homeostasis and dynamics in Alzheimer's disease. Neurobiol Dis 2013; 51: 3-12.

[28] Barnett A and Brewer GJ. Autophagy in aging and Alzheimer's disease: pathologic or protective? J Alzheimers Dis 2011; 25: 385-394.

[29] Stutzmann GE and Mattson MP. Endoplasmic reticulum Ca(2+) handling in excitable cells in health and disease. Pharmacol Rev 2011; 63: 700-727.

[30] Bernales S, Soto MM and McCullagh E. Unfolded protein stress in the endoplasmic reticulum and mitochondria: a role in neurodegeneration. Front Aging Neurosci 2012; 4: 5

[31] Hoozemans JJ, van Haastert ES, Nijholt DA, Rozemuller AJ and Scheper W. Activation of the unfolded protein response is an early event in Alzheimer's and Parkinson's disease. Neurodegener Dis 2012; 10: 212-215.

[32] Wang XZ, Harding HP, Zhang Y, Jolicoeur EM, Kuroda M and Ron D. Cloning of mammalian Ire1 reveals diversity in the ER stress responses. EMBO J 1998; 17: 5708-5717.

[33] Cox JS, Shamu CE and Walter P. Transcriptional induction of genes encoding endoplasmic reticulum resident proteins requires a transmembrane protein kinase. Cell 1993; 73: 1197-1206.
[34] Nikawa J and Yamashita S. IRE1 encodes a putative protein kinase containing a membrane-spanning domain and is required for inositol phototrophy in Saccharomyces cerevisiae. Mol Microbiol 1992; 6: 1441-1446.
[35] Meurs E, Chong K, Galabru J, Thomas NS, Kerr IM, Williams BR and Hovanessian AG. Molecular cloning and characterization of the human double-stranded RNA-activated protein kinase induced by interferon. Cell 1990; 62: 379-390.
[36] Haze K, Yoshida H, Yanagi H, Yura T and Mori K. Mammalian transcription factor ATF6 is synthesized as a transmembrane protein and activated by proteolysis in response to endoplasmic reticulum stress. Mol Biol Cell 1999; 10: 3787-3799.
[37] Zhu C, Johansen FE and Prywes R. Interaction of ATF6 and serum response factor. Mol Cell Biol 1997; 17: 4957-4966.
[38] Hai TW, Liu F, Coukos WJ and Green MR. Transcription factor ATF cDNA clones: an extensive family of leucine zipper proteins able to selectively form DNA-binding heterodimers. Genes Dev 1989; 3: 2083-2090.
[39] Hollien J. Evolution of the unfolded protein response. Biochim Biophys Acta 2013; 1833: 2458-2463.
[40] Nadanaka S, Okada T, Yoshida H and Mori K. Role of disulfide bridges formed in the luminal domain of ATF6 in sensing endoplasmic reticulum stress. Mol Cell Biol 2007; 27: 1027-1043.
[41] Ye J, Rawson RB, Komuro R, Chen X, Davé UP, Prywes R, Brown MS and Goldstein JL. ER stress induces cleavage of membrane-bound ATF6 by the same proteases that process SREBPs. Mol Cell 2000; 6: 1355-1364.
[42] Adachi Y, Yamamoto K, Okada T, Yoshida H, Harada A and Mori K. ATF6 is a transcription factor specializing in the regulation of quality control proteins in the endoplasmic reticulum. Cell Struct Funct 2008; 33: 75-89.
[43] Harding HP, Zhang Y and Ron D. Protein translation and folding are coupled by an endoplasmic-reticulum-resident kinase. Nature 1999; 397: 271-274.
[44] Marciniak SJ, Garcia-Bonilla L, Hu J, Harding HP and Ron D. Activation-dependent substrate recruitment by the eukaryotic translation initiation factor 2 kinase PERK. J Cell Biol 2006; 172: 201-209.
[45] Sood R, Porter AC, Ma K, Quilliam LA and Wek RC. Pancreatic eukaryotic initiation factor-2alpha kinase (PEK) homologues in humans, Drosophila melanogaster and Caenorhabditis elegans that mediate translational control in response to endoplasmic reticulum stress. Biochem J 2000; 346: 281-293.
[46] Harding HP, Novoa I, Zhang Y, Zeng H, Wek R, Schapira M and Ron D. Regulated translation initiation controls stress-induced gene expression in mammalian cells. Mol Cell 2000; 6: 1099-1108.
[47] Ernst V, Levin DH and London IM. Inhibition of protein synthesis initiation by oxidized glutathione: activation of a protein kinase that phosphorylates the alpha subunit of eukaryotic initiation factor 2. Proc Natl Acad Sci U S A 1978; 75: 4110-4114.
[48] Ma Y, Brewer JW, Diehl JA and Hendershot LM. Two distinct stress signaling pathways converge upon the CHOP promoter during the mammalian unfolded protein response. J Mol Biol 2002; 318: 1351-1365.
[49] Lee YY, Cevallos RC and Jan E. An upstream open reading frame regulates translation of GADD34 during cellular stresses that induce eIF2alpha phosphorylation. J Biol Chem 2009; 284: 6661-6673.
[50] Tabas I and Ron D. Integrating the mechanisms of apoptosis induced by endoplasmic reticulum stress. Nat Cell Biol 2011; 13: 184-190.
[51] Novoa I, Zeng H, Harding HP and Ron D. Feedback inhibition of the unfolded protein response by GADD34-mediated dephosphorylation of eIF2alpha. J Cell Biol 2001; 153: 1011-1022.
[52] Liu CY, Schröder M and Kaufman RJ. Ligand-independent dimerization activates the stress response kinases IRE1 and PERK in the lumen of the endoplasmic reticulum. J Biol Chem 2000; 275: 24881-24885.
[53] Tirasophon W, Lee K, Callaghan B, Welihinda A and Kaufman RJ. The endoribonuclease activity of mammalian IRE1 autoregulates its mRNA and is required for the unfolded protein response. Genes Dev 2000; 14: 2725-2736.
[54] Ali MM, Bagratuni T, Davenport EL, Nowak PR, Silva-Santisteban MC, Hardcastle A, McAndrews C, Rowlands MG, Morgan GJ, Aherne W, Collins I, Davies FE and Pearl LH. Structure of the Ire1 autophosphorylation complex and implications for the unfolded protein response. EMBO J 2011; 30: 894-905.
[55] Mannan MA, Shadrick WR, Biener G, Shin BS, Anshu A, Raicu V, Frick DN and Dey M. An ire1-phk1 chimera reveals a dispensable role of autokinase activity in endoplasmic reticulum stress response. J Mol Biol 2013; 425: 2083-2099.
[56] Korennykh AV, Korostelev AA, Egea PF, Finer-Moore J, Stroud RM, Zhang C, Shokat KM and Walter P. Structural and functional basis for RNA cleavage by Ire1. BMC Biol 2011; 9: 47.

[57] Yoshida H, Nadanaka S, Sato R and Mori K. XBP1 is critical to protect cells from endoplasmic reticulum stress: evidence from Site-2 protease-deficient Chinese hamster ovary cells. Cell Struct Funct 2006; 31: 117-125.
[58] Yamamoto K, Suzuki N, Wada T, Okada T, Yoshida H, Kaufman RJ and Mori K. Human HRD1 promoter carries a functional unfolded protein response element to which XBP1 but not ATF6 directly binds. J Biochem 2008; 144: 477-486.
[59] Wang S, Chen Z, Lam V, Han J, Hassler J, Finck BN, Davidson NO and Kaufman RJ. IRE1alpha-XBP1s induces PDI expression to increase MTP activity for hepatic VLDL assembly and lipid homeostasis. Cell Metab 2012; 16: 473-486.
[60] Kanemoto S, Kondo S, Ogata M, Murakami T, Urano F and Imaizumi K. XBP1 activates the transcription of its target genes via an ACGT core sequence under ER stress. Biochem Biophys Res Commun 2005; 331: 1146-1153.
[61] Urano F, Wang X, Bertolotti A, Zhang Y, Chung P, Harding HP and Ron D. Coupling of stress in the ER to activation of JNK protein kinases by transmembrane protein kinase IRE1. Science 2000; 287: 664-666.
[62] Hollien J, Lin JH, Li H, Stevens N, Walter P and Weissman JS. Regulated Ire1-dependent decay of messenger RNAs in mammalian cells. J Cell Biol 2009; 186: 323-331.
[63] Iwakoshi NN, Lee AH, Vallabhajosyula P, Otipoby KL, Rajewsky K and Glimcher LH. Plasma cell differentiation and the unfolded protein response intersect at the transcription factor XBP-1. Nat Immunol 2003; 4: 321-329.
[64] Reimold AM, Iwakoshi NN, Manis J, Vallabhajosyula P, Szomolanyi-Tsuda E, Gravallese EM, Friend D, Grusby MJ, Alt F and Glimcher LH. Plasma cell differentiation requires the transcription factor XBP-1. Nature 2001; 412: 300-307.
[65] Teske BF, Wek SA, Bunpo P, Cundiff JK, McClintick JN, Anthony TG and Wek RC. The eIF2 kinase PERK and the integrated stress response facilitate activation of ATF6 during endoplasmic reticulum stress. Mol Biol Cell 2011; 22: 4390-4405.
[66] Wang Y, Shen J, Arenzana N, Tirasophon W, Kaufman RJ and Prywes R. Activation of ATF6 and an ATF6 DNA binding site by the endoplasmic reticulum stress response. J Biol Chem 2000; 275: 27013-27020.
[67] Yamamoto K, Yoshida H, Kokame K, Kaufman RJ and Mori K. Differential contributions of ATF6 and XBP1 to the activation of endoplasmic reticulum stress-responsive cis-acting elements ERSE, UPRE and ERSE-II. J Biochem 2004; 136: 343-350.
[68] Roy B and Lee AS. The mammalian endoplasmic reticulum stress response element consists of an evolutionarily conserved tripartite structure and interacts with a novel stress-inducible complex. Nucleic Acids Res 1999; 27: 1437-1443.
[69] Kokame K, Kato H and Miyata T. Identification of ERSE-II, a new cis-acting element responsible for the ATF6-dependent mammalian unfolded protein response. J Biol Chem 2001; 276: 9199-9205.
[70] Yoshida H, Okada T, Haze K, Yanagi H, Yura T, Negishi M and Mori K. Endoplasmic reticulum stress-induced formation of transcription factor complex ERSF including NF-Y (CBF) and activating transcription factors 6alpha and 6beta that activates the mammalian unfolded protein response. Mol Cell Biol 2001; 21: 1239-1248.
[71] Misiewicz M, Déry MA, Foveau B, Jodoin J, Ruths D and le Blanc AC. Identification of a Novel Endoplasmic Reticulum Stress Response Element Regulated by XBP1. J Biol Chem 2013; 288: 20378-20391.
[72] Yoshida H, Haze K, Yanagi H, Yura T and Mori K. Identification of the cis-acting endoplasmic reticulum stress response element responsible for transcriptional induction of mammalian glucose-regulated proteins. Involvement of basic leucine zipper transcription factors. J Biol Chem 1998; 273: 33741-33749.
[73] Acosta-Alvear D, Zhou Y, Blais A, Tsikitis M, Lents NH, Arias C, Lennon CJ, Kluger Y and Dynlacht BD. XBP1 controls diverse cell type- and condition-specific transcriptional regulatory networks. Mol Cell 2007; 27: 53-66.
[74] Prostko CR, Brostrom MA, Malara EM and Brostrom CO. Phosphorylation of eukaryotic initiation factor (eIF) 2 alpha and inhibition of eIF-2B in GH3 pituitary cells by perturbants of early protein processing that induce GRP78. J Biol Chem 1992; 267: 16751-16754.
[75] Shinjo S, Mizotani Y, Tashiro E and Imoto M. Comparative analysis of the expression patterns of UPR-target genes caused by UPR-inducing compounds. Biosci Biotechnol Biochem 2013; 77: 729-735.
[76] Katayama T, Imaizumi K, Sato N, Miyoshi K, Kudo T, Hitomi J, Morihara T, Yoneda T, Gomi F, Mori Y, Nakano Y, Takeda J, Tsuda T, Itoyama Y, Murayama O, Takashima A, St George-Hyslop P, Takeda M and Tohyama M. Presenilin-1 mutations downregulate the signalling pathway of the unfolded-protein response. Nat Cell Biol 1999; 1: 479-485.
[77] Niwa M, Sidrauski C, Kaufman RJ and Walter P. A role for presenilin-1 in nuclear accumulation of Ire1 fragments and induction of the mammalian unfolded protein response. Cell 1999; 99: 691-702.

[78] Steiner H, Winkler E, Shearman MS, Prywes R and Haass C. Endoproteolysis of the ER stress transducer ATF6 in the presence of functionally inactive presenilins. Neurobiol Dis 2001; 8: 717-722.
[79] Haapasalo A and Kovacs DM. The many substrates of presenilin/gamma-secretase. J Alzheimers Dis 2011; 25: 3-28.
[80] Copanaki E, Schürmann T, Eckert A, Leuner K, Müller WE, Prehn JH and Kögel D. The amyloid precursor protein potentiates CHOP induction and cell death in response to ER Ca2+ depletion. Biochim Biophys Acta 2007; 1773: 157-165.
[81] Vattemi G, Engel WK, McFerrin J and Askanas V. Endoplasmic reticulum stress and unfolded protein response in inclusion body myositis muscle. Am J Pathol 2004; 164: 1-7.
[82] Chafekar SM, Zwart R, Veerhuis R, Vanderstichele H, Baas F and Scheper W. Increased Abeta1-42 production sensitizes neuroblastoma cells for ER stress toxicity. Curr Alzheimer Res 2008; 5: 469-474.
[83] Esposito L, Gan L, Yu GQ, Essrich C and Mucke L. Intracellularly generated amyloid-beta peptide counteracts the antiapoptotic function of its precursor protein and primes proapoptotic pathways for activation by other insults in neuroblastoma cells. J Neurochem 2004; 91: 1260-1274.
[84] Kang EB, Kwon IS, Koo JH, Kim EJ, Kim CH, Lee J, Yang CH, Lee YI, Cho IH and Cho JY. Treadmill exercise represses neuronal cell death and inflammation during Abeta-induced ER stress by regulating unfolded protein response in aged presenilin 2 mutant mice. Apoptosis 2013; 18: 1332-1347.
[85] Li H, Chen Q, Liu F, Zhang X, Li W, Liu S, Zhao Y, Gong Y and Yan C. Unfolded protein response and activated degradative pathways regulation in GNE myopathy. PLoS One 2013; 8: e58116.
[86] Costa RO, Ferreiro E, Oliveira CR and Pereira CM. Inhibition of mitochondrial cytochrome c oxidase potentiates Abeta-induced ER stress and cell death in cortical neurons. Mol Cell Neurosci 2013; 52: 1-8.
[87] Lee JH, Won SM, Suh J, Son SJ, Moon GJ, Park UJ and Gwag BJ. Induction of the unfolded protein response and cell death pathway in Alzheimer's disease, but not in aged Tg2576 mice. Exp Mol Med 2010; 42: 386-394.
[88] Yu MS, Suen KC, Kwok NS, So KF, Hugon J and Chang RC. Beta-amyloid peptides induces neuronal apoptosis via a mechanism independent of unfolded protein responses. Apoptosis 2006; 11: 687-700.
[89] Chafekar SM, Hoozemans JJ, Zwart R, Baas F and Scheper W. Abeta 1-42 induces mild endoplasmic reticulum stress in an aggregation state-dependent manner. Antioxid Redox Signal 2007; 9: 2245-2254.
[90] Kondo T, Asai M, Tsukita K, Kutoku Y, Ohsawa Y, Sunada Y, Imamura K, Egawa N, Yahata N, Okita K, Takahashi K, Asaka I, Aoi T, Watanabe A, Watanabe K, Kadoya C, Nakano R, Watanabe D, Maruyama K, Hori O, Hibino S, Choshi T, Nakahata T, Hioki H, Kaneko T, Naitoh M, Yoshikawa K, Yamawaki S, Suzuki S, Hata R, Ueno S, Seki T, Kobayashi K, Toda T, Murakami K, Irie K, Klein WL, Mori H, Asada T, Takahashi R, Iwata N, Yamanaka S and Inoue H. Modeling Alzheimer's disease with iPSCs reveals stress phenotypes associated with intracellular Abeta and differential drug responsiveness. Cell Stem Cell 2013; 12: 487-496.
[91] Lai CS, Preisler J, Baum L, Lee DH, Ng HK, Hugon J, So KF and Chang RC. Low molecular weight Abeta induces collapse of endoplasmic reticulum. Mol Cell Neurosci 2009; 41: 32-43.
[92] Yoon SO, Park DJ, Ryu JC, Ozer HG, Tep C, Shin YJ, Lim TH, Pastorino L, Kunwar AJ, Walton JC, Nagahara AH, Lu KP, Nelson RJ, Tuszynski MH and Huang K. JNK3 perpetuates metabolic stress induced by Abeta peptides. Neuron 2012; 75: 824-837.
[93] Pardossi-Piquard R and Checler F. The physiology of the beta-amyloid precursor protein intracellular domain AICD. J Neurochem 2012; 120 Suppl 1: 109-124.
[94] Takahashi K, Niidome T, Akaike A, Kihara T and Sugimoto H. Amyloid precursor protein promotes endoplasmic reticulum stress-induced cell death via C/EBP homologous protein-mediated pathway. J Neurochem 2009; 109: 1324-1337.
[95] Kögel D, Concannon CG, Müller T, König H, Bonner C, Poeschel S, Chang S, Egensperger R and Prehn JH. The APP intracellular domain (AICD) potentiates ER stress-induced apoptosis. Neurobiol Aging 2012; 33: 2200-2209.
[96] Guo Q, Robinson N and Mattson MP. Secreted beta-amyloid precursor protein counteracts the proapoptotic action of mutant presenilin-1 by activation of NF-kappaB and stabilization of calcium homeostasis. J Biol Chem 1998; 273: 12341-12351.
[97] Eckert GP, Chang S, Eckmann J, Copanaki E, Hagl S, Hener U, Müller WE and Kögel D. Liposome-incorporated DHA increases neuronal survival by enhancing non-amyloidogenic APP processing. Biochim Biophys Acta 2011; 1808: 236-243.
[98] Unterberger U, Höftberger R, Gelpi E, Flicker H, Budka H and Voigtländer T. Endoplasmic reticulum stress features are prominent in Alzheimer disease but not in prion diseases in vivo. J Neuropathol Exp Neurol 2006; 65: 348-357.

[99] Hoozemans JJ, van Haastert ES, Nijholt DA, Rozemuller AJ, Eikelenboom P and Scheper W. The unfolded protein response is activated in pretangle neurons in Alzheimer's disease hippocampus. Am J Pathol 2009; 174: 1241-1251.

[100] Nijholt DA, van Haastert ES, Rozemuller AJ, Scheper W and Hoozemans JJ. The unfolded protein response is associated with early tau pathology in the hippocampus of tauopathies. J Pathol 2012; 226: 693-702.

[101] Ho YS, Yang X, Lau JC, Hung CH, Wuwongse S, Zhang Q, Wang J, Baum L, So KF and Chang RC. Endoplasmic reticulum stress induces tau pathology and forms a vicious cycle: implication in Alzheimer's disease pathogenesis. J Alzheimers Dis 2012; 28: 839-854.

[102] Spatara ML and Robinson AS. Transgenic mouse and cell culture models demonstrate a lack of mechanistic connection between endoplasmic reticulum stress and tau dysfunction. J Neurosci Res 2010; 88: 1951-1961.

[103] Abisambra JF, Jinwal UK, Blair LJ, O'Leary JC 3rd, Li Q, Brady S, Wang L, Guidi CE, Zhang B, Nordhues BA, Cockman M, Suntharalingham A, Li P, Jin Y, Atkins CA and Dickey CA. Tau accumulation activates the unfolded protein response by impairing endoplasmic reticulum-associated degradation. J Neurosci 2013; 33: 9498-9507.

[104] Fu ZQ, Yang Y, Song J, Jiang Q, Lin ZC, Wang Q, Zhu LQ, Wang JZ and Tian Q. LiCl attenuates thapsigargin-induced tau hyperphosphorylation by inhibiting GSK-3beta in vivo and in vitro. J Alzheimers Dis 2010; 21: 1107-1117.

[105] Sakagami Y, Kudo T, Tanimukai H, Kanayama D, Omi T, Horiguchi K, Okochi M, Imaizumi K and Takeda M. Involvement of endoplasmic reticulum stress in tauopathy. Biochem Biophys Res Commun 2013; 430: 500-504.

[106] Resende R, Ferreiro E, Pereira C and Oliveira CR. ER stress is involved in Abeta-induced GSK-3beta activation and tau phosphorylation. J Neurosci Res 2008; 86: 2091-2099.

[107] Liu ZC, Fu ZQ, Song J, Zhang JY, Wei YP, Chu J, Han L, Qu N, Wang JZ and Tian Q. Bip enhanced the association of GSK-3beta with tau during ER stress both in vivo and in vitro. J Alzheimers Dis 2012; 29: 727-740.

[108] Nogalska A, Engel WK and Askanas V. Increased BACE1 mRNA and noncoding BACE1-antisense transcript in sporadic inclusion-body myositis muscle fibers--possibly caused by endoplasmic reticulum stress. Neurosci Lett 2010; 474: 140-143.

[109] Page G, Rioux Bilan A, Ingrand S, Lafay-Chebassier C, Pain S, Perault Pochat MC, Bouras C, Bayer T and Hugon J. Activated double-stranded RNA-dependent protein kinase and neuronal death in models of Alzheimer's disease. Neuroscience 2006; 139: 1343-1354.

[110] O'Connor T, Sadleir KR, Maus E, Velliquette RA, Zhao J, Cole SL, Eimer WA, Hitt B, Bembinster LA, Lammich S, Lichtenthaler SF, Hébert SS, de Strooper B, Haass C, Bennett DA and Vassar R. Phosphorylation of the translation initiation factor eIF2alpha increases BACE1 levels and promotes amyloidogenesis. Neuron 2008; 60: 988-1009.

[111] Ill-Raga G, Palomer E, Wozniak MA, Ramos-Fernández E, Bosch-Morató M, Tajes M, Guix FX, Galán JJ, Clarimón J, Antúnez C, Real LM, Boada M, Itzhaki RF, Fandos C and Muñoz FJ. Activation of PKR causes amyloid ss-peptide accumulation via de-repression of BACE1 expression. PLoS One 2011; 6: e21456

[112] Lammich S, Schöbel S, Zimmer AK, Lichtenthaler SF and Haass C. Expression of the Alzheimer protease BACE1 is suppressed via its 5'-untranslated region. EMBO Rep 2004; 5: 620-625.

[113] Mouton-Liger F, Paquet C, Dumurgier J, Bouras C, Pradier L, Gray F and Hugon J. Oxidative stress increases BACE1 protein levels through activation of the PKR-eIF2alpha pathway. Biochim Biophys Acta 2012; 1822: 885-896.

[114] Dumurgier J, Mouton-Liger F, Lapalus P, Prevot M, Laplanche JL, Hugon J and Paquet C. Cerebrospinal fluid PKR level predicts cognitive decline in Alzheimer's disease. PLoS One 2013; 8: e53587

[115] Mitsuda T, Hayakawa Y, Itoh M, Ohta K and Nakagawa T. ATF4 regulates gamma-secretase activity during amino acid imbalance. Biochem Biophys Res Commun 2007; 352: 722-727.

[116] Ohta K, Mizuno A, Li S, Itoh M, Ueda M, Ohta E, Hida Y, Wang MX, Furoi M, Tsuzuki Y, Sobajima M, Bohmoto Y, Fukushima T, Kobori M, Inuzuka T and Nakagawa T. Endoplasmic reticulum stress enhances gamma-secretase activity. Biochem Biophys Res Commun 2011; 416: 362-366.

[117] Koyama Y, Matsuzaki S, Gomi F, Yamada K, Katayama T, Sato K, Kumada T, Fukuda A, Matsuda S, Tano Y and Tohyama M. Induction of amyloid beta accumulation by ER calcium disruption and resultant upregulation of angiogenic factors in ARPE19 cells. Invest Ophthalmol Vis Sci 2008; 49: 2376-2383.

[118] Saftig P and Reiss K. The "A Disintegrin And Metalloproteases" ADAM10 and ADAM17: novel drug targets with therapeutic potential? Eur J Cell Biol 2011; 90: 527-535.

[119] Rzymski T, Petry A, Kračun D, Riess F, Pike L, Harris AL and Görlach A. The unfolded protein response controls induction and activation of

ADAM17/TACE by severe hypoxia and ER stress. Oncogene 2012; 31: 3621-3634.
[120] Reinhardt S, Schuck F, Grösgen S, Riemenschneider M, Hartmann T, Postina R, Grimm M and Endres K. Unfolded protein response signaling by transcription factor XBP-1 regulates ADAM10 and is affected in Alzheimer's disease. FASEB J 2013; [Epub ahead of print].
[121] Kuhn PH, Wang H, Dislich B, Colombo A, Zeitschel U, Ellwart JW, Kremmer E, Rossner S and Lichtenthaler SF. ADAM10 is the physiologically relevant, constitutive alpha-secretase of the amyloid precursor protein in primary neurons. EMBO J 2010; 29: 3020-3032.
[122] Jorissen E, Prox J, Bernreuther C, Weber S, Schwanbeck R, Serneels L, Snellinx A, Craessaerts K, Thathiah A, Tesseur I, Bartsch U, Weskamp G, Blobel CP, Glatzel M, de Strooper B and Saftig P. The disintegrin/metalloproteinase ADAM10 is essential for the establishment of the brain cortex. J Neurosci 2010; 30: 4833-4844.
[123] Chaimowitz NS, Kang DJ, Dean LM and Conrad DH. ADAM10 regulates transcription factor expression required for plasma cell function. PLoS One 2012; 7: e42694.
[124] Elder GA, Gama Sosa MA and de Gasperi R. Transgenic mouse models of Alzheimer's disease. Mt Sinai J Med 2010; 77: 69-81.
[125] Abisambra JF, Blair LJ, Hill SE, Jones JR, Kraft C, Rogers J, Koren J 3rd, Jinwal UK, Lawson L, Johnson AG, Wilcock D, O'Leary JC, Jansen-West K, Muschol M, Golde TE, Weeber EJ, Banko J and Dickey CA. Phosphorylation dynamics regulate Hsp27-mediated rescue of neuronal plasticity deficits in tau transgenic mice. J Neurosci 2010; 30: 15374-15382.
[126] Santacruz K, Lewis J, Spires T, Paulson J, Kotilinek L, Ingelsson M, Guimaraes A, DeTure M, Ramsden M, McGowan E, Forster C, Yue M, Orne J, Janus C, Mariash A, Kuskowski M, Hyman B, Hutton M and Ashe KH. Tau suppression in a neurodegenerative mouse model improves memory function. Science 2005; 309: 476-481.
[127] Hsiao K, Chapman P, Nilsen S, Eckman C, Harigaya Y, Younkin S, Yang F and Cole G. Correlative memory deficits, Abeta elevation, and amyloid plaques in transgenic mice. Science 1996; 274: 99-102.
[128] Oakley H, Cole SL, Logan S, Maus E, Shao P, Craft J, Guillozet-Bongaarts A, Ohno M, Disterhoft J, van Eldik L, Berry R and Vassar R. Intraneuronal beta-amyloid aggregates, neurodegeneration, and neuron loss in transgenic mice with five familial Alzheimer's disease mutations: potential factors in amyloid plaque formation. J Neurosci 2006; 26: 10129-10140.
[129] Casas C, Sergeant N, Itier JM, Blanchard V, Wirths O, van der Kolk N, Vingtdeux V, van de Steeg E, Ret G, Canton T, Drobecq H, Clark A, Bonici B, Delacourte A, Benavides J, Schmitz C, Tremp G, Bayer TA, Benoit P and Pradier L. Massive CA1/2 neuronal loss with intraneuronal and N-terminal truncated Abeta42 accumulation in a novel Alzheimer transgenic model. Am J Pathol 2004; 165: 1289-1300.
[130] Lin JH, Li H, Yasumura D, Cohen HR, Zhang C, Panning B, Shokat KM, Lavail MM and Walter P. IRE1 signaling affects cell fate during the unfolded protein response. Science 2007; 318: 944-949.
[131] Hoozemans JJ, Veerhuis R, van Haastert ES, Rozemuller JM, Baas F, Eikelenboom P and Scheper W. The unfolded protein response is activated in Alzheimer's disease. Acta Neuropathol 2005; 110: 165-172.
[132] Teske BF, Fusakio ME, Zhou D, Shan J, McClintick JN, Kilberg MS and Wek RC. CHOP induces activating transcription factor 5 (ATF5) to trigger apoptosis in response to perturbations in protein homeostasis. Mol Biol Cell 2013; 24: 2477-2490.
[133] Soejima N, Ohyagi Y, Nakamura N, Himeno E, Iinuma KM, Sakae N, Yamasaki R, Tabira T, Murakami K, Irie K, Kinoshita N, Laferla FM, Kiyohara Y, Iwaki T and Kira J. Intracellular accumulation of toxic turn amyloid-beta is associated with endoplasmic reticulum stress in Alzheimer's disease. Curr Alzheimer Res 2013; 10: 11-20.
[134] Oddo S, Caccamo A, Cheng D, Jouleh B, Torp R and Laferla FM. Genetically augmenting tau levels does not modulate the onset or progression of Abeta pathology in transgenic mice. J Neurochem 2007; 102: 1053-1063.
[135] Umeda T, Tomiyama T, Sakama N, Tanaka S, Lambert MP, Klein WL and Mori H. Intraneuronal amyloid beta oligomers cause cell death via endoplasmic reticulum stress, endosomal/lysosomal leakage, and mitochondrial dysfunction in vivo. J Neurosci Res 2011; 89: 1031-1042.
[136] Tomiyama T, Matsuyama S, Iso H, Umeda T, Takuma H, Ohnishi K, Ishibashi K, Teraoka R, Sakama N, Yamashita T, Nishitsuji K, Ito K, Shimada H, Lambert MP, Klein WL and Mori H. A mouse model of amyloid beta oligomers: their contribution to synaptic alteration, abnormal tau phosphorylation, glial activation, and neuronal loss in vivo. J Neurosci 2010; 30: 4845-4856.
[137] de La Monte SM, Re E, Longato L and Tong M. Dysfunctional pro-ceramide, ER stress and insulin/IGF signaling networks with progression of Alzheimer's disease. J Alzheimers Dis 2012; 30 Suppl 2: S217-S229.

[138] Casas-Tinto S, Zhang Y, Sanchez-Garcia J, Gomez-Velazquez M, Rincon-Limas DE and Fernandez-Funez P. The ER stress factor XBP1s prevents amyloid-beta neurotoxicity. Hum Mol Genet 2011; 20: 2144-2160.
[139] Honjo Y, Ito H, Horibe T, Takahashi R and Kawakami K. Protein disulfide isomerase-immunopositive inclusions in patients with Alzheimer disease. Brain Res 2010; 1349: 90-96.
[140] Kaneko M, Koike H, Saito R, Kitamura Y, Okuma Y and Nomura Y. Loss of HRD1-mediated protein degradation causes amyloid precursor protein accumulation and amyloid-beta generation. J Neurosci 2010; 30: 3924-3932.
[141] Safra M, Ben-Hamo S, Kenyon C and Henis-Korenblit S. The ire-1 ER stress-response pathway is required for normal secretory-protein metabolism in C. elegans. J Cell Sci 2013; 126: 4136-4146.
[142] Taylor RC and Dillin A. XBP-1 is a cell-nonautonomous regulator of stress resistance and longevity. Cell 2013; 153: 1435-1447.
[143] Halliday M and Mallucci GR. Targeting the unfolded protein response in neurodegeneration: A new approach to therapy. Neuropharmacology 2014; 76: 169-174.
[144] Chadwick W, Mitchell N, Martin B and Maudsley S. Therapeutic targeting of the endoplasmic reticulum in Alzheimer's disease. Curr Alzheimer Res 2012; 9: 110-119.
[145] Rochet JC. Novel therapeutic strategies for the treatment of protein-misfolding diseases. Expert Rev Mol Med 2007; 9: 1-34.
[146] Valera E, Dargusch R, Maher PA and Schubert D. Modulation of 5-lipoxygenase in proteotoxicity and Alzheimer's disease. J Neurosci 2013; 33: 10512-10525.
[147] Lassot I, Estrabaud E, Emiliani S, Benkirane M, Benarous R and Margottin-Goguet F. p300 modulates ATF4 stability and transcriptional activity independently of its acetyltransferase domain. J Biol Chem 2005; 280: 41537-41545.
[148] Uemura A, Taniguchi M, Matsuo Y, Oku M, Wakabayashi S and Yoshida H. UBC9 regulates the stability of XBP1, a key transcription factor controlling the ER stress response. Cell Struct Funct 2013; 38: 67-79.
[149] Park SW, Zhou Y, Lee J, Lu A, Sun C, Chung J, Ueki K and Ozcan U. The regulatory subunits of PI3K, p85alpha and p85beta, interact with XBP-1 and increase its nuclear translocation. Nat Med 2010; 16: 429-437.
[150] Winnay JN, Boucher J, Mori MA, Ueki K and Kahn CR. A regulatory subunit of phosphoinositide 3-kinase increases the nuclear accumulation of X-box-binding protein-1 to modulate the unfolded protein response. Nat Med 2010; 16: 438-445.
[151] Carrara M, Prischi F and Ali MM. UPR Signal Activation by Luminal Sensor Domains. Int J Mol Sci 2013; 14: 6454-6466.
[152] Vattem KM and Wek RC. Reinitiation involving upstream ORFs regulates ATF4 mRNA translation in mammalian cells. Proc Natl Acad Sci U S A 2004; 101: 11269-11274.
[153] Hai T and Curran T. Cross-family dimerization of transcription factors Fos/Jun and ATF/CREB alters DNA binding specificity. Proc Natl Acad Sci U S A 1991; 88: 3720-3724.
[154] Chérasse Y, Maurin AC, Chaveroux C, Jousse C, Carraro V, Parry L, Deval C, Chambon C, Fafournoux P and Bruhat A. The p300/CBP-associated factor (PCAF) is a cofactor of ATF4 for amino acid-regulated transcription of CHOP. Nucleic Acids Res 2007; 35: 5954-5965.
[155] Lyckman AW, Confaloni AM, Thinakaran G, Sisodia SS and Moya KL. Post-translational processing and turnover kinetics of presynaptically targeted amyloid precursor superfamily proteins in the central nervous system. J Biol Chem 1998; 273: 11100-11106.

7.2 CURRICULUM VITAE

[redacted]

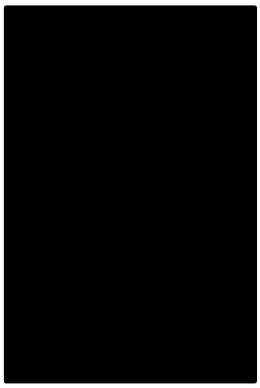

[redacted]

[redacted]